

# Modulation of cellular IKK complexes by human Adenovirus Type 5

DISSERTATION

with the aim of achieving a doctoral degree at the  
Faculty of Mathematics, Informatics and Natural Sciences,  
Department of Biology,  
University of Hamburg

submitted

by

Wing Hang Ip

August 2016 in Hamburg

Tag der Disputation: 27.01.2017

Gutachter: Prof. Dr. T. Dobner  
Prof. Dr. N. Fischer



**Max-Planck-Institut für molekulare Genetik**  
Max Planck Institute for Molecular Genetics

MPI für molekulare Genetik • Ihnestr. 63-73 • D-14195 Berlin

Otto-Warburg-Laboratory

Sarah Kinkley, Ph-D  
Epigenomics

Ihnestr. 63 - 73  
D-14195 Berlin

Tel.: + 49 - 30 - 84 13 1875  
Fax: + 49 - 30 - 84 13 1960  
kinkley@molgen.mpg.de

22. Juli 2016

The English language in Wing Hang Ip's PhD thesis entitled "Modulation of cellular IKK complexes by human Adenovirus Type 5" reads fluently and is well written. I give my support that the English language is correctly articulated in Wing Hang Ip's thesis.

Sincerely,

*Dr. Sarah Kinkley*  
Dr. Sarah Kinkley



Max-Planck-Gesellschaft, c/o MPI für molekulare Genetik  
Deutsche Bank AG, München  
BLZ: 700 700 10 BIC Code (Swift): DEUTDEMMXXX  
Kto-Nr.: 195 130 045 IBAN: DE06 7007 0010 0195 1300 45

UST-Nr.: 143/219/10158  
UST-ID-Nr.: DE129517720

[www.molgen.mpg.de](http://www.molgen.mpg.de)



MAX-PLANCK-GESELLSCHAFT

### Statutory Declaration

I declare that this thesis is a result of my personal work and that no other than the indicated aids have been used for its completion. Furthermore, I assure that all quotations and statements that have been inferred literally or in a general manner from published or unpublished writings are marked as such. Beyond this I assure that the work has not been used, neither completely nor in parts, to achieve an academic grading or is being published elsewhere.

Hamburg, 28. 7. '16

Signature

*Wingkeg p*



## Table of contents

<b>1</b>	<b>Introduction</b>	<b>1</b>
1.1	Adenoviruses	1
1.1.1	Classification	1
1.1.2	HAdV pathogenicity and treatment	3
1.1.3	Structure and genome organization	5
1.2	Life cycle of Human mastadenoviruses	8
1.3	HAdV-C5 early regulatory proteins	9
1.3.1	Early region 1	9
1.3.2	Early region 2	13
1.3.3	Early region 3	14
1.3.4	Early region 4	15
1.4	Innate viral immunity	17
1.4.1	Immune response upon HAdV-C5 infection	18
1.4.2	NF- $\kappa$ B and I $\kappa$ B proteins	21
1.5	NF- $\kappa$ B signaling pathways	23
1.5.1	The canonical NF- $\kappa$ B pathway	23
1.5.2	The non-canonical NF- $\kappa$ B pathway	25
1.5.3	The IKK complex	28
1.5.4	Manipulation of NF- $\kappa$ B signaling upon viral infection	30
<b>2</b>	<b>Material</b>	<b>37</b>
2.1	Cells	37
2.1.1	Bacterial strains	37
2.1.2	Mammalian cell lines	37
2.1.3	Viruses	37
2.2	Nucleic acids	38
2.2.1	Oligonucleotides	38
2.2.2	Vectors	38
2.2.3	Recombinant plasmids	39
2.3	Antibodies	41
2.3.1	Primary antibodies	41
2.4	Secondary antibodies	43
2.4.1	Antibodies for western blotting	43
2.4.2	Antibodies for immunofluorescence staining	43
2.5	Standards and markers	44

2.6	Commercial systems.....	44
2.7	Chemicals, enzymes, reagents, equipment.....	44
2.8	Software and databases .....	44
<b>3</b>	<b>Methods .....</b>	<b>46</b>
3.1	Bacteria.....	46
3.1.1	Culture and Storage.....	46
3.2	Chemical transformation.....	46
3.3	Tissue culture techniques .....	47
3.3.1	Maintenance and passage of cell lines .....	47
3.3.2	Cryopreservation of cell lines .....	47
3.3.3	Determination of cell number .....	48
3.4	Transfection of mammalian cells .....	48
3.4.1	Transfection with Polyethylenimine.....	48
3.4.2	Transfection with calcium phosphate.....	49
3.4.3	Harvest of mammalian cells.....	49
3.4.4	Generation of stable knock-down cell lines .....	49
3.5	Adenovirus.....	50
3.5.1	Infection with adenovirus .....	50
3.5.2	Propagation and storage of high-titer virus stocks.....	50
3.5.3	Titration of virus stocks .....	51
3.5.4	Determination of virus yield.....	51
3.6	DNA techniques .....	52
3.6.1	Preparation of plasmid DNA from <i>E.coli</i> .....	52
3.6.2	Quantitative determination of nucleic acid concentrations .....	52
3.6.3	Agarose gel electrophoresis .....	52
3.6.4	Polymerase chain reaction (PCR) .....	53
3.6.5	Site-directed mutagenesis.....	54
3.7	Cloning of DNA fragments .....	54
3.7.1	Enzymatic DNA restriction .....	54
3.7.2	DNA sequencing.....	55
3.8	RNA techniques.....	55
3.8.1	Isolation of total RNA from mammalian cells.....	55
3.8.2	Quantitative reverse transcription (RT)-PCR .....	55
3.8.3	Real-Time PCR (RT-PCR) .....	55
3.9	Protein techniques.....	56
3.9.1	Preparation of total-cell lysates.....	56
3.9.2	Quantitative determination of protein concentrations.....	57

3.9.3	Immunoprecipitation .....	57
3.9.4	Subcellular fractionation.....	57
3.9.5	Denaturing purification and analysis of conjugates.....	59
3.9.6	SDS polyacrylamide gel electrophoresis (SDS-PAGE).....	60
3.9.7	Western blotting.....	61
<b>3.10</b>	<b>GST Pull-down Assays from Cell Lysates .....</b>	<b>62</b>
3.10.1	GST-Protein Expression.....	62
3.10.2	GST-Protein Purification .....	62
3.10.3	GST Pull-Down Assays.....	63
3.10.4	Indirect immunofluorescence analysis.....	63
3.10.5	Reporter Gene Assay.....	64
<b>4</b>	<b>Results.....</b>	<b>65</b>
4.1	<b>Role of the NF-<math>\kappa</math>B mediated innate immune pathway during HAdV-C5 infection.....</b>	<b>65</b>
4.2	<b>Interplay between HAdV-C5 and the NF-<math>\kappa</math>B pathway .....</b>	<b>65</b>
4.2.1	NF- $\kappa$ B expression activates HAdV-C5 promoters .....	65
4.2.2	NF- $\kappa$ B promoter activity is highly regulated by transient expression of HAdV-C5 proteins .....	67
4.2.3	Role of IKK complex proteins during HAdV-C5 infection .....	71
4.3	<b>Interplay between HAdV-C5 and IKK complex components .....</b>	<b>74</b>
4.3.1	HAdV-C5 reduces the IKK complex formation .....	74
4.3.2	HAdV-C5 E1B-55K interacts with the IKK complex upon infection .....	75
4.3.3	HAdV-C5 E1B-55K and E1B-156R interact with the IKK complex .....	77
4.3.4	Characterization of the binding between host IKK $\alpha$ and HAdV-C5 E1B-55K	79
4.3.5	IKK $\alpha$ enhances viral protein expression upon HAdV-C5 infection .....	95
4.4	<b>NEMO reduces expression level of E1B-55K upon cotransfection .....</b>	<b>98</b>
<b>5</b>	<b>Discussion .....</b>	<b>116</b>
5.1	<b>HAdV-C5 regulates NF-<math>\kappa</math>B pathway during lytic infection.....</b>	<b>116</b>
5.1.1	Interplay between HAdV-C5 proteins and the NF- $\kappa$ B pathway .....	116
5.1.2	HAdV-C5 infection counteracts TNF $\alpha$ -induced NF- $\kappa$ B activation .....	118
5.1.3	IKK complex proteins are targeted upon adenoviral infection .....	119
5.2	<b>IKK<math>\alpha</math> exerts pro-viral functions upon HAdV-C5 infection.....</b>	<b>121</b>
5.3	<b>NEMO regulates stability of important HAdV-C5 regulatory proteins .....</b>	<b>123</b>
5.4	<b>The nuclear localization of NEMO might play a role upon adenovirus infection.....</b>	<b>124</b>

6	Literature .....	128
7	Publications.....	158
8	Acknowledgements .....	160

## Abbreviations

---

aa	amino acid
AAV	Adeno-associated virus
Ab	Antibody
HAdV	Adenovirus
AP-1	Activating protein-1
APS	Ammonium persulfate
ARD	Ankyrin repeat domains
ARTI	Adenovirus respiratory tract infection of airway epithelial cells
ASFV	African swine fever virus
ATP	Adenosine triphosphate
ATM	Ataxia telangiectasia mutated protein
ATR	Ataxia telangiectasia and Rad3 related
ATRX	Alpha thalassemia/mental retardation syndrome X-linked
B	B-Box
BAFF-R	B-cell activating factor receptor
BAK1	BCL2-antagonist/killer 1
BCL-1	B-cell leukemia/lymphoma 1
BRK	baby rat kidney cells
BSA	Bovine serum albumin
c-FLIP	cellular FLICE inhibitory protein
CAR	Coxsackie-and-Adenovirus-receptor
CBP	CREB-binding protein
CC	coiled-coil
CH	Cysteine Histidine
CPV	Chordopoxviruses
CPXV	Cowpox virus
CR	conserved region
CRM1	Chromosome region maintenance 1
CTL	Cytotoxic T-lymphocytes
CYLD	Cylindromatosis
DAPI	4', 6-Diamidine-2-phenylindole dihydrochloride
Daxx	Death-associated protein 6

---

dd	double-distilled
DDR	DNA damage response
DEPC	Diethylpyrocarbonate
DISC	Death-inducing signaling complex
DMEM	Dulbecco's Modified Eagle Medium
DMSO	Dimethylsulfoxide
DNA	Desoxyribonucleic acid
dNTP	Desoxyribonucleoside-5'-triphosphate
ds	double-stranded
DTT	Dithiotreitol
E	early region
EBV	Epstein-Barr virus
ECL	Enhanced Chemiluminescence
<i>E. coli</i>	<i>Escherichia coli</i>
EDTA	Ethylenediaminetetraacetic acid
EMCV	Encephalomyocarditis virus
ERK	Extracellular signal-regulated kinases
ETOH	Ethanol
FCS	Fetal calf serum
FITC	Fluorescein isothiocyanate
ffu	Fluorescence forming units
fw	forward
HAdV	Human mastadenoviruses
HAT	Histone acetyltransferase
HBV	Hepatitis B virus
HCMV	Human Cytomegalovirus
HCV	Hepatitis C virus
HDAC	Histone deacetylase
HEK	Human embryonic kidney
HHV-8	Herpesvirus-8
HLH	Helix-loop-helix
HP1	Heterochromatin protein 1
hpi	hours post infection
HRP	horse-radish peroxidase

---

HSCT	Hematopoietic stem cell transplantation
HSV-1	Herpes simplex virus 1
HTLV-1	Human T-cell lymphotropic virus type 1
HVS	Herpesvirus saimiri
IAP	Inhibitor of apoptosis
ICAM-1	Intercellular adhesion molecule-1
ICP0	Infected Cell Polypeptide 0 protein
IE	immediate early
IFN	Interferon
Ig	Immunoglobulin
IgH	Immunoglobulin heavy chain
IgL	Immunoglobulin light chain
I $\kappa$ B $\alpha$	Inhibitor of kappa B
IKK	I-kappa-B kinase
IL	Interleukin
IP	Immunoprecipitation
IRF	Interferon regulatory factors
ITR	Inverted terminal repeat
JNK	c-Jun N-terminal kinases
kDa	Kilodalton
KSHV	Kaposi's sarcoma-associated herpesvirus
L	late region
LB	Luria Bertani
LPS	Lipopolysaccharide
LT $\beta$ R	Lymphotoxin- $\beta$ receptor
LZ	Leucine zipper
mAB	monoclonal antibody
MAPK	Mitogen-Activated Protein Kinase
MCL-1	Myeloid leukemia sequence 1
MCMV	Mouse cytomegalovirus
MPyV	Merkel cell polyoma virus
MHC	major histocompatibility complex
MLP	major late promoter
MLTU	major late transcription unit

---

MOI	multiplicity of infection
MRN	Mre11-Rad50-Nbs1
mRNA	messenger RNA
MTOC	Microtubule organizing centers
MyD88	Myeloid differentiation primary response gene 88
NBD	NEMO-binding domain
ND10	nuclear domain 10
NEM	N-ethylmaleimide
NEMO	NF- $\kappa$ B essential modifier
NES	Nuclear export signal
NF- $\kappa$ B	Nuclear factor 'kappa-light-chain-enhancer' of activated B-cells
NHEJ	non-homologous end joining
NIK	NF- $\kappa$ B-inducing kinase
NLR	Nod-like receptors
NLS	Nuclear localization signal
NPC	Nuclear pore complex
nt	nucleotide
Oct-1	Octamer transcription factor 1
OD	optical density
ORF	open reading frame
PAMPS	Pathogen-associated molecular patterns
PBS	Phosphate buffered saline
PCAF	p300/CBP-associated factor
PFA	Paraformaldehyde
PI3K	Phosphatidylinositol 3-kinase
PMA	phorbol 12-myristate 13-acetate
PML	Promyelocytic leukemia protein
PML-NB	PML nuclear body
POD	PML oncogenic domain
PP2A	Protein phosphatase 2A
PRR	Pattern recognition receptors
PVDF	Polyvinylidene fluoride
Rb	Retinoblastoma protein

---

RBCC motif	RING, B-Box, coiled-coil domain
rev	reverse
Rev-T	Reticuloendotheliosis virus
RHD	Rel homology domain
RING	Really interesting new gene
RIP-1	Receptor-interacting protein 1
RLR	RIG-I-like receptors
RNA	Ribonucleic acid
rpm	rounds per minute
RSV	Respiratory syncytial virus
RT	room temperature
SAE	SUMO activating enzyme
SARS	Severe acute respiratory syndrome
SCC	Squamous cell carcinomas
SCM	SUMO conjugation motif
SDS	Sodium dodecyl sulfate
SDS-PAGE	SDS polyacrylamide gel electrophoresis
SENp	Sentrin specific protease
SIM	SUMO interaction motif
Sp100	Speckled protein 100
SPOC1	Survival-time associated PHD protein in ovarian cancer 1
SRC	Steroid receptor coactivator
STAT1	Signal transducer and activator of transcription 1
SUMO	Small ubiquitin related modifier
TAP	Transporter associated with antigen presentation
TCR	T-cell receptor
TEMED	N, N, N', N'-Tetra-methylethylenediamine
Tip60	Tat interacting protein
TLR	Toll like receptors
TNF	Tumor necrosis factor
TP	terminal protein
TRADD	Tumor necrosis factor receptor type 1-associated DEATH domain protein

TRAF2	TNF receptor-associated factor 2
TRIF	TIR-domain-containing adapter inducing interferon- $\beta$
TRIM	Tripartite motif
Tris	Tris-(hydroxymethyl)-aminomethane
U	unit
Uba	Ubiquitin activating enzyme
UV	Ultraviolet
VA	virus associated
VACV	Vaccinia virus
VCAM-1	Vascular cell adhesion molecule-1
vol	volume
VSV	Vesicular stomatitis virus
v/v	volume per volume
w/v	weight per volume

## Abstract

---

Human Adenoviruses (HAdV) employ various strategies to interfere with the innate and the adaptive host immune response. Therefore, they encode multiple proteins especially the early proteins, which are capable to inhibit the expression of interferon-stimulated genes (E1A, VA-RNA), certain pro-inflammatory cytokines such as IL-6 (E1A) and down-regulation of MHC class I molecules (E3). The complexity of regulation by adenoviruses is obvious in regard to TNF $\alpha$ . The early HAdV-C5 protein E1A sensitizes cells to TNF $\alpha$  induced apoptosis, which is in turn counteracted by products of the E3 region and E1B-19K. Further, many publications applying adenovirus vectors show cell line-dependent activation of different subsets of cytokines, which are activated by NF- $\kappa$ B. However, the mechanism of NF- $\kappa$ B pathway modulation in lytic infection is yet unknown and hence was investigated in the present study. The results presented here show for the first time that HAdV-C5 infection inhibits TNF $\alpha$  mediated NF- $\kappa$ B activation in human non-small cell lung carcinoma cells (H1299) during the late phase of infection. This is presumably mediated by attenuated I $\kappa$ B kinase (IKK) complex formation comprising the proteins IKK $\alpha$ , IKK $\beta$  and NEMO upon adenoviral infection. Furthermore, E1B-55K interacts with IKK $\alpha$  of the IKK complex that is relocalized into the nucleus juxtaposed to viral replication centers in an E1B-55K-independent manner. However, NEMO is relocalized into viral replication centers and counteracts E1B-55K expression levels. Results presented here show that both host factors IKK $\alpha$  and NEMO promote efficient adenoviral gene expression and replication representing proviral factors of the IKK complex.

Taken together, data obtained during this thesis show that HAdV-C5 is able to inhibit TNF $\alpha$ -mediated NF- $\kappa$ B activation and that the virus benefits from processes sequestering NEMO and IKK $\alpha$  into the nucleus in order to promote viral life cycle.

## Zusammenfassung

---

Humane Adenoviren (HAdV) haben im Laufe der Evolution vielfältige Strategien entwickelt, um sowohl die angeborene als auch die erworbene Immunantwort auf molekularer Ebene zu modulieren. Dafür sind vor allem virale Proteine zuständig, die in der frühen Phase der Infektion exprimiert werden und Interferon-stimulierte Gene (E1A, VA-RNA), bestimmte proinflammatorische Zytokine wie z. B. IL-6 (E1A) inhibieren, sowie die Expression von MHC Klasse I Antigenen (E3) reprimieren. Die Modulation der zellulären Immunantwort durch HAdV wird im Falle der TNF $\alpha$  Regulation besonders deutlich. Das frühe virale E1A Protein sensibilisiert Zellen für die TNF $\alpha$ -induzierte Apoptose, welche durch das E1B-19K Protein wieder aufgehoben wird. Zahlreiche Ergebnisse anderer Arbeitsgruppen haben gezeigt, dass adenovirale Vektoren die zelllinienabhängige Expression von unterschiedlichen Zytokinen durch NF- $\kappa$ B Aktivierung induzieren können. Allerdings ist der molekulare Mechanismus der NF- $\kappa$ B Modulation während der lytischen Infektion weitgehend unbekannt und wurde in der vorliegenden Arbeit untersucht.

Die Ergebnisse dieser Arbeit zeigen zum ersten Mal, dass die TNF $\alpha$  vermittelte NF- $\kappa$ B Aktivierung während der späten Phase der HAdV-C5 Infektion in humanen Lungenkarzinomzellen (H1299) inhibiert wird. Weitere Untersuchungen haben gezeigt, dass die HAdV-C5 vermittelte Reduktion der IKK Komplexbildung die Repression der TNF $\alpha$ -vermittelten NF- $\kappa$ B Aktivierung darstellt. Es konnte gezeigt werden, dass E1B-55K mit IKK $\alpha$ , einer Komponente des IKK Komplexes, interagiert und die E1B-55K-unabhängige Relokalisation des zellulären Faktors in den Zellkern induziert. NEMO stellt ein weiteres Protein aus dem IKK Komplex dar und wird ebenfalls E1B-55K-unabhängig in virale Replikationszentren relokalisiert. Außerdem konnte gezeigt werden, dass beide IKK Proteine die Produktion von Nachkommenviren unterstützt. Die spezifische Relokalisation von IKK $\alpha$  und NEMO in unterschiedliche Zellkernkompartimente zeigt folglich einen positiven Effekt auf die effiziente Virusreplikation und deutet darauf hin, dass HAdV-C5 den IKK Komplex gezielt inaktiviert, um die TNF $\alpha$  vermittelte NF- $\kappa$ B Aktivierung zu reduzieren sowie die NF- $\kappa$ B-unabhängigen Funktionen von IKK $\alpha$  und NEMO zu nutzen.

Zusammengefasst zeigt diese Arbeit, dass der IKK Komplex nach HAdV-C5 Infektion gezielt moduliert wird, um einen positiven Nutzen für die adenovirale Replikation zu erlangen.

# 1 Introduction

## 1.1 Adenoviruses

### 1.1.1 Classification

Adenoviruses (HAdV), which were first discovered and isolated in 1956, were named after the adenoid tissue in which they were discovered (Enders *et al.*, 1956). Subsequent investigations revealed that the family of *Adenoviridae* comprises five approved genera by the International Committee on Taxonomy of Viruses (Viruses, 2012). They are divided depending on their host range into *Mastadenovirus* (infecting mammalian hosts), *Aviadenovirus* (infecting avian hosts), *Atadenovirus* (infecting reptilian and ruminant hosts), *Siadenovirus* (infecting amphibian hosts) and *Ichtadenovirus* (infecting fish hosts) (Benko *et al.*, 2002; Benkö & Harrach, 1998; Davison, 2003). There are more than 130 types in those 5 genera classified so far (Figure 1).

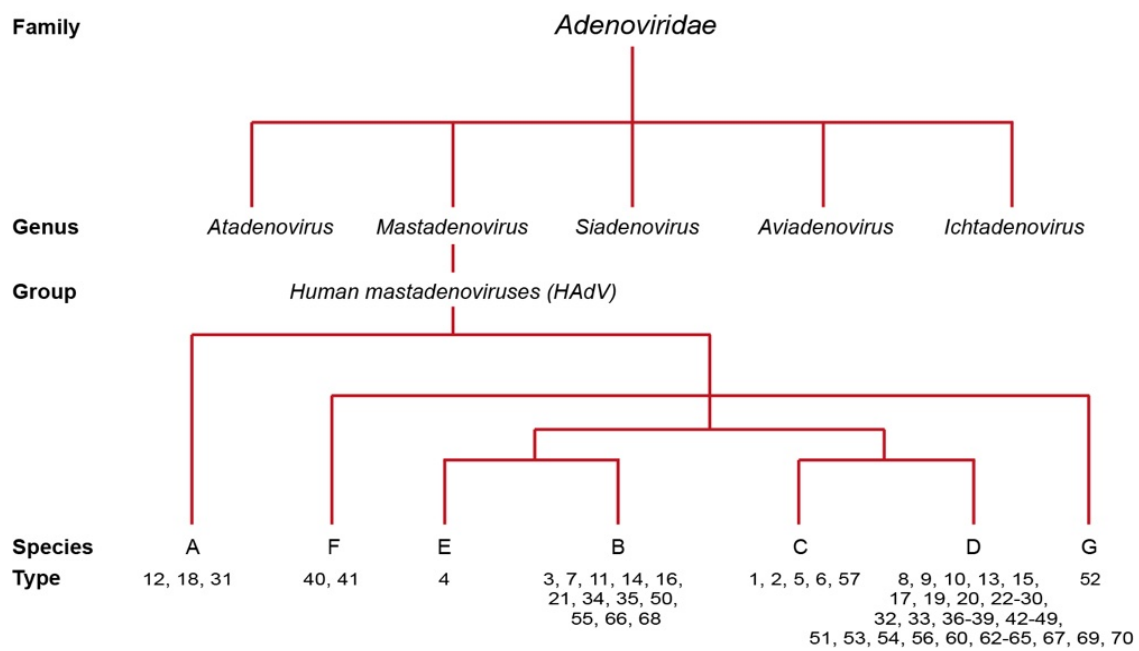


**Figure 1: Classification of the family *Adenoviridae*.**

Simplified illustration of the family *Adenoviridae* taxonomy including HAdV types 1-70. HAdV types 1-52 are classified according to Davison *et al.* and the International Committee of the Taxonomy of Viruses (ICTV).

Human mastadenoviruses (HAdV) were first classified by hemagglutination and serum neutralization characteristics leading to identification of 51 serotypes

(Bailey & Mautner, 1994; Wadell, 1984); however, this has been replaced by genomic data analysis since 2007, which revealed up to now 70 types (Buckwalter *et al.*, 2012; Davison, 2003; Jones *et al.*, 2007; Lion, 2014) (Figure 1). Mastadenoviruses are the most extensively studied genera and comprise bat, bovine, canine, equine, human, murine, ovine, porcine, simian and tree shrew adenoviruses.

Furthermore, these types are subgrouped into seven species (A-G) according to their sequence homology (GC-richness of the genome), hemagglutination and oncogenicity in immunosuppressed rodents. In particular, the prototypical species C Human mastadenovirus types 2 and 5 (HAdV-C2 and HAdV-C5) are the most intensively investigated types due to their non-oncogenic properties (Figure 1) (Shenk, 2001). Besides, the Human mastadenovirus type 12 was the first virus that has been shown to induce malignant tumors in rodents (Trentin *et al.*, 1962). Although there is still no evidence linking HAdV infection to human malignancy, this initial finding led to a tremendous amount of research in Adenovirus-mediated transformation and the classification of HAdV as a DNA tumor virus (Figure 2).

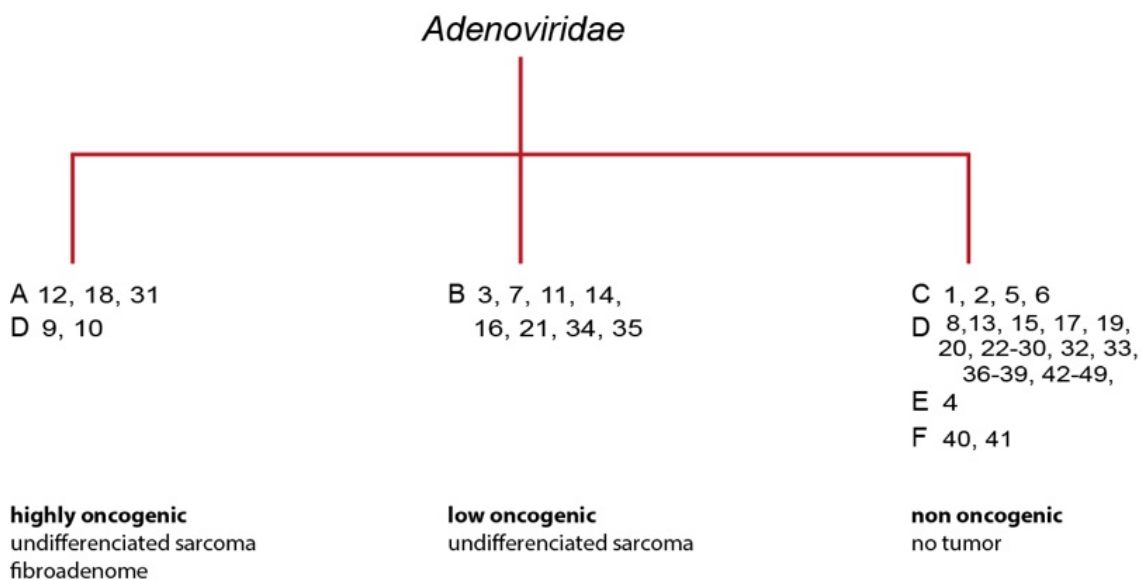


**Figure 2: Oncogenicity of HAdV.**

Overview of the oncogenicity of different so far investigated HAdV subtypes and the kind tumors they induce. Recently discovered types are not classified so far.

### 1.1.2 HAdV pathogenicity and treatment

Subsequent investigations showed that HAdVs generally cause infections of the upper and lower respiratory tract (Dingle & Langmuir, 1968; Ginsberg *et al.*, 1955), the gastrointestinal tract (Chhabra *et al.*, 2013; Yolken *et al.*, 1982) or the eye (Jawetz *et al.*, 1955) (Table 1). Therefore, HAdVs are frequently associated with diseases like acute respiratory disease (usually; caused by species 1, 2, 5, and 6) (Ampuero *et al.*, 2012), pneumonia (occasionally; caused by species A, E) (Esposito *et al.*, 2013), epidemic keratoconjunctivitis (species 1, 2, 5, and 6) (Centers for Disease & Prevention, 2013), and gastroenteritis (occasionally; caused by serotypes 40, 41 of species F) (Celik *et al.*, 2015). In rare cases HAdVs were also found to cause hepatitis (species B) (Detrait *et al.*, 2015), meningoencephalitis (species B) (de Ory *et al.*, 2013), cystitis (species A, B, E) (Hofland *et al.*, 2004) and myocarditis (species C, B, E) (Shauer *et al.*, 2013). Moreover, HAdVs (species D, serotype 36) have been linked to non-inflammatory conditions, such as obesity (Esposito *et al.*, 2012).

**Table 1: Human mastadenoviruses grouped according to their subtypes, types, infectious sites, oncogenic potential and receptor binding (Leen & Rooney, 2005; Shenk, 2001).**

Subtypes	Types	Infectious sites	Oncogenic potential		Receptor
			Tumor in animals	<i>In vitro</i> transformation	
A	12, 18, 31	GI*	high	+	CAR
B	16, 21, 50, 11, 34, 35	Lung, Pharynx, Conjunctiva	high	+	CD46 CD46
	3, 7, 11, 14				DSG-2
C	1, 2, 5, 6	Pharynx	high	+	CAR
D	10, 13, 15, 17, 19, 20, 22-30, 32, 33, 36-39, 42-49, 8, 9, 37	Conjunctiva, GI Conjunctiva	high	+	CAR Salicylic acid, GD1a (37)
	E	4	Respiratory tract	low	+
F	40, 41	GI	low	unknown	CAR
G	52	GI		unknown	unknown

\*GI=Gastrointestinal

HAdV is highly prevalent in human populations and causes in most cases asymptomatic infections. Most known HAdV species circulate globally, but the most prevalent circulating types differ between countries or geographic regions, and they change over time (Ampuero *et al.*, 2012; Ishiko *et al.*, 2008; Lin *et al.*, 2004). The HAdV species and types that are most commonly reported to be associated with human diseases worldwide are HAdV-C1, -C2, -C5, -B3, -B7, -B21, -E4, and -F41 (Barrero *et al.*, 2012; Guo *et al.*, 2012; Qurei *et al.*, 2012; Ylihärsilä *et al.*, 2013). Whereas in immunocompromised patients the types HAdV-C1, -C2, -C5, -A12, -A31, -B3, -B11, -B16, -B34, and -B35 are the most commonly reported, being species C predominant (Leen & Rooney, 2005; Lion *et al.*, 2010; Madisch *et al.*, 2006). Among immunocompetent individuals HAdV epidemics are observed in winter and early spring, but infections in immunocompromised patients are revealed throughout the year. This indicates reactivation of HAdV from a persistent state rather than from a newly acquired infection. Non-infectious persistent HAdV has been found in lymphocytes from tonsils and adenoids (Garnett *et al.*, 2002; Garnett *et al.*, 2009; Roy *et al.*, 2011). It is thought that persistent HAdV might reactivate in immunosuppressed patients as a consequence of their compromised immune system; however, the mechanisms driving this reactivation are still unknown. Epidemiological data indicate that 80% of children have suffered by 5 years of age a primary infection, usually followed by development of humoral immunity (Ison, 2006; Mitchell *et al.*, 2000). The infection of immunocompetent hosts is mostly mild, self-limiting and highly contagious but there were also reports of severe and even fatal cases of infection (Carr *et al.*, 2011; Savón *et al.*, 2008; Siminovich & Murtagh, 2011). Infections may cause local outbreaks with severe courses that can develop into a lethal outcome even in immunocompetent individuals (Alharbi *et al.*, 2012; Berciaud *et al.*, 2012; Chen *et al.*, 2013; Lewis *et al.*, 2009; Savón *et al.*, 2008).

Adenoviruses play a particularly important role in patients with strongly impaired immune responses, such as AIDS patients or hematopoietic stem cell transplantation recipients (HSCT). In those patients, adenoviral infections are associated with high morbidity and mortality rates (Lion *et al.*, 2003; Lion *et al.*, 2010).

Currently, there is no effective treatment for HAdV infections, only general antiviral agents, such as ribavirin and cidofovir, are administered to treat severe HAdV infections, which in most cases are not effective and very toxic (Ganapathi *et al.*, 2016; Gavin P. J., 2002). From those two antivirals, cidofovir has been shown reliable efficacy (Ljungman *et al.*, 2003). However, the main disadvantage is its low bioavailability with >90% of non-metabolized product excreted in urine (Cundy, 1999). Cidofovir also accumulates intracellularly and leads to substantial tubular necrosis in the kidneys (Safrin *et al.*, 1997). Current treatment guidelines suggest administration of low doses as a preemptive treatment to stabilize viral load while waiting for T cell reconstitution after adoptive transfer in HAdV-specific T cell therapy (Lindemans *et al.*, 2010). The capacity of cidofovir to clear adenoviral infection alone is limited, resulting in a significant mortality (Robin *et al.*, 2007; Symeonidis *et al.*, 2007). In both, immunocompetent and immunocompromised patients, sequential or concomitant infections with different HAdV types from the same or different species have been observed (Lion, 2014) leading to the assumption that recombination of different HAdV can take place. This has been confirmed by genome sequencing and bioinformatics within genomes of HAdV species A, B, and D, particularly within the penton base, hexon and fiber genes (Lukashev *et al.*, 2008; Robinson *et al.*, 2009; Robinson *et al.*, 2011; Walsh *et al.*, 2009). Especially HAdV-D genomes seem to recombine more frequently than other species and some of the currently known HAdV-D types emerged via homologous recombination (HR) between hexon and fiber coding regions (Lukashev *et al.*, 2008; Matsushima *et al.*, 2013; Robinson *et al.*, 2013).

### **1.1.3 Structure and genome organization**

Human mastadenoviruses are large non-enveloped viruses with an icosahedral capsid of ~80-110 nm that harbors nine structural proteins (Figure 3). The adenoviral genome consists of a linear double-stranded (ds) DNA of 26-45 kDa in size, flanked by inverted terminal repeats of 43-369 bp (Chiocca *et al.*, 1996; Sprengel *et al.*, 1994). The virus-encoded terminal protein (TP) is covalently attached to the 5'-end of each strand, serving as primer for the initiation of viral DNA replication (Pronk *et al.*, 1992; Rux & Burnett, 2004; Tamanoi & Stillman, 1982). Furthermore, the viral DNA genome is tightly complexed within the

virion with arginine-rich 'core' proteins that interact with and condense the viral genome for efficient packaging (Russell, 1969). The core proteins comprise: the highly basic protein VII (pVII), which condenses the viral genome into repetitive nucleoprotein complexes assuming to have homologous functions to cellular histones (Mirza & Weber, 1982; Mirza & Weber, 1981; Rux & Burnett, 2004; San Martin & Burnett, 2003); a small peptide termed  $\mu$  which is poorly investigated but is thought to have similar function as protein VII (Anderson *et al.*, 1989; Murray *et al.*, 2001); and protein V (pV) that link the core of the virion to the capsid via interaction with protein VI and the penton base (Everitt *et al.*, 1975; Matthews & Russell, 1998). The icosahedral capsid consists of 252 structural units (capsomeres), including 240 trimeric hexon (II) proteins forming the faces and 12 penton (III) proteins located at the vertices. Each penton is associated with a protruding fiber protein (spikes) thereby forming a unit to mediate the receptor-coordinated cell adsorption and internalization of the virus.

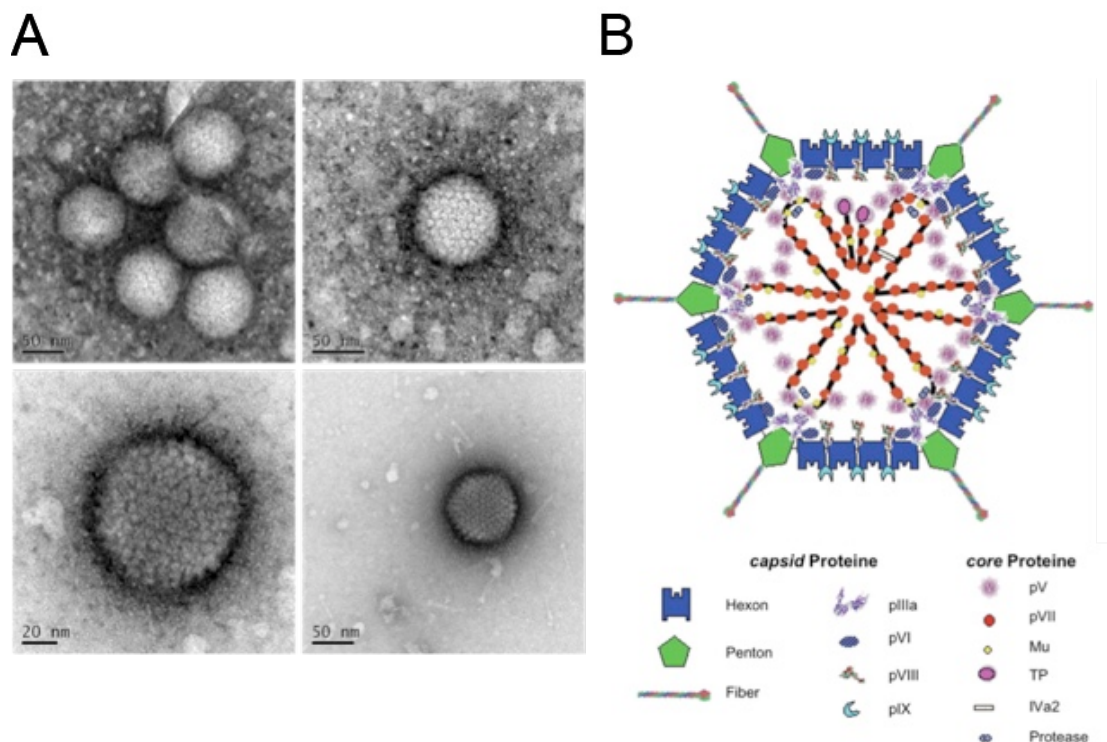


**Figure 3: Electron microscopic images and schematic representation of HAdV-C5.**

The electron microscope images (A) illustrate the icosahedral structure of adenoviral particle as well as the sub-structuration in multiple capsomeres (Department of Electron Microscopy, Heinrich Pette Institute, Leibniz Institute for Experimental Virology, Hamburg). Virion organization of a HAdV-C5 particle, including core and capsid proteins (B) (Russell, 2009; Stewart *et al.*, 1993).

Further, proteins IIIa, VI, VIII, and IX associate with the internal or external surfaces of the capsid (Liu *et al.*, 2010; Philipson, 1983), and serve as the ‘cement’ between individual hexons (Furcinitti *et al.*, 1989; Pérez-Berná *et al.*, 2009; Stewart *et al.*, 1991), and hexons and pentons (Liu *et al.*, 2010; Stewart *et al.*, 1993), respectively.

The most studied HAdV types are 2 and 5 from species C. Their genome organization is highly conserved and is divided into three groups of transcripts including early, intermediate and late transcriptional units (Figure 4). DNA strands have inverted terminal repeats serving as replication origins during viral DNA replication (Berk, 2007). There are several cis-acting packaging sequences between the left inverted terminal repeat and the first coding region (E1A), which are essential for proper encapsidation of the viral genome (Gräble & Hearing, 1992; Hearing *et al.*, 1987). Viral messenger RNAs (mRNAs) were first mapped by hybridization with enzyme-digested viral DNA fragments (Sharp *et al.*, 1975) and later confirmed by other techniques (Berk & Sharp, 1977; Chow *et al.*, 2000; Wilson *et al.*, 1979). The results show that the adenoviral genome comprises a total of nine transcription units encoding approximately 40 regulatory and structural proteins as well as two non-coding RNAs (virus-associated RNAs, VA-RNAs). Individual promoters control the expression of each gene in the early group, which includes the first five transcription units, E1, E2A, E2B, E3 and E4, respectively. The major late promoter controls the expression of five late transcription units: L1, L2, L3, L4, L5. Additionally, pIX, Iva, and VA RNAI and VA RNAII transcripts are transcribed from their own promoters.

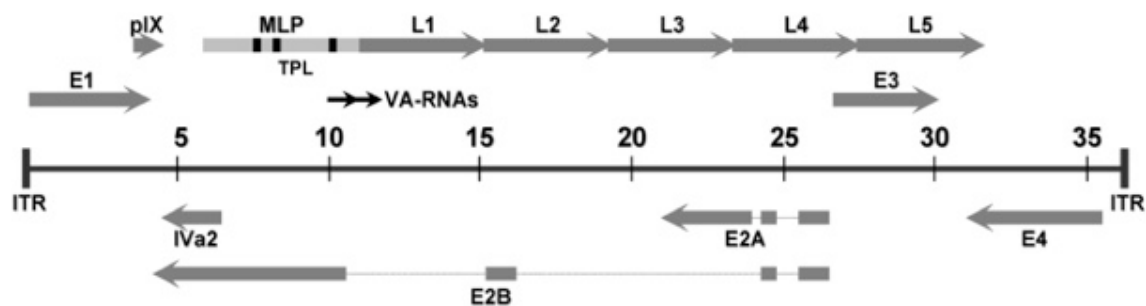


**Figure 4: Genome organization of HAdV-C5.**

The genome is represented as map units (mu) from the 5' end of the rightward strand. Arrows illustrate the organization and transcriptional direction of early (E1, E2A, E2B, E3, E4), delayed (IX, IVa2) and late (L1-L5, MLTU) transcription units on both DNA strands in relation to the 35,9 kbp DNA genome. The genome is transcribed primarily by polymerase II. The units L1-L5 are expressed under the control of the major late promoter (MLP). In addition, two virus-associated RNA (VA-RNA) are transcribed by polymerase III, Pol-Polymerase; ITR inverted terminal repeat; VA-RNA-Virus-associated RNA (White, 2012).

**1.2 Life cycle of Human mastadenoviruses**

Lytic HAdV infections occur in a wide range of cell types *in vivo*, generally, in post-mitotic resting cells, such as differentiated epithelial cells of the respiratory/gastrointestinal tract. Furthermore, several tumor and primary cell lines can be infected in tissue culture. However, infection of animal cells, in particular rodent cells, results in an abortive infection (Liebermann *et al.*, 1996). The adenoviral replicative cycle is divided into two major phases termed early and late, and is distinguished by the onset of viral DNA replication. The early phase comprises adsorption, particle disassembling and early gene expression, whereas the late phase is initiated by the viral DNA replication, late viral gene expression, virus progeny production and viral egress.

Except of species B, all HAdVs bind to the coxsackie-and-adenovirus-receptor (CAR) via their knob-domain of the fiber protein (Roelvink *et al.*, 1998). Additional interaction with integrin  $\alpha\beta1$ ,  $\alpha\beta3$  and  $\alpha\beta5$  promotes virus internalization (Li *et al.*, 1998; Wickham *et al.*, 1993). Viral particles enter the cell via receptor-mediated endocytosis. Subsequent endosome acidification partially disrupts the viral particles, enabling their entry into the cytosol. The viral DNA/Core complex is subsequently imported along microtubules to the microtubule organizing centers (MTOC) adjacent to the nucleus (Bremner *et al.*, 2009; Leopold *et al.*, 2000). Once approaching the MTOC, the nuclear export factor chromosome region maintenance 1 (CRM1), or an associated factor, enables the transition from the microtubule to the nuclear pore complex (NPC) (Strunze *et al.*, 2005). The early phase of adenoviral productive infection starts with entry of the genome into the nucleus and it is initiated by transcription/expression of the "immediate early" gene E1A (Avvakumov *et al.*, 2002a; Avvakumov *et al.*, 2002b; Moran *et al.*, 1986; Schaeper *et al.*, 1998).

Subsequently, E1A induces transcription of E1B and E4 mRNAs, which are alternatively spliced and then translated into the viral early regulatory proteins. The L1-52/55K protein from the major late transcription unit MLTU is also expressed exclusively in the early phase of infection, although at low levels (Akusjarvi & Persson, 1981; Nevins & Wilson, 1981; Shaw & Ziff, 1980). These proteins exert multifunctional roles and establish an optimal environment for virus replication.

The late phase of viral infection begins with the onset of DNA replication and activation of the major late promoter (MLP), followed by production of late mRNAs, controlling the expression of around 15 MLTU products via alternative splicing and polyadenylation (Nevins & Wilson, 1981; Shaw & Ziff, 1980). These result in mRNAs (L1-L5) that contain a common 5'-non-coding sequence of 201 nucleotides (tripartite leader; TPL), which mainly encoding structural, core and capsid proteins. In order to facilitate the production of the full set of MLTU mRNAs, L4-22K and L4-33K need to be expressed as they mediate transcriptional and posttranscriptional changes of MLTU (Farley *et al.*, 2004; Morris & Leppard, 2009; Törmänen *et al.*, 2006). Hence, those proteins have their own promoter to regulate MLP activity (Morris *et al.*, 2010). Further, IVa2 is needed to activate MLTU (Lutz & Kedinger, 1996; Tribouley *et al.*, 1994) or to cooperate with L4-22K and/or L4-33K (Ali *et al.*, 2007; Morris & Leppard, 2009; Ostapchuk *et al.*, 2006). Host mRNA transport and translation pathways are shut-off during the late phase of infection. However, viral late mRNAs are efficiently synthesized, transported to the cytoplasm and translated. The final step of the HAdV life cycle comprises viral DNA packaging/encapsidation in the nucleus, and it is regulated by late (L4-100K, -33K, -22K) and early regulatory (E1B-55K, E4orf6, E2A) proteins. After approximately 24-36 hours, the viral life cycle is completed and up to  $1 \times 10^4$  viral particles are released upon host cell lysis (Shenk, 2001)

### **1.3 HAdV-C5 early regulatory proteins**

#### **1.3.1 Early region 1**

E1A is the first transcription unit being transcribed in the immediate early phase of infection. The expression of E1A is facilitated by the HAdV capsid

protein pVI (Schreiner *et al.*, 2012a). Alternative splicing of the primary E1A transcript yields in five mRNAs, which in HAdV-C5 have the sedimentation coefficients of 13S, 12S, 11S, 10S and 9S (Stephens & Harlow, 1987; Ulfendahl *et al.*, 1987). They encode for the 289 residues (R), 243R, 217R, 171R and 55R proteins. At late stages of infection, the splicing preferences switch through temporal changes in splice site usage to the 9S mRNA product, whereas 11S and 10S mRNA species are less abundant (Stephens & Harlow, 1987; Ulfendahl *et al.*, 1987).

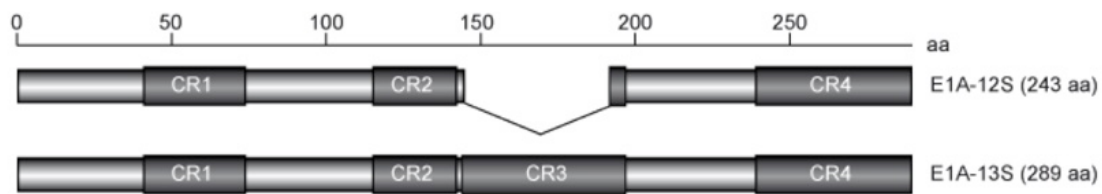


**Figure 5: Schematic domain structure of HAdV-C5 E1A-13S/12S.**

Schematic linear representation of E1A-13S/12S domain structure with conserved regions (Pelka *et al.*, 2008). For more detailed explanation/references see text. Abbr.: CR: *conserved region*.

In contrast, the protein products 289R (13S) and 243R (12S) from E1A are immediately expressed upon entry of the viral genome into the host cell nucleus. The two major E1A products harbor four conserved regions (CR1-CR4), separated by non-conserved domains (Kimelman *et al.*, 1985; van Ormondt *et al.*, 1980) (Figure 5). The largest E1A protein 13S is needed for transcriptional activation of the four early adenoviral transcription units (E1-E4), by recruitment of and association with cellular transcription factors that, in turn, binds to the early adenoviral promoters (Berk *et al.*, 1979; Jones & Shenk, 1979; Liu & Green, 1994; Webster & Ricciardi, 1991). Further, it was found that E1A-13S can also bind to the cellular transcriptional co-activators CREB binding proteins (p300/CBP) (Arany *et al.*, 1995; Avantaggiati *et al.*, 1996; Eckner *et al.*, 1994; Lundblad *et al.*, 1995; Somasundaram & El-Deiry, 1997; Yang *et al.*, 1996) and to MED23, a subunit of the Mediator complex (Stevens, 2002), to activate transcription *in vitro*.

Besides, both 13S and 12S E1As are able to promote cell cycle entry into S-phase in infected cells (Braithwaite *et al.*, 1983; Spindler *et al.*, 1984; Zerler *et al.*, 1987). This function of E1A, together with the activity of E1B or activated RAS, is sufficient to transform primary rodent cells (Howe *et al.*, 1990; Spindler *et al.*,

1984; Stein *et al.*, 1990). Furthermore, E1A interacts with the so-called “pocket proteins”, which include the cellular retinoblastoma protein (pRB) (Buchkovich *et al.*, 1990; Dyson *et al.*, 1989; Giordano *et al.*, 1991) and the RB-related proteins, p107 and p130 (Barbeau *et al.*, 1992; Classon & Dyson, 2001; Dyson *et al.*, 1992). Additionally, further transcriptional regulators such as PCAF, CtBP, p21<sup>Cip1/Waf1</sup>, p27<sup>Kip1</sup>, DYRKs, p400 and TRRAP (Ferrari *et al.*, 2009; Ferrari *et al.*, 2008; Frisch & Mymryk, 2002) enable E1A to dynamically and temporally modulate approximately 70% of all gene promoters (Ferrari *et al.*, 2009; Ferrari *et al.*, 2008). A further host cell regulatory role of E1A is the attenuation of p53 function in two ways. First, acetylation is prevented followed by inhibition of p53. Second, the inhibition of the interaction between the transcription factor SP1 and the p21 promoter, prevents p21 up-regulation and thereby inhibits downstream proliferation regulator of p53 (Savelyeva & Dobbelstein, 2011). Regarding E1A function, expression of E1A alone induces apoptosis in host cells (Debbas & White, 1993; Rao *et al.*, 1992; Yageta *et al.*, 1999). On the one hand, E1A interferes with proteasome function, which stabilizes p53 (Lowe & Ruley, 1993; Zhang *et al.*, 2005). On the other hand, E1A triggers apoptosis in a p53-independent mechanism by inducing proteasomal degradation of a B-cell leukemia/lymphoma 2 (BCL-2) family member, the myeloid leukaemia sequence 1 (MCL-1) protein, leading to the release of pro-apoptotic BCL2-Antagonist/Killer (BAK) and the initiation of apoptosis (Cuconati, 2003; Cuconati & White, 2002). In order to achieve proper viral replication, the induction of apoptosis by E1A has to be counteracted, as early apoptosis of the host cell would prevent the completion of the viral life cycle. Therefore, a multitude of HAAdV proteins act to prevent p53-dependent and independent apoptosis, including products of the E1B transcriptional unit.

The major gene products of the E1B region are the E1B-19K and E1B-55K proteins (Figure 6). Both are expressed from overlapping reading frames of the 2.28 kb E1B-mRNA. E1B-55K and E1B-19K proteins suppress p53-dependent and independent cell cycle arrest, and apoptosis induced by E1A (Debbas & White, 1993). E1B-19K is a functional homologue of the cellular anti-apoptotic protein BCL-2 (Rao *et al.*, 1992) and inhibits the initiation of the apoptotic cascade by binding pro-apoptotic cellular proteins like BAK and BAX (Cuconati, 2003; Cuconati & White, 2002). Moreover, E1B-19K prevents p53-

mediated apoptosis induced by TNF- $\alpha$  and Fas ligand by the same mechanism (Debbas & White, 1993).

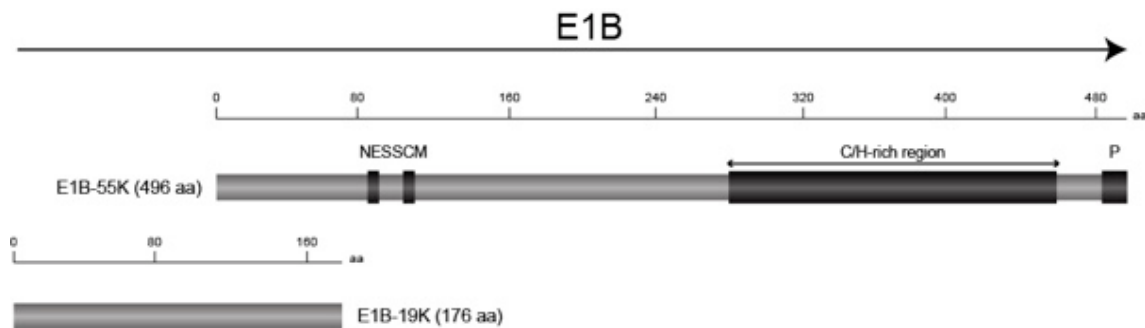


**Figure 6: Schematic domain structure of HAAdV-C5 E1B-55K/19K.**

Schematic linear representation of E1B-55K/19K domain structure. The line on the top represents the transcriptional direction. The second line denotes the number of amino acids (aa). NES: nuclear export signal; SCM: SUMO conjugation motif; C/H-rich region: cysteine/histidine-rich region.

E1B-55K sequesters p53 in perinuclear bodies, also called aggresomes (Liu *et al.*, 2005b; Sarnow *et al.*, 1982; Zantema *et al.*, 1985), which are subcellular structures formed at the MTOC in response to misfolded proteins (Garcia-Mata *et al.*, 2002; Kopito, 2000). In the nucleus, E1B-55K interacts with p53 to prevent p53-mediated transcriptional activation (Martin & Berk, 1999; Querido *et al.*, 1997; Teodoro & Branton, 1997; Yew & Berk, 1992). Furthermore, E1B-55K acts as an E3 small ubiquitin-like modifier 1 (SUMO1) ligase of p53. This function leads to SUMOylation and following sequestration of p53 in nuclear promyelocytic leukemia protein nuclear bodies (PML-NBs) supporting p53 nuclear export (Pennella *et al.*, 2010). P53 suppression is also mediated by preventing its acetylation by p300/CBP-associated factor (PCAF) (Liu *et al.*, 2000). Acetylation of p53 promotes high-affinity binding to DNA, which enhances the transcription of p53-targeted promoters. Interaction of E1B-55K with HDAC complexes suppresses p53-dependent transcription (Punga & Akusjarvi, 2000).

In order to counteract the DNA damage response, E1B-55K forms an ubiquitin ligase complex with the HAAdV E4 open reading frame 6 (E4orf6) protein (Sarnow *et al.*, 1984) and the cellular proteins elongins B and C, cullin 5 and Rbx-1 (Yew *et al.*, 1994). E1B-55K serves as the substrate recognition domain, while E4orf6 binds elongin C (Blanchette *et al.*, 2004b). This complex formed by

viral and cellular proteins promotes ubiquitination and proteasomal degradation of proteins that are part of the DNA damage response, including p53 (Harada *et al.*, 2002; Querido *et al.*, 2001) and HIV-Tat interacting protein (Tip60) (Gupta *et al.*, 2012), the MRN complex (Stracker *et al.*, 2002a), which is part of the DNA double-strand break repair (Carson *et al.*, 2003; D'Amours & Jackson, 2002; Petrini & Stracker, 2003; Stracker *et al.*, 2002a; van den Bosch *et al.*, 2003), DNA ligases IV (Baker *et al.*, 2007) and chromatin remodeling proteins like ATRX (Schreiner *et al.*, 2013a) and SPOC1 (Survival-time associated PHD protein in ovarian cancer 1) (Schreiner *et al.*, 2013b). The cellular MRN complex promotes concatemerization of viral genomes by non-homologous end-joining (NHEJ) (Boyer *et al.*, 1999; Evans & Hearing, 2005; Weiden & Ginsberg, 1994). PML-NBs are multi-protein complexes, which are present in nearly all human cell lines (Chan *et al.*, 1997). These complexes are associated with currently 166 known PML-associated proteins that are important for multiple cellular processes, like proteins of the DNA repair machinery (e. g. Mre11, Rad50), cell cycle regulation (e. g. pRb, p53), telomere metabolism (e. g. TRF), epigenetic regulation (e. g. HDACs) and apoptosis (e. g. Daxx) (Van Damme *et al.*, 2010). The viral protein E4orf3 targets the PML-NBs and re-organizes them into nuclear tracks, while E4orf6 interacts with MRN within the modified PML-NBs (Carvalho *et al.*, 1995; Doucas & Evans, 1996; Evans & Hearing, 2003). Then, a complex of E1B-55K, E4orf6, E4orf3 and MRN is exported to the cytoplasmic aggresomes, where degradation of ubiquitinated MRN complex proteins takes place (Liu *et al.*, 2005b).

### **1.3.2 Early region 2**

The HAdV early region 2 encoded proteins are crucial for viral replication and comprises the viral DNA binding protein (DBP; E2A), the viral DNA polymerase (E2B) and the precursor of the terminal protein (pTP) (de Jong *et al.*, 2003). The E2 gene expression is driven from two different promoters, whereas the E2 early promoter is activated early after infection. However, at intermediate time of infection, E2 gene transcription is controlled by the E2 late promoter (Swaminathan & Thimmapaya, 1996). This switch is regulated by the adenovirus E1A protein that activates the E2 early but represses the E2 late

promoter (Guilfoyle *et al.*, 1985). The interplay between these viral proteins and cellular proteins, including octamer transcription factor 1 (Oct-1) and NF- $\kappa$ B, is necessary for efficient virus replication (de Jong *et al.*, 2003).

### 1.3.3 Early region 3

The early region 3 of HAdV transcript is alternatively spliced resulting in products of at least four mRNAs. They encode for a 19-kDa glycoprotein (gp19) and E3 10.4K, 14.5K, and 14.7K. The early transcription unit E3 of HAdV is not required for viral replication in tissue culture and for *in vivo* infection in cotton rat (Ginsberg *et al.*, 1991). Nevertheless, it is present in all HAdV and thus it is believed to have key functions in regulating virus-host interactions (Burgert & Blusch, 2000; Mahr & Gooding, 1999; Wold *et al.*, 1995). This might provide the basis for immune evasion and establishment of persistent infections (Burgert & Blusch, 2000; Burgert *et al.*, 2002; Mahr & Gooding, 1999; Wold *et al.*, 1995). Intriguingly, there are specific variations of size and composition of the E3 regions in different adenovirus subgenera (Figure 7). The so-called E3A region comprising 10.4K, 14.5K and 14.7K genes, is the region with the highest variability within the HAdV genome of different subgenera (Bailey & Mautner, 1994). Therefore, it is reasonable to assume that the E3 region contributes to subgenus-specific pathogenesis (Table 1), since subgenus-specific differences in pathogenesis cannot be explained by differential utilization of cell surface receptors for virus adsorption (Burgert & Blusch, 2000). Furthermore, most proteins from the E3 region are transmembrane proteins, which localize to the ER, the Golgi/TGN, the plasma and nuclear membrane (Burgert & Blusch, 2000; Wold *et al.*, 1995). This property is unique for E3 region proteins as it is the only known adenoviral transcription unit encoding for transmembrane proteins.

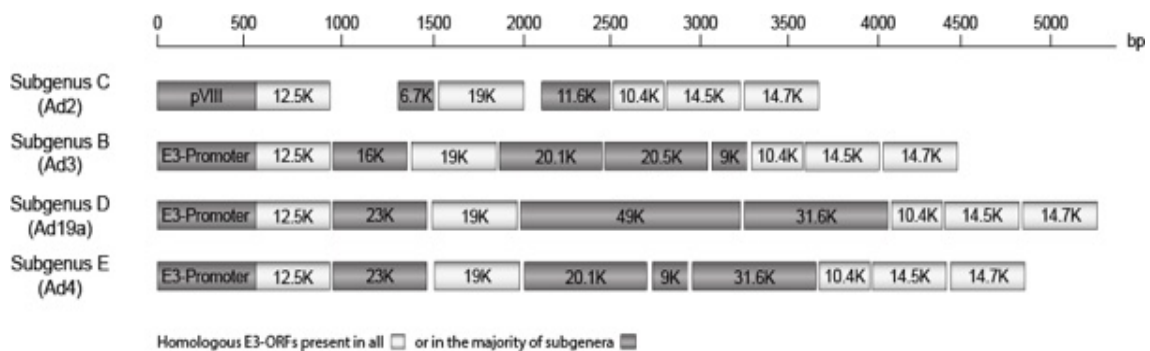


**Figure 7: Organization of the E3 region in different HAdV-C5 subgenera.**

The line on top denotes the size in base pairs and ORFs are indicated as bars and drawn to scale. The size or name of common ORFs is only given once. The shading code is depicted below the figure (adapted from (Windheim & Burgert, 2002)).

In order to exert immunomodulatory functions upon HAdV infection, membrane integration of proteins from the E3 region seems to be most critical. Hence, lytic attack of the cellular defense system is thereby prevented (Burgert *et al.*, 2002). The gp19 protein downregulates class I major histocompatibility complex (MHC)-mediated antigen presentation to cytotoxic T-lymphocytes (CTL) by interacting with the heavy chain of class I MHC molecule and inhibiting its transport from the ER to the cell surface (Andersson *et al.*, 1985; Burgert & Kvist, 1985) Further, gp19 prevents loading of class I MHC molecules to the transporter associated with antigen presentation (TAP) (Bennett *et al.*, 1999). The other proteins from the E3 region (10.4K, 14.5K, and 14.7K) inhibit tumor necrosis factor- $\alpha$  (TNF $\alpha$ )-induced apoptosis (Tufariello *et al.*, 1994; Wold & Gooding, 1991). Therefore, the 10.4K and 14.5K proteins act as a TNF $\alpha$ -and Fas-induced apoptosis inhibition complex (Shisler *et al.*, 1997; Tollefson *et al.*, 1996). 14.7K counteracts ligand-induced TNFR1 internalization in order to inhibit the death-inducing signaling complex (DISC). (Schneider-Brachert *et al.*, 2006). However, 14.7K does not affect TNF-induced NF- $\kappa$ B activation, which depends on recruitment of receptor-interacting protein 1 (RIP-1) and TNF receptor-associated factor 2 (TRAF-2) (Schneider-Brachert *et al.*, 2006).

### 1.3.4 Early region 4

The E4 region encodes for several proteins with a variety of important functions (Figure 8). The first protein product is E4orf1, which has been shown to have tumorigenic and transforming properties for HAdV-D9 (Javier, 1994). The putative role of E4orf1 in lytic infection may be the induction of cell quiescence in certain cell types. Recent studies have shown that E4orf1 fulfills its oncoprotein function by activating phosphatidylinositol 3-kinase (PI3K) and the cellular transcription factor Myc (Kong *et al.*, 2014; 2015). E4orf2 is a soluble cytoplasmic protein produced at early times after infection with so far unknown function (Dix & Leppard, 1995). The E4orf3/4 protein is a putative

predicted protein, based on HAdV-C2 mRNA analysis (Dix & Leppard, 1993; Virtanen *et al.*, 1984).

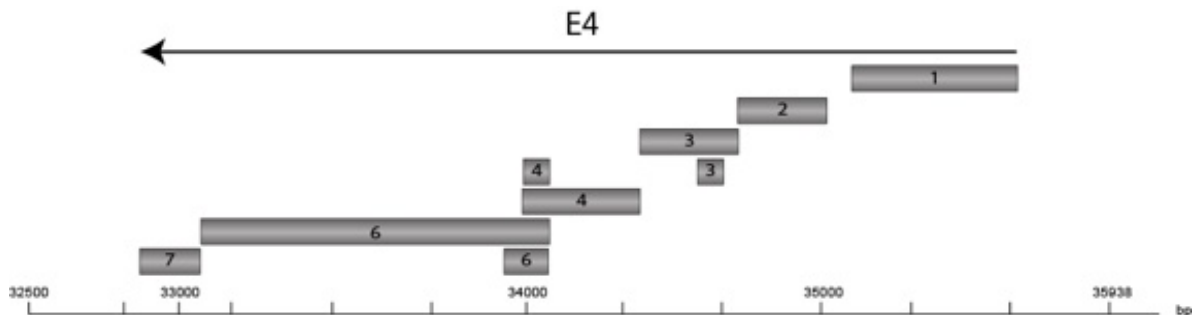


**Figure 8: E4-region proteins of HAdV-C5.**

The scheme shows the HAdV-C5 5'end genome. The line on the bottom denotes the size in base pairs. The line on top shows the length and direction of transcription of the pre-RNA. Grey bars depict the open reading frames (ORF) 1 to 6/7. The gene products of the orf 1, 2, 3, 4, 6 and 6/7 were detected in infected cells. E4orf3/4 was only shown at the mRNA level. ITR: inverted terminal repeat; P: E4-promoter; cap: starting point of the pre-RNA; Poly (A): site of polyadenylation.

However, the functions of E4orf3 and orf6 have been intensively investigated. Both proteins share partially redundant functions (Bridge & Ketner, 1989; Huang & Hearing, 1989) which are important for efficient viral replication, i.e. efficient DNA replication (Bridge *et al.*, 2003), viral late protein synthesis, shut-off of host protein synthesis, late viral mRNA transport (Nordqvist & Akusjarvi, 1990; Nordqvist *et al.*, 1994) and progeny virus production (Huang & Hearing, 1989). Furthermore, they inhibit MRN complex function independent of the E1B-55K/E4orf6 ubiquitin ligase activity (Boyer *et al.*, 1999; Shepard & Ornelles, 2004).

Transfected E4orf3 is sufficient to re-organize PML-NBs into so-called track-like structures. PML-NBs are nuclear protein aggregates with anti-viral/anti-tumor functions (Carvalho *et al.*, 1995; Doucas & Evans, 1996; Puvion-Dutilleul *et al.*, 1995). This modulation of the PML-NB is conserved among various species of HAdVs (Hoppe *et al.*, 2006), indicating that counteraction of this cellular anti-viral mechanism is important for a proper HAdV infection (Doucas *et al.*, 1996; Everett, 2001; Everett & Chelbi-Alix, 2007). Additionally, E4orf3 modulates certain transient components of the PML-NBs, such as p53, the Mre11-Rad50-NBS1 (MRN) complex of the DNA repair machinery and the transcriptional

modulator Tif1 $\alpha$  (Araujo *et al.*, 2005; Konig *et al.*, 1999; König *et al.*, 1999; Liu *et al.*, 2005a; Weiden & Ginsberg, 1994; Yondola & Hearing, 2007).

E4orf6 has an amphipathic  $\alpha$ -helix containing a nuclear localization signal (NLS) and a nuclear export signal (NES) motif that allows it to shuttle between nucleus and cytoplasm (Orlando & Ornelles, 1999; Weigel & Dobbelstein, 2000), and it can interact with p53 thereby, inhibiting its function (Dobner *et al.*, 1996). Together with E1B-55K, E4orf6 enhances HAdV mRNA transport leading to cytoplasmic accumulation of viral mRNAs and subsequent increase in viral late protein production (Imperiale *et al.*, 1995). Besides the function of the ubiquitin ligase complex formed by E4orf6 and E1B-55K on p53 (Sarnow *et al.*, 1984) (see chapter 1.3.2), this complex can also regulate the degradation of other cellular proteins, such as Mre11, DNA ligase IV, Bloom Helicase, Tip60, integrin  $\alpha$ 3, ATRX and SPOC1 in order to shape the cellular environment for proper viral propagation (Baker *et al.*, 2007; Blanchette *et al.*, 2004b; Dallaire *et al.*, 2009a; Gupta *et al.*, 2012; Harada *et al.*, 2002; Schreiner *et al.*, 2013a; Schreiner *et al.*, 2013b). E4orf6 with its various regulatory functions is not only important for HAdVs, but also for adeno-associated virus (AAV), a parvovirus of the genus *Dependovirus* (Samulski & Shenk, 1988). AAV needs the presence of adenoviruses or other helper viruses to undergo an efficient productive replicative life cycle. Thereby, E4orf6 induces second strand synthesis of the single stranded DNA genome of AAV that is important to be transcriptionally active (Ferrari *et al.*, 1996; Fisher, 1996).

#### **1.4 Innate viral immunity**

The innate immune response plays an important role in shaping the adaptive immune system. It is directly activated upon pathogen recognition and provides the first line of defense by generating an immediate, non-specific response against pathogen components (Karin, 2011).

A virus- or bacteria-infected cell undergoes rapid changes through pathogen modulation of cellular components as well as innate immune response activation (Karin, 2011). This is mediated by diverse families of pattern recognition receptors (PRRs) that recognize conserved structural components of pathogens also called pathogen-associated molecular patterns (PAMPs) (Kumar *et al.*, 2011; Thompson *et al.*, 2011). Those PAMPs comprise diverse classes of

molecules like lipopolysaccharides (LPS), bacterial flagellin, zymosan and nucleic acids which are rarely or never found in host cells (Lee & Kim, 2007; Takeuchi & Akira, 2010). The cell employs an array of PRRs like Toll-like receptors (TLRs), RIG-I-like receptors (RLRs), and Nod-like receptors (NLR) to recognize signs of infection (Janeway Jr & Medzhitov, 2002; Kawai & Akira, 2010; Thompson *et al.*, 2011). The diverse spatial distribution of the PRRs in the plasma membrane, endosomes, cytosol or extracellular receptors enhance their recognition capability at different stages of infection (Janeway Jr & Medzhitov, 2002; Kawai & Akira, 2010; Kumar *et al.*, 2011).

So far, ten different TLRs are known (TLR1-10) and stimulation of them triggers activation of nuclear factor kappaB (NF- $\kappa$ B) (Doyle & O'Neill, 2006; Medzhitov, 2001).

Once distinct ligands bind their cellular receptors, specific signal transduction pathways are activated, leading to transcription of numerous cytokines and chemokines as well as type-1 interferon (IFN) genes (Medzhitov, 2007).

The most important transcription factors activated by PRRs are NF- $\kappa$ B, activating protein-1 (AP-1) and interferon regulatory factors (IRFs) (Kawai & Akira, 2006). IRFs are main regulators of type-1 IFN, comprising IFN $\beta$  and multiple IFN $\alpha$  variants (Honda *et al.*, 2006). Secreted IFNs bind to type-1 IFN receptor activating the signal transducer and activator of transcription 1 (STAT1) and STAT2, and the formation of ISGF3, leading to stimulation of a broader spectrum of IFN-responsive genes (McCaffrey *et al.*, 2008).

#### **1.4.1 Immune response upon HAdV-C5 infection**

Immune response is activated early upon interaction of the adenoviral virions with host cell components (Reich *et al.*, 1988) (Figure 9). The first event of immune response is triggered by the adenoviral fiber binding with the CAR (Tamanini *et al.*, 2006). Hence, downstream signaling of extracellular signal-regulated kinases (ERK1/2), c-Jun N-terminal kinases (JNK) and mitogen-activated protein kinase (MAPK) is induced, followed by NF- $\kappa$ B activation and the up-regulation of chemokines (Thaci *et al.*, 2011). However, ERK1/2 pathway activation is also linked to the production of IL-10 that induces Th differentiation into Th2-type that is known to produce and release anti-inflammatory cytokines such as IL-4, IL-5, IL-9, and IL-13 (Mosmann *et al.*,

2009). Furthermore, IL-10 is a negative regulator of inflammation to prevent tissue damage (Bosschaerts *et al.*, 2010; Guilliams *et al.*, 2009; Haddad *et al.*, 2003; Romagnani, 2006). IFN-responsive genes are activated six hours after administration of “first-generation” adenoviral vector lacking E1 and E3 region or a “gutless” adenoviral vector. These genes are induced by a primary IFN response and a secondary response following autocrine and paracrine detection of IFNs (Fejer *et al.*, 2008; McCaffrey *et al.*, 2008).

However, during wild type HAdV infection, interferon (IFN) production is suppressed by the immediate-early protein E1A (Anderson & Fennie, 1987; Leonard & Sen, 1996; 1997; Reich *et al.*, 1988). Besides, E1A inhibits the transcriptional co-activator function of the CREB binding proteins CBP/p300 by directly competing with nuclear STATs for CBP/p300 binding (Bhattacharya *et al.*, 1996; Zhang *et al.*, 1996). Additionally, E1A competes with IFN response factor 3 (IRF-3) for binding to CBP/p300 interfering with INF $\alpha$  and IFN $\beta$  induction (Juang *et al.*, 1998). However, an E1A CBP/p300 binding mutant still blocks IFN $\gamma$  signaling by directly interacting with the nuclear STAT1 homodimer during infection, suggesting that other molecules, apart from CBP/p300, might be involved in the binding to STAT1 (Look *et al.*, 1998). Furthermore, E1A is able to inhibit the JAK/STAT signaling pathway, suppressing a number of IFN-responsive genes that influence the immune response (Burgert *et al.*, 2002).

The IFN response is also blocked at a later stage of infection. This is mediated by the virus-associated (VA) RNAs (Ma & Mathews, 1996), which are abundantly transcribed in the late phase of infection by RNA polymerase III (Söderlund *et al.*, 1976). The secondary structure of VA-RNA is capable of binding PKR to inhibit its activity (Kitajewski *et al.*, 1986). PKR is an ubiquitously expressed serine/threonine protein kinase that can be activated by double-stranded RNA, cytokines, growth factors and stress signals (Williams, 1999). Upon HAdV infection, VA-RNA can regulate the IFN response by preventing PKR activation thereby affecting the inflammatory response and apoptosis.

Besides regulation of IFN, HAdV infection induces TNF in the infected tissue (Ginsberg *et al.*, 1991), which is hampered by E1A, E1B and E3, as the absence of these proteins sensitized the cells to TNF-dependent lysis (Chen *et al.*, 1987;

Duerksen-Hughes *et al.*, 1989; Gooding *et al.*, 1988; Shisler *et al.*, 1996). Therefore, E1A inhibits NF- $\kappa$ B in an indirect way presumably by IKK-mediated I $\kappa$ B phosphorylation and subsequent NF- $\kappa$ B release to the nucleus to avoid TNF-induced apoptosis (Shao *et al.*, 1999). However, the way how E1A regulates NF- $\kappa$ B is diverse and seems to depend on the cell type, the phase within the HAdV life cycle, the influence of further viral gene products as well as the experimental setup (Schmitz *et al.*, 1996; Shao *et al.*, 1999; Shisler *et al.*, 1996).

Additionally, four adenovirus proteins are contributed to counteract TNF-mediated cytolysis upon infection: the E1B-19K protein (White *et al.*, 1991) and the E3 proteins, 14.7K, 10.4K and 14.5K (Wold *et al.*, 1995) (see chapter 1.3.4).

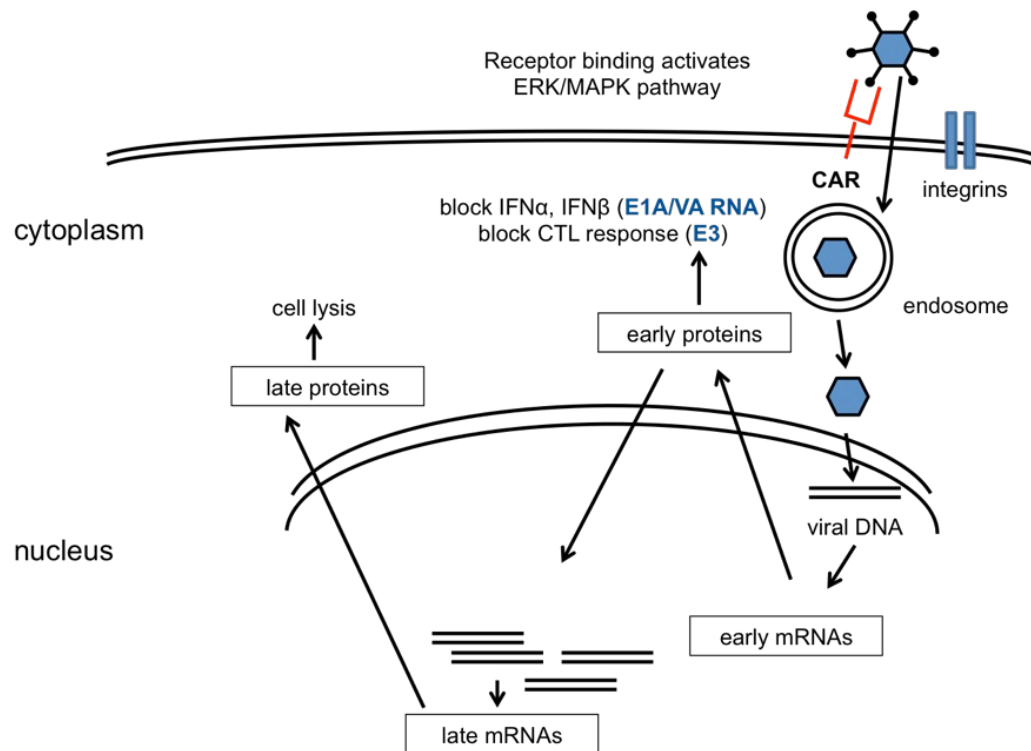


**Figure 9: Schematic representation of immune response after HAdV infection.**

Interaction of the protruding knob domain of the fiber protein with its main recognition receptor CAR on the cell surface activates the ERK/MAPK pathway. The early viral protein E1A and VA RNA have been shown to block IFN $\alpha$  and IFN $\beta$  response. Further, proteins from the E3 region block the CTL response.

### 1.4.2 NF- $\kappa$ B and I $\kappa$ B proteins

NF- $\kappa$ B transcription factor represents a group of evolutionarily conserved and structurally related proteins and belongs to the Rel protein family (Ghosh *et al.*, 1998). The large NF- $\kappa$ B family of proteins is composed by two subfamilies, namely the “NF- $\kappa$ B” proteins and the “Rel” proteins. All of these proteins share a highly conserved Rel homology domain (RHD) at its N-terminus with a length of 300 amino acids. RHD was first identified in avian reticuloendotheliosis virus (Chen *et al.*, 1981; Graef *et al.*, 2001) (Figure 10). This domain is important for mediating protein-protein interactions as well as for DNA-binding (Hayden & Ghosh, 2004). Furthermore, it contains the nuclear localization sequence (NLS) at the C-terminal end of RHD (Karin, 1999) (Figure 10).

The C-terminal transactivation domains of the Rel proteins are often not conserved across species even though the transcriptional activation is functional in a variety of species (Gilmore, 2006). So far two NF- $\kappa$ B proteins NF- $\kappa$ B1 (p50/p105) and NF- $\kappa$ B2 (p52/p100) have been described. The mature proteins p50 and p52 are first synthesized as large precursor molecules p105 and p100, respectively (Betts & Nabel, 1996; Fan & Maniatis, 1991). Both precursor proteins p105 and p100 have multiple copies of the so-called ankyrin repeat at their C-termini, which are cleaved upon maturation, and have putatively regulatory functions in the cell by forming a trimeric complex with p50/RelA or p50/RelB dimers (Dobrzanski *et al.*, 1995; Kanno *et al.*, 1994).

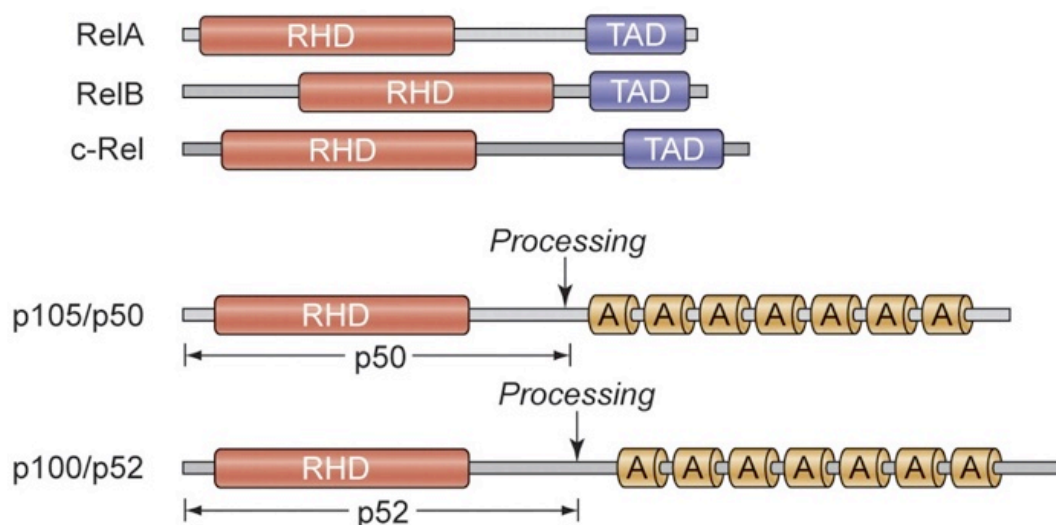


**Figure 10: Schematic representation of NF- $\kappa$ B subunits (Jost & Ruland, 2007).**

Rel proteins share highly conserved Rel homology domain (RHD) at their N-terminus which is responsible for dimerization, nuclear translocation, DNA binding and interaction with its inhibitory I $\kappa$ B proteins. At their C-termini they share a carboxy-terminal transactivation domain (TAD) initiating transcription from NF- $\kappa$ B-binding sites in target genes. A further group of NF- $\kappa$ B subunit comprises proteins with ankyrin repeats (A) at their C-terminus instead of TAD.

The NF- $\kappa$ B proteins are only transcriptionally active as a dimer, but some combinations are thought to act as inactive or repressive complexes. It has been shown that p50/p65, p50/c-rel, p65/p65, and p65/c-rel are all transcriptionally active, whereas p50 homodimer and p52 homodimer are transcriptionally repressive (Brown *et al.*, 1994; Hansen *et al.*, 1994a; Hansen *et al.*, 1994b; Kang *et al.*, 1992). The classical heterodimeric NF- $\kappa$ B transcription factor, which is usually referred to, is the abundant expressed dimer of p50 and RelA (p65), and it has been the most intensively studied dimer of the NF- $\kappa$ B pathway (Ghosh *et al.*, 1998). This heterodimer p50/p65 activates the classical NF- $\kappa$ B signaling pathway upon translocation into the nucleus (Link *et al.*, 1992; Liu *et al.*, 2015; Nolan *et al.*, 1993; Totzke *et al.*, 2006; Whiteside *et al.*, 1997; Zabel & Baeuerle, 1990) (Hoffmann *et al.*, 2006).

NF- $\kappa$ B dimers localize in their inactive state within the cytoplasm, forming a complex with members of the I $\kappa$ B (inhibitor of  $\kappa$ B) family. The family comprises I $\kappa$ B $\alpha$ , I $\kappa$ B $\beta$ , I $\kappa$ B $\epsilon$ , I $\kappa$ B $\gamma$ , I $\kappa$ B $\delta$ , BCL3 and recently described I $\kappa$ B $\zeta$  proteins with large ankyrin repeat domains (ARD) (Figure 11). These domains mediate the interaction and inactivation of NF- $\kappa$ B through masking one or both nuclear localization signals in the dimer (Chen & Greene, 2004).



**Figure 11: Schematic representation of I $\kappa$ B subunits (Jost & Ruland, 2007).**

I $\kappa$ B proteins are characterized by 6 or 7 ankyrin repeats mediating protein-protein interactions. The ankyrin repeats interact with the localization sequence of NF- $\kappa$ B proteins, which is important to keep NF- $\kappa$ B in an inactive state in the cytoplasm.

## 1.5 NF- $\kappa$ B signaling pathways

Two main signaling pathways activate NF- $\kappa$ B: the canonical pathway and the non-canonical pathway (Bonizzi & Karin, 2004). It has been shown that both pathways have different regulatory functions: the canonical pathway is mostly involved in innate immunity whereas the non-canonical pathway regulates the development of lymphoid organs and the adaptive immunity (Bonizzi & Karin, 2004; Whiteside & Israel, 1997).

### 1.5.1 The canonical NF- $\kappa$ B pathway

The canonical pathway is activated through a plethora of stimuli like pro-inflammatory cytokines, such as tumor necrosis factor- $\alpha$  (TNF $\alpha$ ) and interleukin-1 (IL-1), pathogen-associated molecular patterns (PAMPS), lipopolysaccharides (LPS), ultraviolet (UV) radiation, phorbol 12-myristate 13-acetate (PMA), ligation of the T-cell receptor (TCR), double strand RNA, reactive oxygen intermediates and the human T-cell lymphotropic virus type 1 (HTLV-1) Tax protein (Baldwin, 1996; Ghosh *et al.*, 1998). This pathway is characterized by its rapid activation upon stimuli exposure, as *de novo* protein synthesis is not required to fully activate the pathway. Upon activation, receptors coupled with myeloid differentiation primary response gene 88 protein (MyD88) (IL-1R and all TLRs except of TLR3) or with the TIR-domain-containing adapter-inducing interferon- $\beta$  protein (TRIF) (TLR3 and TLR4) activate the first step in the cascade resulting in stepwise activation of downstream proteins by posttranslational modifications such as ubiquitinylation and phosphorylation. Hence, activation of the serine/threonine kinase complex formed by I-kappa-B Kinase-alpha (IKK $\alpha$ ) (catalytic subunit), I-kappa-B Kinase-beta (IKK $\beta$ ) and I-kappa-B Kinase-gamma (IKK $\gamma$ ) (regulatory subunit), also called NF- $\kappa$ B essential modifier (NEMO) induces phosphorylation of inhibitor of kappa B (I $\kappa$ B $\alpha$ ) at serine-32 and serine-36 (Adli *et al.*, 2010; Li *et al.*, 2002) followed by subsequent polyubiquitinylation and proteasomal degradation (DiDonato *et al.*, 1996). Thereby, the signal transduction of the canonical NF- $\kappa$ B pathway mostly depends on the IKK subunit NEMO (Rudolph *et al.*, 2000). Additionally, the IKK $\beta$  is important for the phosphorylation of I $\kappa$ B $\alpha$ . Some cases are known in which IKK $\alpha$  is also

needed for the phosphorylation of I $\kappa$ B $\alpha$  (Adli *et al.*, 2010; Li *et al.*, 2002). Proteasomal degradation of I $\kappa$ B $\alpha$  uncovers the NLS of the p50/p65 dimer followed by its nuclear translocation, binding to consensus NF- $\kappa$ B binding motifs and subsequent transcription of NF- $\kappa$ B dependent genes (Hayden & Ghosh, 2011).

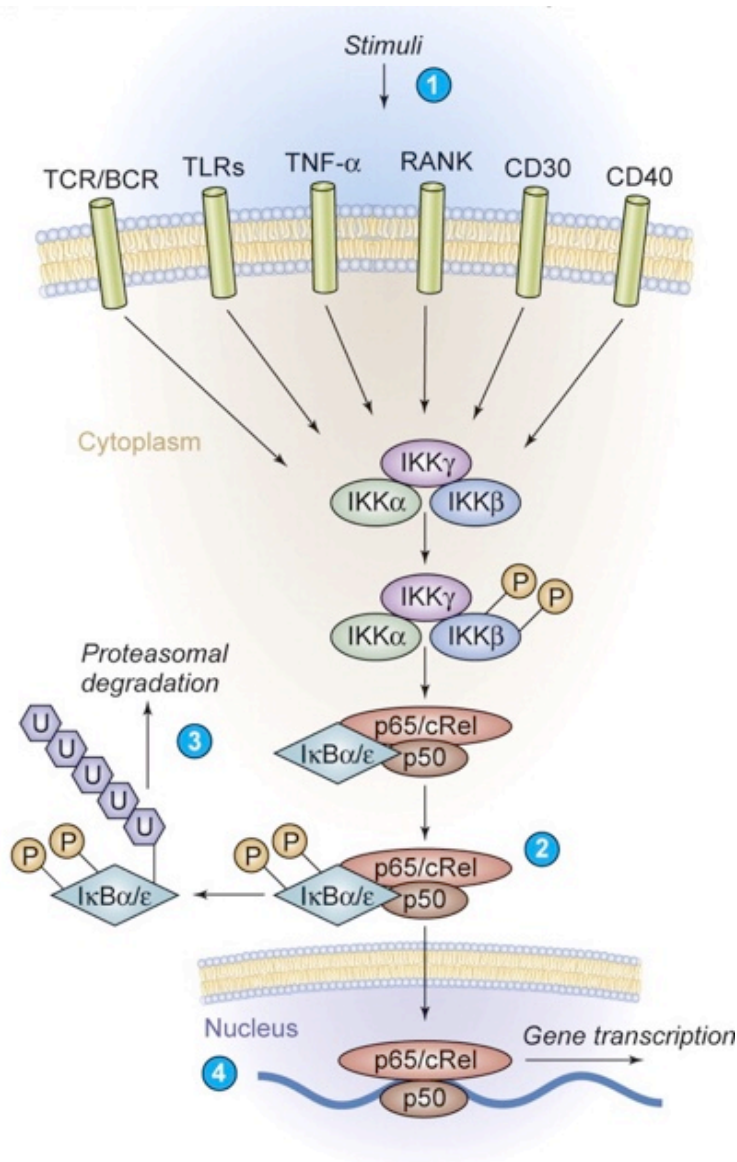


**Figure 12: Activation of the canonical NF- $\kappa$ B pathway (Jost & Ruland, 2007).**

A wide range of stimuli activates the canonical pathway. Inducers are proinflammatory cytokines such as IL-1, TNF $\alpha$ , or pathogen-associated molecular patterns (PAMPs) that bind to TLRs (1), the antigen receptors TCR/BCR, or lymphocyte coreceptors such as CD40, CD30, or receptor activator of NF- $\kappa$ B (RANK). (2) Activated IKK phosphorylates I $\kappa$ B proteins, (3) induces I $\kappa$ B polyubiquitinylation and subsequent degradation. The cytoplasmic NF- $\kappa$ B is free to translocate into the nucleus, (4) where inflammatory genes are activated.

The NF- $\kappa$ B dependent proteins regulate a large number of pro-inflammatory cytokines and acute phase proteins such as TNF $\alpha$ , IL-1, IL-2, IL-6, interferon  $\gamma$  (IFN $\gamma$ ) and C3 complement, thus playing various roles in immunity and inflammation, as well as the expression of cell adhesion molecules, like vascular cell adhesion molecule-1 (VCAM-1) and intercellular adhesion molecule-1 (ICAM-1) (Baldwin, 1996; Ghosh *et al.*, 1998). Further, NF- $\kappa$ B dependent proteins are important for expression of proteins that are involved in anti-apoptotic processes such as inhibitor of apoptosis (IAP) proteins, cellular FLICE inhibitory protein (c-FLIP) and Bcl-2 (Delhalle *et al.*, 2004). A further NF- $\kappa$ B induced gene is its inhibitor I $\kappa$ B $\alpha$ , also disrupting the transcription factor from the DNA and relocalizes it back into the cytoplasm (Sun *et al.*, 1993; Zabel & Baeuerle, 1990). A permanent activation of the NF- $\kappa$ B signaling is inhibited by this negative feedback loop or by deubiquitinylation of NEMO through the deubiquitinases and NF- $\kappa$ B target genes A20, and the cylindromatosis (CYLD) (Häcker & Karin, 2006). In an acute inflammation the equilibrium between cytoplasmic and nuclear NF- $\kappa$ B levels returns to its initial state. However, chronic long-lasting and elevated chronic inflammation, can contribute to cancers and tumor progression (Diamant & Dikstein, 2013; Hoesel & Schmid, 2013).

The lymphotoxin- $\beta$  receptors (LT $\beta$ R), a subgroup of the TNFR-family, activate both the canonical and the non-canonical NF- $\kappa$ B pathway (Dejardin *et al.*, 2002; Müller & Siebenlist, 2003).

### **1.5.2 The non-canonical NF- $\kappa$ B pathway**

In contrast to the canonical pathway, this alternative pathway is activated by a rather limited number of TNFR family members, comprising BAFF-R and CD40 (on B cells) and LT $\beta$ R (on stromal cells) (Claudio *et al.*, 2002; Coope *et al.*, 2002a; Coope *et al.*, 2002b; Dejardin *et al.*, 2002; Kayagaki *et al.*, 2002) (Figure 13). In contrast to the canonical pathway, the NF- $\kappa$ B transcription factor dimer p100/RelB contributes to the activation of the non-canonical pathway. In its inactive state, p100 is bound to RelB within the cytoplasm. Upon activation of the non-canonical NF- $\kappa$ B pathway, an inducible NF- $\kappa$ B2/p100 processing occurs. Therefore, p100 is phosphorylated and its I $\kappa$ B-like domain is targeted for a proteasome-dependent proteolysis. The proteolysis of p100 is partial,

producing the mature transcription factor p52/RelB, which translocates into the nucleus to regulate gene expression (Amir *et al.*, 2004). Proteolysis of p100 upon activation of the non-canonical NF- $\kappa$ B pathway requires two kinases: NIK and IKK $\alpha$  (Senftleben *et al.*, 2001; Xiao *et al.*, 2001). Formation and phosphorylation of IKK $\alpha$  homodimer allows the stabilization of NF- $\kappa$ B signaling kinase (NIK), which is normally ubiquitinated and degraded when the non-canonical NF- $\kappa$ B pathway is inactive (Vallabhapurapu *et al.*, 2008; Zarnegar *et al.*, 2008). The catalytic activity of both kinases is required for inducible p100 processing. It has been shown *in vitro*, that NIK is a potent IKK $\alpha$ -activating kinase. By itself, IKK $\alpha$  binds only weakly to p100, which is significantly enhanced in the presence of NIK, suggesting that NIK serves as an adaptor for IKK $\alpha$  to dock to its substrate (Kallunki *et al.*, 1996; Xiao *et al.*, 2004).

The termination of the non-canonical NF- $\kappa$ B pathway is mediated through dephosphorylation of IKK T-loop serines by the protein phosphatase 2A (PP2A) (Häcker & Karin, 2006). The non-canonical response in contrast to the canonical response, is usually more slowly but shows an increased longevity (Dejardin *et al.*, 2002; DiDonato *et al.*, 1997; Xiao *et al.*, 2001; Zandi *et al.*, 1997).

It is important to mention, that there is not a strict separation between both pathways, as a crosstalk between the canonical and non-canonical pathway exists, as p100 can also inhibit the DNA-binding activity of p50/RelA and p50/RelB dimers. Thus, activation of the non-canonical pathway also results in the activation of canonical NF- $\kappa$ B pathway downstream of NIK and IKK $\alpha$  (Basak *et al.*, 2007).

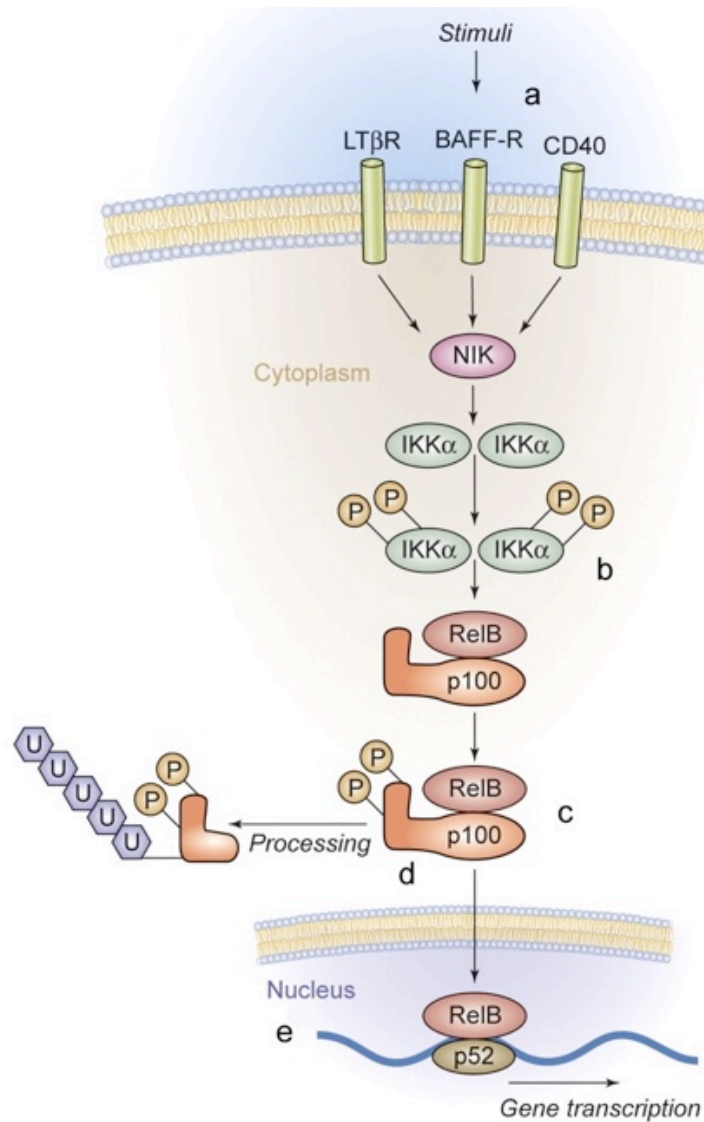


**Figure 13: Activation of the non-canonical NF-κB pathway (Jost & Ruland, 2007).**

(a) A restricted set of cell-surface receptors that belong to the TNF receptor superfamily activates the non-canonical NF-κB pathway, including CD40, the lymphotoxin β receptor, and the BAFF receptor, (b) leading to activation of IKKα, which can directly phosphorylate NF-κB2/p100. (c) This results in partial proteolysis of p100 to p52 by the proteasome, (d) which lacks the inhibitory ankyrin repeats and preferentially dimerizes with RelB to translocate into the nucleus activating gene transcription.

### 1.5.3 The IKK complex

Activation of both NF- $\kappa$ B signaling pathways converges at the activation of IKK. Therefore, it is the most important regulatory component of the pathway and activates NF- $\kappa$ B through two distinct mechanisms (Ghosh *et al.*, 1998). The IKK kinase complex is a 700-900 kDa complex containing the catalytic subunits IKK $\alpha$  (Chuk) and IKK $\beta$  and the regulatory subunit IKK $\gamma$  (also known as NF- $\kappa$ B essential modifier or NEMO, IKKAP1 and Fip-3) (Bonizzi & Karin, 2004; Ghosh *et al.*, 1998)(Figure 14).

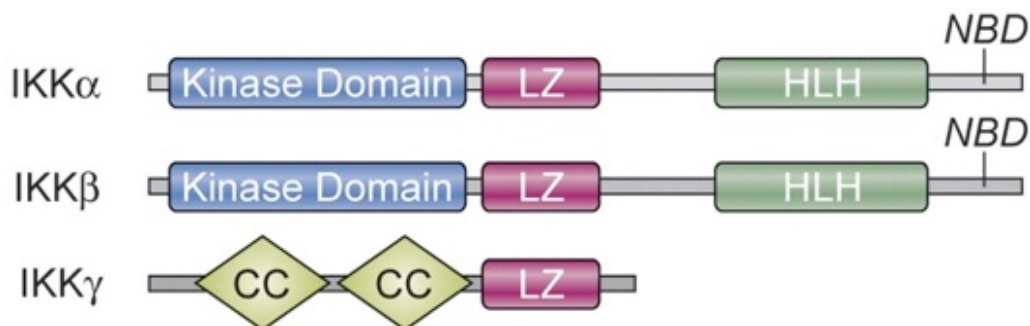


**Figure 14: Schematic representation of IKK complex proteins (Jost & Ruland, 2007).**

The IKK complex contains the catalytic kinase subunits IKK $\alpha$  and IKK $\beta$ , as well as the regulatory subunit IKK $\gamma$  (NEMO). IKK $\alpha$  and IKK $\beta$  possess a helix-loop-helix region (HLH) and a leucine zipper (LZ) domain whereas NEMO has two coiled-coil (CC) domains at its C-terminus.

As described above, the canonical NF- $\kappa$ B pathway catalyzes the phosphorylation of I $\kappa$ Bs in mainly IKK $\beta$ - and IKK $\gamma$ -dependent manner, while the non-canonical NF- $\kappa$ B pathway is strictly activated through IKK $\alpha$  and is independent of IKK $\beta$  and IKK $\gamma$ .

IKK $\alpha$  was the first component of the IKK complex, which was identified by an RT-PCR-based approach in an attempt to isolate Myc-like genes and was first proposed to be involved in transcriptional regulation (Mock *et al.*, 1995). Later on, Chuk was renamed as IKK $\alpha$ . IKK $\beta$  was discovered shortly thereafter through biochemical purification and sequence homology search (Choi *et al.*, 2011; Mercurio *et al.*, 1997).

The third member of the IKK complex, the regulatory subunit IKK $\gamma$ , was initially isolated through genetic complementation cloning using two NF- $\kappa$ B

defective cell lines 1.3E2 and HTLV-1 Tax-transformed rat fibroblast 5R (Yamaoka *et al.*, 1998). IKK $\gamma$  was described as a protein interacting with IKK $\alpha$  and IKK $\beta$  (Mercurio *et al.*, 1999; Rothwarf *et al.*, 1998), and as an Adenovirus E3-14.7K-binding protein (Li *et al.*, 1999). IKK $\alpha$  and IKK $\beta$  share 65 % sequence identity within the kinase domain and have 52 % overall sequence identity. Both are serine/threonine kinases characterized by the presence of a kinase domain at their N-terminus, followed by a leucine zipper domain and a helix-loop-helix (HLH) domain at their C-terminus. The leucine zipper domain of IKK $\alpha$  and IKK $\beta$  is important for their dimerization. Although they can homodimerize, heterodimers are highly favoured and are clearly more catalytically efficient (Mercurio *et al.*, 1997). Both are capable of interacting with NEMO through their C-terminal NEMO-binding domain (NBD) (May *et al.*, 2002).

NEMO (IKK $\gamma$ ) is a 48 kDa protein with a C-terminal zinc finger-like domain, a leucine zipper, and N-terminal and C-terminal coiled-coil domains. In contrast to IKK $\alpha$  and IKK $\beta$ , it is a regulatory- or a scaffold protein and has therefore no structural similarity to them. Activation of the canonical NF- $\kappa$ B pathway leads to IKK $\gamma$  oligomerization and its interaction with upstream signaling adapters such as RIP1 or IRAK1 (Li *et al.*, 1999; Windheim *et al.*, 2008; Wu *et al.*, 2006; Zhang *et al.*, 2000). Thereafter, K63-linked ubiquitinylation, SUMOylation and phosphorylation of downstream proteins takes place (Sebban *et al.*, 2006). This interaction leads to subsequent phosphorylation of T-loop serines of at least one of the IKK subunits, either through the action of an upstream kinase or by transautophosphorylation (Makris *et al.*, 2002).

#### 1.5.4 Manipulation of NF- $\kappa$ B signaling upon viral infection

Activation of NF- $\kappa$ B in response to the appearance of pathogens is associated with the establishment of protective immunity. On the one hand, viruses evolved diverse and sophisticated strategies to subvert host defenses that enhance their virulence and survival time in the infected hosts (Bowie & Unterholzner, 2008) (Table 3). But on the other hand, the NF- $\kappa$ B pathways provide an attractive target to viruses through the rapid and immediate early (IE) event. This results in a strong transcriptional stimulation not only for cellular, but also for several early viral genes to enhance viral replication as they also harbor NF- $\kappa$ B binding sites in their promoters (Hiscott *et al.*, 2001) (Table 2). NF- $\kappa$ B regulates gene expression of retroviruses (HIV) (Bachelierie *et al.*, 1991; Chirmule *et al.*, 1994; Fiume *et al.*, 2012), adenoviruses (Pahl *et al.*, 1996; Shurman *et al.*, 1989), papova viruses (JC virus) (Ranganathan & Khalili, 1993) and herpes viruses (herpes simplex virus-1 [HSV-1] and CMV) (Gimble *et al.*, 1988; Sambucetti *et al.*, 1989). Additionally, viruses take advantage of the NF- $\kappa$ B activation pathway by modulating host cell survival and by evading immune responses. Therefore, some viruses like human herpesvirus 8 (HHV-8) encoding for vFLIP, activate NF- $\kappa$ B to prevent the cell from undergoing apoptosis (Keller *et al.*, 2006). In contrast, the protease 3Cpro of Coxsackie virus blocks NF- $\kappa$ B to increase apoptosis leading to a decrease in viral replication, which is beneficial to the infected host cell and prolongs the viral infection state (Zaragoza *et al.*, 2006). The viral ICP0 protein from herpes simplex virus-1 (HSV-1) is a key intermediate-early gene in viral replication and contains also NF- $\kappa$ B binding sequences (Rong *et al.*, 1992). Low level NF- $\kappa$ B activation allows some viruses to maintain their chronic infections, like it has been shown in HIV-1 chronically infected cells (DeLuca *et al.*, 1999).

Tumor viruses like HTLV-1 and EBV, through their viral proteins Tax and LMP1 respectively, are capable of activating NF- $\kappa$ B in order to enable their transforming functions. Therefore, Tax associates with NEMO in the IKK complex to form higher order complexes that are resistant to dissociation *in vitro*, leading to chronic IKK activation, continuous I $\kappa$ B turnover, and persistent NF- $\kappa$ B expression (Chu *et al.*, 1999). In contrast, LMP1 activates NF- $\kappa$ B through

Tumor necrosis factor receptor type 1-associated DEATH domain protein (TRADD) and RIP activating a kinase cascade that includes NIK and the IKK complex (Karin, 1999).

**Table 2: Viral activators of NF- $\kappa$ B (adapted from (Hiscott *et al.*, 2006)).**

Level of action	Virus	Viral protein	Mechanism of inhibition	Reference
<b>Cytokine receptors</b>	EBV	LMP-1	CD40 receptor mimic	(Hatzivassiliou <i>et al.</i> , 1998)
	EMCV	Capsid protein	Triggers Mda-5	(Gitlin <i>et al.</i> , 2006)
	HCMV	US28	Constitutive transmembrane receptor signaling through the G protein q (Gq)/ phospholipase C pathway	(Miller <i>et al.</i> , 2012)
	HSV-8	ORF74	G protein coupled chemokine receptor	(Sandford <i>et al.</i> , 2009)
	HIV	Gp120	Engages CD4 receptor	(Ugolini <i>et al.</i> , 1997)
	MCMV	M33	Constitutive transmembrane receptor	(Waldhoer <i>et al.</i> , 2002)
	SARS	Nucleocapsid	Multiple functions (RIG-I signaling?)	(Che <i>et al.</i> , 2003)
<b>TLR signaling</b>	HCV	Core protein	Triggers IFN response	(Bode <i>et al.</i> , 2003)
	HCMV	StpC	Interacts with TRAF2	(Merlo & Tsygankov, 2001)
	KSHV-8	K15	Mediates TRAF2 induction of NF- $\kappa$ B	(Brinkmann <i>et al.</i> , 2003; Brinkmann & Schulz, 2006)
	Influenza A	NS1, NS2	Triggers RIG-I	(Pang <i>et al.</i> , 2013)
	VSV	Ribonucleoprotein	Activates TBK-1	(tenOever <i>et al.</i> , 2004)
<b>IKK complex</b>	ASFV	A224L	IAP-like activator of IKK	(Rodriguez <i>et al.</i> , 2002)
	KSHV	vFLIP	Associates with NEMO and activates IKK	(Field <i>et al.</i> , 2003)
	HTLV	Tax	Adaptor for NEMO	(Iha <i>et al.</i> , 2003)
	Influenza A	HA, M and NP	Hemagglutinin, matrix and nucleoprotein induces IKK activation	(Veckman <i>et al.</i> , 2006)

	Rotavirus	VP4 capsid protein	Activates IKK	(Holloway & Coulson, 2006)		
<b>NF-κB</b>	Bluetongue virus	VP2, VP5	Capsid proteins activate NF-κB	(Mortola <i>et al.</i> , 2004)		
	EBV	EBNA-2, LMP	Transcription coactivator of IKK	(Chen & Cooper, 1996)		
	HBV	HBx	Activation of Src, MAPK cascades and NF-κB	(Bouchard <i>et al.</i> , 2006; Lim <i>et al.</i> , 2013)		
	Herpesviruses Saimiri	Tip	Adaptor for LCK leading to NF-κB activation	(Yoon <i>et al.</i> , 1997)		
	HCMV	IE1	Regulation of NF-κB induced genes	(Wang & Sonenshein, 2005)		
				NS5A	Enhances full-length core protein-induced NF-κB activation	(Gong <i>et al.</i> , 2001)
				NS5B	Regulates TNF signaling through effects on cellular IKK	(Choi <i>et al.</i> , 2006)
	HSV-8	K7	Associates with PLIC1 to induce IκB degradation	(Feng <i>et al.</i> , 2004)		
	HIV 1	Tat	Enhances NF-κB mediated LTR activation	(Pieper <i>et al.</i> , 2002)		
		Nef	Stimulates HIV-1 LTR via NF-κB activation	(Varin <i>et al.</i> , 2003)		
	RSV	M2-1	Associates with RelA	(Reimers <i>et al.</i> , 2005)		
	KSHV	Orf74	Encodes for a constitutively active chemokine receptor homologue activating NFκB	(Schwarz & Murphy, 2001)		
	Rev-T	v-Rel	Activated c-Rel	(Richardson & Gilmore, 1991)		

**Table 3: Viral inhibitors of NF- $\kappa$ B (adapted from (Le Negrate, 2011))**

Level of action	Virus	Viral protein	Mechanism of inhibition	Reference
<b>Cytokine receptors</b>	Orthopoxvirus	CrmB, C, D, E	Binds to TNF $\alpha$ , LT $\alpha$ or both	(Hu <i>et al.</i> , 1994; Loparev <i>et al.</i> , 1998; Saraiva & Alcami, 2001)
	CPXV	vCD30	Binds to CD153, prevents CD30/CD153 interaction	(Panus <i>et al.</i> , 2002)
	Poxvirus	TPV2L/TNF-BP	Binds to mammalian TNF $\alpha$ , impairs TNF $\alpha$ signaling	(Brunetti <i>et al.</i> , 2003; Rahman <i>et al.</i> , 2006)
	Orthopoxvirus (VACV, CPXV, ectromelia virus)	vIL-18BP	Binds to IL-18	(Smith <i>et al.</i> , 2000)
<b>TLR signaling</b>	VACV	A52	Binds to IRAK2 and TRAF6, disrupts TRAF6-TAB1 and Mal-IRAK2 interactions	(Harte <i>et al.</i> , 2003)
	VACV	A46	Prevents the interaction between the TIR domain of TLRs and MyD88, Mal, TRIF and TRAM	(Lysakova-Devine <i>et al.</i> , 2010; Stack <i>et al.</i> , 2005)
	HCV	NS5A	Prevents the interaction between IRAK and MyD88	(Abe <i>et al.</i> , 2007)
	HCV	NS3/4A	Cleaves TRIF, prevents the interaction between IRAK and MyD88	(Li <i>et al.</i> , 2005)
	HSV	ICP0	Degrades MyD88 and Mal	(van Lint <i>et al.</i> , 2010)
<b>IKK complex</b>	VACV	N1L	Interacts with IKK $\alpha$ , IKK $\beta$ , NEMO and TANK-binding kinase 1	(DiPerna <i>et al.</i> , 2004)
	VACV	K1L	Prevents IKK phosphorylation or activation	(Shisler & Jin, 2004)
	VACV	B14R	Interacts with IKK $\beta$ and inhibits Ser177 and Ser181 phosphorylation	(Chen <i>et al.</i> , 2008)
	MCPyV	ST	Targets NEMO	(Griffiths <i>et al.</i> , 2013)
	Molluscum contagiosum	MC160	Binds to procaspase-8 and Hsp90 Prevents the interaction between Hsp90 and IKK $\alpha$	(Nichols & Shisler, 2009)

	KSHV	vIRF3	Binds and impairs IKK $\beta$ activity	(Seo <i>et al.</i> , 2004)
	HSV-1	ICP-27	Blocks the phosphorylation and ubiquitination of I $\kappa$ B $\alpha$ and directly interacts with I $\kappa$ B $\alpha$	(Kim <i>et al.</i> , 2008)
<b>SCF<math>^{\beta}</math>-TrCP</b>	VACV	G1R	Interacts with S-phase kinase-associated protein 1	(Mohamed <i>et al.</i> , 2009a)
		CP77	Binds to SCF $^{\beta}$ -TrCP complex	(Chang <i>et al.</i> , 2009)
	Rotavirus	NSP1	Proteasomal degradation of $\beta$ -TrCP	(Graff <i>et al.</i> , 2009)
	HIV	Vpu	Inactivation of $\beta$ -TrCP	(Bour <i>et al.</i> , 2001)
<b>NF-<math>\kappa</math>B</b>	West Nile virus	NS1	Inhibits NF- $\kappa$ B nuclear translocation	(Wilson <i>et al.</i> , 2008)
	Hantaan virus	Nucleo-capsid (N)	Binds to importin $\alpha$ protein and prevents p65 nuclear translocation	(Taylor <i>et al.</i> , 2009a; Taylor <i>et al.</i> , 2009b)
	Myxoma virus	M150	Colocalizes with p65 and prevents NF- $\kappa$ B transcriptional activity	(Camus-Bouclainville <i>et al.</i> , 2004)
	ASFV	A238L	Prevents the binding between p300 and PKC	(Granja <i>et al.</i> , 2006)
	Walley dermal sarcoma virus	Rv-cyclin	Prevents the interaction between TAF9 and p65	(Quackenbush <i>et al.</i> , 2009)
	VARV	G1R	Interacts with NF- $\kappa$ B1/p105	(Mohamed <i>et al.</i> , 2009b)
	VACV	CP77	Interacts with p65	(Chang <i>et al.</i> , 2009)
	Myxoma virus	M013	Interacts with p105 and impairs p65 nuclear translocation	(Rahman <i>et al.</i> , 2009)
	HPV	E7	Inhibits NF- $\kappa$ B activation	(Spitkovsky <i>et al.</i> , 2002)

A biphasic model of NF- $\kappa$ B control has been observed being performed by viruses. A perfectly adopted activation of NF- $\kappa$ B to the viral life cycle has been shown for the African swine fever virus (ASFV), which encodes A238L to block NF- $\kappa$ B release into the nucleus. Besides, the IKK-activating viral late protein A244L turns on NF- $\kappa$ B transcriptional activity at later stages of infection. A244L has anti-apoptotic functions and it is important for proper viral replication (Rodriguez *et al.*, 2002).

Conversely, HCMV as well as MCMV activate NF- $\kappa$ B already through the binding of viral particles to the cell surface, after virus entry and through the immediate early protein IE1 (Compton *et al.*, 2003; Gribaudo *et al.*, 1996; Sambucetti *et al.*, 1989; Yurochko *et al.*, 1997; Yurochko *et al.*, 1995). However, at later stages of infection, pp65 and IE86 block NF- $\kappa$ B signaling (Browne & Shenk, 2003; Taylor & Bresnahan, 2006). Further, HCMV blocks NF- $\kappa$ B activation after IL-1 $\beta$  and TNF $\alpha$  stimulation (Le *et al.*, 2008; Mack *et al.*, 2008; Montag *et al.*, 2006; Popkin & Virgin, 2003). The mechanism and responsible viral protein behind this inhibition is so far unknown, but it has been shown for both cases, that the effect is caused by downregulation of TNFR1. An additional protein of MCMV called M45 terminates the initial MCMV activation in the immediate early phase after PRR- and cytokine receptor stimulation (Mack *et al.*, 2008).

## 2 Material

---

### 2.1 Cells

#### 2.1.1 Bacterial strains

---

Strain	Genotype
DH5 $\alpha$	<i>supE44</i> , $\Delta$ <i>lacU169</i> , ( $\phi$ 80d <i>lacZ</i> $\Delta$ M15), <i>hsdR17</i> , <i>recA1</i> , <i>endA1</i> , <i>gyrA96</i> , <i>thi-1</i> , <i>relA1</i> (Hanahan & Meselson, 1983)

---

#### 2.1.2 Mammalian cell lines

---

Cell line	Genotype
H1299	Human lung carcinoma cell line, p53 negative (Mitsudomi <i>et al.</i> , 1992).
H1299shIKK $\alpha$	H1299 cell line with shRNA against IKK $\alpha$ ; shRNA 5'-GTG AGC CTG TGA TCA ATA A-3' (MISSION® TRC shRNA TRCN0000244902).
A549	Human lung carcinoma cell line expressing wild-type p53 (Giard <i>et al.</i> , 1973).
A549shIKK $\alpha$	A549 cell line with shRNA against IKK $\alpha$ ; shRNA 5'-GTG AGC CTG TGA TCA ATA A-3' (MISSION® TRC shRNA TRCN0000244902).
A549shNEMO	A549 cell line with shRNA against NEMO; shRNA 5'-AGG GAG TAC AGC AAA CTG AAC-3' (MISSION® TRC shRNA TRCN0000022148).
HEK-293	Established HAdV-C5-transformed, human embryonic kidney cell line stably expressing the adenoviral E1A and E1B oncoproteins (Graham <i>et al.</i> , 1977).
HEK-293T	HEK-293 derived cell line expressing the SV40 large T-ag (DuBridge <i>et al.</i> , 1987).

---

#### 2.1.3 Viruses

---

Adenovirus	Characteristics
H5pg4100	Wt Ad5 containing an 1863 bp deletion (nt 28602-30465) in the E3 region (Kindsmüller <i>et al.</i> , 2007).

---

---

H5pm4149	Ad5 E1B-55K null mutant containing four stop codons at the aa positions 3, 8, 86 and 88 of the E1B-55K sequence (Kindsmüller <i>et al.</i> , 2007).
H5pm4154	Ad5 E4orf6 null mutant containing a stop codon at aa 66 within the E4orf6 sequence (Blanchette <i>et al.</i> , 2004b).

---

## 2.2 Nucleic acids

### 2.2.1 Oligonucleotides

The following oligonucleotides were used for sequencing, PCR, RT-PCR and site-directed mutagenesis. All oligonucleotides were ordered from Metabion (Munich) and numbered according to the internal group *Filemaker Pro* database.

---

#	Name	Sequence	Purpose
1371	18S rRNA-fwd	5'-CGG CTA CCA CAT CCA AGG AA-3'	RT-PCR
1372	18S rRNA-rev	5'-GCT GGA ATT ACC GCG GCT-3'	RT-PCR
1686	E1A-fwd	5'-GTG CCC CAT TAA CCA GTT G-3'	RT-PCR
1687	E1A-rev	5'-GGC GTT TAC AGC TCA AGT CC-3'	RT-PCR
64	E1B bp2043-fwd	5'-CGC GGG ATC CAT GGA GCG AAG AAA CCC ATC TGA GC-3'	Sequencing
1569	E1B-fwd	5'-GAG GGT AAC TCC AGG GTG CG-3'	RT-PCR
1570	E1B-rev	5'-TTT CAC TAG CAT GAA GCA ACC ACA-3'	RT-PCR
635	pcDNA3-fwd	5'-ATG TCG TAA CAA CTC CGC-3'	Sequencing
636	pcDNA3-rev	5'-GGC ACC TTC CAG GGT CAA G-3'	Sequencing

---

### 2.2.2 Vectors

---

#	Name	Purpose	Reference
101	pGEX-4T1	Empty vector control	Group database

---

129	pGL4	Reporter gene expression vector for Gal4 fusions	(Sadowski & Ptashne, 1989)
136	pcDNA3	Expression vector for mammalian cells, CMV promoter	Invitrogen
138	pGL3	<i>Firefly</i> -Luciferase-Assay	Promega
152	pCMX3b-Flag	Empty vector control	Group database
180	pRL-TK	<i>Renilla</i> -Luciferase-Assay	Promega
196	pcDNA3-Flu	Empty vector control	Group database

### 2.2.3 Recombinant plasmids

#	Name	Vector	Insert	Reference
129	pGEX E1B-55kDa TOPP6	pGEX-2Tk	E1B-55kDa	Group database
577	pGEX E1BdlS263-D496 TOPP6	pGEX-4T1	E1BdlS263-D496	Group database
578	pGEX E1BdlQ163-D496 TOPP6	pGEX-4T1	E1BdlQ163-D496	Group database
737	pE1A	pML	Ad5 E1A	Group database
1022	pE1B-55K-K104R (SCM)	pcDNA3	Ad5 E1B-55K	Group database
1023	pE1B-55K-NES	pcDNA3	Ad5 E1B-55K	Group database
1188	pFlag-L4-100K	pcDNA3	Ad2 L4-100K	Group database
1319	pE1B-55K	pcDNA3	Ad5 E1B-55K	Group database
1418	pGEX-2T-E1B55Z	pGEX-2T	pGEX-2T-E1B55 (aa83-188)	Group database
1519	pGEX-93R	pGEX-2T	Ad5 E1B-93R	Group database
1520	pGEX-156R	pGEX-2T	Ad5 E1B-156R	Group database
1521	pE1B-55K-delP	pcDNA3	Ad5 E1B-55K	Group database

1664	pE4orf6	pcDNA3	Ad5 E4orf6	Group database
1730	pE1B-55K- C454/456S (RF6)	pcDNA3	Ad5 E1B-55K	Group database
1968	pCMV-VSV-G	pCMV	Envelope protein G of Vesicular Stomatitis Virus	(Beyer <i>et al.</i> , 2002)
1969	pRSV Rev	pRSV	HIV-1 Rev	(Dull <i>et al.</i> , 1998)
1970	pMDLg/pRRE		HIV-1 Gag Pol	(Dull <i>et al.</i> , 1998)
2068	E1B-55K- S490/491/495D (pM)	pcDNA3	Ad5 E1B-55K	Group database
2140	pE1B-55K- R443in	pcDNA3	Ad5 E1B-55K	Group database
2141	pE1B-55K- R443A	pcDNA3	Ad5 E1B-55K	Group database
2193	pE1B-55K-RTR	pcDNA3	Ad5 E1B-55K	Group database
2194	pE1B-55K- E472A (E2)	pcDNA3	Ad5 E1B-55K	Group database
2261	pflu-pVII	pcDNA3-flu	Ad5 pVII	Group database
2420	pGL3-Basic Prom E1A	pGL3	Ad5 E1A promoter reporter gene construct	Group database
2421	pGL3-Basic Prom E1B	pGL3	Ad5 E1B promoter reporter gene construct	Group database
2422	pGL3-Basic Prom pIX	pGL3	Ad5 pIX promoter reporter gene construct	Group database
2423	pGL3-Basic Prom E2E	pGL3	Ad5 E2early promoter reporter gene construct	Group database
2425	pGL3-Basic Prom E3	pGL3	Ad5 E3 promoter reporter gene construct	Group database
2428	pGL3-Basic Prom E2L	pGL3	Ad5 E2early promoter reporter gene construct	Group database
2563	pE1B-55K-EE	pcDNA3	Ad5 E1B-55K	Group database

2628	pflu-pV	pcDNA3-flu	Ad5 pV	Group database
2724	pflu-pIX	pcDNA3-flu	Ad5 pIX	Group database
2744	pFlag-E2A	pCMX3b	Ad5 E2A	Group database
2799	non-target shRNA	pLKO.1.puro	shRNA control	Sigma SHC002
2857	shRNACHUK	pLKO.1.puro	5'-ACA GCG TGC CAT TGA TCT ATA-3'	MISSION® TRC shRNA TRCN0000244902
2858	shRNANEMO	pLKO.1.puro	5'-AGG GAG TAC AGC AAA CTG AAC-3'	MISSION® TRC shRNA TRCN0000022148
2908	Flag-IKK $\alpha$	pcDNA3	Flag-tagged I $\kappa$ B kinase $\alpha$	Thomas Gilmore
2910	Flag-IKK $\beta$	pCMV2	Flag-tagged I $\kappa$ B kinase $\beta$	Addgene 11103
2912	HA-NEMO	pcDNA3-HA	HA-tagged NF- $\kappa$ B essential modifier	Addgene 13512
2913	Flag-NEMO	pCMV-Flag	Flag-tagged NF- $\kappa$ B essential modifier	Addgene 11970
3037	pGL3-Basic 5X NF- $\kappa$ B-Elam- Prom	pGL3	5X NF- $\kappa$ B binding site with Elam-promoter	Group database

## 2.3 Antibodies

### 2.3.1 Primary antibodies

Name	Properties	Source
2A6	Monoclonal mouse Ab; against N-terminus of HAdV-C5 E1B-55K (Sarnow <i>et al.</i> , 1982)	Group database
3F10	Monoclonal rat Ab; against the HA-tag	Roche
4E8	Monoclonal rat Ab; against the central region of HAdV-C5 E1B-55K	Group database
M73	Polyclonal rabbit Ab; against HAdV-C5 E1A	kindly provided by R. Grand/ University of Birmingham
6B10	Monoclonal rat Ab; against HAdV-C5 L4-100K	Group database

6His	Monoclonal mouse Ab; against 6xHis-tag	Clontech
7C11	Monoclonal rat Ab; against the 50 C-terminal aa of HAdV-C5 E1B-55K	kindly provided by E. Kremmer
93H1	Polyclonal rabbit Ab; against Ser 536 phosphorylated p65	Cell Signaling
$\beta$ -actin (AC-15)	Monoclonal mouse Ab; against $\beta$ -actin	Sigma Aldrich
B6-8	Monoclonal mouse Ab; against HAdV-C5 E2A protein (Reich <i>et al.</i> , 1983)	Group database
C-21	Polyclonal rabbit Ab; against C-terminus of I $\kappa$ B $\alpha$	Santa Cruz
DO-I	Monoclonal mouse Ab; against the N-terminal aa 11-25 of human p53	Santa Cruz
E2A	Polyclonal rabbit Ab; against HAdV-C5 E2A-72 kDa protein	kindly provided by R. T. Hay
Flag-M2	Monoclonal mouse AbB; against Flag-tag	Sigma Aldrich
GST	Polyclonal goat Ab; against GST-tag	Amersham
H3	Monoclonal rabbit Ab; against Histone H3	Epitomics
L133	Polyclonal rabbit serum; against HAdV-C5 capsid (Kindsmüller <i>et al.</i> , 2007)	Group database
M-204	Polyclonal rabbit Ab; against the C-terminal aa 248-452 of IKK $\alpha$	Santa Cruz
M58	Monoclonal mouse Ab; against HAdV-C5 E1A-12S and -13S (Harlow <i>et al.</i> , 1985)	Group database
Mre11	Polyclonal rabbit Ab; against human Mre11	Abcam/Novus
RSA3	Monoclonal mouse Ab; against the N-terminus of HAdV-C5 E4orf6 and E4orf6/7 (Marton <i>et al.</i> , 1990)	Group database
C-20	Polyclonal rabbit Ab; against C-terminus of p65	Santa Cruz
FL-419	Polyclonal rabbit Ab; against full length of IKK $\gamma$	Santa Cruz
5A5	Monoclonal mouse Ab; against synthetic phosphopeptide surrounding Ser32/36 of I $\kappa$ B $\alpha$	Cell Signaling
H-207	Polyclonal rabbit Ab; against the C-terminal aa 465-671 of RIP 1	Santa Cruz
TNF $\alpha$	Polyclonal rabbit Ab; against mature as well as	Cell Signaling

precursor TNF- $\alpha$ 

C-20

Polyclonal goat Ab; against Vimentin

## 2.4 Secondary antibodies

### 2.4.1 Antibodies for western blotting

Product	Properties	Company
HRP-Anti-Mouse IgG	HRP (horseradish peroxidase)-coupled; raised in sheep	Jackson
HRP-Anti-Rabbit IgG	HRP (horseradish peroxidase)-coupled; raised in sheep	Jackson
HRP-Anti-Rat IgG	HRP (horseradish peroxidase)-coupled; raised in sheep	Jackson
HRP-Anti-Mouse IgG light chain specific	HRP (horseradish peroxidase)-coupled; raised in sheep	Jackson
HRP-Anti-Rabbit IgG light chain specific	HRP (horseradish peroxidase)-coupled; raised in sheep	Jackson
HRP-Anti-Rat IgG light chain specific	HRP (horseradish peroxidase)-coupled; raised in sheep	Jackson

### 2.4.2 Antibodies for immunofluorescence staining

Product	Properties	Company
Cy3-Anti-Mouse IgG	Affinity purified, Cy3-coupled; raised in donkey (H + L)	Dianova
Cy3-Anti-Rabbit IgG	Affinity purified, Cy3-coupled; raised in donkey (H + L)	Dianova
Cy3-Anti-Rat IgG	Affinity purified, Cy3-coupled; raised in donkey (H + L)	Dianova
Alexa 488 Anti-Mouse IgG	Alexa 488 antibody raised in goat (H + L; F(ab') <sub>2</sub> Fragment)	Invitrogen
Alexa 488 Anti-Rabbit IgG	Alexa 488 antibody raised in goat (H + L; F(ab') <sub>2</sub> Fragment)	Invitrogen

## 2.5 Standards and markers

Product	Company
1 kb/100bp DNA ladder	New England Biolabs
PageRuler Plus Prestained Protein Ladder	Pierce

## 2.6 Commercial systems

Product	Company
Dual-Luciferase Reporter Assay System	Promega
Plasmid Purification Mini, Midi und Maxi Kit	Qiagen
ProFection® Mammalian Transfection System	Promega
Protein Assay	BioRad
QuikChange Site-Directed Mutagenesis Kit	Stratagene
SuperSignal West Pico Chemiluminescent Substrate	Pierce

## 2.7 Chemicals, enzymes, reagents, equipment

Chemicals, enzymes and reagents used in this study were obtained from Agilent, Applichem, Biomol, Merck, New England, Biolabs Roche and Sigma Aldrich. Cell culture materials, general plastic material as well as equipment were supplied by BioRad, Biozym, Brand, Engelbrecht, Eppendorf GmbH, Falcon, Gibco BRL, Greiner, Hartenstein, Hellma, Nunc, Pan, Sarstedt, Protean, Schleicher & Schuell, VWR and Whatman.

## 2.8 Software and databases

Software	Purpose	Source
Acrobat X Pro	PDF data processing	Adobe
CLC Main Workbench 7.0	Sequence data processing	CLC bio
Papers 3.4.2	Reference management	Mekentosj

---

Endnote X 7.5.1.1	Reference management	Thomson Reuters
Filemaker Pro 11	Database management	FileMaker, Inc.
Illustrator CS6	Layout processing	Adobe
Photoshop CS6	Image processing	Adobe
PubMed	Literature database, open sequence analysis software	Open Software (provided by NCBI)
Word 2011	Text processing	Microsoft
Prism 6	data graphing	GraphPad

---

### 3.1 Bacteria

#### 3.1.1 Culture and Storage

##### Solid Plate Culture

Transformed bacteria or bacteria from glycerin culture were plated on solid LB media containing 15 g/l agar with the appropriate antibiotics (100  $\mu\text{g}/\text{ml}$  ampicillin; 50  $\mu\text{g}/\text{ml}$  kanamycin) and incubated at 30 °C/37 °C for 16-20 hours.

Solid plate cultures can be stored for several weeks at 4 °C sealed with *Parafilm* (Pechiney Plastic Packaging).

##### Liquid culture

Sterile LB medium containing the appropriate antibiotic (100  $\mu\text{g}/\text{ml}$  ampicillin; 50  $\mu\text{g}/\text{ml}$  kanamycin) was inoculated with a single bacteria colony to establish liquid *E. coli* culture. Therefore, cultures were incubated at 30 °C/37 °C at 200 rpm in an *Inova 4000 Incubator* (New Brunswick) overnight.

##### Storage

5 ml of liquid cultures from single colony bacteria were centrifuged briefly at 4,000 rpm for 10 min (*Multifuge 3 S-R; Heraeus*) at RT. After discarding the supernatant, the bacteria pellets were then resuspended in 1 ml LB media containing 50 % sterile glycerol and transferred into *CryoTubes<sup>TM</sup>* (Nunc). Resulting glycerol cultures can be stored at -80 °C for years.

<b>LB Medium</b>	10 g/l	Trypton
	5 g/l	Yeast extract
	5 g/l	NaCl (Autoclaved)
<b>Antibiotic solution</b>	50 mg/ml	Ampicillin
	10 mg/ml	Kanamycin (Sterile filtered; storage at -20 °C)

### 3.2 Chemical transformation

For chemical transformation of *E.coli*, 200 ng plasmid DNA were transferred into a 15 ml *Falcon 2059* tube together with 100  $\mu\text{l}$  of chemically competent DH5 $\alpha$  bacterial cells. Incubation for 30 min on ice was followed by a heat shock by incubating the

bacteria in a water bath at 42 °C for 45 s. The cells were immediately chilled on ice for 2 min. Afterwards, 1 ml LB medium without antibiotics were added and incubated for 1 hour at 37 °C and 220 rpm in an *Inova 4000 Incubator* (New Brunswick). The bacteria were plated on LB agar containing appropriate antibiotics and incubated at 30 °C/37 °C overnight.

### 3.3 Tissue culture techniques

#### 3.3.1 Maintenance and passage of cell lines

All tissue culture techniques were performed in specialized flow hoods under sterile conditions. Adherent mammalian cell lines were cultured as monolayers in polystyrene cell culture dishes with *Dulbecco's Modified Eagles Medium* (DMEM; Sigma) containing 0.11 g/l sodium pyruvate, 10 % FCS (Pan) and 1 % of penicillin/streptomycin solution (1000 U/ml penicillin & 10 mg/ml streptomycin in 0.9 % NaCl; Pan). Cells are cultured at 37 °C in a CO<sub>2</sub> incubator (Heraeus) in 5 % CO<sub>2</sub> atmosphere. Cell passage comprises removing existing medium, wash twice with phosphate buffered saline (PBS), adding appropriate amount of trypsin/EDTA (Pan) for 3-5 min at 37 °C. Trypsin activity was inactivated by adding standard culture medium. Detached cells were transferred to a 50 ml tube, centrifuged at 2,000 rpm for 3 min (*Multifuge 3S-R*; Heraeus) and resuspended in an appropriate volume of culture medium. Depending on the experimental procedure, cells were counted and seeded or re-plated in a definite amount for further experiments as described in (3.3.3) or split in an appropriate ratio (1:5-1:20).

PBS		140 mM	NaCl
		3 mM	KCl
		4 mM	Na <sub>2</sub> HPO <sub>4</sub>
		1.5 mM	KH <sub>2</sub> PO <sub>4</sub> (pH 7.0-7.7; autoclaved)

#### 3.3.2 Cryopreservation of cell lines

Subconfluent cultures were trypsinized and pelleted as described above (3.3.1) for long-term storage. These cell pellets were resuspended in pure FCS, supplemented with 10 % dimethyl sulfoxide (DMSO) and transferred to *CryoTubes*<sup>TM</sup> (Nunc). Aliquoted cells were cooled gradually with *Mr. Frosty* (Nalgene) to -80 °C overnight before storage in liquid nitrogen. For re-cultivation, cells were rapidly thawed to 37

°C, pelleted to remove the DMSO, resuspended in 1 ml of fresh culture medium and seeded in an appropriate cell culture dish followed by incubation at standard conditions (3.3.1).

### 3.3.3 Determination of cell number

Trypsinized cells were centrifuged and resuspended in DMEM. The number of cells was determined by using a *Neubauer cell counter* (C. Roth). A 50  $\mu$ l aliquot of cell suspension was mixed with 50  $\mu$ l trypan blue in a 1.5 ml reaction tube (Eppendorf). A small volume of this mixture was pipetted on to the cell counter. Cells spread within a 16-square area were counted under a light microscope (Leica DM IL). The number of cells was multiplied by the dilution factor and factor  $10^4$  to obtain the cell number in 1 ml of suspension by applying the following formula:

$$\text{cell number/ml} = \text{counted cell} \times 2 \text{ (dilution factor)} \times 10^4$$

Trypan blue solution	0.15 %	Trypan Blue
	0.85 %	NaCl

## 3.4 Transfection of mammalian cells

### 3.4.1 Transfection with Polyethylenimine

DNA was transferred into mammalian cell lines by using a linear 25 kDa polyethylenimine (PEI; Polysciences), which builds complexes with DNA based on electrostatic interactions, and therefore enables cell membrane penetration of DNA. It was dissolved in ddH<sub>2</sub>O at a concentration of 1 mg/ml, neutralized with 0.1 M HCl (pH of 7.2), sterile filtered (0.2  $\mu$ m pore size), aliquoted and stored at -80 °C. Cells were seeded in 12-/6-well or 100 mm tissue culture dishes 24 h before transfection. For transfection, DNA and PEI in a ratio from 1:5 to 1:10 were mixed with 600  $\mu$ l DMEM and incubated in RT for 10 min. The DNA-PEI mixture was added to the cells seeded in DMEM without FCS and antibiotics. Around 4-6 h after transfection, medium was replaced with normal growth medium. Transfected cells were harvested 24 or 48 h post transfection as described in section (3.4.3).

### 3.4.2 Transfection with calcium phosphate

Mammalian cells were seeded in a 6-well or a 100 mm dish (Falcon) 6-24 h before transfection. With calcium phosphate, plasmid or linear DNA molecules were covered with calcium phosphate crystals, which would be adsorbed by the cells and internalized by endocytosis. For this procedure, DNA was first diluted with deionized water to a final volume of 300  $\mu$ l/500  $\mu$ l after adding 37  $\mu$ l/62  $\mu$ l 2M CaCl<sub>2</sub>. 300  $\mu$ l/500  $\mu$ l of 2xHBS was prepared in a second 15 ml conical centrifuge tube. Prepared DNA solution was added slowly to the tube with 2xHBS while it was vortexed continuously. The transfection solution was incubated 30 min before added to seeded cells.

### 3.4.3 Harvest of mammalian cells

Transfected or infected mammalian cells were harvested by using cell scrapers (Sarstedt) and were collected into 15 or 50 ml conical tubes which were then centrifuged at 2,000 rpm for 3 min at RT (*Multifuge 3S-R*; Heraeus). After discarding the supernatant, the pellet was washed once with PBS and stored at -20 °C for following experiments.

### 3.4.4 Generation of stable knock-down cell lines

#### 3.4.4.1 Generation of recombinant lentiviral particles

Recombinant lentiviral particles were generated by cotransfection of HEK 293T cells with a plasmid encoding for either scrambled shRNA or shRNA specific for protein target, as well as the envelope and packaging plasmids pCMV-VSV-G, pMDLg/pRRE and pRSV-Rev. Therefore, cells were transfected with calcium phosphate method as described in 3.4.2. After incubation, cell medium was replaced by 10 ml DMEM including 25  $\mu$ M Chloroquine and DNA-mixture was added drop-wise to the cells. Approximately 6-12 hours after transfection, the medium was replaced by 8 ml DMEM supplemented with 10 % FBS. Supernatant was collected 24 h and 48 h after transfection, which contains viral particles. Therefore, supernatant were harvested with a syringe and filter sterilized (0.45  $\mu$ m) into 2 ml reaction tubes. Virus particle containing supernatant was quickly frozen in liquid nitrogen and stored at -80 °C.

### 3.4.4.2 Infection of mammalian cell lines with lentiviral particles

Chosen cell lines for transduction with lentiviral particles were grown to a confluence of 50 to 70 % in 6-well culture plates. Prior to infection, media was replaced by DMEM without supplements and 100  $\mu$ l lentiviral particles were added drop-wise. Approximately 2 hours post transduction standard culture media was added. For selection of transduced cells, puromycin (1  $\mu$ g/ml) was added to the cells. Cells were cultured and propagated under these conditions at least 48 hours until determining knockdown efficiency via western blot analysis.

## 3.5 Adenovirus

### 3.5.1 Infection with adenovirus

Mammalian cells were seeded 24 h before infection so that they reach a confluency of approximately 60-80 % at infection. Cells were washed once with PBS before adding fresh medium without supplements. Virus dilutions were prepared in an appropriate volume of DMEM without supplements and added to the cell culture plates. The amount of volume of the virus stock solution, which is needed for infection, was calculated with the following formula:

$$\text{volume virus stock solution } (\mu\text{l}) = \frac{\text{multiplicity of infection (MOI)} \times \text{total cell number}}{\text{virus titer (focus forming units (ffu)/}\mu\text{l)}}$$

The infection medium was replaced with standard culture medium after an incubation of 2 h. The infected cells were harvested (3.4.3) or fixed (3.10.4) according to the experimental procedure at the indicated times post infection.

### 3.5.2 Propagation and storage of high-titer virus stocks

For production of high-titer virus stocks, 150 mm cell culture dishes with 60 % confluent HEK-293 cells were infected with established laboratory virus stocks at an MOI of 20 ffu/cell as described in (3.5.1). Infected cells were harvested 3-5 days after infection as described in (3.5.1). After pelleting (2,000 rpm, 5 min, RT; Multifuge 3 S-R; Heraeus) cells were washed once with PBS and resuspended in an appropriate volume of DMEM without supplements (~1 ml/150 mm dish). Viral particles were released by repeated freezing/thawing cycles in liquid nitrogen, centrifuged at 4,500 rpm for 10 min (Multifuge 3 S-R; Heraeus) to pellet cell debris. Virus-containing

supernatant was mixed with 87 % glycerol sterile; 10 % final concentration) for preservation at -80 °C or at 4 °C for short-time storage.

### 3.5.3 Titration of virus stocks

In order to determine the titer of virus stocks, immunofluorescence staining of infected cells was done using an antibody against the adenoviral E2A-72K DNA binding protein (DBP; Reich et al., 1983). 6-well dishes seeded with  $5 \times 10^5$  HEK-293 cells were infected with 1 ml of virus dilution ranging from  $10^{-2}$  to  $10^{-6}$  and were fixed 24 h past infection with 1 ml ice-cold methanol. It was removed after 15 min incubation at -20 °C and cells were air-dried at RT and incubated with 1 ml PBS-Triton for 15 min. Subsequently, the PBS-Triton was removed and blocked with 1 ml TBS-BG for 1 h at RT. Blocking solution was replaced by 1 ml solution of the primary B6-8 antibody (1:10 in TBS-BG) for 2 h at RT, washed three times for 15 min with TBS-BG before adding the Alexa Fluor® 488-coupled secondary antibody (Invitrogen; 1:500 in TBS-BG) for 2 h at RT. After removing the secondary antibody solution, the cells were washed three times for 15 min with TBS-BG and were counted using a fluorescence microscope (Leica). The total number of infectious particles was calculated according to the infected cell number, virus dilutions and microscope magnification. With this titration technique, the fluorescence forming units (ffu) is determined.

TBS-BG	20 mM	Tris-HCl (pH 7.6)
	137 mM	NaCl
	3 mM	KCl
	1.5 mM	MgCl <sub>2</sub>
	0.05 % (v/v)	Tween20
	0.05 % (w/v)	Sodium azide (NaN <sub>3</sub> )
	5 % (w/v)	Glycine
	5 % (w/v)	BSA

### 3.5.4 Determination of virus yield

The viral progeny production is determined by seeding  $2.5 \times 10^5$  A549 cells in a 6-well plate that were infected afterwards with adenoviruses. They were harvested at indicated time points post infection (3.4.3) and cells were resuspended in an appropriate volume of DMEM. After virus particle breaking the cells by repeating

freeze and thaw cycles, the titer of the virus solution was determined as described above (3.5.3) and the particle number produced per cell was calculated (3.5.4).

### 3.6 DNA techniques

#### 3.6.1 Preparation of plasmid DNA from *E.coli*

For a large-scale plasmid preparation, a pre-culture with 2 ml LB medium was set up by inoculation with a single bacteria colony at 30 °C/37 °C (*Inova 4000 Incubator*, New Brunswick). Approximately 8 h later, the pre-culture was added to 0.5 l LB medium supplemented with the appropriate antibiotics to incubate further 16-20 h at 30 °C/37 °C. The bacteria from the culture were pelleted at 6,000 rpm for 10 min (*Avanti J-E*; Beckman & Coulter) and plasmid DNA was isolated according to the manufacturer's instructions using a *MaxiKit* (*Qiagen*).

For analytical purposes, 5 ml liquid culture was inoculated and plasmid DNA was isolated by a modified protocol of Sambrook and Russell (Sambrook, 1989). 1-5 ml liquid culture was centrifuged at 4,000 rpm for 5 min (*Eppendorf 5417R*) and resuspended in 300 µl *resuspension buffer P1* (*Qiagen*). This suspension was gently mixed with 300 µl of *lysis buffer P2* (*Qiagen*) to lyse the cells. After incubation for 5 min at RT; 300 µl neutralization buffer P3 (*Qiagen*) was added and incubated for further 5 min. Finally, cellular debris were pelleted by centrifugation a 14,000 rpm for 10 min at 4 °C (*Eppendorf 5417R*). The supernatant was collected into a new 1.5 ml reaction tube with 1 volume of isopropanol and 0.1 volumes 3 M NaAc to precipitate the DNA by centrifugation at 14,000 rpm for 30 min (*Eppendorf 5417R*). The DNA pellet was washed once with 1 ml of 75 % (v/v) ethanol, air dried and rehydrated in an appropriate volume of ~20-50 µl of 10 mM Tri-HCl (pH 8.0).

#### 3.6.2 Quantitative determination of nucleic acid concentrations

DNA/RNA concentrations were measured with a *NanoDrop* spectrophotometer (PEQLAB) at a wavelength of 260 nm. DNA purity was assessed by calculation of the OD<sub>260</sub>/OD<sub>280</sub> ratio, which should be located at 1.8 for highly pure DNA and at 2.0 for highly pure RNA.

#### 3.6.3 Agarose gel electrophoresis

Agarose (*Seakem*<sup>®</sup> *LE agarose*; Biozym) was dissolved in TBE buffer to a final concentration of 0.6-1.2 % (w/v) to prepare an analytical or preparative agarose gel. Agarose was melted by heating with buffer in a microwave (Moulinex) and ethidium

bromide was added to a final concentration of 0.5  $\mu\text{g}/\text{ml}$  before pouring the liquid agarose solution in an appropriate gel tray. 6x *Loading Buffer* were mixed with DNA samples and subjected to agarose gel electrophoresis at a voltage of 5-10 V/cm gel length. DNA was visualized by applying UV light at 312 nm using the *G:BOX transilluminator system* (SynGene). To minimize harmful UV irradiation for preparative purposes, agarose gels were supplemented with 1 mM guanosine. DNA was extracted from gel slices by centrifugation at 20,000 rpm for 2 h (*RC 5B Plus*; Sorvall), precipitated with isopropanol from the obtained supernatant, washed, dried and rehydrated as described for plasmid DNA in 3.6.1.

5 x TBE	450 mM	Tris (pH 7.8)
	450 mM	Boric Acid
	10 mM	EDTA
6 x loading buffer	10 mM	EDTA
	50 % (v/v)	Glycerol
	0.25 %	Bromphenol blue
	0.25 %	Xylen Cyanol

### 3.6.4 Polymerase chain reaction (PCR)

To amplify DNA template, a 50  $\mu\text{l}$  PCR reaction was prepared by mixing 25 ng DNA template, 125 ng forward primer, 125 ng reverse primer, 1  $\mu\text{l}$  dNTP mixture (dATP, dTTP, dCTP, dGTP; each 1 mM), 5  $\mu\text{l}$  10 x PCR reaction buffer and 5 U Taq-polymerase (Roche) in a 0.2 ml PCR tube. Following PCR program was performed using a thermocycler (*Flexcycler*; Analytic Jena):

DNA denaturation	1 min	95 °C
Primer annealing	45 sec	55 – 70 °C
Extension	1 min/kb	72 °C
		(25-30 cycles)
Final extension	10 min	72 °C
Storage	$\infty$	4 °C

DNA denaturation, primer annealing and extension were performed for 25-30 cycles. To determine PCR efficiency 5  $\mu\text{l}$  PCR reaction were analyzed by gel electrophoresis (3.6.3).

### 3.6.5 Site-directed mutagenesis

Forward and reverse primers were designed with the desired mutations and ordered from Metabion (Munich). Site-directed mutations were introduced into a plasmid with the following PCR programme:

<b>DNA denaturation</b>	1 min	95 °C
<b>Primer annealing</b>	45 sec	55 °C
<b>Extension</b>	45 min/kb	68 °C
		(12-16 cycles)
<b>Final extension</b>	10 min	68 °C
<b>Storage</b>	∞	4 °C

PCR efficiency was determined with gel electrophoresis with 10  $\mu$ l PCR reaction (3.6.3). The remaining 40  $\mu$ l PCR product were incubated with 1  $\mu$ l restriction enzyme *DpnI* (New England Biolabs) for 1 h at 37 °C to remove methylated template DNA. 10  $\mu$ l of the digested PCR product were transformed into chemical competent DH5 $\alpha$  (3.2). Finally, single clones were picked, cultured in 5-10 ml LB medium (3.1.1) and prepared plasmid DNA (3.6.1) was analyzed by restriction digest (3.7.1), agarose gel electrophoresis (3.6.3) and sequencing (3.7.2) before storage (3.6.5).

## 3.7 Cloning of DNA fragments

### 3.7.1 Enzymatic DNA restriction

Restriction enzymes were used according to the manufacturer's instructions in suggested reaction buffers (New England Biolabs; Roche). Analytical restriction digests were done with 1  $\mu$ g DNA which was incubated with 3-10 U of enzyme for 2 hours at 37 °C, unless indicated otherwise. Preparative restriction digests were done with 20  $\mu$ g of DNA which were incubated with 50 U enzyme for at least 3 hours at 37 °C. If necessary, multiple steps of enzymatic restriction were carried out sequentially, following separation by preparative agarose electrophoresis (3.6.3) and isopropanol/ethanol precipitation (3.6.1). If possible a double digest was set up with the online tool Double Digest Finder (NEB) ([www.neb.com/tools-and-resources/interactive-tools/double-digest-finder](http://www.neb.com/tools-and-resources/interactive-tools/double-digest-finder)) in order to find the best reaction buffer for two different enzymes.

### 3.7.2 DNA sequencing

For DNA sequencing, 0.8  $\mu\text{g}$  DNA and 30 pmol of sequencing primer were mixed with ddH<sub>2</sub>O in a total volume of 12  $\mu\text{l}$ . Sequencing was performed by *Seqlab* (Göttingen).

## 3.8 RNA techniques

### 3.8.1 Isolation of total RNA from mammalian cells

Mock and adenovirus infected A549 cells ( $4 \times 10^6$ ) (3.5.1) were harvested (3.4.3) at indicated time points after infection and the pelleted cells were used to extract total RNA. Therefore, the cell pellet was resuspended with 1 ml of *Trizol*<sup>®</sup> *Reagent* (Invitrogen) and after 5 min incubation at RT, 200  $\mu\text{l}$  Chloroform (Sigma) were added, shaken vigorously and was pelleted at 12,000 g for 15 min at 4 °C (*Eppendorf 5417R*). The aqueous supernatant was transferred into a new 1.5 ml reaction tube where the RNA is precipitated with 600  $\mu\text{l}$  isopropanol at 12,000 g for 15 min (4 °C; *Eppendorf 5417R*). The RNA pellet was washed once with 1 ml 75 % (v/v) EtOH (7,500 g, 15 min, 4 °C; *Eppendorf 5417R*), air dried shortly and dissolved in 20  $\mu\text{l}$  nuclease free water. The amount of total RNA was determined with the *NanoDrop* spectrophotometer (*PEQLAB*; Erlangen). RNA was stored at -80 °C or further used for reverse transcription for quantitative RT-PCR (3.8.3).

### 3.8.2 Quantitative reverse transcription (RT)-PCR

To reverse transcribe (RT) RNA into complementary DNA (cDNA), 1  $\mu\text{g}$  of RNA was reverse transcribed using the *Reverse Transcription System* (Promega). The RT was primed with oligo(dT)/random primers to select for processed mRNA and was performed as described by the manufacturer. Samples of cDNA were stored at -80 °C.

### 3.8.3 Real-Time PCR (RT-PCR)

Quantitative reverse transcription (RT)-PCR was measured by a first-strand method in a *Rotor-Gene 6000* (Corbett Life Sciences) in a *0.1 ml Strip Tube* (LTF Labortechnik). Therefore, a 10  $\mu\text{l}$  reaction mixture was prepared by adding 1  $\mu\text{l}$  cDNA dilution (1:100 in nuclease free water), 2.5 pmol forward and reverse primer and 5  $\mu\text{l}$  *SensiMix Plus SYBR* (Quantace). Measurement was performed in triplicate for each sample denaturing at 95 °C for 10 min prior to 40 cycles of PCR reaction as follows:

<b>DNA denaturation</b>	15 sec	95 °C
<b>Primer annealing</b>	30 sec	62 °C
<b>Extension</b>	15 sec	72 °C
		(40 cycles)

The average threshold cycle (CT) value was determined from triplicate reactions, and levels of viral mRNA relative to cellular 18S rRNA were calculated.

### 3.9 Protein techniques

#### 3.9.1 Preparation of total-cell lysates

All total-cell lysates were prepared with highly stringent RIPA lysis buffer to ensure proper solubilization of proteins and to eliminate unspecific or weak protein interactions. Further, all protein analysis steps were carried out on ice or at 4 °C to reduce the activity of proteases. Cell pellets were resuspended in an appropriate volume of lysis buffer with freshly added 0.2 mM PMSF, 1 mg/ml pepstatin A, 5 mg/ml aprotinin, 20 mg/ml leupeptin, 25 mM iodacetamide and 25 mM N-ethylmaleimide. Resuspended cells were incubated for 30 min on ice and were vortexed every 10 min in between. Complete cell disruption as well as genomic DNA shearing was facilitated by sonification (40 pulses, output 0.60; 0.8 Impulse/s; *Branson Sonifier 450*) and cellular debris as well as insoluble components were pelleted by centrifugation (14,000 rpm, 3 min, 4 °C; *Eppendorf 5417R*). Protein concentration of the supernatant was determined by spectrophotometry (3.9.2). Finally, proteins were denatured by addition of 5 x SDS sample buffer and subsequent boiling at 95 °C for 3 min. Protein lysates were stored at -20 °C until analysis by SDS-PAGE/immunoblotting (3.9.6).

<b>RIPA</b>	50 mM	Tris-HCl (pH 8.0)
	150 mM	NaCl
	5 mM	EDTA
	1 % (v/v)	Nonidet P-40
	0.1 % (w/v)	SDS
	0.5 % (w/v)	Sodium Desoxycholate
<b>5 x SDS sample buffer</b>	100 mM	Tris-HCl (pH 6.8)
	10 % (w/v)	SDS
	200 mM	DTT
	0.2 % (w/v)	Bromphenol blue

### 3.9.2 Quantitative determination of protein concentrations

Protein concentrations in samples were measured using *Protein-Assays* (BioRad) according to *Bradford* (Bradford, 1976). To determine protein concentrations, 1  $\mu$ l protein lysate was mixed with 800  $\mu$ l ddH<sub>2</sub>O and 200  $\mu$ l *Bradford Reagent* (BioRad), incubated for 5 min at RT and measured in a *SmartSpec Plus* spectrophotometer (BioRad) at 595 nm against a blank. Protein concentrations were determined by interpolation from a standard curve with BSA (concentrations of 1-16  $\mu$ g/ $\mu$ l; New England Biolabs).

### 3.9.3 Immunoprecipitation

For immunoprecipitation equal amounts (0.1 mg – 3 mg) of total-cell lysates (3.9.3) from each sample were precleared by addition of Pansorbin A for one hour at 4 °C in a rotator (GFL). Simultaneously, indicated amounts of antibody were coupled to 3 mg of sepharose/IP. Antibody-coupled sepharose beads were washed three times with 1.0 ml of lysis buffer and added to the precleared protein lysate in a 1.5 ml reaction tube after clearing by centrifugation (600xg, 5 min, 4 °C; *Eppendorf 5417R*). Immunoprecipitation was performed at 4 °C in a rotator (GFL) for 2 hours. The resulting protein A/protein G immune complexes were pelleted by centrifugation (600xg, 5 min, 4 °C; *Eppendorf 5417R*) and washed three times with 1.5 ml RIPA lysis buffer. Finally, the samples were mixed with an appropriate volume of 2xSDS sample buffer (Sambrook, 1989), boiled for 3 min at 95 °C to elute proteins and stored at -20 °C until further analysis (3.9.6).

<b>2 x SDS sample buffer</b>	100 mM	Tris-HCl (pH 6.8)
	4 % (w/v)	SDS
	200 mM	DTT
	0.2 % (w/v)	Bromphenol blue
	20 %	Glycerol

### 3.9.4 Subcellular fractionation

All following procedures were carried out on ice. Cells were washed once with PBS and detached from the cell culture plate with trypsin/EDTA (Pan) for 3-5 min at 37 °C. Trypsin activity was inactivated by adding standard culture medium and cells were pelleted by centrifugation at 2,000 rpm for 3 min. Cells were resuspended in

500  $\mu$ l isotonic buffer (IB) and lysed by the addition of 33,33  $\mu$ l 10 % NP40. 5 min after incubation, the crude nuclei were pelleted (1,000 rpm, 3 min) and the supernatant was transferred to a new 1.5 ml reaction tube as cytoplasmic fraction (F1). The pellet was washed twice with isotonic buffer, pelleted as before and the first washing supernatant was transferred to the F1 fraction. The supernatant of the second wash was discarded. These wash steps are necessary to achieve a F1 cleaned composition of the nuclear membrane fraction F2. The pellet comprising cell nuclei were resuspended in F2 buffer, followed by a vortexing and pelleting step (1,000 rpm, 3 min) afterwards. The supernatant after this pelleting step is the nuclear membrane fraction F2 (Hodge *et al.*, 1977). The remaining pellet was washed again in 1 ml RSB buffer, pelleted as before and the supernatant was added to F2. This step removes excess detergents prior to DNase I treatment. After centrifugation and discarding the supernatant, the nuclei were resuspended in 0.5 ml RSB and 5  $\mu$ l 10 mg/ml RNase-free DNase I was added. After 30 min incubation, the nuclei were pelleted as before and the supernatant again was transferred into a new reaction tube labeled as F3. In order to deplete digested chromatin from the nuclei, the pellet was resuspended in 2 ml RSB and 0.25 ml 5 M NaCl was added (Long *et al.*, 1979; van Eekelen & van Venrooij, 1981). The chromatin-depleted nuclei were pelleted by centrifugation at 2,000 rpm for 5 min and the supernatant F4 was collected in a new tube. The remaining pellet, which has been defined as the nuclear matrix was solubilized in isotonic buffer by adding SDS to 0.2 % and EDTA to 10 mM and is referred to F5.

<b>IB</b> (isotonic buffer)	10 mM	Tris-HCl (pH 7.5)
	150 mM	NaCl
	0.2 mM	PMSF
	1 mg/ml	pepstatinA
	5 mg/ml	aprotinin
	20 mg/ml	leupeptin
	25 mM	iodacetamide
	25 mM	N-ethylmaleimide
<b>RSB</b>	10 mM	Tris-HCl (pH 7.5)
	10 mM	NaCl
	3 mM	MgCl <sub>2</sub>
<b>F5B</b>	10 mM	EDTA
	0.2 %	SDS
	Ad15 ml	IB

### 3.9.5 Denaturing purification and analysis of conjugates

H1299 cells were transiently transfected with p6His-SUMO-1 or 6His-SUMO-2 and were subsequently infected/transfected with the appropriate virus/expression vector. The cells were harvested 48 h later, washed once with 1 x PBS and 20 % of the cells were lysed with RIPA Buffer after centrifugation and removing of PBS for total protein analysis (3.4.3). 80 % of the cells were resuspended in 5 ml Guanidinium containing lysis buffer. Lysates in Guanidinium buffer were incubated for 6 h at 4 °C with in lysis buffer prewashed 25  $\mu$ l Ni-NTA agarose (*Qiagen*). The slurry was washed once with lysis buffer, then once with wash buffer pH 8.0 and twice with wash buffer pH 6.3. 6His-SUMO conjugates were eluted with 40  $\mu$ l elution buffer and subsequent boiling at 95 °C for 5 min. Finally, proteins were separated by SDS-PAGE and visualized by immunoblotting (3.9.6).

<b>Guanidinium lysis buffer</b>	6 M	Guanidinium-HCl
	0.1 M	Na <sub>2</sub> HPO <sub>4</sub>
	0.1 M	NaH <sub>2</sub> PO <sub>4</sub>
	10 mM	Tris-HCl (pH 8.0)
	20 mM	Imidazole
	5 mM	$\beta$ -Mercaptoethanol

<b>Wash buffer pH 8.0</b>	8 M	Urea
	0.1 M	Na <sub>2</sub> HPO <sub>4</sub>
	0.1 M	NaH <sub>2</sub> PO <sub>4</sub>
	10 mM	Tris-HCl (pH 8.0)
	20 mM	Imidazole
	5 mM	$\beta$ -Mercaptoethanol Protease inhibitors

<b>Wash buffer pH 6.3</b>	8 M	Urea
	0.1 M	Na <sub>2</sub> HPO <sub>4</sub>
	0.1 M	NaH <sub>2</sub> PO <sub>4</sub>
	10 mM	Tris-HCl (pH 6.3)
	20 mM	Imidazole
	5 mM	$\beta$ -Mercaptoethanol Protease inhibitors

<b>Elution buffer</b>	200 mM	Imidazole
	0.1 % (w/v)	SDS
	150 mM	Tris-HCl (pH 6.8)
	30 % (v/v)	Glycerol
	720 mM	$\beta$ -Mercaptoethanol
	0.01 % (w/v)	Bromphenol blue

### 3.9.6 SDS polyacrylamide gel electrophoresis (SDS-PAGE)

Protein samples of cell lysates (3.9.1), of immunoprecipitation (3.9.3) or SUMOylation pulldown (3.9.5) were separated according to their molecular weights by SDS-PAGE (Biometra). Polyacrylamide gels were made by using 30 % acrylamide/bisacrylamide solution (37.5:1 *Rotiphorese Gel 30*; Roth) diluted to the final concentration of 8 -15 % with ddH<sub>2</sub>O. Protein samples were concentrated between the lower pH of the stacking gel in comparison to the higher pH value of the separation gel. Acrylamide polymerization was initiated by addition of APS ( $f_{\text{inal}}=0.1$  %) and TEMED ( $f_{\text{inal}}=0.01$  %). All gels were prepared by the *Multigel* SDS-PAGE system of Biometra according to the manufacturer's instructions and run at 15 mA/gel in TGS-buffer. Independent of the preparation of the protein samples, they were prepared for SDS-PAGE by addition of 2 x or 5 x SDS- sample buffer leading to its final concentration of 1 x (Sambrook, 1989) and followed by boiling at 95 °C for 3 min in a thermoblock (*Thermomixer Comfort*; Eppendorf). To determine the protein weights, *Page Ruler*™ *Prestained Protein Ladder Plus* (Fermentas) was loaded onto the gels. Afterwards, separated proteins were transferred onto nitrocellulose membranes (*Protran*®; Whatman) by western blotting (3.9.7).

<b>5 % stacking gel</b>	17 % (v/v)	Acrylamide solution (30 %)
	120 mM	Tris-HCl (pH 6.8)
	0.1 % (w/v)	SDS
	0.1 % (w/v)	APS
	0.1 % (v/v)	TEMED
<b>8 % separating gel</b>	27 % (v/v)	Acrylamide solution (30 %)
	250 mM	Tris-HCl (pH 8.8)
	0.1 % (w/v)	SDS
	0.1 % (w/v)	APS
	0.6 % (v/v)	TEMED
<b>10 % separating gel</b>	34 % (v/v)	Acrylamide solution (30 %)
	250 mM	Tris-HCl (pH 8.8)
	0.1 % (w/v)	SDS
	0.1 % (w/v)	APS
	0.6 % (v/v)	TEMED
<b>12 % separating gel</b>	40 % (v/v)	Acrylamide solution (30 %)
	250 mM	Tris-HCl (pH 8.8)
	0.1 % (w/v)	SDS
	0.1 % (w/v)	APS
	0.6 % (v/v)	TEMED

<b>15 % separating gel</b>	50 % (v/v)	Acrylamide solution (30 %)
	250 mM	Tris-HCl (pH 8.8)
	0.1 % (w/v)	SDS
	0.1 % (w/v)	APS
	0.6 % (v/v)	TEMED
<b>TGS buffer</b>	25 mM	Tris
	200 mM	Glycine
	0.1 % (w/v)	SDS

### 3.9.7 Western blotting

Adjusted amounts of protein samples were separated by SDS-PAGE and transferred onto nitrocellulose (*Whatman*) or in case of proteins smaller than 20 kDa polyvinylidene fluoride (PVDF) membranes using the *Trans-Blot Electrophoretic Transfer Cell System (BioRad)* in Towbin-buffer. PVDF membranes have to be activated with methanol. Gels and membranes were soaked in Towbin-buffer, placed between two soaked blotting papers (*Whatman*) and two blotting pads in a plastic grid. The electrophoretic transfer was performed in “full wet” mode in a blotting tank filled with Towbin-buffer at 400 mA for 90 min. Subsequently, membranes were incubated for at least 2 hours at RT or overnight at 4 °C in PBS containing 5 % non-fat dry milk (*Frema*) on an *orbital shaker* (GFL) to saturate unspecific antibody binding areas on the nitrocellulose membrane. After blocking of the membrane, the blocking solution was discarded, membranes were washed briefly to remove remaining blocking solution and incubated for 2 h at RT with the primary antibody diluted in PBS-Tween. The grade of primary antibodies dilutions as well as the amount of added the non-fat dry milk (*Frema*) have to be determined individually for each antibody. After primary staining, the antibody solution was removed, the nitrocellulose membranes were washed three times for 15 min and incubated for 2 hours at RT in PBS-Tween with the HRP-coupled secondary antibody (1:10,000; *Amersham*) containing 3 % non-fat dry milk (*Frema*). Protein bands were visualized by enhanced chemiluminescence using *SuperSignal West Pico Chemiluminescent Substrate (Pierce)* according to the manufacturer’s instructions and detected by X-ray films (*RP New Medical X-Ray Film; CEA*) using a *GBX Developer (Kodak)*. X-ray films were scanned, cropped using *Photoshop CS5 (Adobe)* and figures were prepared using *Illustrator CS5 (Adobe)*.

<b>Towbin buffer</b>	25 mM	Tris-HCl (pH 8.3)
	200 mM	Glycine
	0.05 % (w/v)	SDS
	20 % (v/v)	Methanol
<b>PBS-Tween</b>	0.1 % (v/v)	Tween20 in 1x PBS

### 3.10 GST Pull-down Assays from Cell Lysates

#### 3.10.1 GST-Protein Expression

GST-tagged constructs from the database were cloned into pGEX4T-1 or pGEX5X-1 (Amersham Pharmacia) vectors and stored in glycerol in *E. coli* as described in (3.1.1). They were applied for inoculating 5 ml starter cultures and incubated at 37 °C overnight (3.1.1). Afterwards, pre-culture was transferred into 500 ml LB-medium and incubated at 37 °C until the OD<sub>600</sub> of the culture reached 0.6 (2-4 h post inoculation). Proteinexpression of the bacteria were induced with 0.5 mM (final concentration) Isopropylthio- $\beta$ -D-galactosid (IPTG). This expression culture was further incubated at 30 °C at 180 rpm rotation for 4 hours. Bacteria were pelleted at 6,000g for 10 min. The pellets were frozen at -80 °C overnight after discarding the supernatant to crack bacteria and improve celllysis.

#### 3.10.2 GST-Protein Purification

Bacteria were thawed on ice for 20 min and 15 ml of MTTBs supplemented with 30 mg of Lysozyme and protease inhibitors were added and resuspended with each pellet and transferred to a 50 ml conical tube. After incubation of 10 min on ice, lysates were sonicated five times for 30 s and centrifuged at 14,000 rpm for 40 min at 4 °C. Supernatants were collected and transferred to 15 ml conical tube containing 600  $\mu$ l of three times with MTTBs pre-washed Glutathione beads. Supernatant and GST-beads were rotated for 4 h at 4°C for conjugation of GST-tagged proteins with the beads. GST-protein beads were precipitated by centrifuging at 4,500 rpm for 5 min and washed five times with ice-cold MTTBs buffer. After adding 50-100  $\mu$ l of MTTBs to the beads, 10  $\mu$ l of each sample were examined by SDS-PAGE (3.9.6) and for protein amount estimation, a BSA concentration row was added. Gels were then incubated in a Coomassie staining solution and left at RT for 20 min with agitation. For destaining, gels were placed in a solution containing 10 % glacial acetic acid, 20

% methanol in water, until proteins became clearly visible. Protein amounts were estimated and adjusted to same levels.

### 3.10.3 GST Pull-Down Assays

For *in vivo* GST pull-down assays, cell lysates were prepared as described (3.9.1) in RIPA. Adjusted amounts of GST-protein beads were incubated with 1 mg of protein lysate overnight. GST-protein complexes were precipitated by centrifuging at 6,000 rpm for 5 min at 4 °C. The beads were washed 5 times with 1 ml of ice-cold lysis buffer containing protease inhibitors. GST-beads bound complexes were disrupted by addition of 10  $\mu$ l 2x Laemmli loading buffer. Samples were analyzed by SDS-PAGE (3.9.6), followed by western blotting (3.9.7).

<b>MTTBs</b>	50 mM	Tris
	150 mM	NaCl
	1 % (w/v)	TritonX-100
	100 $\mu$ l	PMSF
	1:1000	aprotinin
		leupeptin
		pepstatin
<b>Coommassie Stain</b>	50 %	methanol
	10 %	acetic acid
	0.05 %	Brilliant Blue R-250
<b>Destain solution</b>	50 %	methanol
	40 %	milli-Q water
	10 %	acetic acid

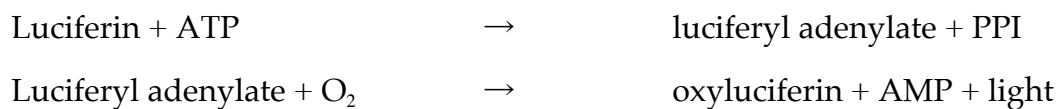
### 3.10.4 Indirect immunofluorescence analysis

For indirect immunofluorescence analysis  $1.5 \times 10^5$  cells were grown on glass coverslips (3.3.1) and transfected/infected according to the experimental setup (3.5.1). Cells were washed once with PBS and fixed with 4 % PFA at 4 °C for 20 min. Afterwards cells were permeabilized by incubation with PBS containing 0.5 % (v/v) Triton X-100 for 10 min at RT. After 1 h blocking in TBS-BG buffer, coverslips were treated for 1 h with the primary antibody diluted in PBS, washed three times with TBS-BG buffer, followed by incubation with the corresponding Alexa488 (Invitrogen) or Cy3-conjugated (*Dianova*) secondary antibodies. Coverslips were washed three times with TBS-BG buffer, mounted in *Glow Mounting Media* (EnerGene) and digital

images were acquired with a *DM6000 fluorescence microscope (Leica)* with a charge-coupled device camera (*Leica*), cropped and decoded by *Photoshop CS5 (Adobe)* and assembled with *Illustrator CS5 (Adobe)*.

### 3.10.5 Reporter Gene Assay

Luciferases are enzymes with catalytic activity that emit visible light upon substrate conversion. The firefly luciferase is the most commonly used luciferase catalyzing following reaction:



Transcriptional activity of a promoter of interest was investigated by transiently transfecting cells with a reporter construct harboring a luciferase ORF under the control of this particular promoter. Expression levels of the luciferase reporter gene are then quantified by adding the luciferase substrate and ATP to the cellular lysates prior to measuring the intensity of emitted light. In addition, *Renilla* luciferase is cotransfected as an internal transfection control. Therefore, measurements of the firefly luciferase (*Photinus pyralis*) activity are always normalized to the activity of *Renilla* luciferase. For quantitative determination of promoter activities, the *Dual-Luciferase<sup>®</sup> Reporter Assay System (Promega)* was used according to the manufacturer's instructions with some modifications. Luciferase reporter gene assays were performed in H1299 cells in 12-well plates. 24 hours after transfection the supernatant was removed. After washing the cells with 1 x PBS, 100  $\mu\text{l}$  of *passive lysis buffer (Promega)* was added to each well and the plates were incubated for 10 min at RT on an orbital shaker (*GFL*) and assayed immediately. Therefore, 10  $\mu\text{l}$  of lysate were subjected to sequential measuring of *Firefly* (10 sec) with 3  $\mu\text{l}$  *firefly luciferase substrate (Promega)* and *Renilla* luciferase activity (10 sec) with *Renilla* luciferase substrate (*Promega*) in a *Lumat LB 9507 luminometer (Berthold Technologies)*. This sequential measurement is possible as firefly luciferase activity is blocked by the pH conditions of the *Renilla* substrate.

The relative luciferase unit (RLU) was calculated through dividing the *firefly*-value by the corresponding *Renilla*-value.

### 3 Results

#### 4.1 Role of the NF- $\kappa$ B mediated innate immune pathway during HAdV-C5 infection

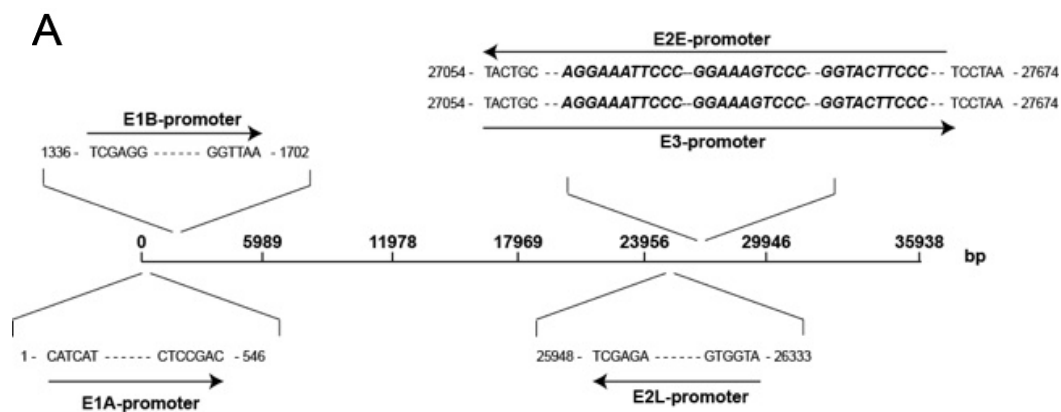
Many studies showed numerous strategies of HAdV-C5 to suppress or activate the antiviral immune response of the host either after infection or administration of adenoviral vectors (Burgert *et al.*, 2002; Hendrickx *et al.*, 2014; Lam & Falck-Pedersen, 2014; Mahr & Gooding, 1999; Wold, 1993). Although great efforts have been made to investigate the immune response induced by HAdV-C5, the molecular mechanisms behind this activation are still poorly investigated and not understood in detail.

#### 4.2 Interplay between HAdV-C5 and the NF- $\kappa$ B pathway

##### 4.2.1 NF- $\kappa$ B expression activates HAdV-C5 promoters

NF- $\kappa$ B-binding sites have been revealed within the promoter regions of HAdV-C5 E2 and E3 transcriptional units (Machitani *et al.*, 2016). This is associated with activation of the NF- $\kappa$ B pathway at the early time point after infection, which is beneficial for HAdV-C5 gene expression and replication. Besides HAdV-C5, there are several human pathogenic DNA viruses harboring NF- $\kappa$ B sites within their early promoter regions (Pahl, 1999; Sambucetti *et al.*, 1989; Williams *et al.*, 1990). Thus, timely regulation of NF- $\kappa$ B pathway in order to take advantage from its function as a transcription factor is a common viral strategy to overcome antiviral host response.

To test whether HAdV-C5 early promoter regions of different adenoviral genes can be also activated by the NF- $\kappa$ B transcription factor, H1299 cells were transfected with constructs encoding HAdV-C5 promoter sequences upstream of a reporter luciferase gene and co-transfected with a plasmid encoding p65, a subunit of NF- $\kappa$ B.



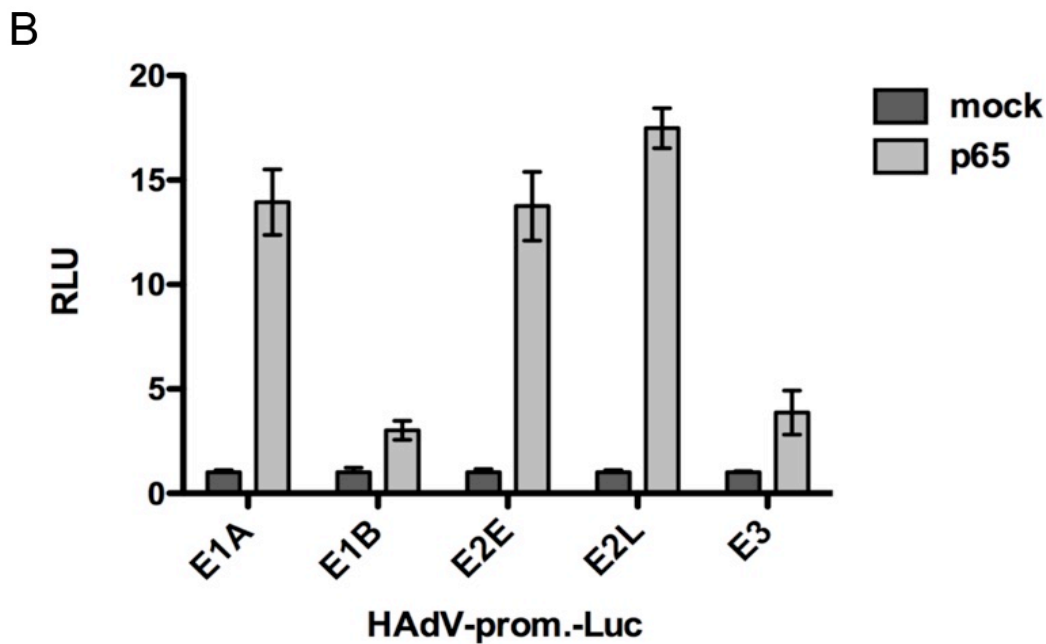


**Figure 15: NF- $\kappa$ B overexpression activates HAdV-C5 promoters.**

(A) Schematic overview of HAdV promoter region. The line in the middle denotes the size of the adenoviral genome in base pairs. The arrows depict the direction of transcription. The bold italic letters show the NF- $\kappa$ B binding motifs within the promoter regions. (B) H1299 cells were transfected with 1  $\mu$ g of either HAdV promoter, 0.5  $\mu$ g of pRL-TK (*Renilla*-Luc), 0.5  $\mu$ g of pGL3 Basic and 1  $\mu$ g of p65 (3.4.1). Whole cell extracts were prepared and luciferase activity was determined (3.10.5). The firefly luciferase activity measured for the different HAdV promoter constructs was normalized to its respective *Renilla* luciferase activity as an internal transfection control. The mean and standard deviations from three dependent experiments are presented.

As illustrated in Figure 15, p65 activated each, E1A and E2E promoters, to 14-fold, while it increased to 17-fold for the E2L promoter. The results obtained with the viral E2E promoter construct were expected since it has been described that the viral E2E promoter has two NF- $\kappa$ B binding sites (Machitani *et al.*, 2016). We could verify activation of this promoter upon cotransfection with p65 (Figure 15).

However, activation of the E1A and E2L promoter was not expected, as both promoters do not harbor conserved NF- $\kappa$ B binding sites. Further, this assay revealed a 4.5-fold induction of luciferase activity when the E3 promoter construct was cotransfected with p65. The E3 promoter construct in this assay does not include the potential NF- $\kappa$ B binding site, which explains the low level of induction of this promoter. In line with this, we could detect induction of the E1B promoter to 4-fold comparable to the E3 promoter.

In summary the results show a regulatory mechanism between viral components with the cellular NF- $\kappa$ B pathway.

#### 4.2.2 NF- $\kappa$ B promoter activity is highly regulated by transient expression of HAdV-C5 proteins

In the last years, many publications have described viral mechanisms for activation or inhibition of the NF- $\kappa$ B pathway, revealing an unlimited diversity in the regulation of this pathway by viruses (Amaya *et al.*, 2014; Brady & Bowie, 2014; Hodgson & Wan, 2015; Le Negrate, 2011; Pahl, 1999; Pham & Tenover, 2010; Rahman & McFadden, 2011; Zhao *et al.*, 2015). Viruses tightly regulate the immediate early step of immune activation in order to benefit from activation or inhibition of the immune determinants. Viral targets of the immune pathway can be broadly classified into three categories based on the site of inhibition within the NF- $\kappa$ B pathway comprising the TLRs, IKK complex or the transcriptional level.

To elucidate the role of adenoviral proteins on NF- $\kappa$ B pathway regulation, H1299 cells were co-transfected with the NF- $\kappa$ B promoter construct and either early or late adenoviral protein expressing constructs (see Figure 16). The reporter gene expression construct used in this assay encodes a luciferase gene under the control of a (5x) NF- $\kappa$ B-ELAM-promoter. Firefly luciferase expression/activity directly correlates with transcriptional activation of NF- $\kappa$ B. p*Renilla*-Luc was cotransfected to determine the transfection efficiency for normalization.

This experiment showed that the early protein E1A highly increased the NF- $\kappa$ B promoter to 7-fold, while the late protein L4-100K and the core protein pV and pVII activated the NF- $\kappa$ B promoter 4-fold compared to the control.

Previous results have shown activation of NF- $\kappa$ B upon HAdV-C5 infection either with a high multiplicity of infection (MOI) (Rajaiya *et al.*, 2008) or transduction with a high titer of adenoviral vectors (Borgland *et al.*, 2000; Gloria P Bowen & Daniel, 2004; Muruve *et al.*, 1999).

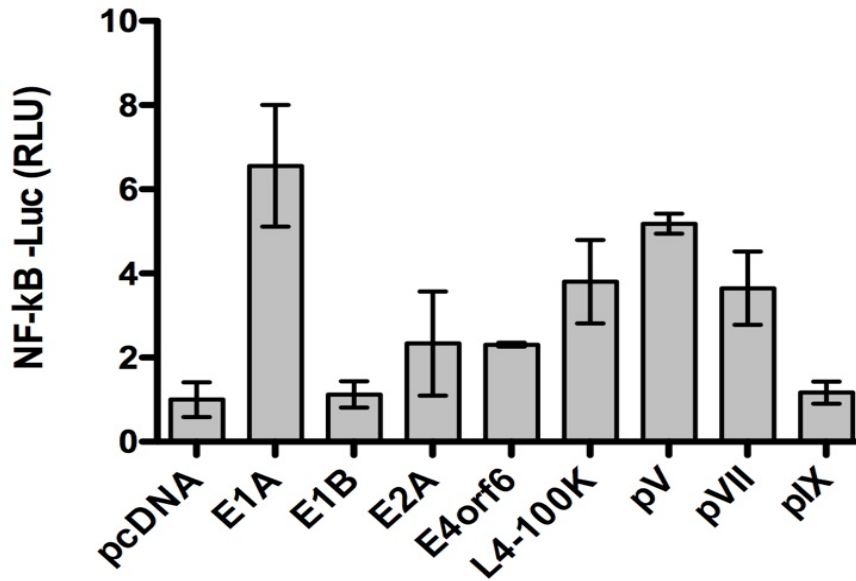


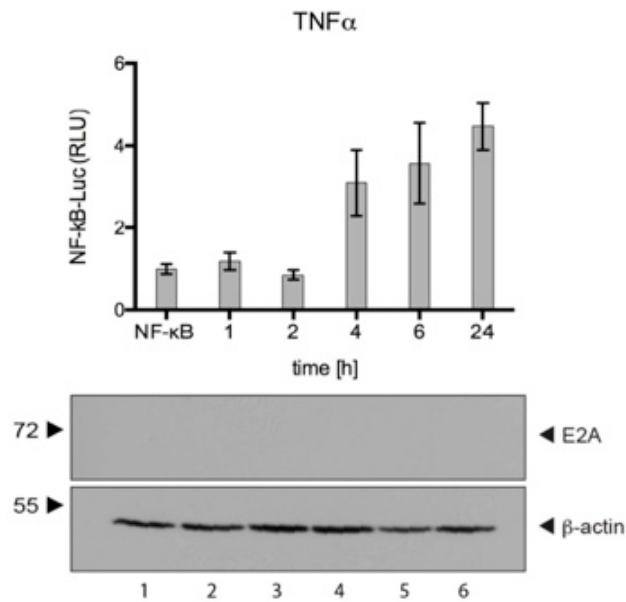
**Figure 16: Overexpression of HAdV-C5 proteins modulates NF- $\kappa$ B promoter activation.**

H1299 cells were transfected with 0.5  $\mu$ g of pRL-TK (Renilla-Luc), 0.5  $\mu$ g pGL3 Basic 5x NF- $\kappa$ B-Elam-prom as indicated and 1  $\mu$ g of plasmid expressing viral proteins (3.4). Total protein extracts were prepared and luciferase activity was determined (3.10.5). The *Firefly*-luciferase activity was normalized to the 5x-Elam-prom expressed alone and its respective Renilla luciferase activity as a transfection control efficiency control. The mean and standard deviations are presented for three technical replicates.

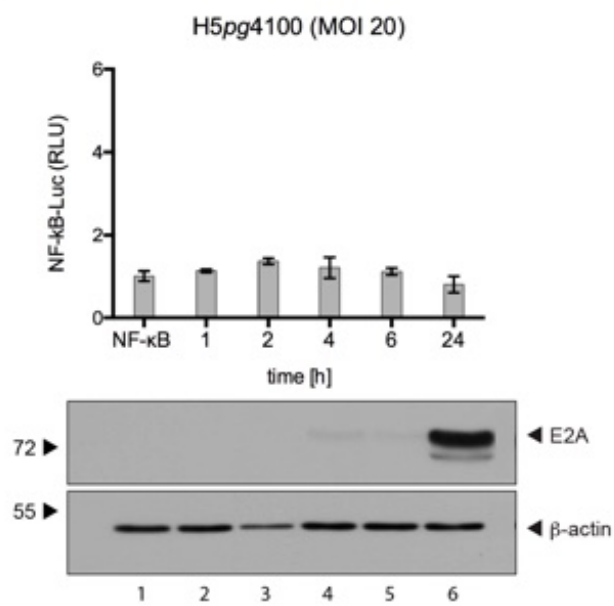
It has been shown that proteins from the E3 region have immunomodulatory functions (Burgert & Blusch, 2000). Therefore, we used a HAdV-C5 that is deleted in the viral region E3 in order to elucidate the role of HAdV-C5 proteins on NF- $\kappa$ B regulation during viral infection, in an E3-independent manner. H1299 were infected with a low (MOI 20) and a high virus concentration (MOI 100) to mimic a more physiological situation and to force a putative induction of the immune response, respectively (Figure 17). The activation of NF- $\kappa$ B promoter was then analyzed in a transient reporter gene assay after HAdV-C5 wild type delta E3 virus infection (see Figure 17BC). Tumor necrosis factor  $\alpha$  (TNF $\alpha$ ) is a pro-inflammatory cytokine that induces diverse cellular responses varying from apoptosis to the expression of genes involved in both early inflammatory and acquired immune responses (Rahman & McFadden, 2011). TNF $\alpha$  is known as one of the most potent physiological inducers of the nuclear transcription factor NF- $\kappa$ B (Schutze *et al.*, 1995). So, in order to analyze the effects of HAdV-C5 infection on TNF $\alpha$ -mediated NF- $\kappa$ B induction, we treated H1299 cells with 20 ng/ml TNF $\alpha$ , and then infected treated and non-treated cells with HAdV-C5. We have observed, as expected, that TNF $\alpha$  treatment induced 3-fold

luciferase expression starting at 4 hours after treatment and lasting up to 24 hours (4.5-fold) after treatment (Figure 17A, lanes 4-6).

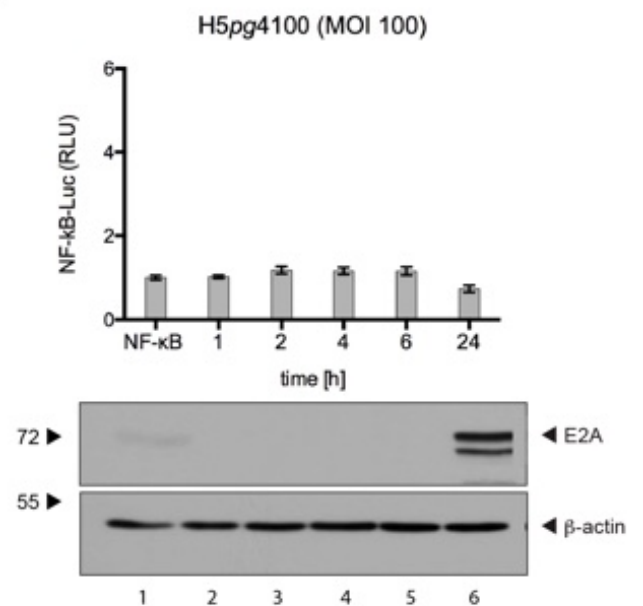
A



B



C



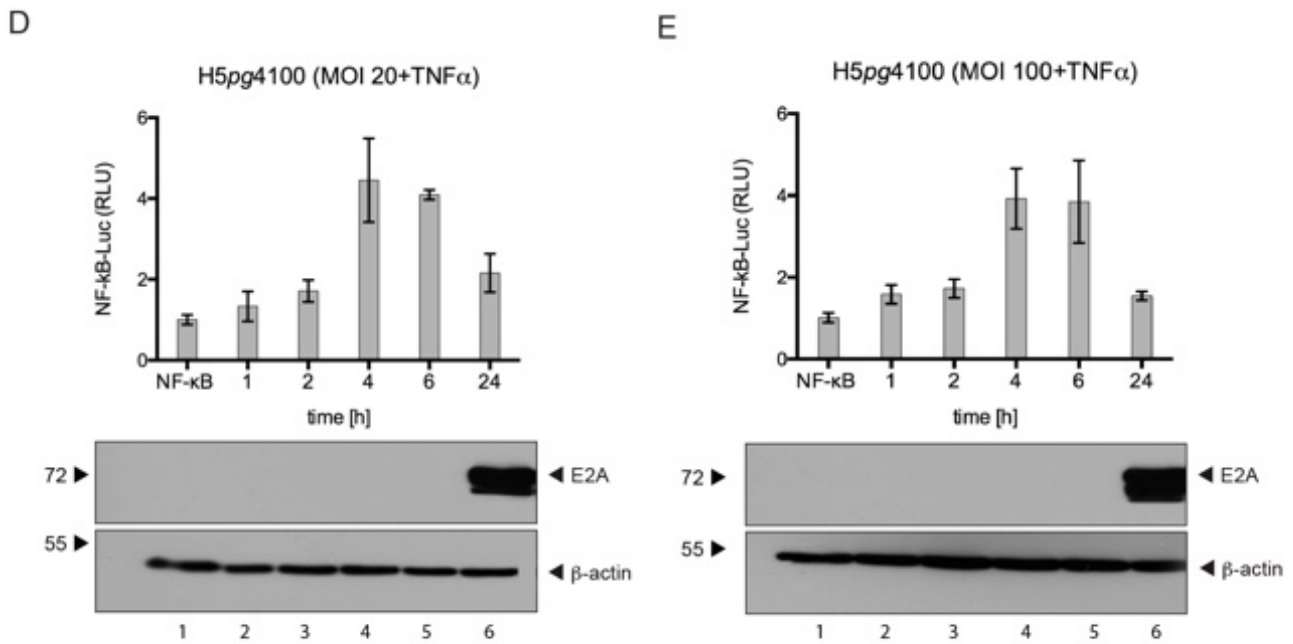


**Figure 17: NF- $\kappa$ B promoter is not activated during HAdV-C5 productive infection.**

H1299 cells were transfected with 0.5  $\mu$ g of pRL-TK (Renilla-Luc), 0.5  $\mu$ g pGL3-Basic Prom NF- $\kappa$ B (5x-NF- $\kappa$ B-ELAM-promoter) (3.4.1). Cells were (A) treated with 20 ng/ml TNF $\alpha$  at indicated time points before cell lysis or (B, C) infected with Ad wt (*H5pg4100*) at a multiplicity of 20 or 100 ffu/cell at indicated (3.5.1). (D, E) Cells were treated with TNF $\alpha$  1 hour before infection and were infected for indicated hours prior to cell lysis (3.5.1). Total-cell extracts were prepared and luciferase activity was determined (3.10.5). Firefly-luciferase activity derived from the NF- $\kappa$ B-responsive reporter measurement was normalized to its respective Renilla luciferase activity for transfection efficiency. The mean and standard deviations are presented for three technical replicates. To determine adenoviral infection and the usage of equal amount of cell lysate for measurement, total-cell lysates were resolved by 10 % SDS-PAGE and visualized by immunoblotting (3.9). E2A levels as infection control was detected using mAb B6-8 ( $\alpha$ -E2A) and actin using mAb AC-15 ( $\alpha$ - $\beta$ -actin) served as loading control. Molecular weights in kDa are indicated on the *left*, while corresponding proteins are labeled on the *right*.

However, H1299 cells only infected with HAdV-C5, without TNF $\alpha$  treatment, at either MOI 20 (Figure 17B) or MOI 100 (Figure 17C) did not show activation at any time point after infection (Figure 17BC, lane 1-6). Interestingly, the level of NF- $\kappa$ B activity at 24 hpi at MOI 20 (Figure 17B, lane 6) and MOI 100 (Figure 17C, lane 6) was slightly lower than in non-infected cells (Figure 17A, lane 6). In contrast, when cells were first treated with TNF $\alpha$  and then infected, HAdV-C5 could counteract NF- $\kappa$ B activation by TNF $\alpha$  at late time points of infection (24 h), coinciding with E2A expression (Figure 17DE). Therefore, we assume that HAdV-C5 encodes for a protein that counteracts this host defense mechanism.

### 4.2.3 Role of IKK complex proteins during HAdV-C5 infection

NF- $\kappa$ B pathway activation converges from various signals at the IKK complex, which could be a potential target complex upon HAdV-C5 infection. In order to investigate the fate of IKK complex proteins after adenoviral infection, we examined their expression level in a time course experiment (see Figure 18). Therefore, A549 cells were chosen to study infection experiments as this cell line has been used extensively to investigate the NF- $\kappa$ B pathway especially with influenza viruses (Gao *et al.*, 2012; Pauli *et al.*, 2008; Wang *et al.*, 2012). Further, they are derived from respiratory epithelial cells, which as been shown to be the cellular target for natural HAdV-C5 infection *in vivo* (Schmitz *et al.*, 1983). However, A549 is not transfectable with the methods established in our lab. Conversely, all transient transfection experiments were done in H1299 cells, another lung epithelial cell line, as this cell line has higher transfection efficiency than A549 cells. For analysis of IKK protein levels across a time course of infection, A549 cells were HAdV-C5 infected and harvested at 0, 2, 4, 8, 16, 24, 48, and 72 hpi. Proteins from whole-cell lysates were analyzed by SDS-PAGE and western blotting.

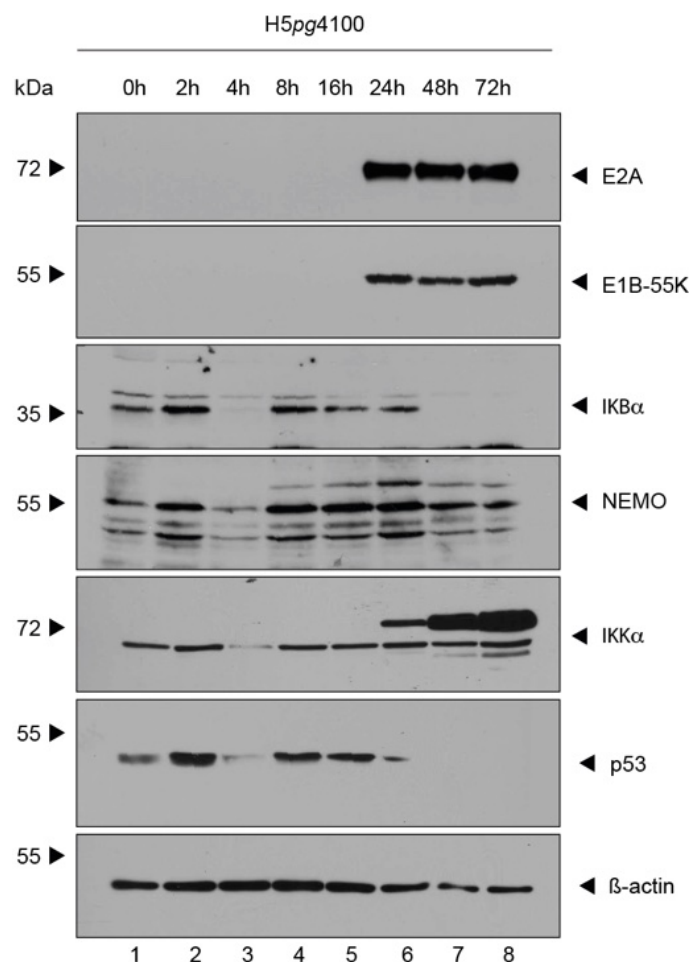


**Figure 18: Expression levels of IKK proteins upon HAdV-C5 infection in A549 cells.**

A549 cells were infected with H5pg4100 at a multiplicity of 20 ffu/cell and proteins from whole-cell extracts were separated by SDS-PAGE (3.9) and subjected to immunoblotting using Ab rabbit C-21 ( $\alpha$ -I $\kappa$ B $\alpha$ ), Ab rabbit FL-419 ( $\alpha$ -NEMO), Ab rabbit M-204 ( $\alpha$ -IKK $\alpha$ ), mAb AC-15 ( $\alpha$ - $\beta$ -actin), mAb DO-I ( $\alpha$ -p53), mAb B6-8 ( $\alpha$ -E2A) and mAb 2A6 ( $\alpha$ -E1B-55K). Molecular weights are indicated in kDa on the left side of the panels, while the corresponding proteins are labeled on the right side.

The levels of NF- $\kappa$ B pathway proteins I $\kappa$ B $\alpha$ , NEMO and IKK $\alpha$  were investigated over a time course. Expression levels of I $\kappa$ B $\alpha$  served as an indicator for the NF- $\kappa$ B activity as activation of the NF- $\kappa$ B pathway is linked to the proteasomal degradation of I $\kappa$ B $\alpha$  (Palombella *et al.*, 1994; Traenckner *et al.*, 1994). I $\kappa$ B $\alpha$  expression level is reduced 16 hpi and completely disappeared at 48 and 72 hpi (Figure 18, lane 5-7). This reduction indicates activation of NF- $\kappa$ B at later time points after infection. The cellular level of the IKK complex proteins IKK $\alpha$  and NEMO appeared to stay stable at all time points tested. Besides, NEMO specific antibody detected a slower migrating band at 8 hpi, which migrates at approximately 70 kDa (Figure 18, lane 4). An additional higher migrating band at around 100 kDa is also visible in the staining with IKK $\alpha$  specific antibody at 24 hpi (Figure 18, lane 4). Viral infection was evidenced by detection of the early proteins E2A and E1B-55K at 24 hours after infection (Figure 18, lane 6). Activation of NF- $\kappa$ B is accompanied with complete nuclear relocalization of p65 as shown for many other viruses (reviewed in (Hiscott *et al.*, 2001)). In order to verify whether NF- $\kappa$ B is activated upon adenoviral infection, H1299 cells were transfected with p65 a subunit of NF- $\kappa$ B heterodimer, and infected at 6 hpt with HAdV-C5 (MOI 20). At 24 hpi, cells were subjected to immunofluorescence analysis (Figure 19).

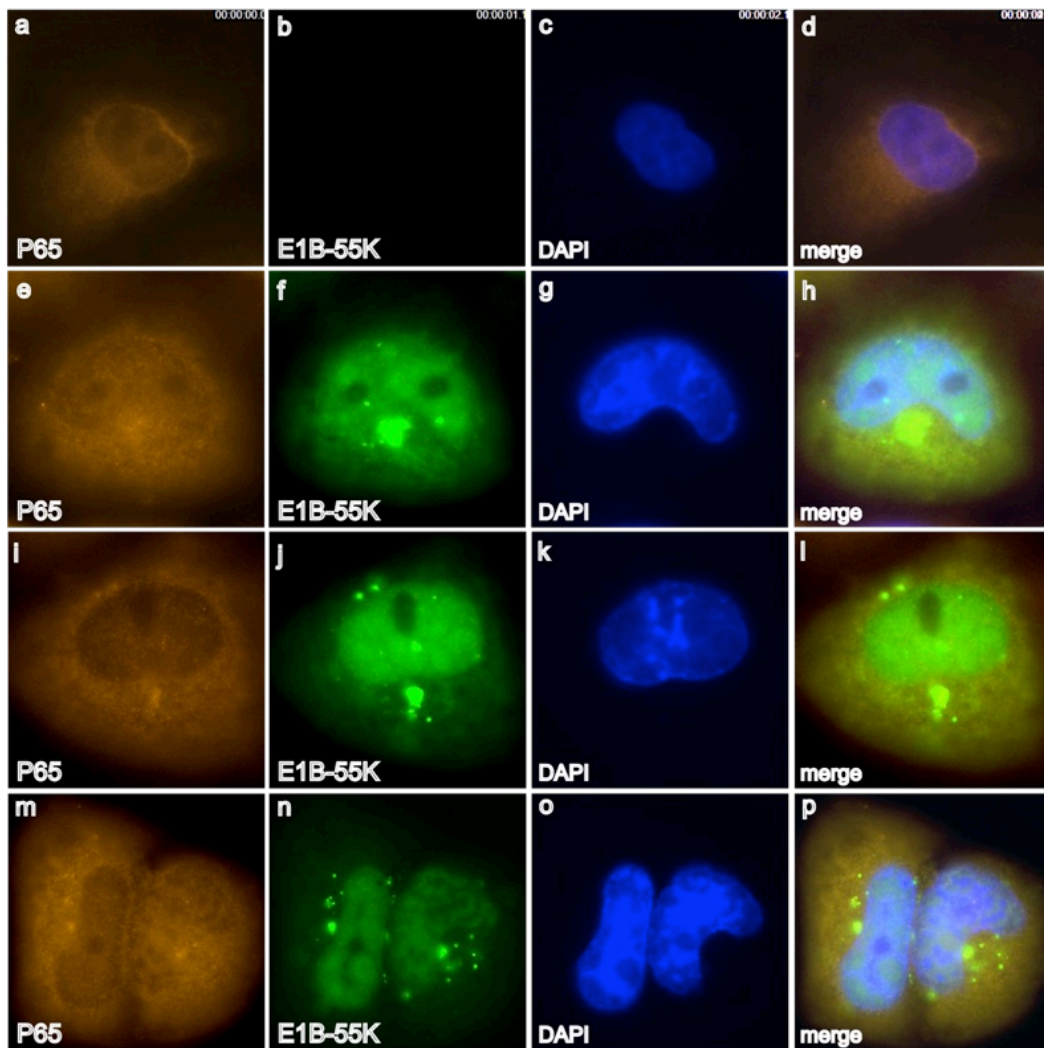


**Figure 19: p65 fails to relocalize into the nucleus upon HAdV-C5 infection.**

A549 cells were infected with H5pg4100 and were fixed 24 hpi with 4 % PFA and double labeled with mAb 2A6 ( $\alpha$ -E1B-55K) and mAb C-20 ( $\alpha$ -p65). Primary Abs were detected with Cy3 ( $\alpha$ -p65) and Alexa 488 ( $\alpha$ -E1B-55K) conjugated secondary Abs. For nuclear staining, the DNA intercalating dye DAPI was used. Representative  $\alpha$ -E1B-55K and  $\alpha$ -p65 staining patterns of at least 29 analyzed cells are shown. Overlays of single images (merge) are shown (magnification  $\times$  7600). One representative field for mock cells is shown (a-d) and three representative fields are shown for HAdV-infected cells.

As shown in (Figure 19) endogenous p65 localized mainly within the cytoplasm at the nuclear lamina, but it was also detectable within the nucleus (Figure 19a). Adenoviral infected cells are indicated by staining of the viral E1B-55K protein (Figure 19f, j, n). After infection the overall distribution of p65 within the cell was comparable to non-infected cells (Figure 19e, i, m). Taken together, the putative activation of NF- $\kappa$ B after adenoviral infection shown by western blot analysis could not be verified by immunofluorescence analysis, as p65 still localizes within the cytoplasm after HAdV-C5 infection (Figure 19e, m). This result confirms the

luciferase measurement (Figure 17) where no activation of NF- $\kappa$ B was measurable after adenoviral infection (Figure 17BC).

### 4.3 Interplay between HAdV-C5 and IKK complex components

#### 4.3.1 HAdV-C5 reduces the IKK complex formation

Many viruses encode for viral proteins in order to target the NF- $\kappa$ B pathway. As an example, HCV expresses the proteases NS3-NS4 causing proteolysis of TRIF, which is important for TLR9-mediated activation of NF- $\kappa$ B (Abe *et al.*, 2007). Besides, NS5B and the core proteins of HCV inhibit activation of the IKK complex by interaction with IKK proteins (Choi *et al.*, 2006; Joo *et al.*, 2005). Regulation of the NF- $\kappa$ B pathway by adenoviruses could be maintained at several steps after infection at multiple NF- $\kappa$ B signaling molecules. In order to investigate whether HAdV interfere or cooperate with the main kinase complex of the NF- $\kappa$ B pathway, H1299 cells were co-transfected with constructs expressing human Flag-tagged IKK $\alpha$ , IKK $\beta$  and human HA-tagged NEMO alone and then infected with H5pg4100 virus (MOI 20). Cells were harvested 24 h later and subjected to immunoprecipitation analysis.

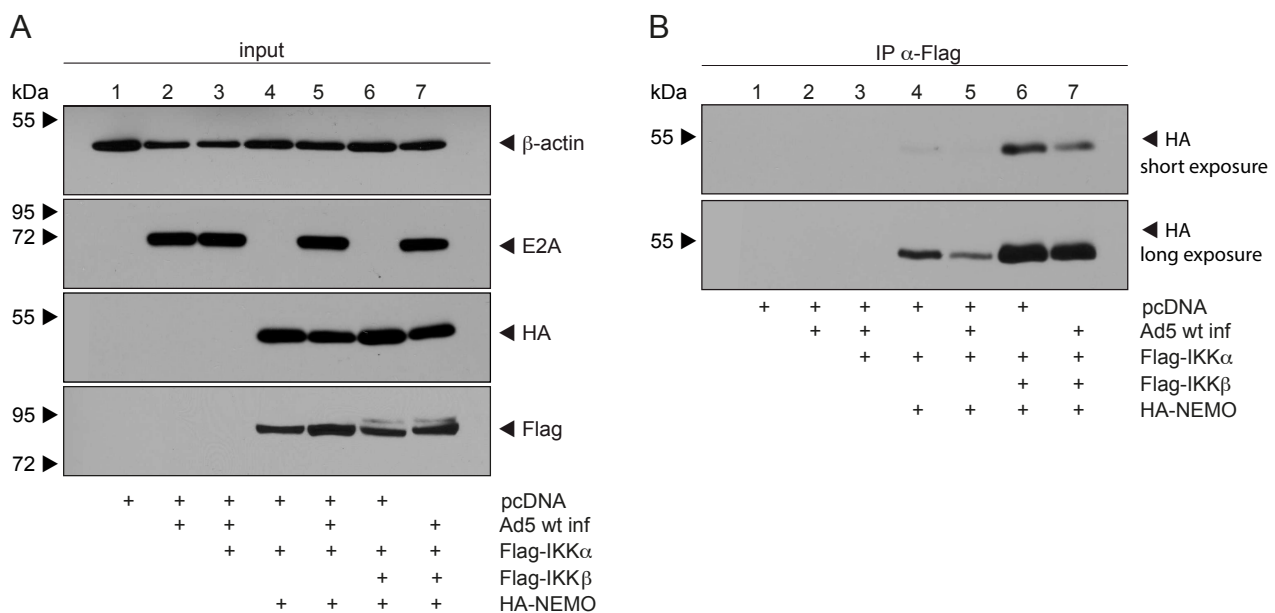


**Figure 20: HAdV infection reduces the interaction between IKK proteins.**

Subconfluent H1299 cells were transfected with 5  $\mu$ g of human Flag-tagged IKK $\alpha$  and IKK $\beta$  and HA-tagged NEMO (3.4). Cells were infected 24 hours after transfection with H5pg4100 at a multiplicity of 20 ffu/cell (3.5.1) and harvested 24 hpi (3.3). After total protein extraction, immunoprecipitation of Flag-tagged proteins was performed by using Flag-beads M2, resolved by 10 % SDS-PAGE and visualized by immunoblotting (3.9). Input levels (A) of total cell lysates were detected using mAb Flag-M2 ( $\alpha$ -Flag), mAb B6-8 ( $\alpha$ -E2A) and mAb

AC-15 ( $\alpha$ - $\beta$ -actin). Coprecipitated proteins (B) were stained with mAb 3F10 ( $\alpha$ -HA). Molecular weights are indicated in kDa on the left side of the panels, while the corresponding proteins are labeled on the right side.

The results showed that IKK $\alpha$  is able to co-immunoprecipitate with NEMO both in the absence and in the presence of IKK $\beta$  (Figure 20B, lanes 4 and 6, respectively), in concordance with what has been previously published (May, 2000; May *et al.*, 2002). Interestingly, HAdV-C5 infected cells showed a decrease in the amount of immunoprecipitated Flag-tagged-proteins, indicating that HAdV-C5 interferes with the binding capacity of the IKK complex components (Figure 20B, lanes 5 and 7).

#### **4.3.2 HAdV-C5 E1B-55K interacts with the IKK complex upon infection**

The HAdV-C5 E1B-55K protein is a multifunctional protein, which has been extensively studied, with different roles during adenovirus lytic life cycle. It contributes to degrade specific cellular proteins by forming an ubiquitin ligase complex together with E4orf6 in the early phase of infection (Blanchette *et al.*, 2008; Querido, 2001; Querido *et al.*, 2000).

It has been reported that the E1B-55K protein controls expression of genes that are involved in the NF- $\kappa$ B pathway regulation and in the interferon response (Miller *et al.*, 2009). Due to the role of E1B-55K on the immune response and as HAdV-C5 infection showed a reduced IKK complex formation capacity, immunoprecipitation experiments were performed to elucidate a putative role of E1B-55K in regulating the IKK complex (see Figure 21). Therefore, H1299 cells were transfected with human Flag-tagged IKK $\alpha$ , IKK $\beta$  and NEMO and infected with H5pg4100 at 8 hpt.

The staining for Flag-tagged proteins revealed interaction between E1B-55K and Flag-tagged IKK $\alpha$  and NEMO (Figure 21B, lane 3 and 5). Short exposure of the membrane showed a strong interaction between E1B-55K and NEMO (Figure 21B, lane 5) whereas the interaction between IKK $\alpha$  and E1B-55K shown in Figure 22 upon cotransfection was only detectable after long exposure time.

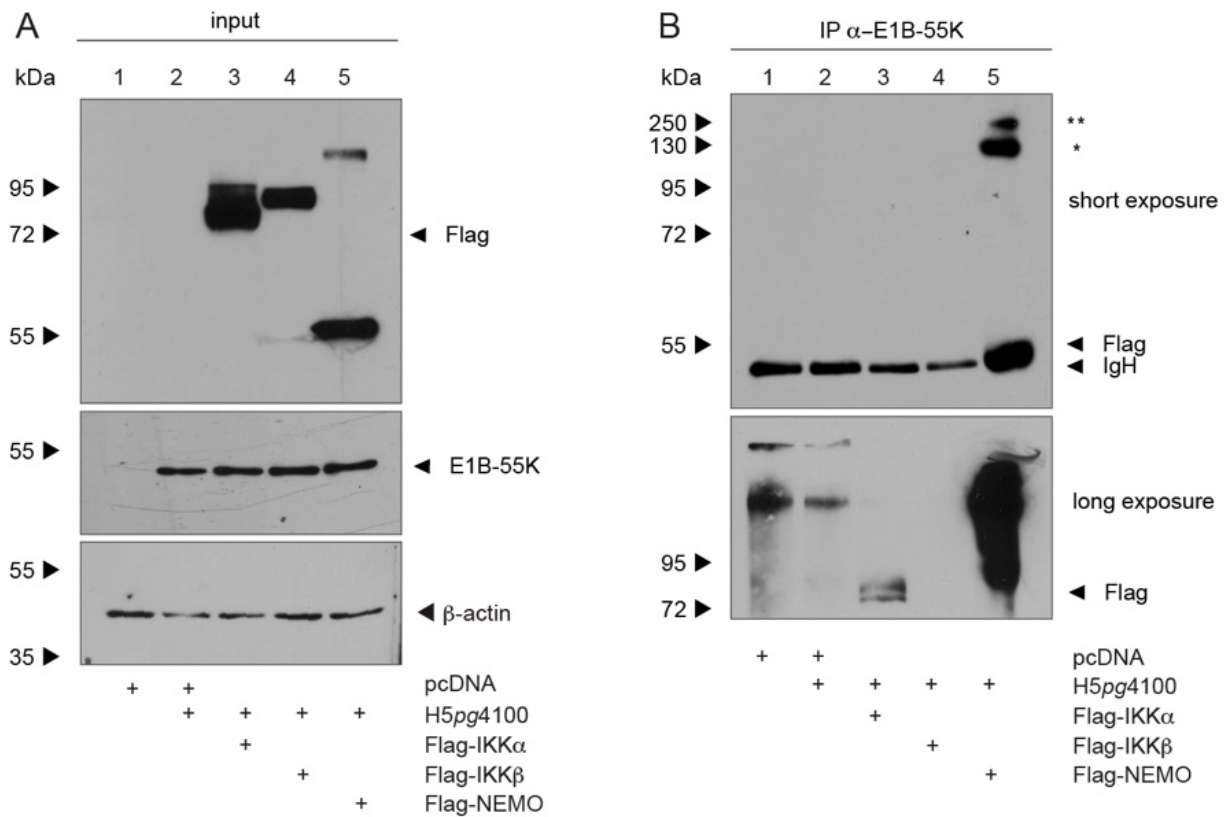


**Figure 21: E1B-55K interacts with IKK $\alpha$  and NEMO upon HAdV infection.**

Subconfluent H1299 cells ( $4 \times 10^6$ ) were transfected with 5  $\mu$ g of human Flag-tagged IKK $\alpha$  and IKK $\beta$  and NEMO and infected 8 hpt with H5pg4100 at a multiplicity of 20 ffu/cell (3.5.1). Cells were harvested 24 hpi and then whole-cell extracts were prepared (3.4.3). Immunoprecipitation of Flag-tagged proteins was performed with Flag antibody conjugated to sepharose beads, resolved by 10 % SDS-PAGE and visualized by immunoblotting (3.9). Input levels (A) of total cell lysates were detected using mAb Flag-M2 ( $\alpha$ -Flag), mAb 2A6 ( $\alpha$ -E1B-55K) and mAb AC-15 ( $\alpha$ - $\beta$ -actin). Coprecipitated proteins (B) samples were stained with mAb Flag-M2 ( $\alpha$ -Flag). NEMO oligomerization is indicated by asterisks whereas (\*) denotes NEMO dimer and (\*\*) NEMO trimer. Molecular weights are indicated in kDa on the left side, while corresponding proteins are labeled on the *right*.

Beside the interaction between NEMO with E1B-55K, western blot results show a higher migrating band upon overexpression of NEMO, which is recognized by a NEMO specific antibody indicating its dimerization by size (Figure 21B, lane 5). NEMO has a size of 48 kDa protein, which usually migrate at around 55 kDa on a 10 % SDS-gel. Upon cotransfection of NEMO and subsequent virus infection, two slower migrating bands at around 110 kDa and 250 kDa appeared. This band corresponds assumably to NEMO dimers (\*) and trimers (\*\*) because of the sizes and the specific detection by the NEMO antibody. Intriguingly, it has been shown that oligomerization of NEMO is important for its full functionality (Agou *et al.*, 2004; Agou *et al.*, 2002; Fontan *et al.*, 2007; Herscovitch M., 2008; Marienfeld *et al.*, 2006;

Vinolo *et al.*, 2006). Interestingly, E1B-55K seems to interact after adenoviral infection. The results indicate a regulatory role of E1B-55K on the IKK complex proteins.

### 4.3.3 HA $\Delta$ V-C5 E1B-55K and E1B-156R interact with the IKK complex

The interaction between E1B-55K and the IKK proteins was investigated more in detail in order to reveal whether the interaction occurs independent on further viral proteins. Therefore, immunoprecipitation experiments were repeated with E1B-55K, which were cotransfected with each of the Flag-tagged IKK proteins in H1299 cells (Figure 22).

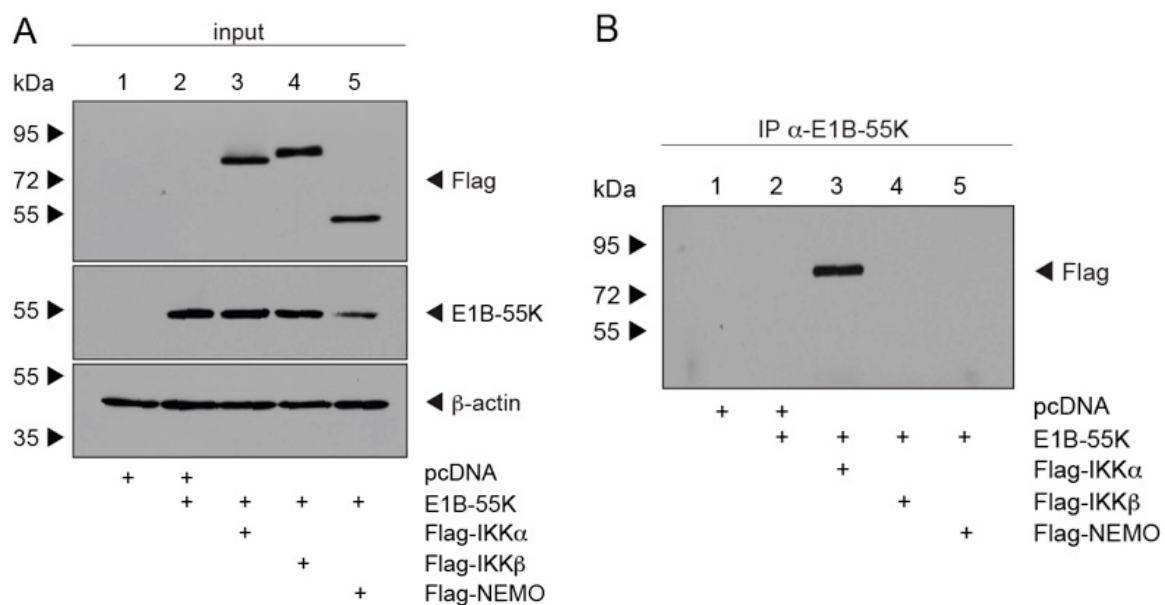


**Figure 22: Overexpressed E1B-55K interacts with IKK complex components.**

Subconfluent H1299 cells ( $4 \times 10^6$ ) were cotransfected with  $5 \mu\text{g}$  of E1B-55K and  $5 \mu\text{g}$  of human Flag-tagged IKK $\alpha$  and IKK $\beta$  and NEMO (3.4). Cells were harvested 48 hpt before preparing whole-cell extracts (3.4.3). Immunoprecipitation of Flag-tagged proteins was performed with mAb Flag-M2 ( $\alpha$ -Flag), resolved by 10 % SDS-PAGE and visualized by immunoblotting (3.9). Input levels (A) of total cell lysates were detected using mAb Flag-M2 ( $\alpha$ -Flag), mAb 2A6 ( $\alpha$ -E1B-55K), mAb FL-419 ( $\alpha$ -NEMO) and mAb AC-15 ( $\alpha$ - $\beta$ -actin). Coprecipitated proteins (B) samples were stained with mAb Flag-M2 ( $\alpha$ -Flag). Molecular weights are indicated in kDa on the left side, while corresponding proteins are labeled on the *right*.

Input samples for direct immunoprecipitation of E1B-55K showed sufficient and similar amounts of the transfected and the endogenous proteins (see Figure 22A).

E1B-55K could only interact with IKK $\alpha$  but not with NEMO, in contrast to a full virus infection (Figure 21, lane 3). This would indicate that other viral proteins are necessary to interact with NEMO. Interestingly, E1B-55K expression levels were lower in NEMO cotransfected cells (Figure 22, lane 5).

In order to confirm the interaction through a further assay and to narrow down the binding site between E1B-55K and IKK $\alpha$ , a GST-pull down experiment was performed (3.10). Therefore, bacterial expressed GST-tagged E1B-55K wt, different truncation mutants and isoforms of E1B-55K were purified and conjugated to glutathione-sepharose beads. These beads were then incubated with A549 cell lysates and later analyzed by SDS-PAGE and western blotting.

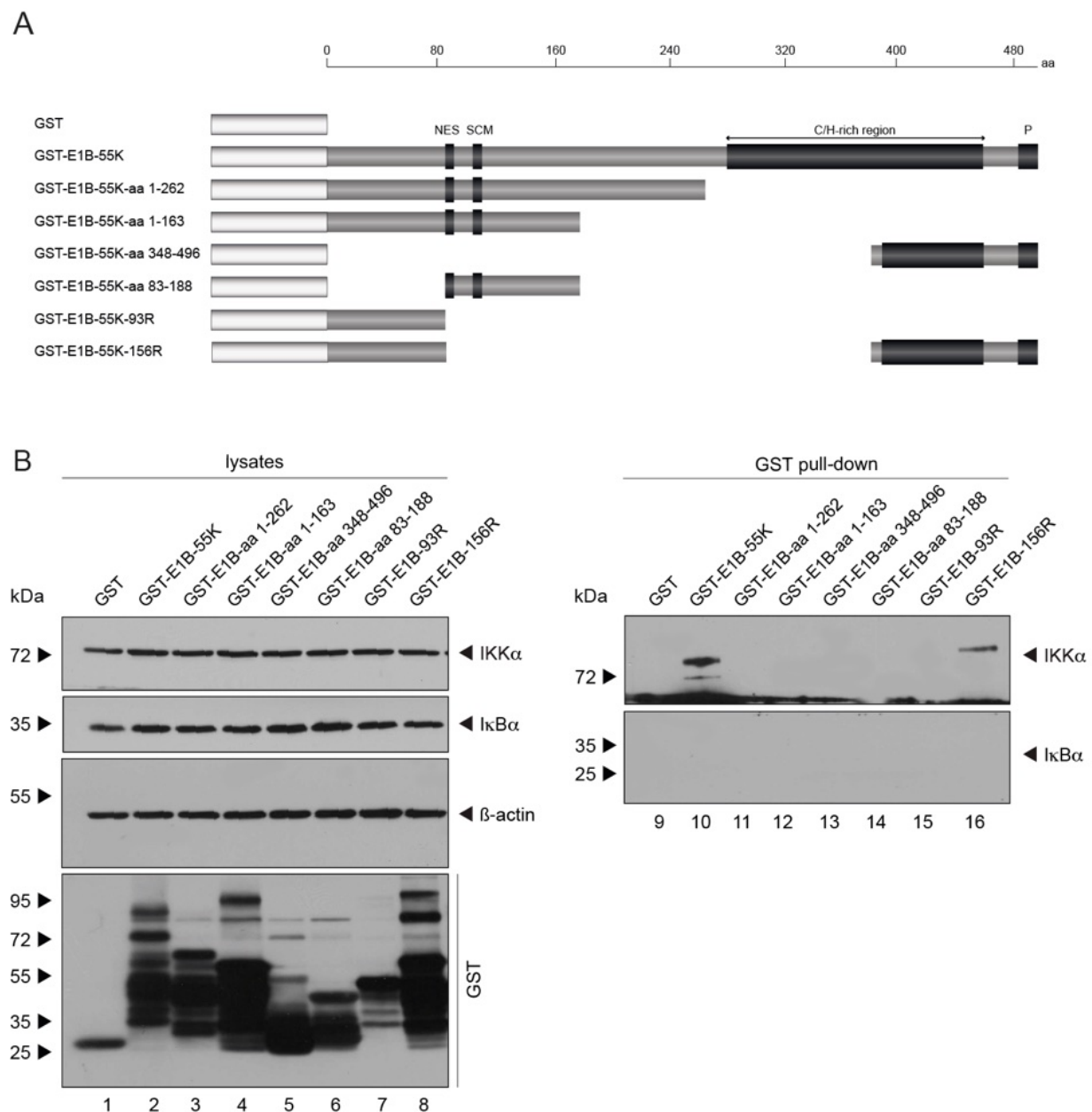


**Figure 23: IKK $\alpha$  interacts with GST-E1B-55K wt and GST-E1B-156R isoform.**

Subconfluent A549 cells were harvested and whole cell extracts were prepared (3.4.3). Bacterial (*E. coli*) expressed GST-tagged E1B-55K truncation mutants (A) were conjugated to

glutathione sepharose beads and incubated with 750  $\mu$ g of protein lysates, resolved by 10 % SDS-PAGE and visualized by immunoblotting with Ab M-204 ( $\alpha$ -IKK $\alpha$ ) (4.9) (B; *right*). As a control, the same experiment was done in duplicate and stained also with Ab C-21 ( $\alpha$ -IKB $\alpha$ ) (B; *right*). Input levels (B; *left*) of total-cell lysates were detected using Ab M-204 ( $\alpha$ -IKK $\alpha$ ), Ab C-21 ( $\alpha$ -IKB $\alpha$ ) and mAb AC-15 ( $\alpha$ - $\beta$ -actin). Molecular weights are indicated in kDa on the left side, while corresponding proteins are labeled on the *right*. aa: amino acid; NES: nuclear export signal; SCM: SUMO conjugation motif; C/H-rich region: Cysteine/Histidine-rich region; P: phosphorylation site.

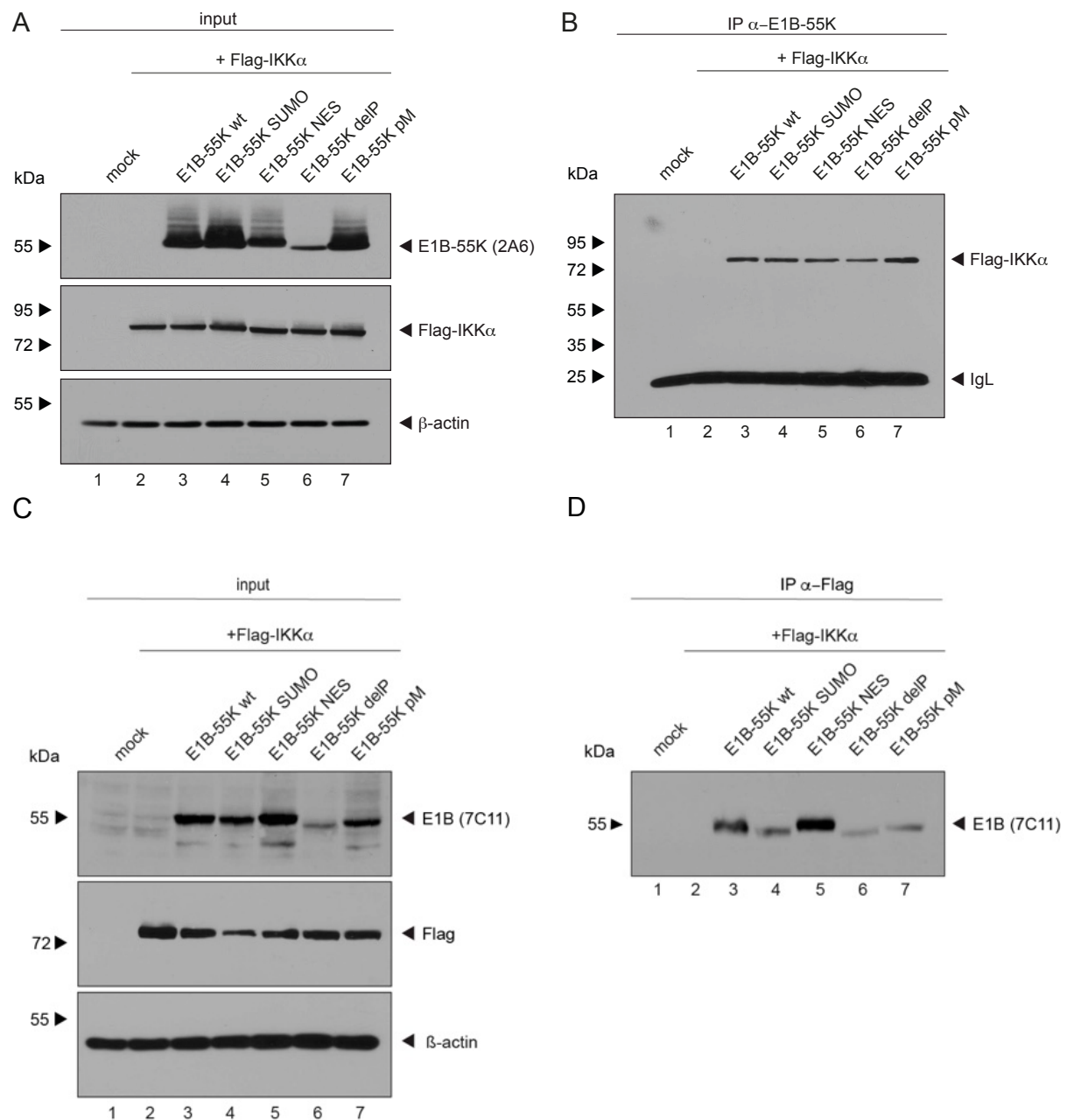
GST-pull down experiments confirmed the interaction between IKK $\alpha$  and E1B-55K as shown in Figure 21 and 22 (Figure 23, lane 10). Additionally, IKK $\alpha$  interacts with the isoform 156R of E1B-55K, which shares the same N- and C-terminus as E1B-55K but misses the central part (Figure 23A). This isoform lacks the NES and SUMO conjugation motif, therefore localizes in the cytoplasm and is not SUMOylated. However, 156R is phosphorylated at its C-terminus like E1B-55K. These results indicate that the central part of E1B-55K is not necessary for its interaction with IKK $\alpha$ , whereas protein folding or phosphorylation of E1B could be crucial for their interaction.

#### 4.3.4 Characterization of the binding between host IKK $\alpha$ and HAAdV-C5 E1B-55K

##### 4.3.4.1 Posttranslational modification of E1B-55K is dispensable for IKK $\alpha$ interaction

Posttranslational modifications of proteins are strategies to increase the diversity of protein functions, such as subcellular localization, stability as well as interaction properties. E1B-55K is a viral protein, which is posttranslationally modified by several posttranslational modifiers. So far it has been described that it is SUMOylated at lysine 104 (Endter & Dobner, 2004; Endter *et al.*, 2001) and phosphorylated at the serines 490 and 491 (S490/491) and threonine 495 (T495) (Teodoro & Branton, 1997; Teodoro *et al.*, 1994). It has been shown that inhibition of E1B-55K SUMO modification enhances its preference for cytoplasmic localization (Endter *et al.*, 2001). Accordingly, mutation of the *nuclear export signal* (NES) by changing its leucines 83, 87, 91 to alanines results in E1B-55K nuclear retention and subsequently more SUMOylated E1B-55K within the nucleus (Krätzer *et al.*, 2000). The E1B-55K delP variant has a mutation in the phosphorylation site and it is therefore not phosphorylated, which, in turn, has been shown to influence its SUMOylation of the viral factor (Wimmer *et al.*, 2012). In contrast, E1B-55K pM is a phosphomimetic mutant in which amino acid substitutions are introduced by changing serines to aspartic acid (Schwartz *et al.*, 2008). Aspartic acid is chemically similar to phospho-

serine, mimicking phosphorylated E1B-55K protein, leading to its increased SUMOylation rate. In order to investigate whether those posttranslational modifications of E1B-55K are important to mediate interaction with IKK $\alpha$ , we cotransfected Flag-tagged IKK $\alpha$  with E1B-55K wt and the respective variants and co-immunoprecipitated E1B-55K (see Figure 24BD).



E

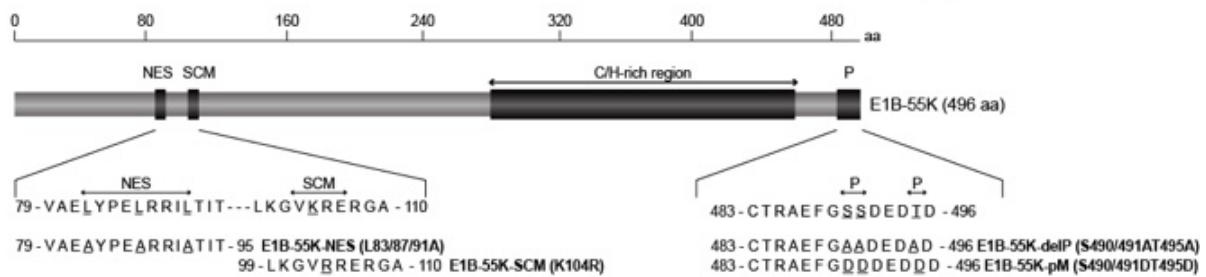


**Figure 24: IKK $\alpha$  interacts with E1B-55K PTM mutants.**

Subconfluent H1299 cells were cotransfected with 5  $\mu$ g of E1B-55K wt or indicated E1B-55K mutants and 5  $\mu$ g of human Flag-tagged IKK $\alpha$  (3.4). Cells were harvested 48 hpt before preparing whole cell extracts (3.9). Immunoprecipitation of E1B-55K was performed with mAb 2A6 ( $\alpha$ -E1B-55K), resolved by 10 % SDS-PAGE and visualized by immunoblotting (3.9.3). Input levels (A, C) of whole cell lysates were detected using mAb Flag-M2 ( $\alpha$ -Flag), mAb 2A6 ( $\alpha$ -E1B-55K), 7C11 ( $\alpha$ -E1B-55K) and mAb AC-15 ( $\alpha$ - $\beta$ -actin). Coprecipitated protein (B, D) samples were stained with mAb Flag-M2 ( $\alpha$ -Flag) or 7C11 ( $\alpha$ -E1B-55K). (E) Schematic overview of E1B-55K PTM mutants. Molecular weights are indicated in kDa (*left*), while corresponding proteins are shown in the right side of the panels. aa: amino acid; NES: nuclear export signal; SCM: SUMO conjugation motif; C/H-rich region: Cysteine/Histidine-rich region; P: phosphorylation sites

The immunoprecipitation with  $\alpha$ -E1B-55K antibody showed that E1B-55K PTM mutants were still able to interact with IKK $\alpha$  (see Figure 24B). Similar results were obtained when immunoprecipitating IKK $\alpha$  with  $\alpha$ -Flag AB and detecting E1B-55K with a different antibody (7C11), which recognizes the C-terminal part of E1B-55K (Figure 24D). Immunoprecipitation with two E1B-55K antibodies recognizing different antigens indicated that interaction between IKK $\alpha$  and E1B-55K is independent of posttranslational modifications, such as SUMOylation and phosphorylation.

#### 4.3.4.2 IKK $\alpha$ has reduced binding affinity to E1B-55K-RF6 and E1B-55K-E2 mutants

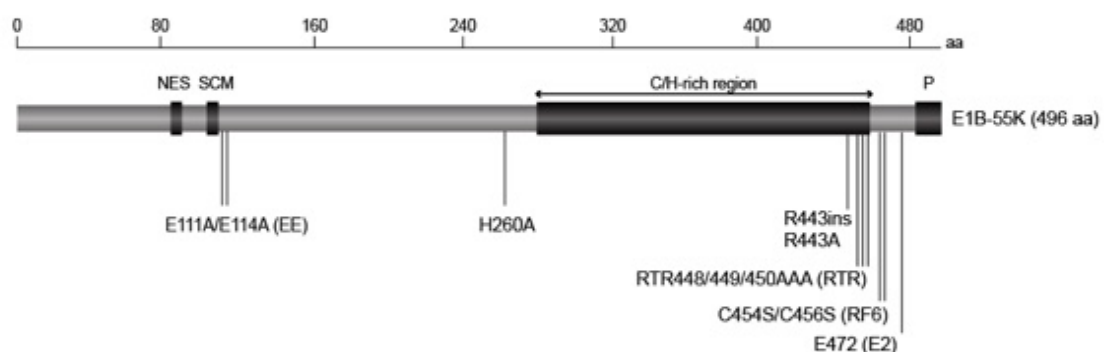
Many efforts were made to characterize the multifunctional E1B-55K protein by generating different single-amino-acid substitution mutants as well as multiple-amino-acid substitution in order to disrupt motifs or post transcriptional modification (Kindsmüller *et al.*, 2007; Schwartz *et al.*, 2008; Shen *et al.*, 2001). The experiment described above strongly suggested that those posttranslational modifications of E1B-55K are not important for interaction with IKK $\alpha$  (see Figure 24BD). However, E1B-55K PTMs are not the only determinant for interaction with other proteins. Studies by Cardoso *et al.* could narrow down one amino acid on E1B-

55K that is important for binding to cellular proteins resulting in specific phenotypes like repression of p53 and its oncogenic potential in combination with E1A (Cardoso *et al.*, 2008). These mutants were used to characterize important function of E1B-55K like the modulation of the p53 level, interaction with E4orf6 protein (Rubenwolf *et al.*, 1997), the regulation of late viral gene expression and the support of virus replication in human cancer cells.

E1B-55K-H260A has been shown to be defective in its degradation functions on p53, as well as on its interaction with E4orf6 (Härtl *et al.*, 2008). Furthermore, E1B-55K mutant R443ins is defective for inhibition of all three components of the MRN complex resulting in activation of the cellular DNA damage response, however it retains its ability to degrade p53 (Gonzalez & Flint, 2002; Yew *et al.*, 1990). The E1B-55K-EE mutant harbors mutations in the central part of the protein and its phenotype has not been published. E1B-55K-RF6 has been shown to repress p53 comparable to E1B-55K wt leading to the assumption that transformation capacity has to be comparable as both processes were believed to be prerequisites for efficient cellular transformation (Zeller, 2003). However, although transactivation of p53 is repressed, E1B-55K-RF6 mutation abolished E1B-55K transforming potential (Härtl *et al.*, 2008). E1B-55K mutants R443A, RTR and E2 were initially designed to disrupt previously described Daxx interaction motifs (Schreiner *et al.*, 2010). However, further investigations showed that only the E1B-55K-E2 mutant is able to abolish Daxx/E1B-55K interaction (Schreiner *et al.*, 2010).

To further characterize the interaction between IKK $\alpha$  and E1B-55K, we used different E1B-55K constructs and tested IKK $\alpha$  binding capacity (Figure 25). H1299 cells were cotransfected with IKK $\alpha$  and either E1B-55K-wt, E1B-55K-EE, E1B-55K-H260A, E1B-55K-R443ins, E1B-55K-R443A, E1B-55K-RTR, E1B-55K-RF6 or E1B-55K-E2 encoding plasmids before being analyzed by immunoprecipitation (Figure 25).

A



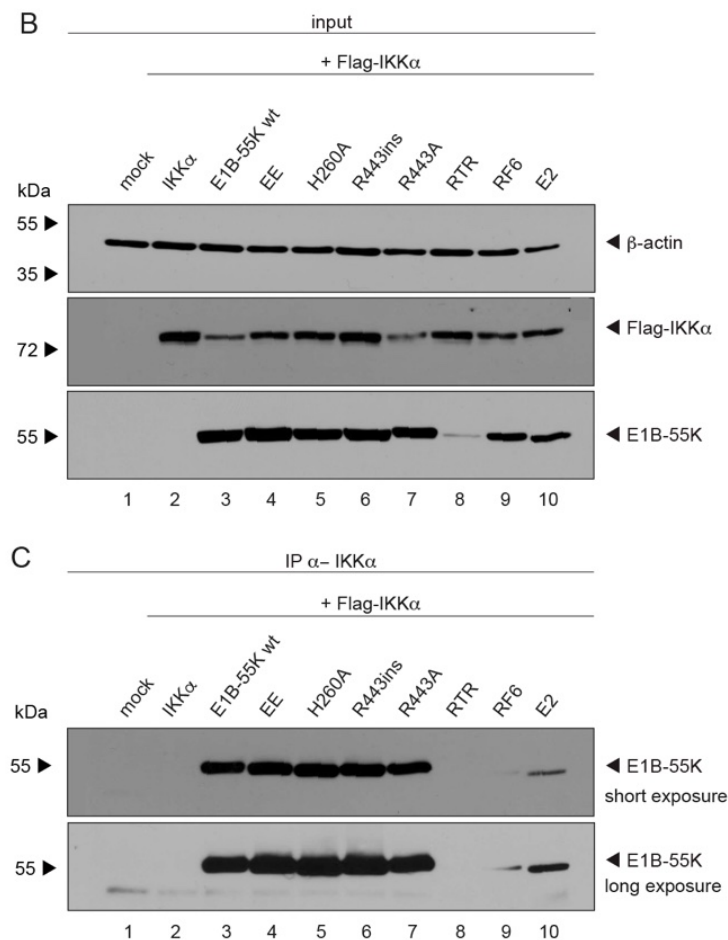


**Figure 25: IKK $\alpha$  shows impaired interaction with E1B-55K RF6 and E2 mutants.**

(A) Schematic overview of E1B-55K. The line on top denotes the amino acid (aa) of E1B-55K. Triangles show the introduced mutation within E1B-55K. (B) Subconfluent H1299 cells were cotransfected with 5  $\mu$ g of E1B-55K wt or indicated E1B-55K mutants and 5  $\mu$ g of human Flag-tagged IKK $\alpha$  (3.4). Cells were harvested 48 hpt before preparing total-cell extracts (3.9). Immunoprecipitation of E1B-55K was performed with mAb 2A6 ( $\alpha$ -E1B-55K) (3.9.3), resolved by 10 % SDS-PAGE and visualized by immunoblotting (3.9). Input levels (A) of whole cell lysates were detected using mAb Flag-M2 ( $\alpha$ -Flag), mAb 2A6 ( $\alpha$ -E1B-55K) and mAb AC-15 ( $\alpha$ - $\beta$ -actin). Coprecipitated proteins (C) samples were stained with mAb Flag-M2 ( $\alpha$ -Flag). Molecular weights are indicated in kDa on the left side, while corresponding proteins are labeled on the *right*.

Mutation of E1B-55K often alters protein stability although minor changes with usually few amino acids are modified. Hence, reduced stability of steady state protein expression in this experiment was observed for E1B-55K-RF6 and the E1B-55K-E2 mutants (Figure 25A, 9 and 10). In case of E2, the lower expression level correlates with lower amount of the loading control,  $\beta$ -actin (Figure 25A, 10). However, the significantly reduced amounts in the input of the E1B-55K-RTR in this experiment might be due to low transfection efficiency or reduced protein stability (Figure 25A, 9). As shown in Figure 25B, comparable amounts of E1B-55K-wt, E1B-

55K-EE, E1B-55K-H260A, E1B-55K-R443ins could be detected after immunoprecipitation with IKK $\alpha$ . This might be due to its low input levels (Figure 25B, lane 8). Although E1B-55K-RF6 mutant shows a higher input level in comparison to E1B-55K-E2, it is repeatedly less precipitated and precipitation efficiency seems to be less pronounced than for E1B-55K-wt.

#### 4.3.4.3 IKK $\alpha$ is diffusely distributed within the cell upon cotransfection with E1B-55K

Immunoprecipitation of overexpressed E1B-55K and IKK proteins indicated that in contrast to IKK $\beta$  and NEMO, E1B-55K interacts with IKK $\alpha$  (see Figure 22). This interaction is investigated more in detail by performing immunofluorescence analysis. Therefore, H1299 cells were cotransfected similar to the immunoprecipitation experiments with Flag-tagged IKK $\alpha$  and E1B-55K, fixed with 4 % PFA 48 hpt and visualized by using double-labeled IKK $\alpha$  and E1B-55K immunofluorescence microscopy (Figure 26).

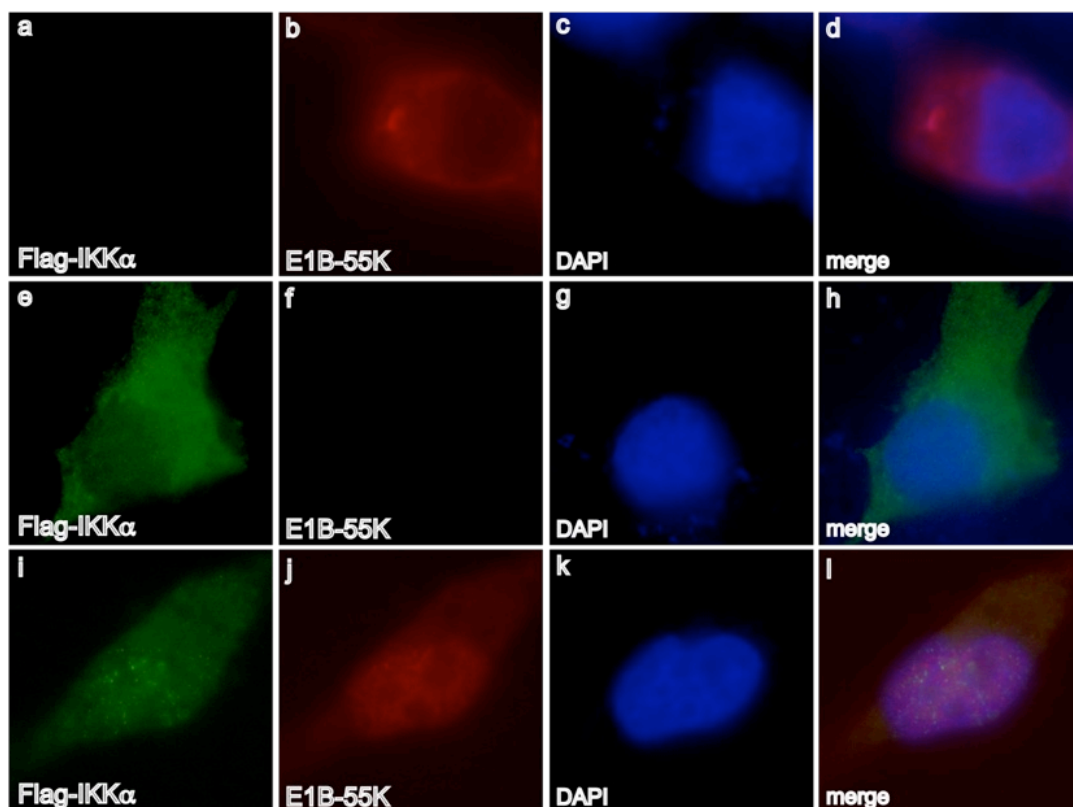


**Figure 26: Cotransfection changes subcellular localization of E1B-55K and IKK $\alpha$ .**

H1299 cells were transfected with 1.5  $\mu$ g of Flag-tagged IKK $\alpha$  and E1B-55K, fixed with 4 % PFA 48 hpt and double labeled with mAb 2A6 ( $\alpha$ -E1B-55K) and mAb M2 ( $\alpha$ -Flag) (3.10.4). Primary Abs were detected with Alexa 488 ( $\alpha$ -Flag) and texas red ( $\alpha$ -E1B-55K) conjugated secondary Abs. For nuclear staining, the DNA intercalating dye DAPI was used. Representative  $\alpha$ -E1B-55K and  $\alpha$ -Flag staining patterns of at least 29 analyzed cells are shown. Overlays of single images (merge) are shown (magnification x 7600).

In Flag-tagged E1B-55K and IKK $\alpha$  single transfected cells, both proteins show mainly cytoplasmic localization (Figure 26, b and e). However, upon cotransfection of both proteins, E1B-55K nearly showed a complete diffuse nuclear relocalization (Figure 26, j). In contrast, Flag-tagged IKK $\alpha$  lost its cytoplasmic localization and seemed to be diffusely distributed throughout the whole cell upon cotransfection with E1B-55K (Figure 26, i).

**4.3.4.4 IKK $\alpha$  is relocalized into the nucleus and excluded from viral replication centers upon adenoviral infection**

The reduced capability of the IKK complex formation after adenoviral infection could be induced by changes in the subcellular localization of the complex component as it has already been shown in the case of NEMO by the MCMV protein M45. M45 relocalizes NEMO into autophagosomes leading to its degradation (Fliss & Brune, 2012). Analysis performed by Jenner and Young (2005) resulted in a cluster of 511 deregulated genes, which have been designated as the common host response to infection with several different pathogen species (like HCV, KSHV, HPV) (Jenner & Young, 2005). This cluster analysis showed that the common host response is enriched for genes involved in the immune response. Monitoring of host responses against pathogens by transcriptional profiling with DNA microarrays clarified that pathogenesis is driven by modulation of the host immune response. In particular, the cluster of genes that mediate inflammation, and the group of IFN-stimulated genes (ISGs) (Jenner & Young, 2005). Later on, studies by Miller *et al.* have shown the important role of E1B-55K on the suppression of immune response genes after HAdV-C5 infection.

In order to investigate whether E1B-55K exerts its immune suppressive function by counteracting the NF- $\kappa$ B pathway, targeting its main complex consisting of IKK proteins, an immunofluorescence experiment was performed to analyze the subcellular distribution of the IKK $\alpha$  after HAdV-C5 infection. Therefore, A549 cells were infected with HAdV-C5 (MOI 20) and co-stained for E1B-55K and IKK $\alpha$  (see

Figure 27). Consistent with previous publications, E1B-55K localizes 24 hours after (H5pg4100) infection within the cytoplasm and nucleus (Gonzalez & Flint, 2002; Ornelles & Shenk, 1991). Staining of E1B-55K revealed its nuclear localization with a few cytoplasmic and nuclear membrane intensely stained bodies, which were diffusely distributed (Figure 27, f; j; n; r). Within the nucleus, E1B-55K showed mostly a granular diffuse distribution (Figure 27, f; j; n; r). However, there were usually also some cells with E1B-55K localized in globular structures, which is mostly associated with E2A-induced globular ring-like structures (Figure 27, r). Therefore, HAdV-C5 E1B-55K localizes to sites of viral replication and transcription, cytoplasmic aggresomes and nuclear track-like structures (Dosch *et al.*, 2001; Zantema *et al.*, 1985). Endogenous IKK $\alpha$  showed the expected cytoplasmic localization as it acts as member of the NF- $\kappa$ B signaling pathway within the cytoplasm, but a small proportion of IKK $\alpha$  is also detectable within the nucleus to exert its NF- $\kappa$ B-dependent as well as independent functions (Figure 27, a). IKK $\alpha$  is a nuclear-cytoplasmic shuttled protein (Anest *et al.*, 2003; Yamamoto *et al.*, 2003b). However, IKK $\alpha$  shows a distinct localization pattern upon infection, being completely relocalized into the nucleus and excluded from certain nuclear structures together with E1B-55K (Figure 27, e; i; m).

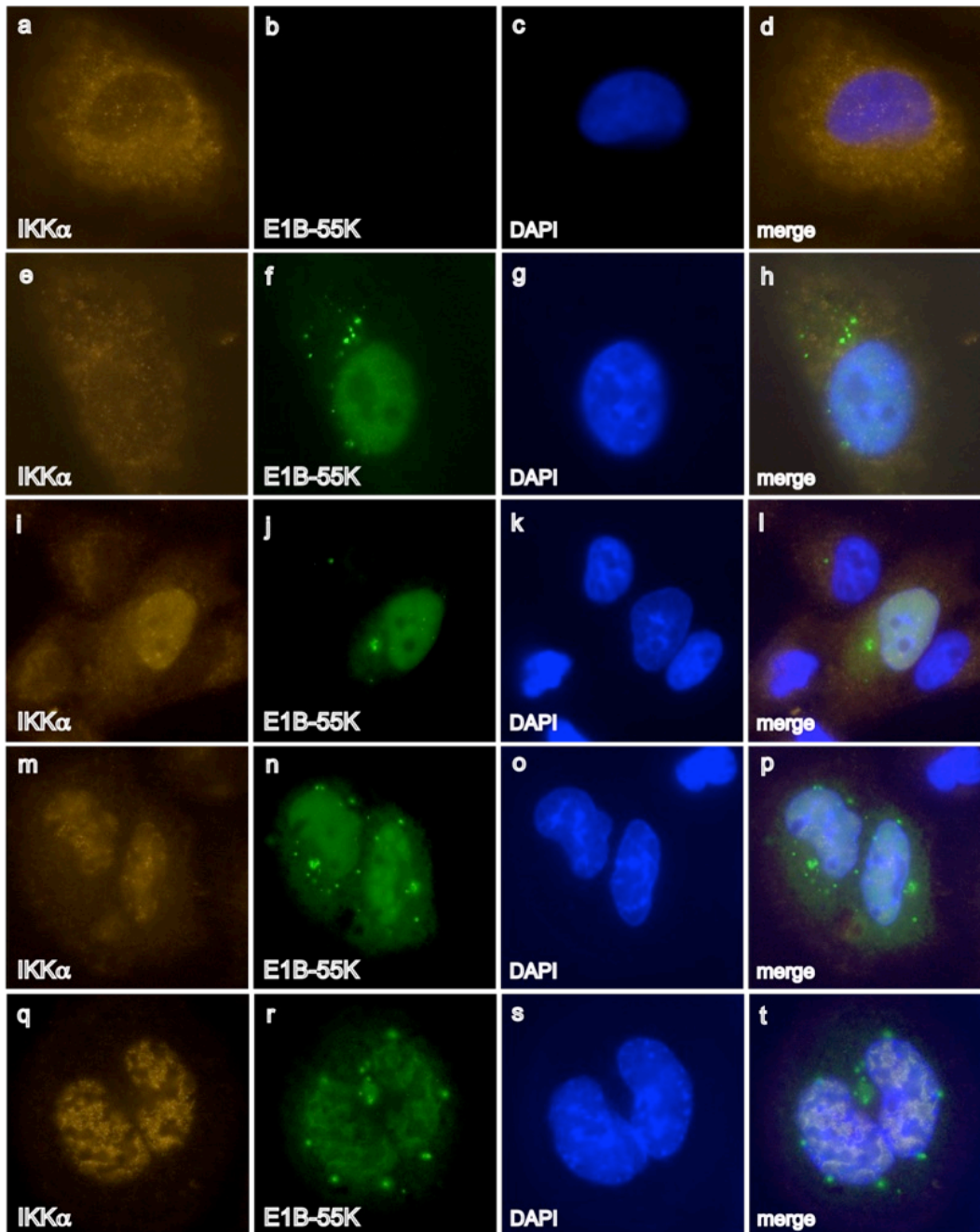


**Figure 27: HAdV-C5 induces nuclear relocalization of IKK $\alpha$ .**

A549 cells were infected with wt H5pg4100 for 24 hours, fixed with 4 % PFA and double-labeled either with (A) AB M-204 ( $\alpha$ -IKK $\alpha$ ) and mAB 2A6 ( $\alpha$ -E1B-55K) or with (3.10.4). Primary Abs were detected with Cy3 ( $\alpha$ -IKK $\alpha$ ; orange) and Alexa488 ( $\alpha$ -E1B-55K; green) conjugated secondary Abs. The DNA intercalating dye DAPI was used for nuclear staining. Representative  $\alpha$ -IKK $\alpha$  and  $\alpha$ -E2A staining patterns of at least 40 analyzed cells are shown. Overlays of single images (merge) are shown (magnification x 7600).

#### 4.3.4.5 Nuclear relocalization of IKK $\alpha$ upon infection is E1B-55K-independent

Beside intensive IKK $\alpha$ -E1B-55K binding studies, and revealing nuclear relocalization of IKK $\alpha$  after adenoviral infection, the responsibility of E1B-55K for IKK modification was tested (Figure 28). Therefore, H1299 cells were infected with an E1B-55K null mutant virus, H5pm4149, and co-stained for the viral DNA binding protein (E2A) and IKK $\alpha$ . The early adenoviral protein E2A is widely considered as a marker for the viral replication centers, which are globular condensations that are constituted within the nucleus by E2A upon HAdV-C5 infection (Weitzman *et al.*, 1996).

These structures are known to accumulate predominantly diffusely upon expression but around 16 hpi, depending on the multiplicity of infection, they localize at the periphery of the viral replication centers to fulfill their various functions in the regulation of viral replication (Monaghan *et al.*, 1994; van Breukelen *et al.*, 2000).

Therefore, the E2A protein was used as a control for infection and as a marker of the viral replication centers (Figure 28, b; f; j). Costaining of IKK $\alpha$  and E2A revealed different localization patterns of IKK $\alpha$  early upon infection (Figure 28, e; i). At this time point, cells showing a diffuse E2A localization (Ornelles & Shenk, 1991), displayed a dispersed IKK $\alpha$  localization, which was in contrast with its preferred nuclear lamina localization observed in the mock cells (Figure 28, e). Additionally, the expression levels of IKK $\alpha$  seem to be reduced in comparison to non-infected cells (Figure 28, e). However, cells, where the viral replication centers are formed, presented IKK $\alpha$  relocalization in the space between these structures (Figure 28, i).

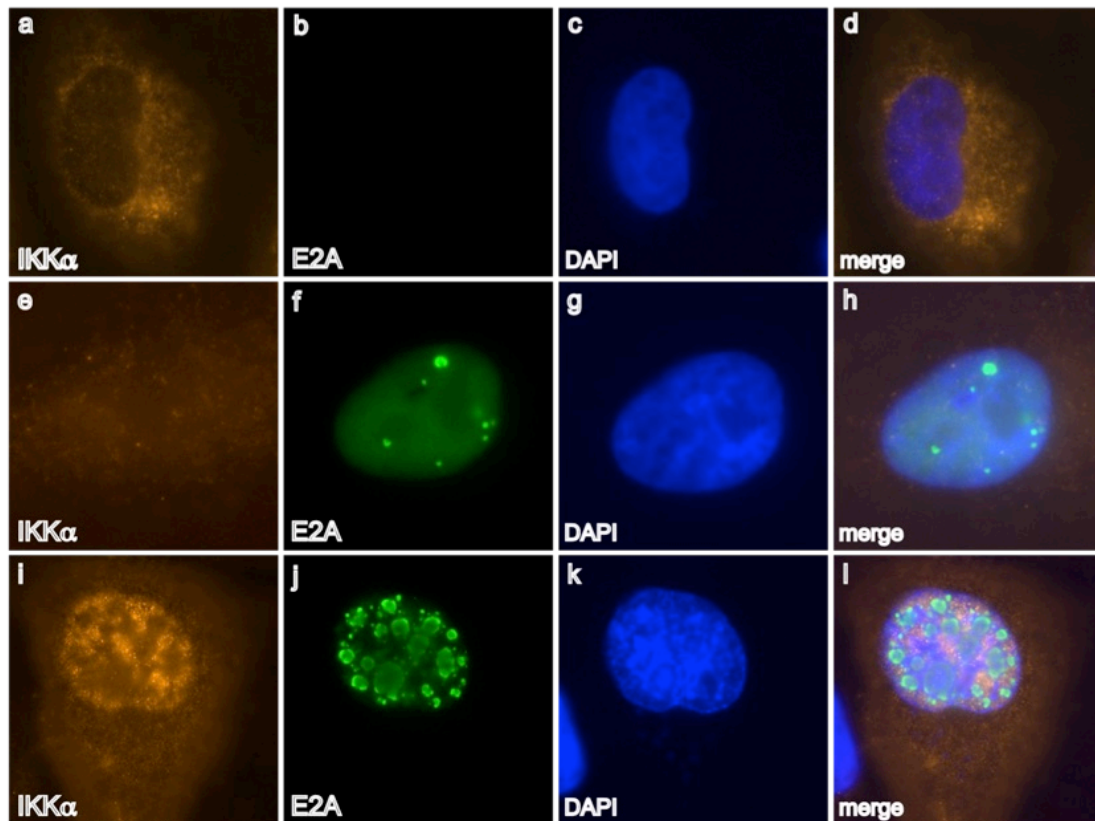


**Figure 28: Nuclear relocation of IKK $\alpha$  is independent of E1B-55K.**

A549 cells were infected with H5pg4149 (E1B-null mutant) for 24 hours, fixed with 4 % PFA and double-labeled either with Ab M-204 ( $\alpha$ -IKK $\alpha$ ) or mAb B6-8 ( $\alpha$ -E2A) (3.10.4). Primary Abs were detected with Cy3 ( $\alpha$ -IKK $\alpha$ ; orange) and Alexa488 ( $\alpha$ -E2A; green) conjugated secondary Abs. The DNA intercalating dye DAPI was used for nuclear staining. Representative  $\alpha$ -IKK $\alpha$  and  $\alpha$ -E2A staining patterns of at least 40 analyzed cells are shown. Overlays of single images (merge) are shown (magnification  $\times$  7600).

In summary, infection with an E1B-55K null mutant virus revealed that although IKK $\alpha$  is relocated upon infection, it is not dependent on E1B-55K indicating that further viral factors could induce relocation of IKK $\alpha$ .

#### 4.3.4.6 E1B-55K does not affect the IKK complex formation

As shown in Figure 20 adenoviral infection disrupts the IKK complex formation. Moreover, it has been published that E1B-55K modulates the host immune response (Miller *et al.*, 2009). Therefore, several binding studies were performed in order to analyze whether E1B-55K can interact with IKK complex components especially with IKK $\alpha$ , after infection (Figure 21) and transient transfection (Figure 22). To test the influence of E1B-55K without the presence of other viral proteins, E1B-55K was transiently cotransfected with Flag-tagged IKK $\alpha$ , IKK $\beta$  and HA-tagged NEMO similar to Figure 22. The immunoprecipitation assay showed that E1B-55K has no

effect on the IKK complex formation indicating that another viral protein might be involved in this process (Figure 29, B).

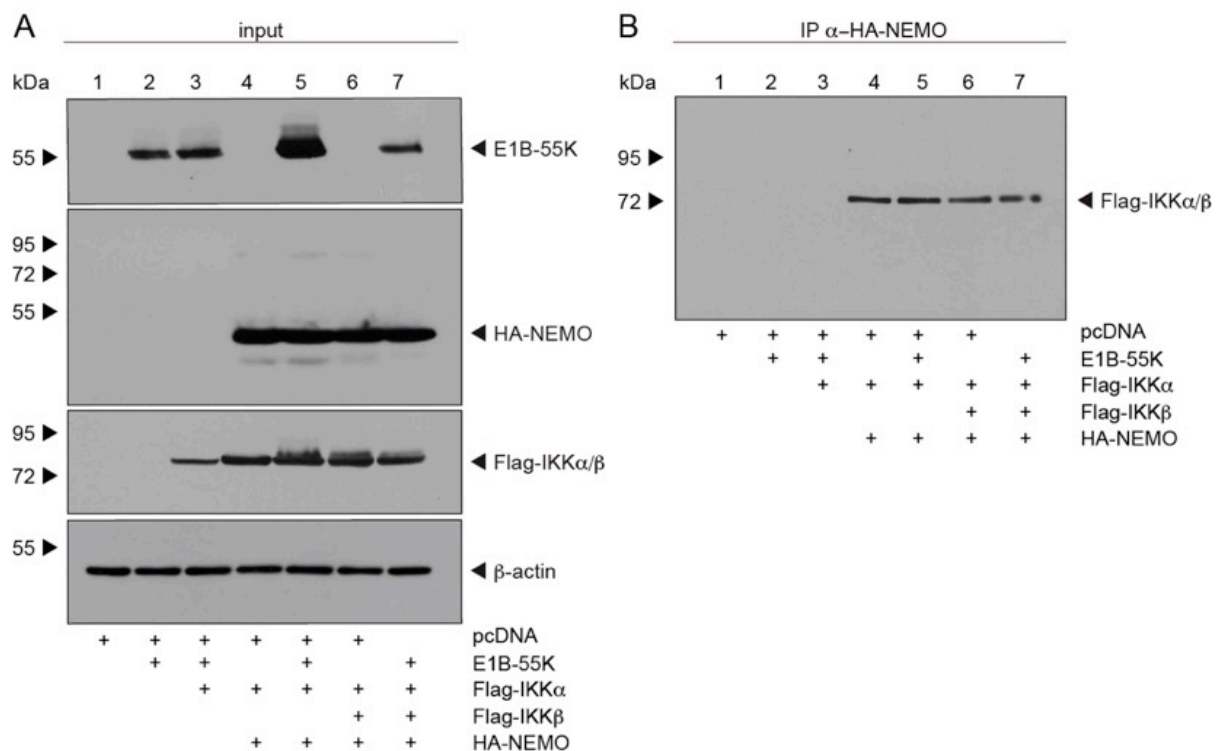


**Figure 29: E1B-55K does not affect IKK complex formation.**

Subconfluent H1299 cells were transfected with 5  $\mu$ g of human Flag-tagged IKK $\alpha$  and IKK $\beta$  HA-tagged NEMO and E1B-55K (3.4). Cells were harvested 48 hpt before preparing whole cell extracts (3.9.1). Immunoprecipitation of Flag-tagged proteins was performed by using Flag-beads M2, resolved by 10 % SDS-PAGE and visualized by immunoblotting (3.9.3). Input levels (A) of whole cell lysates were detected using mAb Flag-M2 ( $\alpha$ -Flag), mAb 3F10 ( $\alpha$ -HA), mAb 2A6 ( $\alpha$ -E1B) and mAb AC-15 ( $\alpha$ - $\beta$ -actin). Coprecipitated proteins (B) were stained with mAb 3F10 ( $\alpha$ -HA). Molecular weights are indicated in kDa on the left side, while corresponding proteins are labeled on the *right*.

#### 4.3.4.7 IKK $\alpha$ supports adenovirus progeny production in human cancer cell lines

Viruses modulate their hosts in order to achieve a microenvironment that will promote a productive viral infection. Therefore, cells have to counteract anti-viral defense measurements by either being targeted to protein degradation, subcellular localization changes or they are inactivated by modulation of their posttranslational modifications. To analyze the effect of IKK $\alpha$  on HAdV-C5 progeny production, lentiviral particles harboring shRNA against IKK (shIKK $\alpha$ ) were transduced to deplete endogenous protein in H1299 and A549 cells, and then infected with

H5pg4100 virus (3.4.4). IKK $\alpha$  protein levels were efficiently depleted in both cell lines, shown by western blot analysis (Figure 30A). Growth curve analysis indicated that the IKK $\alpha$  knock-down did not substantially affect the growth rate of the cells (Figure 30BC).

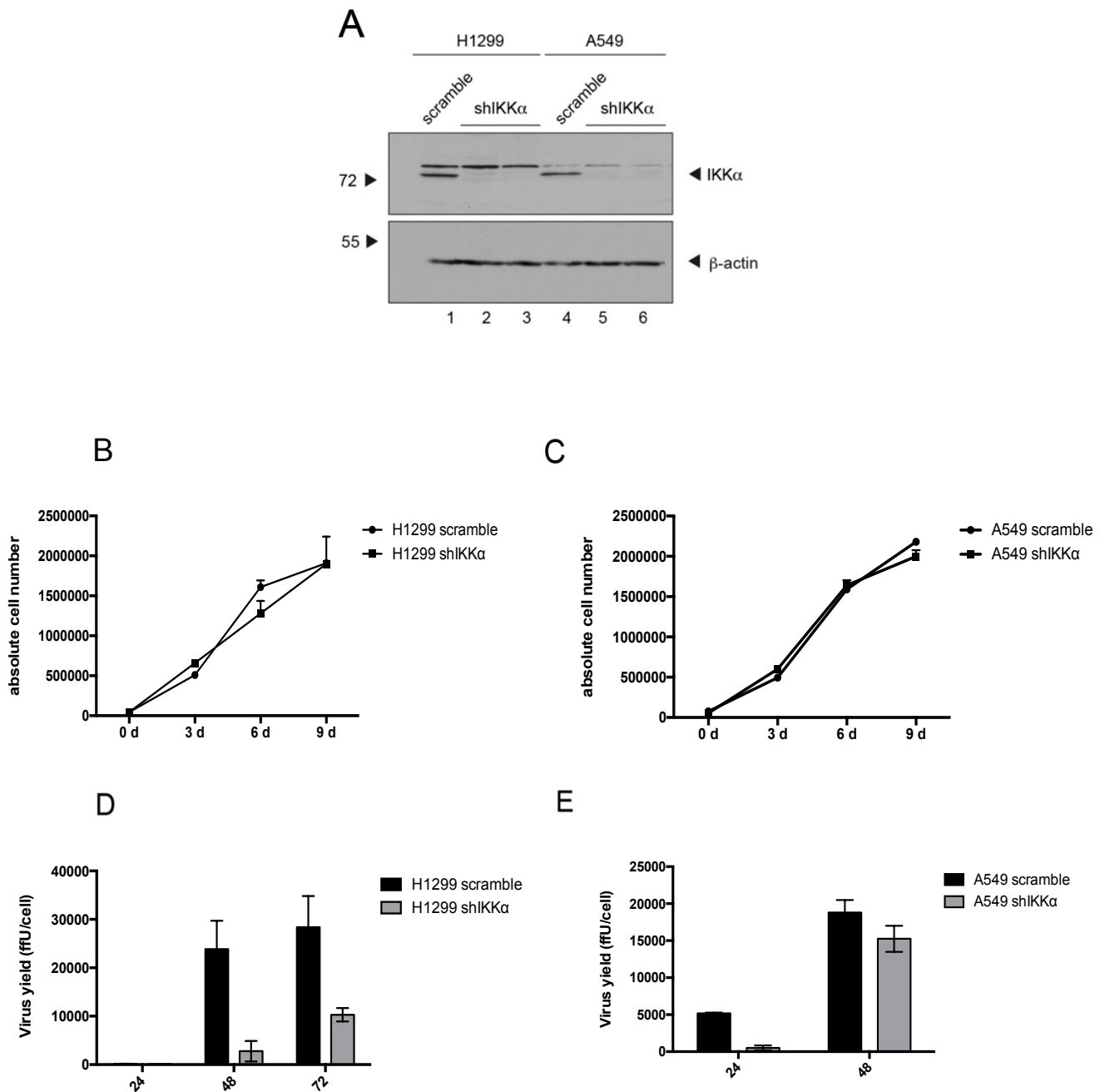


**Figure 30: IKK $\alpha$  depletion promotes HAdV-C5 progeny production.**

(A) Control of IKK $\alpha$  knockdown efficiency in H1299 and A549 cells. Lentiviral particles with shIKK $\alpha$  were harvested 24 (lanes 2 and 5) and 48 hours (lanes 3 and 6) after transfection of respective constructs. H1299 and A549 cells were harvested 3 rounds after puromycin selection with the first round started at 48 hours after lentiviral transduction before preparing total cell extracts (3.9). Lysates were resolved by 10 % SDS-PAGE and visualized by immunoblotting using Ab M-204 ( $\alpha$ -IKK $\alpha$ ) and mAb AC-15 ( $\alpha$ - $\beta$ -actin) (3.9). (B) Total cell numbers of parental and shIKK $\alpha$  H1299 and A549 cells were determined at indicated time points (3.3.3). (C) H1299 and A549 parental and respective shIKK $\alpha$  cells were infected with wt virus H5pg4100 at a multiplicity of 20 ffu/cell (3.5.1). Viral particles were harvested 24, 48 and 72 h pi and virus yield was determined by quantitative E2A-72K immunofluorescence staining of HEK-293 cells (3.5.4). The results represent the averages from two independent experiments and error bars indicate the standard error of the mean.

In comparison to the parental cell lines, which were transduced with lentiviral particles harboring scramble shRNA, knockdown of IKK $\alpha$  decreased the production of infectious virus particles at 2.5-fold in H1299 (Figure 30D). Knockdown of IKK $\alpha$  in A549 showed a 10-fold induction of adenoviral progeny production at 24 hpi (Figure 30E). However, a minor effect of IKK $\alpha$  is detectable at 48 hpi in A549 cells. Therefore, the data indicate, that IKK $\alpha$  acts as a negative regulator of HAdV-C5 progeny production which effect is more pronounced in H1299 in comparison to A549 cells. In the next steps, the role of IKK $\alpha$  on adenoviral replication cycle was investigated in the context of gene transcription and protein expression.

#### **4.3.4.8 IKK $\alpha$ regulates adenovirus gene transcription**

Recent studies have identified IKK $\alpha$  as a nuclear-cytoplasmic shuttling protein (Birbach *et al.*, 2002; Yamamoto *et al.*, 2003a). Besides its cytoplasmic NF- $\kappa$ B pathway-dependent role, a nuclear NF- $\kappa$ B independent role has also been described. Thus, TNF $\alpha$  treatment is sufficient to induce nuclear localization of IKK $\alpha$  leading to its association with the I $\kappa$ B $\alpha$  promoter, which induces the phosphorylation of H3 at Ser 10 and promotes NF- $\kappa$ B transcriptional activity (Yamamoto *et al.*, 2003b; Yoshida *et al.*, 2008). Furthermore, nuclear IKK $\alpha$  stabilizes the transcription factor p73, which is a member of the p53 family, and promotes the expression of tumor suppressor genes (Furuya *et al.*, 2007). After describing the E1B-55K-independent nuclear relocalization of IKK $\alpha$  (Figure 28) and its positive effect on adenoviral progeny production after infection (Figure 30DE), the role of IKK $\alpha$  on the transcriptional regulation of adenoviral genes was investigated (Figure 31). Therefore, E1A and E1B promoter activities were analyzed in shIKK $\alpha$  cells. As a proof of principle, transiently overexpressed IKK $\alpha$  in H1299 cells were also investigated for E1A and E1B promoter activity (Figure 31AB).

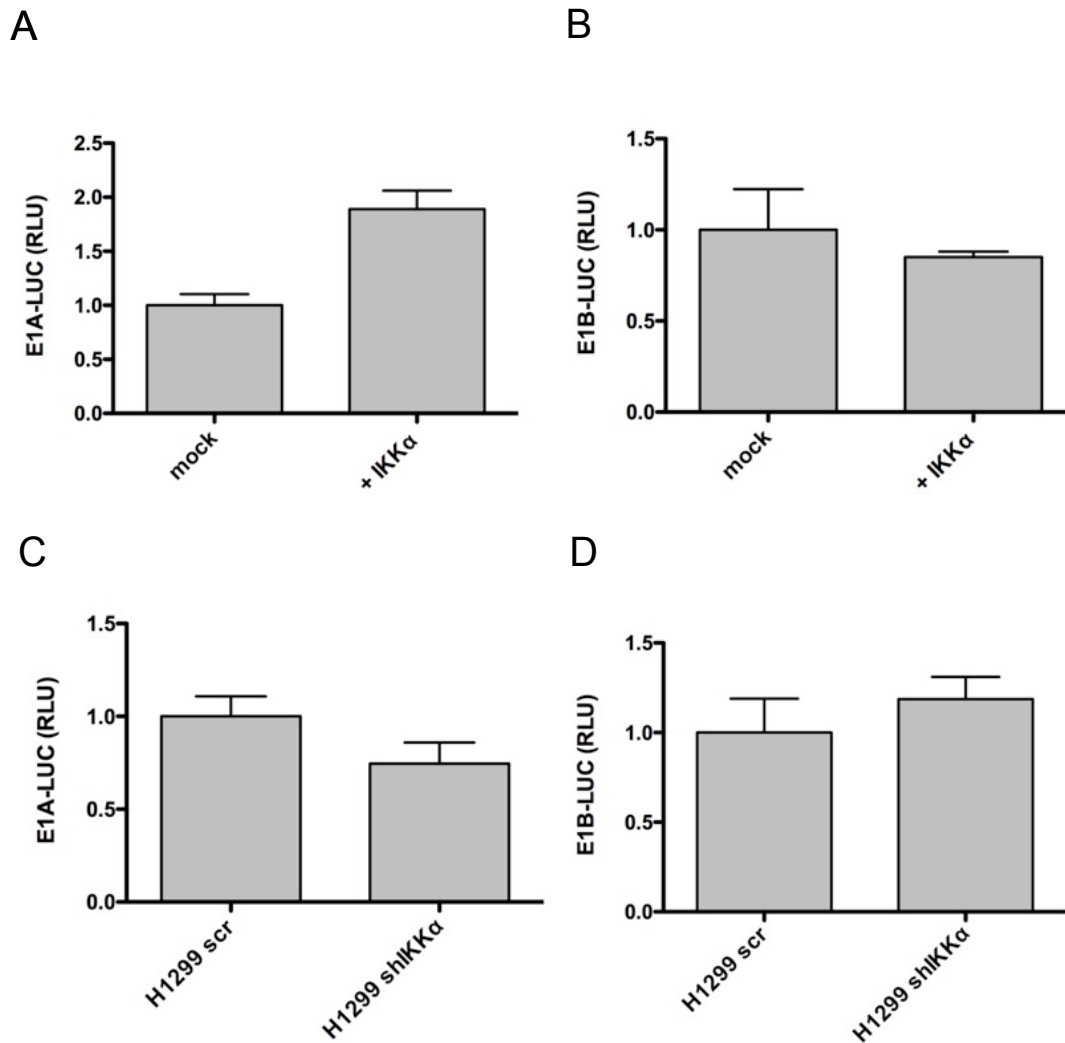


**Figure 31: IKK $\alpha$  regulates HAdV-C5 E1A gene transcription.**

(A) H1299 cells were transfected with 0.5  $\mu$ g of pRL-TK (*Renilla-Luc*), 0.5  $\mu$ g pGL3-Basic-Prom E1A (E1A promoter) or 0.5  $\mu$ g pGL3-Basic-Prom E1B (E1B promoter), plus 1  $\mu$ g Flag-tagged IKK $\alpha$  (3.4). (B) H1299 and shIKK $\alpha$  H1299 cells were transfected with 0.5  $\mu$ g of pRL-TK (*Renilla-Luc*), 0.5  $\mu$ g pGL3-Basic-Prom E1A (E1A promoter) or 0.5  $\mu$ g pGL3-Basic-Prom E1B (E1B promoter) (3.4). Total-cell extracts were prepared and luciferase activity determined 24 hpt (3.10.5). Absolute *Firefly*-luciferase activity is shown. The mean and standard deviations of two independent experiments are presented.

As shown in Figure 31A, IKK $\alpha$  specifically stimulated transcription of E1A by 1.8-fold in H1299 after transient overexpression (Figure 31A). However, knock-down of IKK $\alpha$  showed a modest reduction of E1A promoter activity (Figure 31C). In contrast to the influence of IKK $\alpha$  to the promoter activity of E1A, E1B showed no significant decrease in the promoter activity upon IKK $\alpha$  overexpression (Figure 31B), which is not significantly increased upon IKK $\alpha$  knock-down (Figure 31D). To confirm the results of IKK $\alpha$  on viral transcription in a replication-competent virus-system,

mRNA expression was measured after adenoviral infection of H1299 parental as well as shIKK $\alpha$  knock-down cell lines (Figure 32).

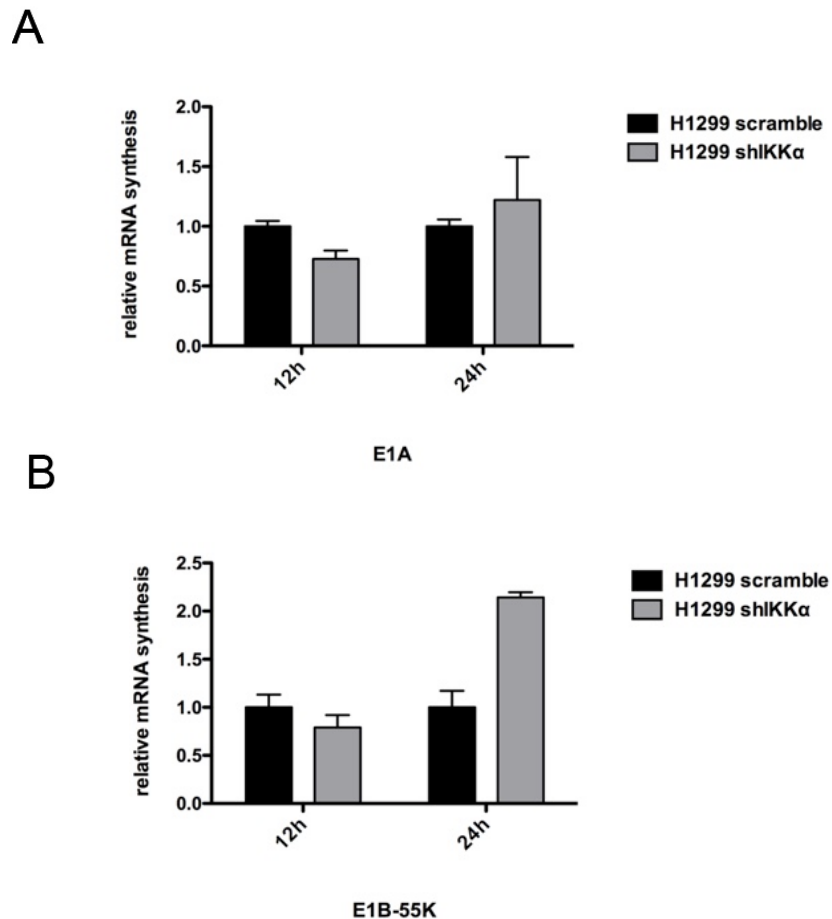


**Figure 32: IKK $\alpha$  regulation of HAdV-C5 gene transcription.**

H1299 parental and respective shIKK $\alpha$  cells were infected with H5pg4100 at a multiplicity of 20 ffu/cell (3.5.1). Cells were harvested 12 and 24 hpi, total RNA was extracted, reverse transcribed and quantified by RT-PCR analysis using primers specific for E1A and E1B-55K (3.8.3). Data were normalized to 18S rRNA levels.

As shown in Figure 32, depletion of IKK $\alpha$  resulted in about 25 % decrease of E1A as well as E1B mRNA transcripts at 12 hpi, which increased slightly at 24 hpi for E1A (Figure 32A) but more pronounced for E1B with around 2-fold (Figure 32B). In summary, the role of IKK $\alpha$  in regulating viral transcription is not solved with the obtained data. Moreover, further experiments are needed to clarify the influence of IKK $\alpha$  on viral gene transcription.

#### 4.3.5 **IKK $\alpha$ enhances viral protein expression upon HAdV-C5 infection**

In order to investigate the role of IKK $\alpha$  on viral early and late protein expression in H1299 cells, western blot analysis were performed to monitor viral protein expression levels at different time points after infection (Figure 33). Consistent with the affected HAdV-C5 progeny production, expression levels of the early protein E1A are decreased, whereas the early protein E1B-55K is expressed delayed in IKK $\alpha$  depleted cells compared to the parental cells (Figure 33). However, protein levels of E1B-19K and adenoviral capsids remain similar during the course of infection with and without IKK $\alpha$ . Mre11 levels are higher in the parental cells compared to the shIKK $\alpha$  knock-down cells. Moreover, consequences of NF- $\kappa$ B pathway protein expression levels upon IKK $\alpha$  depletion were investigated. Staining of p65, a subunit of the transcription factor NF- $\kappa$ B heterodimer, showed lower expression levels upon IKK $\alpha$  knock-down. In line with this, the amount of phosphorylated form of p65 (p-p65) in shIKK $\alpha$  knock-down cells is reduced indicating dampened activation of the NF- $\kappa$ B pathway in this cell line. I $\kappa$ B $\alpha$  in the parental cell line shows reduced levels upon infection starting from 48 hours after infection, which is in line with the decrease of the internal loading control  $\beta$ -actin level (Figure 33, lanes 5 and 6). This indicates that the I $\kappa$ B $\alpha$  level stays constant during infection. However, I $\kappa$ B $\alpha$  levels are reduced without IKK $\alpha$  in H1299 cells (Figure 33, lanes 7-12). The expression level of I $\kappa$ B $\alpha$  is under the detection limit of this western blot assay upon 48 hours after infection (Figure 33, lanes 11 and 12).

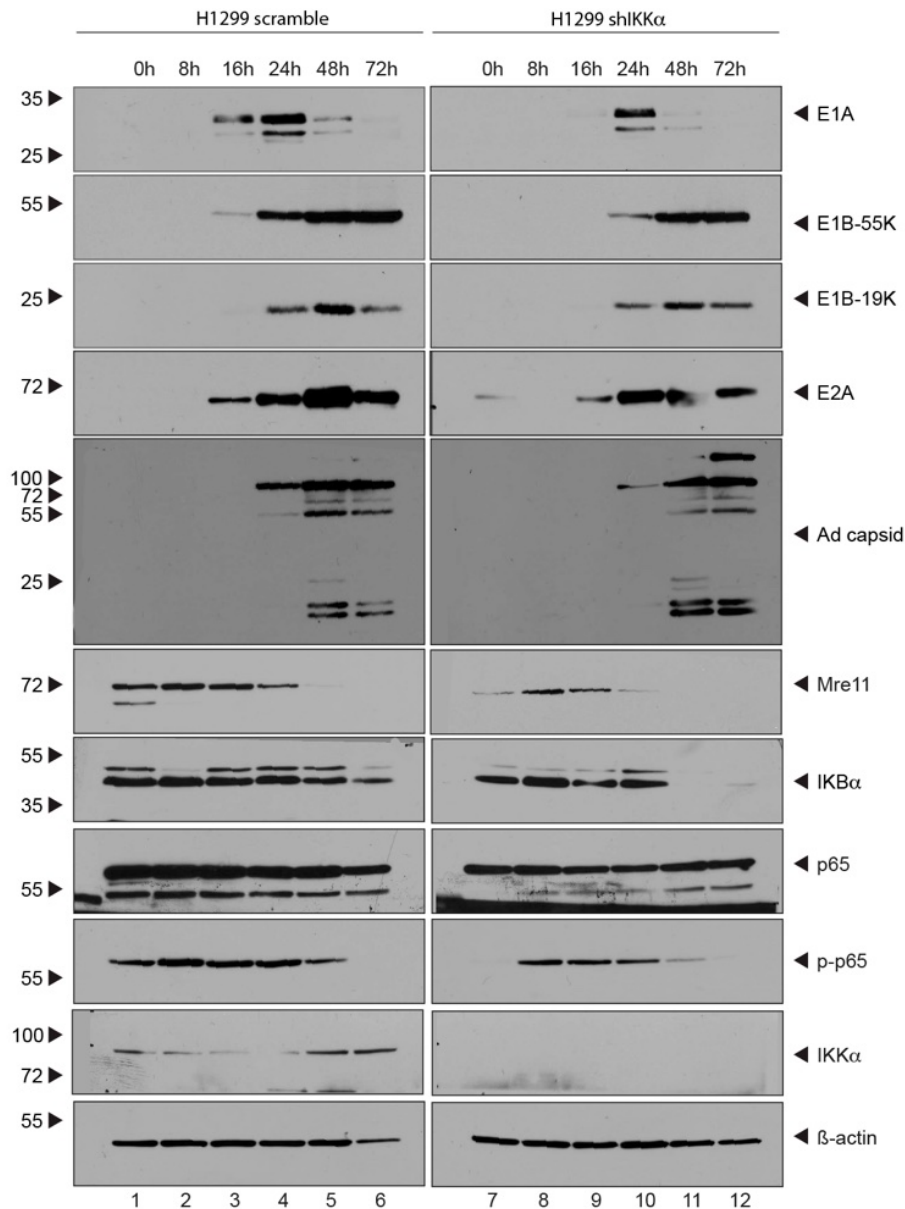


**Figure 33: IKK $\alpha$  enhances viral protein expression upon infection in H1299 cells.**

H1299 parental (H1299 par) and H1299 shIKK $\alpha$  cells were infected with wt H5pg4100 at a multiplicity of 20 ffu/cell and proteins from total-cell extracts were separated by SDS-PAGE and subjected to immunoblotting using rabbit Ab ( $\alpha$ -Mre11), C-21 ( $\alpha$ -IkB $\alpha$ ), C-20 ( $\alpha$ -p65), 93H1 ( $\alpha$ -p-p65), M-204 ( $\alpha$ -IKK $\alpha$ ), AC-15 ( $\alpha$ - $\beta$ -actin) mouse mAb M-58 ( $\alpha$ -E1A), B6-8 ( $\alpha$ -E2A), 2A6 ( $\alpha$ -E1B-55K), RSA3 ( $\alpha$ -E4orf6), rabbit 19K ( $\alpha$ -19K) and rabbit antiserum L133 to Ad capsid.

Taken together, these data indicate that IKK $\alpha$  is a positive regulator of HAdV-C5 replication during infection. In Figure 30, the infection of A549 and H1299 with H5pg4100 resulted in cell line dependent differences in viral progeny production upon IKK $\alpha$  depletion.

In order to test, whether a difference of viral protein expression is detectable in A549 cells, a time course experiment including early time points after infection was done

(Figure 34). Knock-down of IKK $\alpha$  in A549 cell lines showed slight differences in expression of viral proteins E1B-55K, L4-100K and E2A in comparison to parental cells. Interestingly, staining of E1B-55K showed loss of the lower migrating bands at 72 hpi in the shIKK $\alpha$  cells. Staining of p53 in parental cell line exhibited the expected degradation starting at around 48 hpi, which is mediated by the E1B-55K/E4orf6 E3 ubiquitin ligase complex together with cellular factors (Harada *et al.*, 2002; Querido, 2001). Furthermore, levels of p53 were increased upon depletion of IKK $\alpha$  (Figure 34, lanes 10-17). However, NF- $\kappa$ B pathway associated protein p65 level was slightly decreased in the same cell line (Figure 34, lanes 10-17). Further, phosphorylated p65 (p-p65) was under the detection limit of this assay upon IKK $\alpha$  depletion in uninfected cells as well as up to 1 hpi (Figure 34, lanes 10-12) in contrast to A549 scramble cell line as a modest constitutive phosphorylation of p65 was detectable (Figure 20, lanes 1-3).

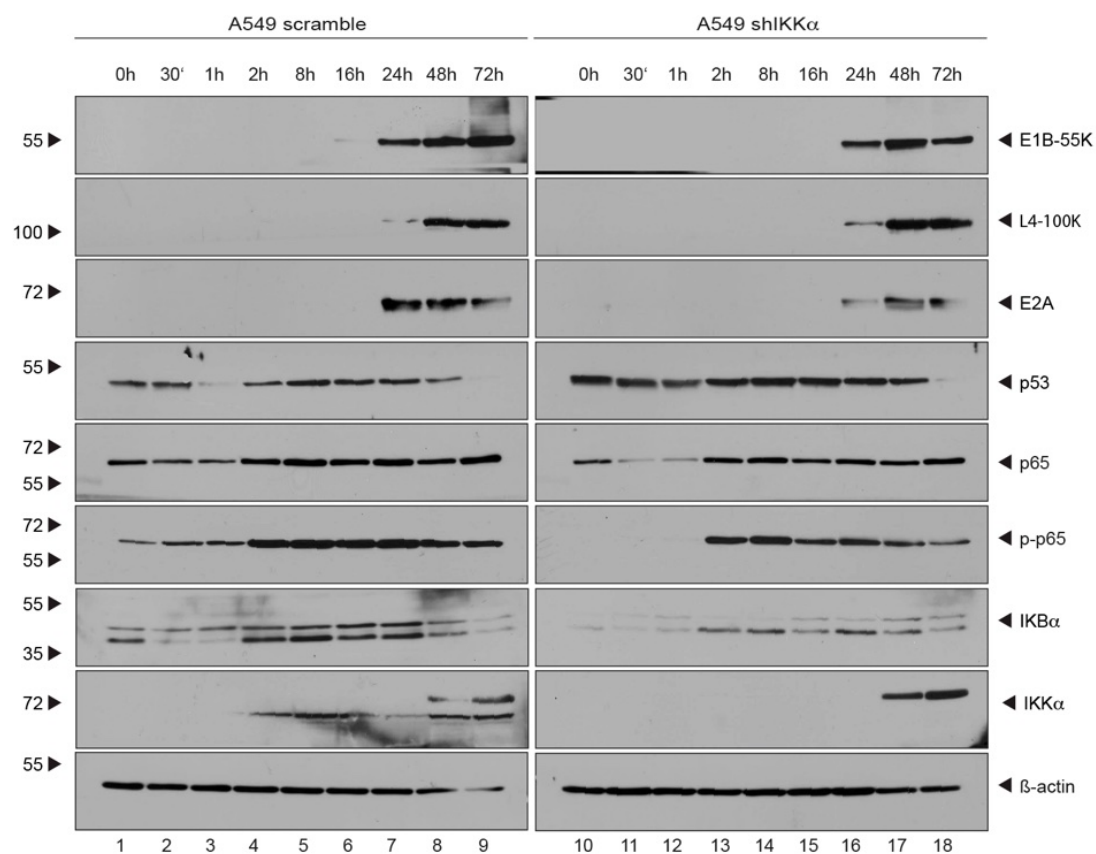


**Figure 34: IKK $\alpha$  is necessary to enhance viral protein expression upon infection in A549 cells.**

A549 parental (A549 par) and A549 shIKK $\alpha$  cells were infected with wt H5pg4100 at a multiplicity of 20 ffu/cell and proteins from total-cell extracts were separated by SDS-PAGE and subjected to immunoblotting using rabbit Ab ( $\alpha$ -Mre11), C-21 ( $\alpha$ -IKB $\alpha$ ), C-20 ( $\alpha$ -p65),

93H1 ( $\alpha$ -p-p65), M-204 ( $\alpha$ -IKK $\alpha$ ), L133 ( $\alpha$ -Ad capsid), 19K ( $\alpha$ -19K) and mouse mAb M-58 ( $\alpha$ -E1A), B6-8 ( $\alpha$ -E2A), 2A6 ( $\alpha$ -E1B-55K), RSA3 ( $\alpha$ -E4orf6), AC-15 ( $\alpha$ - $\beta$ -actin).

However, p65 was phosphorylated with a peak at 8 hpi, which decreased over time (Figure 34, lanes 13-18). In summary, modest influence of IKK $\alpha$  on viral protein expression levels was detectable. However, p53 protein was still degraded, although higher protein levels could be observed in absence of IKK $\alpha$  (Figure 34, lane 18).

The reduction of I $\kappa$ B $\alpha$  was already detectable in Figure 19 upon infection of H1299 cells. The enhancement of phosphorylated p65 (p-p65) levels is usually correlated with the decrease of I $\kappa$ B $\alpha$ , as the proteasomal degradation of I $\kappa$ B $\alpha$  is induced by the activation of the NF- $\kappa$ B pathway leading to phosphorylation of p65 followed by its nuclear relocalization (Baldwin, 1996; Ghosh *et al.*, 1998). However, this part of the NF- $\kappa$ B pathway is often targeted upon viral infection as reviewed by Hiscott *et al.* (Hiscott *et al.*, 2006).

#### 4.4 NEMO reduces expression level of E1B-55K upon cotransfection

As already mentioned in 4.3.3, cotransfection of NEMO with E1B-55K reduces its levels. In order to reproduce this result, increasing amounts of NEMO were cotransfected with E1B-55K in H1299 cells and harvested 48 hpt. Upon cotransfection of 15  $\mu$ g NEMO with 5  $\mu$ g E1B-55K, levels of E1B-55K were strongly reduced dependent on the expression level of Flag-tagged-NEMO (Figure 35, lanes 3-6). Actin is shown as a loading control.

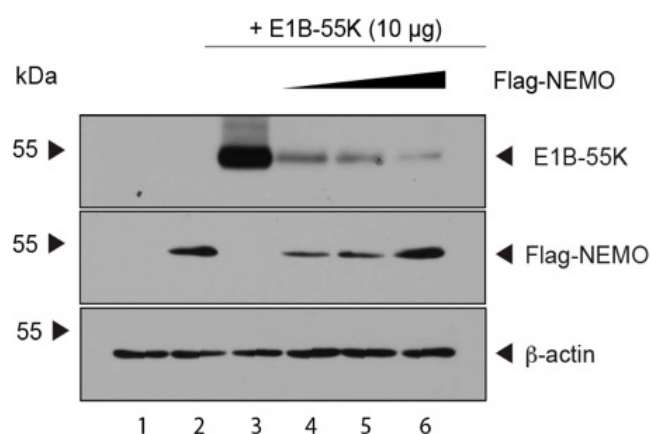


**Figure 35: NEMO induces reduced steady state level of E1B-55K upon cotransfection in H1299 cells.**

Subconfluent H1299 cells ( $4 \times 10^6$ ) were cotransfected with 10  $\mu\text{g}$  of E1B-55K wt and increasing amount (5  $\mu\text{g}$ , 10  $\mu\text{g}$ , 15  $\mu\text{g}$ ) of Flag-NEMO (3.4). Cells were harvested 48 hpt before preparing total-cell extracts (3.9.1). Cell lysates were resolved by 10 % SDS-PAGE and visualized by immunoblotting (3.9.6). Input levels of total-cell lysates were detected using mAb Flag-M2 ( $\alpha$ -Flag), mAb 2A6 ( $\alpha$ -E1B-55K) and mAb AC-15 ( $\alpha$ - $\beta$ -actin). Triangle illustrates the increasing amount of transfected Flag-tagged NEMO. Molecular weights in kDa are indicated on the *left*, while corresponding proteins are labeled on the *right*.

These results indicate an indirect influence of NEMO on the levels of E1B-55K upon cotransfection, however both proteins do not interact with each other as already shown in Figure 8.

**4.4.1.1 NEMO is relocalized into the nucleus and perinuclear bodies upon cotransfection with E1B-55K**

It has been shown, that NEMO is involved in both ubiquitin-dependent proteasomal degradation as well as in ubiquitin-independent lysosomal degradation (Ashida *et al.*, 2010; Qing *et al.*, 2006). So far it has only been described for NEMO itself to be degraded by viral proteins (Fliss *et al.*, 2012). Proteins that are targeted for lysosomal degradation are usually localized in punctate or vesicular structures within the cytoplasm. In order to better understand how NEMO reduces the levels of E1B-55K and if this could be related to different subcellular localization, we cotransfected both proteins in H1299 cells and performed immunofluorescence analysis (see Figure 36).

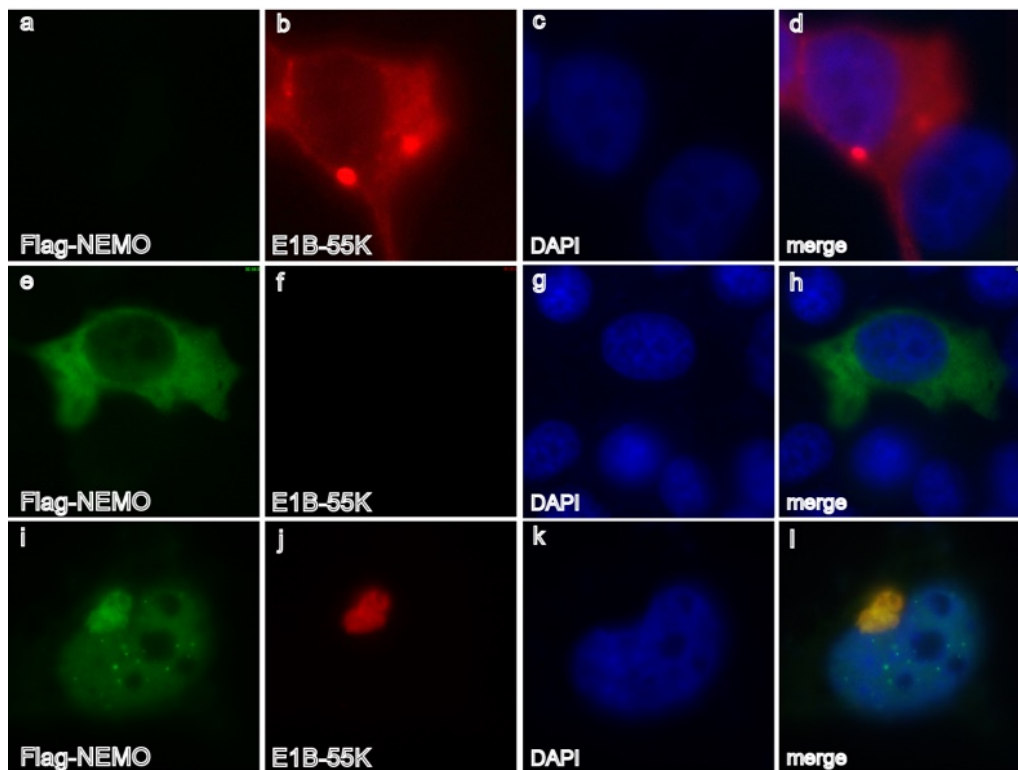


**Figure 36: NEMO redirects E1B-55K into perinuclear bodies upon cotransfection.**

H1299 cells were transfected with 1,5  $\mu\text{g}$  of Flag-tagged NEMO and E1B-55K, fixed with 4 % PFA 48 hpt and double labeled with mAb 2A6 ( $\alpha$ -E1B-55K) and mAb M2 ( $\alpha$ -Flag) (3.10.4). Primary Abs were detected with Alexa 488 ( $\alpha$ -Flag) and Texas Red ( $\alpha$ -E1B-55K) conjugated secondary Abs. For nuclear staining, the DNA intercalating dye DAPI was used. Representative  $\alpha$ -E1B-55K and  $\alpha$ -Flag staining patterns of at least 29 analyzed cells are shown. Overlays of single images (merge) are shown (magnification  $\times 7600$ ).

As already shown, transiently overexpressed E1B-55K localized in the cytoplasm (Figure 36, b), and it was completely relocated into a perinuclear body upon cotransfection with Flag-tagged NEMO (Figure 36, j). NEMO itself is mainly detectable within the cytoplasm whereas weak nuclear staining is also detectable (Figure 36, e). However, complete relocation into the nucleus as well as perinuclear bodies containing NEMO was detected upon cotransfection with E1B-55K (Figure 36, i) where they colocalized (Figure 36, i, l).

#### **4.4.1.2 NEMO-mediated reduction of E1B-55K is not mediated by proteasomal degradation**

Reduced expression levels of proteins after cotransfection can generally be induced through regulatory mechanisms on DNA-, RNA- or protein levels. It is possible to exclude the reduction of E1B-55K on DNA- and RNA- level, as the experiment is based on cotransfection and if the reduction occurs on DNA- or RNA- level, this

would be unspecific and true for all proteins which are cotransfected with NEMO. A hint excluding this possibility is the interaction between NEMO and the mouse cytomegalovirus (MCMV) viral protein M45 after cotransfection. In contrast to the reduction of the expression levels of E1B-55K upon cotransfection with NEMO, viral protein M45 degrades NEMO on protein level by redirecting it into cytoplasmic autophagosomes (Fliss *et al.*, 2012). Transfected cDNA of the viral protein M45 was cloned into pcDNA3 backbone like E1B-55K, which is under the control of a CMV promoter. As no further manipulation of the cells occurs, the stability of transfected DNA is not influenced in this assay. Furthermore, NEMO itself does not change promoter activity of the CMV promoter as shown in case of M45 (Fliss *et al.*, 2012). Therefore, it is possible to assume that the regulation of protein stability occurs at the protein level. In order to test whether E1B-55K is degraded by NEMO through proteasomal degradation, H1299 cells were cotransfected with E1B-55K and increasing amounts of NEMO (Figure 37) and then treated with MG132, an inhibitor of proteasome-mediated degradation. In our experiments we could not see an increase in E1B-55K levels in the presence of NEMO after MG132 treatment (Figure 37B), indicating, that the reduction of E1B-55K levels in the presence of NEMO is not mediated by proteasomal degradation. However, when using a positive control of a protein which degradation is mediated by the proteasome such as c-Myc, we could see that the MG132 treatment restored c-Myc levels (Figure 37B).

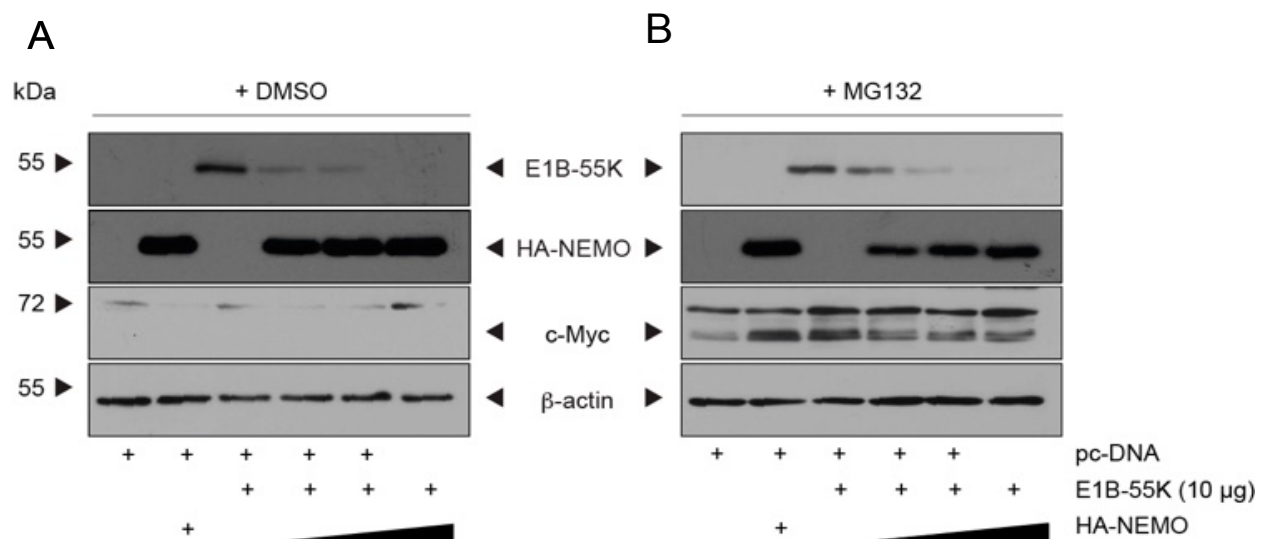


**Figure 37: NEMO-induced reduction of E1B-55K is not mediated by proteasomal degradation.**

Subconfluent H1299 cells ( $4 \times 10^6$ ) were cotransfected with 5  $\mu\text{g}$  of E1B-55K wt and increasing amount (5  $\mu\text{g}$ , 10  $\mu\text{g}$ , 15  $\mu\text{g}$ ) of HA-tagged NEMO (3.4). Cells were treated 8 hours before harvesting with DMSO (A) only or 10  $\mu\text{g}$  (final concentration) of MG132 (B). Cells were harvested 48 hpt before preparing total-cell extracts (3.9). Cell lysates were resolved by 10 % SDS-PAGE and visualized by immunoblotting (3.9.6). Input levels of total-cell lysates were detected using mAb 3F10 ( $\alpha$ -HA), mAb 2A6 ( $\alpha$ -E1B-55K), mAb c-Myc and mAb AC-15 ( $\alpha$ - $\beta$ -actin). Triangle illustrates the increasing amount of transfected HA-tagged NEMO. Molecular weights in kDa are indicated on the *left side*, while corresponding proteins are labeled between panels A and B.

**4.4.1.3 NEMO reduces the levels of the E4orf6 and E1B-55K complex**

Previous results of this work showed different subcellular localization of IKK proteins and E1B-55K depending on viral infection or transfection of the viral protein E1B-55K (see Figure 26, Figure 27). This could influence the interaction between proteins leading to different experimental results depending on transient transfection or viral infection. It has been shown that E1B-55K and E4orf6 form a functional complex (Bridge & Ketner, 1990; Rubenwolf *et al.*, 1997). E1B-55K protein sequence presents a nuclear export signal (NES), which determines its cytoplasmic localization. In order to act as a nucleocytoplasmic transporter for viral mRNAs E1B-55K interacts with E4orf6, which has a nuclear localization signal (NLS) to shuttle between both cellular and nuclear compartments (Dobbelstein *et al.*, 1997; Ornelles & Shenk, 1991; Weigel & Dobbelstein, 2000). It has been shown that E4orf6 cotransfected with E1B-55K shifts its cytoplasmic localization towards the nucleus (Dosch *et al.*, 2001; Krätzer *et al.*, 2000).

In order to examine the direct influence of NEMO on the viral proteins out of the context of infection and the dependency of E1B-55Ks localization on its expression levels, viral proteins E4orf6 and E1B-55K were overexpressed together with increasing amounts of NEMO (Figure 38).

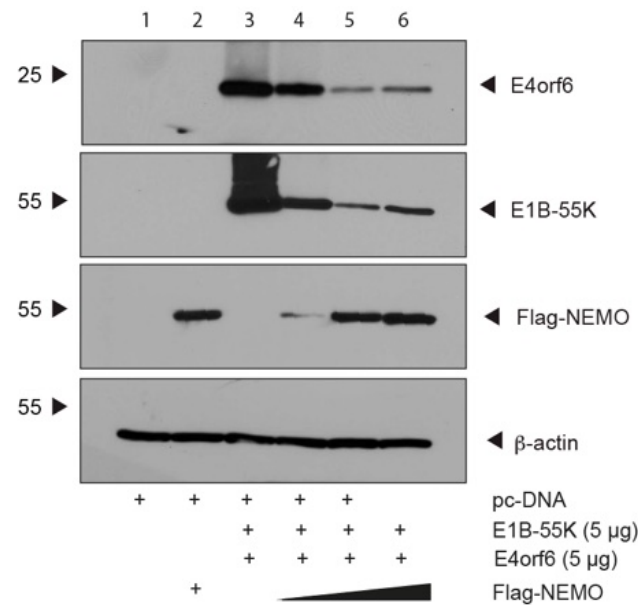


**Figure 38: Expression level of E1B-55K is reduced by NEMO upon cotransfection with E4orf6.**

Subconfluent H1299 cells ( $4 \times 10^6$ ) were cotransfected with 5  $\mu$ g of E1B-55K and E4orf6 together with increasing amount (1  $\mu$ g, 5  $\mu$ g, 10  $\mu$ g) of Flag-tagged NEMO (3.4). Cells were harvested 48 hpt before preparing total-cell extracts (3.9). Cell lysates were resolved by 10 % SDS-PAGE and visualized by immunoblotting (3.9.6). Input levels of total cell lysates were detected using mAb Flag-M2 ( $\alpha$ -Flag), mAb 2A6 ( $\alpha$ -E1B-55K), mAb B6-8 ( $\alpha$ -E4orf6) and mAb AC-15 ( $\alpha$ - $\beta$ -actin). Triangle illustrates the increasing amount of transfected Flag-tagged NEMO. Molecular weights in kDa are indicated on the *left*, while corresponding proteins are labeled in the *right*.

Cotransfection of the viral proteins E4orf6 and E1B-55K with NEMO showed that the presence of this cellular protein can not only decreases the levels of E1B-55K but also the levels of E4orf6, and this was shown to be dependent on increasing amount of NEMO (Figure 38).

In order to test whether the reduction of viral protein levels is an unspecific phenomenon upon cotransfection with NEMO, the same assay was repeated with Flag-tagged L4-100K protein (Figure 39).

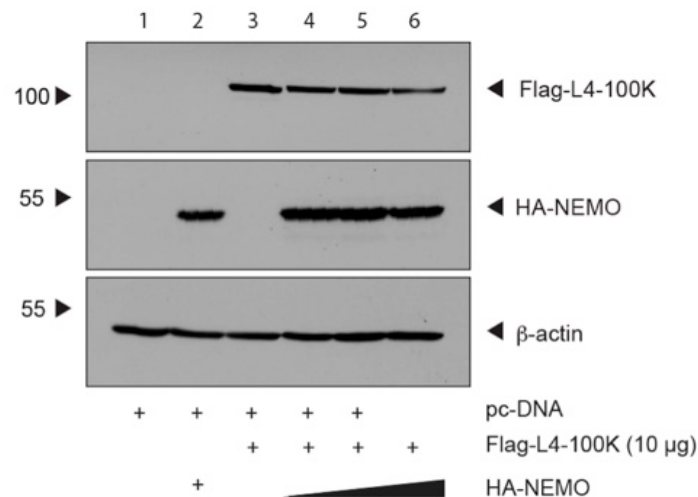


**Figure 39: Expression level of L4-100K is stable upon cotransfection with NEMO.**

Subconfluent H1299 cells ( $4 \times 10^6$ ) were cotransfected with 5  $\mu\text{g}$  of E1B-55K and E4orf6 in increasing amount (1  $\mu\text{g}$ , 5  $\mu\text{g}$ , 10  $\mu\text{g}$ ) of Flag-tagged NEMO (3.4). Cells were harvested 48 hpt before preparing total cell extracts (3.9). Cell lysates were resolved by 10 % SDS-PAGE and visualized by immunoblotting (3.9.6). Input levels of total-cell lysates were detected using mAb Flag-M2 ( $\alpha$ -Flag), mAb 2A6 ( $\alpha$ -E1B-55K), mAb B6-8 ( $\alpha$ -E4orf6) and mAb AC-15 ( $\alpha$ - $\beta$ -actin). Triangle illustrates the increasing amount of transfected Flag-tagged NEMO. Molecular weights in kDa are indicated on the *left*, while corresponding proteins are labeled on the *right*.

The control experiment showed no effect of NEMO on L4-100K levels, indicating that reduced levels of E1B-55K and E4orf6 viral proteins cotransfected with NEMO are specific (Figure 39). Degradation experiments in Figure 37 and Figure 38 showed, that both NEMO constructs although differing in their tags did not influence the detected reduction of E1B-55K levels.

#### **4.4.1.4 NEMO is partially relocalized after adenovirus infection to the virus-induced nuclear globular compartments**

So far, cotransfection experiments suggest that NEMO does not interact with E1B-55K (Figure 22) and consequently indirectly influences subcellular localization of each other. Further, NEMO reduces the levels of E1B-55K (Figure 35).

Next, the observed results were repeated in the presence of further viral proteins upon infection. Therefore, A549 cells were infected with H5pg4100 wt virus fixed with 4 % PFA and stained for NEMO and E1B-55K (Figure 40).

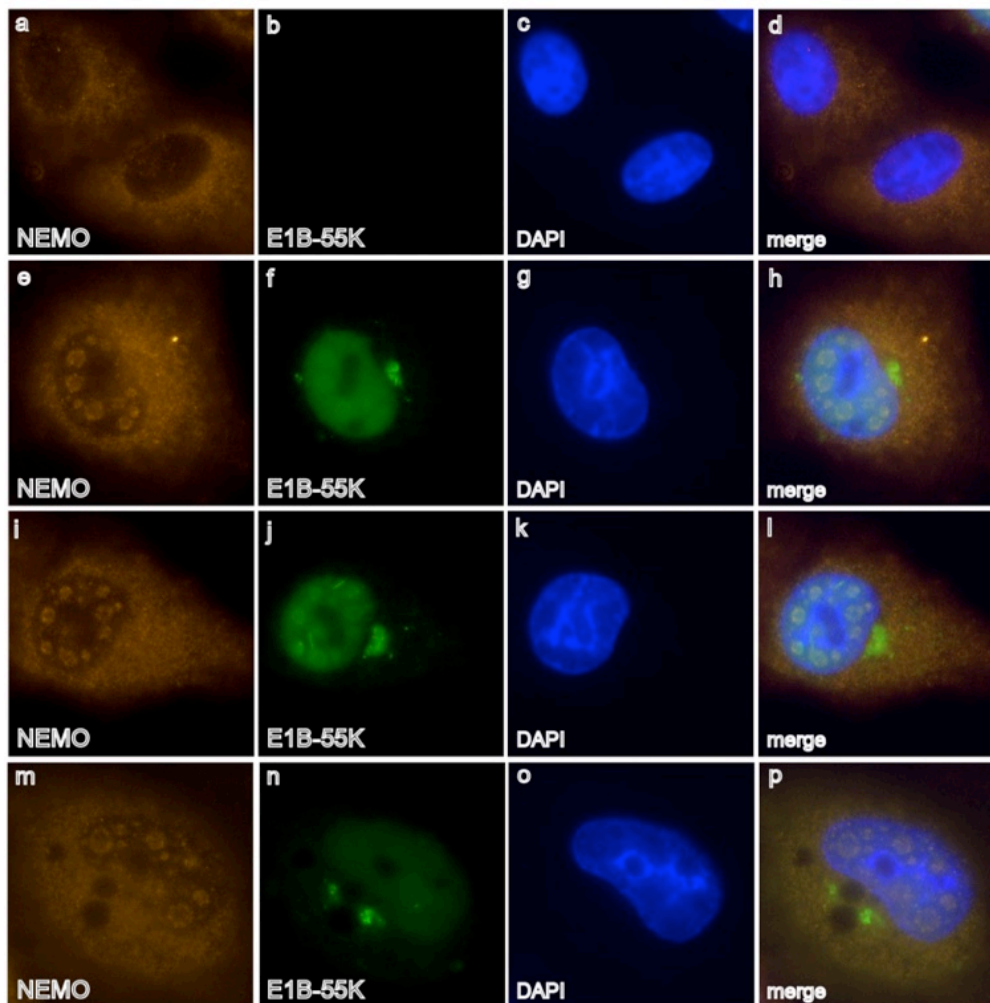


**Figure 40: HAdV induces nuclear relocalization of NEMO.**

A549 cells were infected with wt H5pg4100 (moi 20) for 24 hours, fixed with 4 % PFA and double-labeled either with (A) Ab FL-419 ( $\alpha$ -NEMO) and mAb 2A6 ( $\alpha$ -E1B-55K). Primary Abs were detected with Cy3- ( $\alpha$ -NEMO; orange) and Alexa488 ( $\alpha$ -E1B-55K; green) conjugated secondary Abs. The DNA intercalating dye DAPI was used for nuclear staining. Representative  $\alpha$ -NEMO and  $\alpha$ -E1B-55K staining patterns of at least 40 analyzed cells are shown. Overlays of single images (merge) are shown (magnification  $\times$  7600).

The cellular localization of E1B-55K upon adenoviral infection showed the expected staining pattern with specific staining of the nucleus and the perinuclear bodies (Figure 40, f; j; n). Moreover, some cells showed also partial localization of E1B-55K within the viral replication centers (Figure 40, j). It has been published that E1B-55K transiently colocalizes with viral replication centers depending on the expression of E4orf6, whereas E4orf3 rather mediates its localization in the PML-tracks (König *et al.*, 1999).

Endogenous NEMO showed cytoplasmic localization in the absence of infection (Figure 40, a). However, upon infection with HAdV-C5 wt, it is partially relocalized into the nucleus, colocalizing with E1B-55K within the viral replication centers (Figure 40, e ; i; m).

#### 4.4.1.5 NEMO relocalizes with the viral replication centers in an E1B-55K-independent manner

Viral replication centers are nuclear structures, which are assembled upon adenoviral infection. By approximately 6 hpi, E2 gene products accumulate to sufficient levels, form E2A (DBP) protein-containing centers and are active for both replication and transcription. E2A is a single-stranded DNA (ssDNA) binding protein, found colocalized with sites of viral ssDNA as well as double-stranded DNA, forming sphere-shaped pattern within the nucleus and is thus a marker for sites of transcription and replication, respectively (Weitzman *et al.*, 1996). Thereby, it has been shown that ssDNA accumulates in replication centers, while dsDNA is released to the surrounding nucleoplasm, where it serves for transcription (Pombo *et al.*, 1994). There, the viral E1B-55K and E4orf6 proteins also accumulate (Ornelles & Shenk, 1991; Sarnow *et al.*, 1984) at the late phase of infection, and DNA replication continues until the host cell lyses and dies.

To examine whether NEMO relocalizes to sites of viral DNA replication centers and whether this is dependent on E1B-55K, A549 cells were infected with H5pm4133 (E1B-55K null mutant) at a MOI of 20 ffu/cell and 4 % PFA fixed at 24 hpi. Fixed cells were stained for NEMO and E2A and this costaining showed that the expression of E2A (DBP) was not sufficient to change the cytoplasmic localization of NEMO (Figure 41). However, upon formation of viral replication centers by E2A, a part of NEMO was relocalized into the nucleus to viral replication centers (Figure 41, j). Thereby, NEMO localizes like E2A at the periphery of the spherical shape structure of the replication centers (Figure 41, i). Taken together, these results indicate that NEMO partially relocalized in the viral replication centers in an E1B-55K-independent manner after adenoviral infection (Figure 41, e; i; m; q).

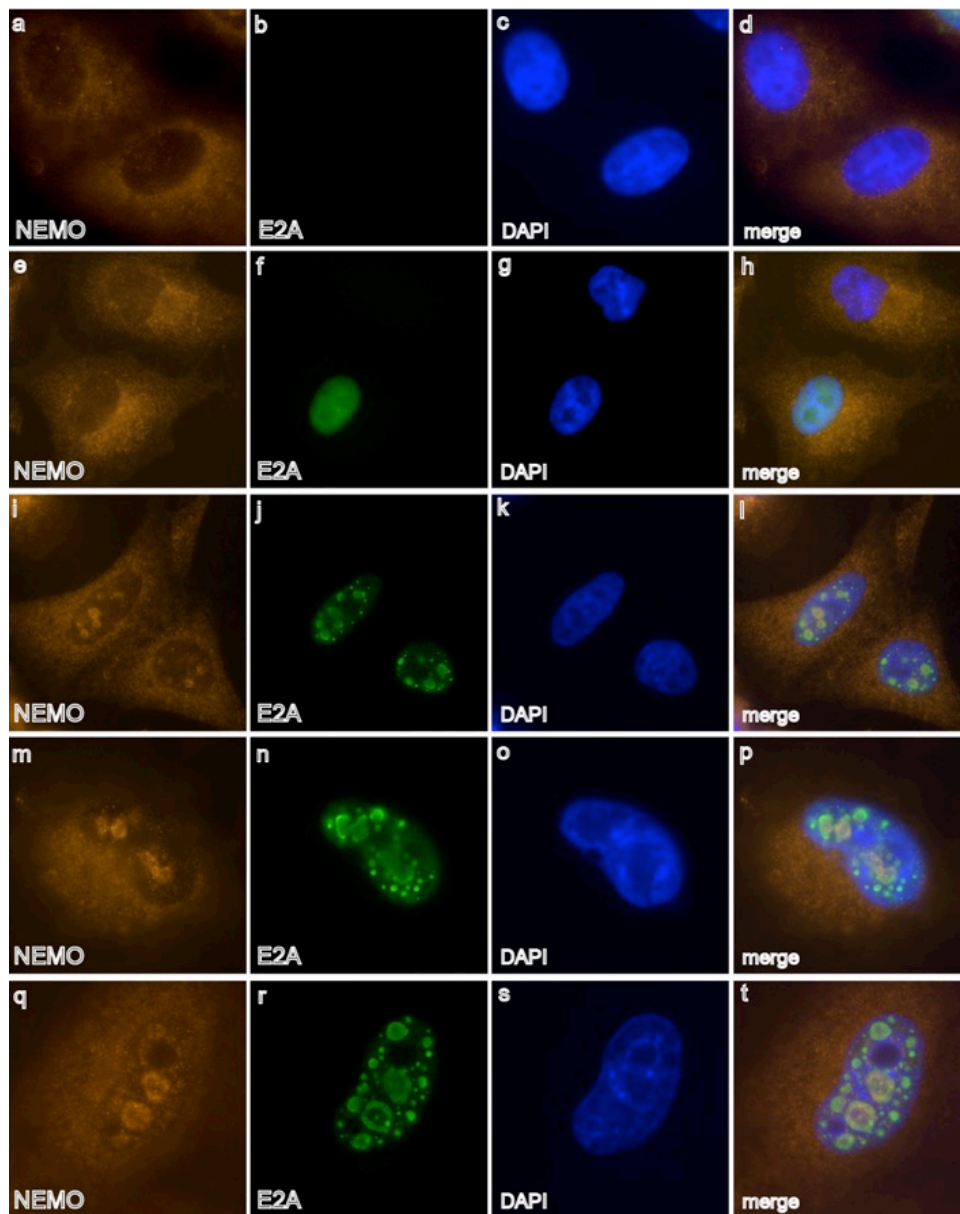


**Figure 41: HA $\nu$ -C5 induces E1B-55K independent nuclear relocalization of NEMO.**

A549 cells were infected with an E1B-55K deletion mutant virus H5 $\rho$ m4133 for 24 hours, fixed with 4 % PFA and double-labeled with Ab FL-419 ( $\alpha$ -NEMO) and mAb B6-8 ( $\alpha$ -E2A) (3.10.4). Primary Abs were detected with Cy3 ( $\alpha$ -NEMO; orange) and Alexa488 ( $\alpha$ -E2A; green) conjugated secondary Abs. The DNA intercalating dye DAPI was used for nuclear staining. Representative  $\alpha$ -IKK $\alpha$  and  $\alpha$ -E2A staining patterns of at least 40 analyzed cells are shown. Overlays of single images (merge) are shown (magnification x 7600).

In order to confirm the immunofluorescence results, adenovirus infected A549 cells were separated into five fractions immediately after harvest. The first fraction (F1) represented the cytoplasmic portion of the cell (Figure 42, lanes 1; 6; 11), whereas F2-F5 comprise fractions of the nuclear compartment starting with the nuclear membrane (Figure 42, lanes 2; 7; 12), DNase I eluate (Figure 42, lanes 3; 8; 13), high salt eluate (Figure 42, lanes 4; 9; 14) and the nuclear matrix fraction (Figure 42, lanes 5; 10; 15) (Leppard & Everett, 1999; Leppard & Shenk, 1989). Non-infected cells as

control and infected cells were processed through a protocol with various buffer and centrifugation steps (3.9.4).

Staining of E1B-55K after HAdV-C5 wt infection and subsequent subcellular fractionation showed an expected staining pattern with the most abundant amount within the cytoplasm and nuclear matrix fraction. The nuclear matrix fraction is defined as the insoluble residue after detergent lysis of the cell and extraction of the nucleus with DNaseI and salt and includes structures termed PML-NB (Lethbridge, 2003). As expected, E1B-55K was not expressed upon infection of A549 cells with H5pm4149 virus mutant that does not express E1B-55K after introduction of four stop codons within the E1B-55K coding region. NEMO localized within the cytoplasm (F1) and the nuclear membrane fraction (F2) in non-infected A549 cells (Figure 42,

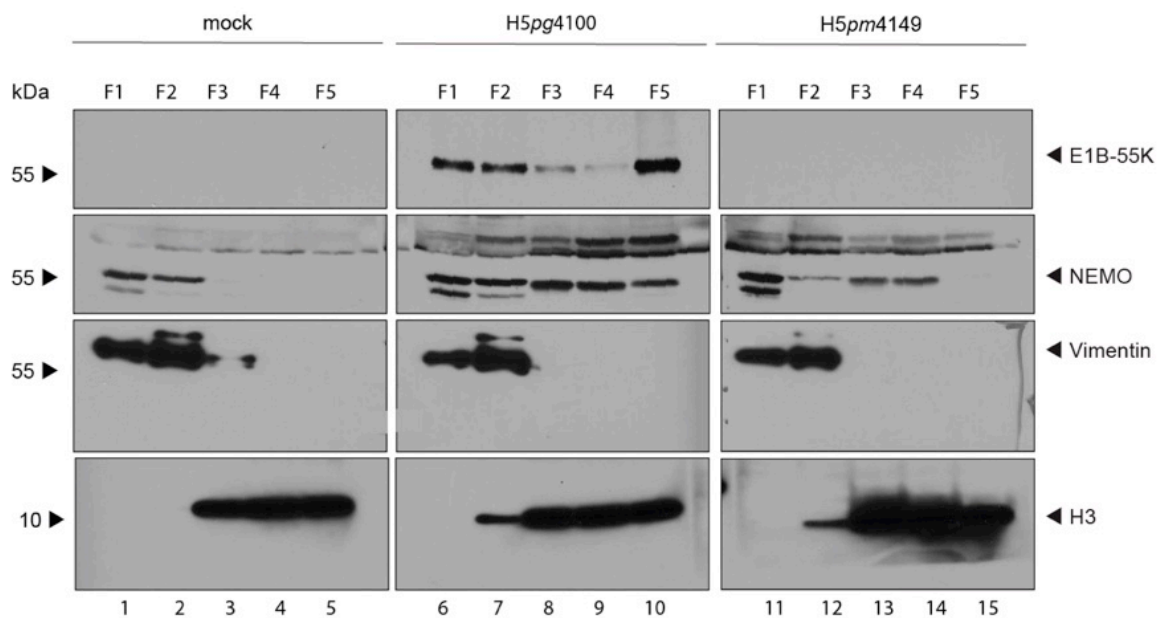


**Figure 42: HAdV-C5 induces nuclear relocalization of NEMO.**

A549 cells were infected with wt H5pg4100 or H5pm4149 and harvested 24 hpi. Fractionation was performed as described in (3.9.4). Fractions 1-5 were separated by SDS-PAGE and subjected to immunoblotting using mAb 2A6 ( $\alpha$ -E1B-55K), Ab rabbit FL-419 ( $\alpha$ -NEMO), Ab rabbit M-204 ( $\alpha$ -IKK $\alpha$ ), mAb ( $\alpha$ -Vimentin), mAb rbH3 ( $\alpha$ -Histone 3).

lane 1 and 2). In adenovirus-infected cells, NEMO was detected not only in the F1 and F2 but also in all other separated fractions (F3-F5) (Figure 42, lanes 8-10). Moreover, the SDS-PAGE showed a faster migrating band of NEMO in the F3 and F4 fractions (Figure 42, lane 8 and 9). The results of the fractionation assays suggest, that E1B-55K directs the localization of NEMO towards the insoluble nuclear matrix fraction (F5) (Figure 42, lane 10). Vimentin and Histone3 were stained as control for proper cytoplasmic and nuclear fractionation, respectively.

#### 4.4.1.6 Endogenous NEMO interacts with E2A and L4-100K upon infection

As shown before, NEMO modulates the levels of E1B-55K and NEMO is relocalized upon infection in an E1B-55K-independent manner (Figure 40). In order to investigate the role of other viral proteins on NEMO subcellular localization, an immunoprecipitation experiment was assessed with endogenous NEMO after adenoviral infection (Figure 43). Therefore, A549 cells were infected for 24 h with H5pg4100 wt at a MOI at 20 ffu/cell and cell lysates were subjected to immunoprecipitation with NEMO specific antibody and as a negative control a non-reactive rabbit IgG antibody was used. Bound proteins were eluted, resolved by SDS-PAGE and detected by western blotting using the appropriate antibodies.

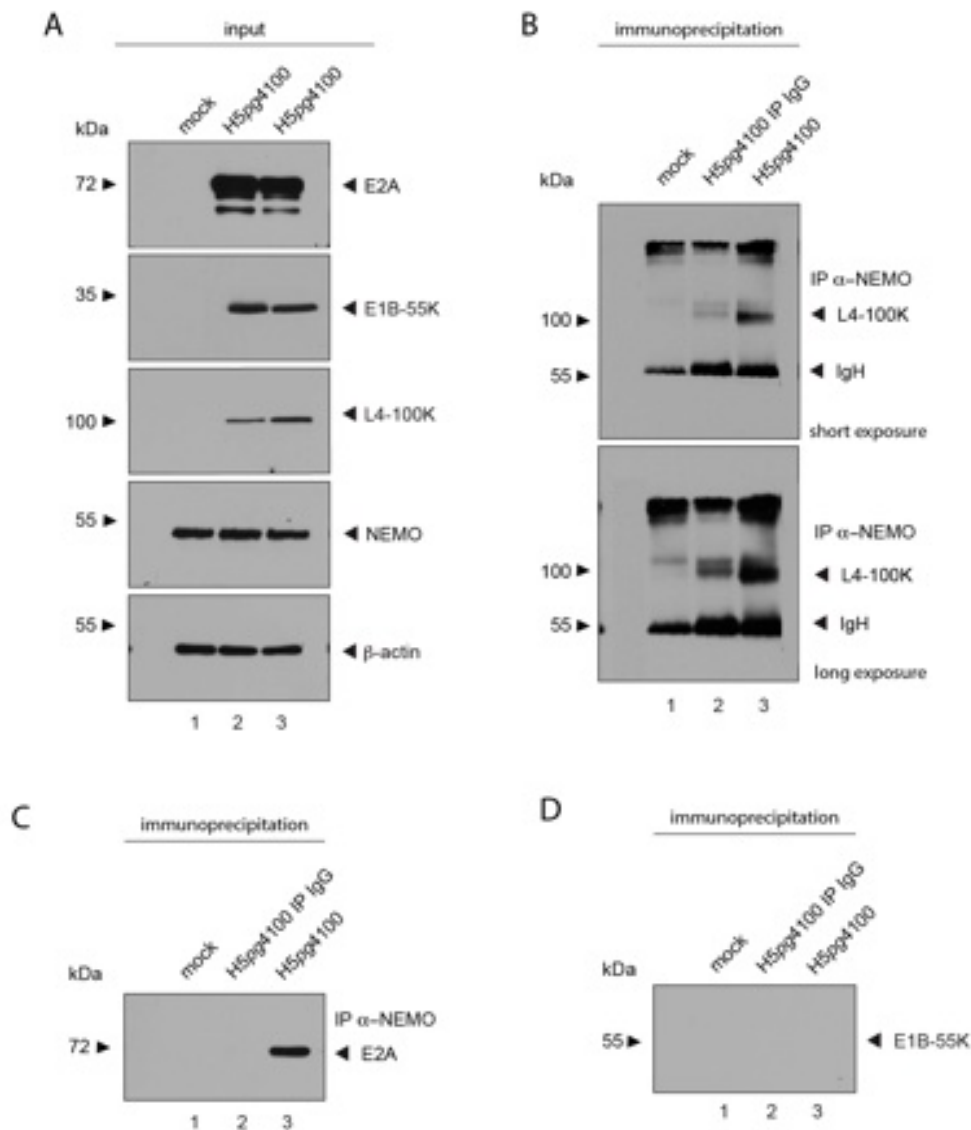


**Figure 43: NEMO interacts with the viral proteins E2A and L4-100K upon adenoviral infection.**

Subconfluent A549 cells ( $4 \times 10^6$ ) were infected with H5pg4100 at a multiplicity of 20 ffu/cell (3.5.1). Cells were harvested 24 hpi before preparing total-cell extracts (3.9.1). Immunoprecipitation of NEMO was performed with mAb FL-419 ( $\alpha$ -NEMO) and as a negative control, non-reactive rabbit IgG antibody was applied. Lysates were resolved by 10 % SDS-PAGE and visualized by immunoblotting (3.9.6). Input levels (A) of total-cell lysates were detected using mAb 2A6 ( $\alpha$ -E1B), mAb B6-8 ( $\alpha$ -E2A), mAb 6B10 ( $\alpha$ -L4-100K) and mAb AC-15 ( $\alpha$ - $\beta$ -actin). Coprecipitated protein (B) samples were stained with mAb 6B10 ( $\alpha$ -L4-100K), (C) mAb B6-8 ( $\alpha$ -E2A), and mAb 2A6 ( $\alpha$ -E1B). Molecular weights in kDa are indicated on the *left*, while corresponding proteins are labeled on the *right*.

Staining of the whole-protein lysate as control revealed that comparable initial amounts of cell lysates were used for immunoprecipitation (Figure 43A). Comparable to the reciprocal co-immunoprecipitation experiment where E1B-55K was immunoprecipitated, no interaction between NEMO and E1B-55K was found, which is in concordance with the E1B-55K-independent relocalization of NEMO (Figure 43D). However, immunoprecipitation assays with NEMO showed interaction of this cellular protein with E2A and L4-100K after adenoviral infection (Figure 43BC). Although a moderate amount of L4-100K was detectable after immunoprecipitation with IgG control, the immunoprecipitated amount of L4-100K with NEMO specific antibody was higher than with the IgG control (Figure 29B, lane 2 and 3). The interaction between E2A and NEMO after infection (Figure 43C) confirmed the result from the immunofluorescence analysis, which showed colocalization of both proteins (Figure 41).

**4.4.1.7 SUMOylation of NEMO is not affected upon infection**

Changes in subcellular localization as shown in Figure 40 by immunofluorescence as well as western blot analysis in Figure 42 indicate that posttranslational modification of NEMO with SUMO occurs. NEMO possesses 3 highly conserved motifs  $\Psi$ KxD/E (where  $\Psi$  is a hydrophobic residue and x represents any residue) at K139, K277 and K285, which could serve as SUMOylation sites (Liu *et al.*, 2013). It turned out that K277 is both necessary and sufficient for SUMO2/3 modification (Liu *et al.*, 2013). This is important for prolonged NF- $\kappa$ B activation. However, another publication showed the importance of lysine K277 and K309, which are part of a conserved SUMO conjugation motif necessary for SUMO1 modification. Mutation of both sites showed inhibition of SUMO1 SUMOylation. This SUMOylation is important for DNA damage-dependent IKK activation (Huang *et al.*, 2003). SUMO is an important determinant of subnuclear localization (Pichler & Melchior, 2002).

In order to test the SUMOylation status of NEMO, H1299 cells were cotransfected with 6HIS-SUMO2 and HA-tagged NEMO and subsequently infected with HAdV-C5 8 hpt (Figure 44). Immunoblotting of Ni-NTA-purified HIS-SUMO conjugates and crude lysates revealed unchanged SUMOylation status of NEMO upon infection (3.9.5).

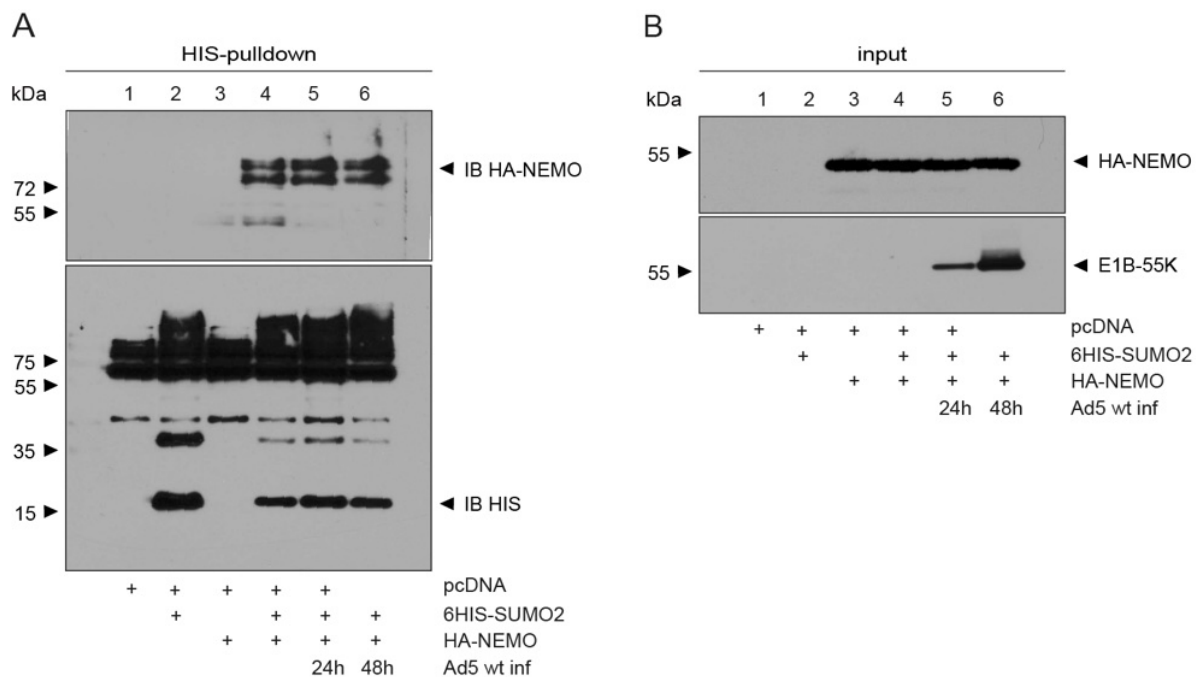


**Figure 44: SUMO modification of NEMO is not altered upon adenoviral infection**

(A, B) H1299 cells were cotransfected with 6HIS-SUMO2 and HA-tagged NEMO and infected with H5pg4100 at a multiplicity of 20 ffu/cells 8 hpt as indicated. Whole-cell lysates were prepared with guanidinium chloride buffer (3.9.5), (A) subjected to Ni-NTA purification of 6HIS-SUMO conjugates and fractionated on a 10 % SDS-gel before immunoblot analysis. Input levels of total-cell lysates (B) and Ni-NTA purified proteins (A) were detected using mAb 3F10 ( $\alpha$ -HA), mAb 2A6 ( $\alpha$ -E1B-55K) and mAb 6xHIS. Molecular weights in kDa are indicated on the *left*, relevant proteins on the *right*.

This result indicates that adenoviral infection does not induce changes in subcellular localization of NEMO by changing its SUMO2 modification.

#### 4.4.1.8 NEMO supports adenovirus progeny production in human cancer cell line A549

We and other groups have recently shown that HAdV-C5 hijacks cellular proteins into distinct newly formed nuclear structures upon infection depending on their function for viral propagation. For example, it has been shown, that cellular factors with proviral functions like Sp100A or TIF1 $\alpha$  are relocated into so called track-like

structures (Berscheminski *et al.*, 2014; Yondola & Hearing, 2007). In contrast, cellular factors with repressive functions like Sp100B, C, HMG, ATRX, Daxx, STAT1 and SPOC1 are trapped within viral replication centers (Berscheminski *et al.*, 2014; Schreiner *et al.*, 2013a; Schreiner *et al.*, 2013b; Sohn & Hearing, 2011). In order to investigate the role of NEMO on adenovirus lytic infection, NEMO knock-down in A549 cell line was performed (Figure 45A). A growth curve was assessed to test whether A549 parental and shNEMO cell lines were comparable, with no significant differences (Figure 45B). Then, A549-NEMO knock-down cells were infected with H5pg4100 virus and virus propagation was determined.

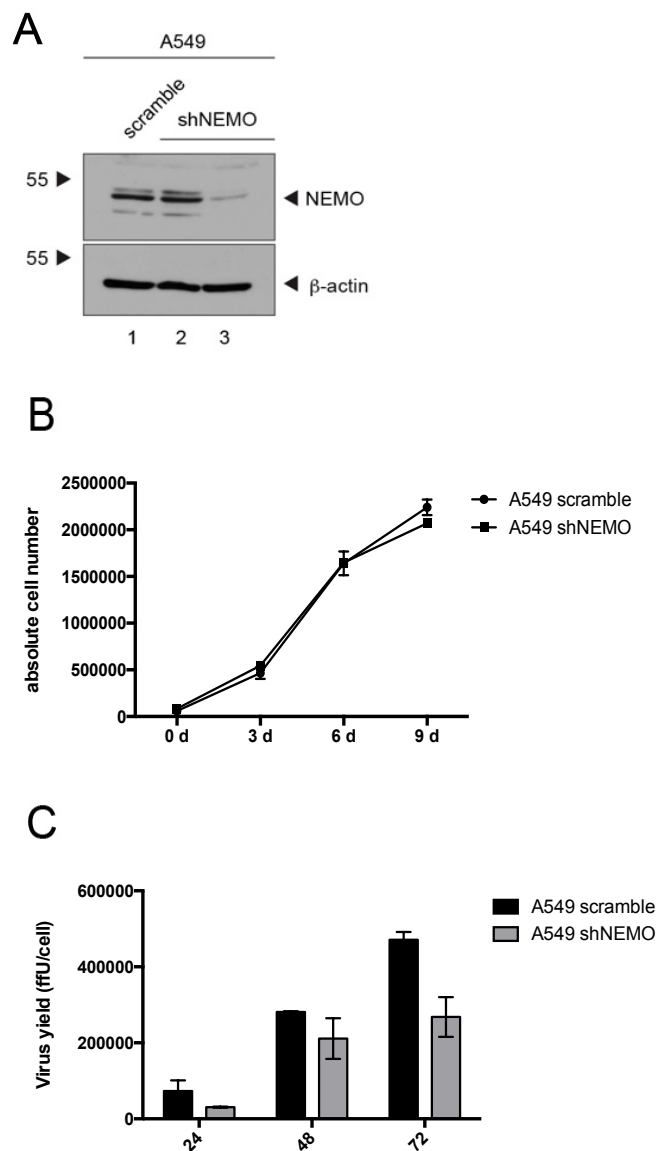


**Figure 45: NEMO depletion affects HAdV progeny production.**

(A) Control of NEMO knockdown efficiency in A549 cells. Lentiviral particles with shNEMO were harvested 24 (lane 2) and 48 hours (lane 3) after transfection of respective constructs. A549 cells were harvested 3 rounds after puromycin selection with the first round started at 48 hours after lentiviral transduction before preparing total-cell extracts (3.4.4). Lysates were resolved by 10 % SDS-PAGE and visualized by immunoblotting using Ab FL-419 ( $\alpha$ -NEMO), and mAb AC-15 ( $\alpha$ - $\beta$ -actin). (B) Total cell numbers of parental and shNEMO A549 cells were determined at indicated time points. (C) A549 parental and respective shNEMO cells were infected with wt virus H5pg4100 at a multiplicity of 20 ffu/cell. Viral particles were harvested 24, 48 and 72 hpi and virus yield was determined by quantitative E2A-72K immunofluorescence staining of HEK-293 cells. The results represent the averages from two independent experiments and error bars indicate the standard error of the mean.

Knock-down of NEMO is presented in Figure 45A, which shows the highest efficiency with around 90 % when the supernatant with lentiviral particles harboring shNEMO harvested at 48 h after transduction was used on A549 cells (Figure 45A, lane 3). However, knock-down of NEMO with the lentiviral supernatant harvested 24 h after transduction was not efficient as expression levels of NEMO were identical to the control cell line. After testing the knock-down efficiency, the cell line was used to determine adenoviral propagation after infection by a virus yield experiment (Figure 45C).

The control knockdown (shscramble) in A549 cells showed progressive increase in virus progeny production over time, as expected (Figure 45C). In contrast, shNEMO cells had a reduction in the amount of viral progeny production at all time points. This was more evident at 72 hpi, where the inhibition reached almost 2-fold when compared to the corresponding shscramble control, showing similar levels of virus progeny to those observed at 48 hpi.

**4.4.1.9 NEMO destabilizes E4orf6 and E1B-55K in A549 cells upon infection**

Knockdown of NEMO showed a decrease on viral progeny production. To test whether the inhibitory effect of NEMO is already measureable on protein level, a further time course experiment followed by immunoblotting was performed (Figure 46). Staining of the first expressed viral protein E1A upon infection showed that its levels are already reduced at 16 hpi. Furthermore, the expression of the viral protein E2A was delayed, shifting from 16 hpi in the control, to 24 hpi in the shNEMO cells. The viral proteins E4orf6 and E1B-55K, although detectable in both cell lines at 24 hpi, presented lower levels in NEMO knocked-down cells compared to the control

cell line. In contrast, L4-100K protein seemed to be more abundant in the NEMO knock-down cell line.

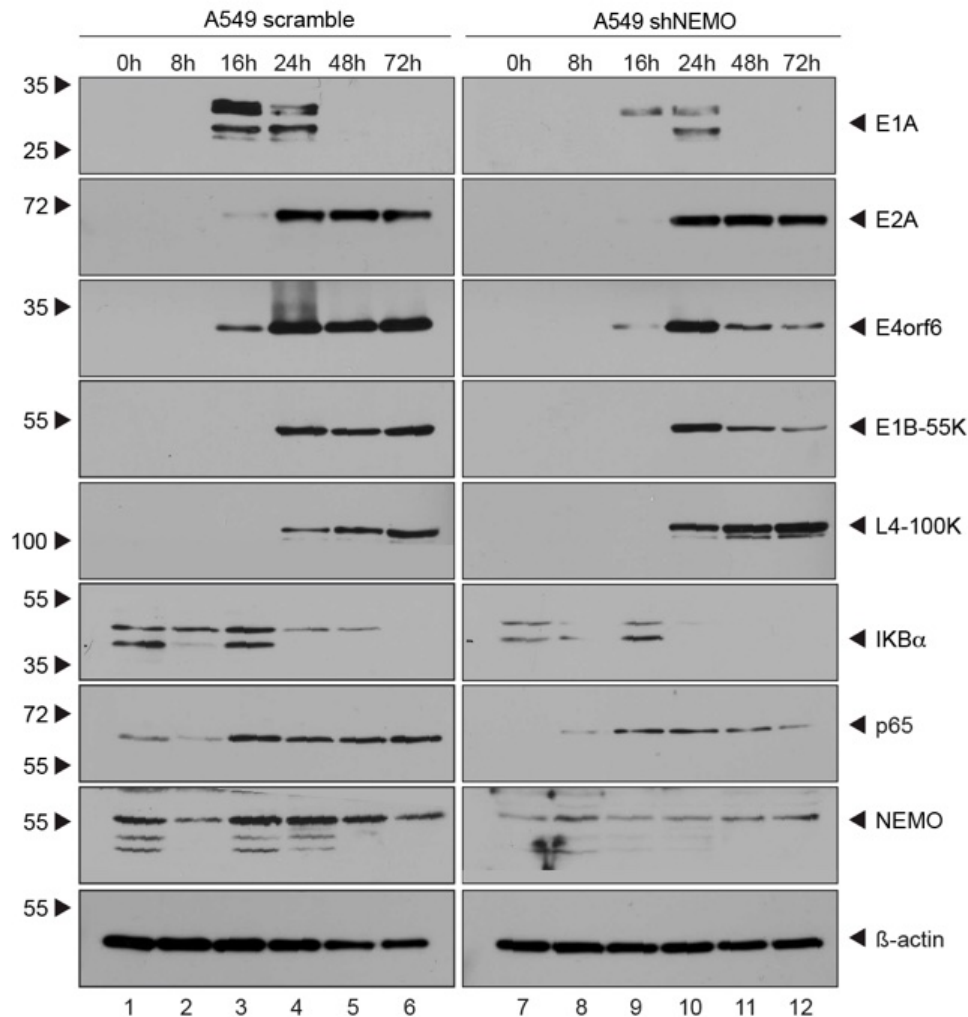


**Figure 46: The absence of NEMO decreases viral protein expression upon infection in A549 cells.**

A549 scramble and A549 shNEMO cells were infected with wt H5pg4100 at a multiplicity of 20 ffu/cell and proteins from total-cell extracts were separated by SDS-PAGE and subjected to immunoblotting using rabbit Ab C-21 ( $\alpha$ -I $\kappa$ B $\alpha$ ), C-20 ( $\alpha$ -p65), FL-419 ( $\alpha$ -NEMO), mouse mAb M-58 ( $\alpha$ -E1A), B6-8 ( $\alpha$ -E2A), 2A6 ( $\alpha$ -E1B-55K), RSA3 ( $\alpha$ -E4orf6), AC-15 ( $\alpha$ - $\beta$ -actin) and rat 6B10 ( $\alpha$ -L4-100K). Molecular weights in kDa are indicated on the left, relevant proteins on the right.

Furthermore, levels of NF- $\kappa$ B pathway proteins, I $\kappa$ B $\alpha$  and p65, were reduced upon reduction of NEMO. Control staining of NEMO showed that the expression of the shRNA against NEMO resulted in a moderate down-regulation.

Taken together, NEMO seems to be a positive regulator of adenovirus infection that, on the one hand, regulates the stability of overexpressed adenoviral proteins and, on the other hand, interacts with several viral proteins upon infection suggesting a complex regulatory network. More experiments are needed to understand the molecular mechanisms controlling these complex processes.

### 5.1 HAdV-C5 regulates NF- $\kappa$ B pathway during lytic infection

Adenoviruses usually cause mild and self-limiting infections in immunocompetent individuals; however, it can also cause severe disease in immunocompromised patients, with fatal cases being reported (Carr *et al.*, 2011; Savón *et al.*, 2008; Siminovich & Murtagh, 2011). This fact denotes the importance of a functional immune system that is needed to control adenovirus infection and progression.

Because adenoviral vectors have been widely generated for vaccine application and gene/cancer therapy, many studies have focused on investigating the innate immune activation upon administration of HAdV-C5 vectors. As a consequence, several reports have described the role of incoming adenoviral proteins from the virus particle on cytokine induction by activation of the NF- $\kappa$ B pathway (Borgland *et al.*, 2000; Duerksen-Hughes *et al.*, 1989; Gooding *et al.*, 1988). Further studies mainly focused on single early viral proteins by either applying plasmids expressing specific viral proteins or replication deficient vectors. However, no studies have focused on the NF- $\kappa$ B pathway in the context of productive infection with lytic wild type. Furthermore, only few reports have analyzed the activation of cytokine/chemokine production upon adenovirus infection. However, these studies were done at high multiplicity of infection (MOI). Therefore, the aim of this thesis is to investigate the molecular mechanisms behind NF- $\kappa$ B pathway and cytokine production in the context of wild type HAdV infection.

#### 5.1.1 Interplay between HAdV-C5 proteins and the NF- $\kappa$ B pathway

This work demonstrates that there is a reciprocal interaction between HAdV-C5 proteins and the NF- $\kappa$ B subunit p65. On the one hand, overexpression of p65 shows increased up-regulation of some adenoviral gene promoters, mainly E1A and E2A promoter genes, confirming the results obtained by Machitani *et al.* On the other hand, overexpression of different adenoviral proteins also increases the luciferase expression of a construct encoding the NF- $\kappa$ B promoter (Figure 16). Specifically, E1A protein shows a significant impact on NF- $\kappa$ B promoter induction. This observation is in line with the reports, which showed that many viral oncoproteins, such as Tax (HTLV) and LMP1 (EBV), also induce NF- $\kappa$ B activity (Hiscott *et al.*, 2001). Such proteins either can be cancerogenic themselves or are associated with tumor development. E1A has been previously described to be both activator and inhibitor

of the NF- $\kappa$ B pathway depending on the viral genetic background (Schaack, 2005). E1A alone is sufficient to activate immune response, whereas fully suppression of HAdV-C5 induced inflammation needs further viral proteins from the E1 region (E1B-55K and E1B-19K) (Schaack, 2005; Schmitz *et al.*, 1996). Moreover, proteins from the E3 region inhibit the immune response by counteracting TNF $\alpha$ -induced chemokine expression.

Besides divergent regulatory mechanisms of E1A on cellular proteins in different cell lines, this viral factor has a multifaceted role as transcription factor in regulating NF- $\kappa$ B pathway activation depending on the proinflammatory stimuli such as IL-1, tumor necrosis factor (TNF) and endotoxin (Siebenlist *et al.*, 1994). It has been published that stably transfected HAdV-C5 E1A, which is transiently expressed in HepG2 and HeLa cells, represses IL-6 transcription after induction with IL-1 or TNF $\alpha$  (Siebenlist *et al.*, 1994). Therefore, E1A interferes with the formation of appropriate NF- $\kappa$ B-DNA complexes (Janaswami *et al.*, 1992). However, stable expression of transfected HAdV-C5 E1A in A549 cells stimulates exclusively adhesion molecule-1 (ICAM-1) and IL-8 expression after lipopolysaccharide (LPS) treatment (Keicho *et al.*, 1999). Besides direct interaction between E1A and NF- $\kappa$ B (Schmitz *et al.*, 1996), it is suggested that transcriptional regulation of E1A on NF- $\kappa$ B is mediated by the coactivators CBP, the cAMP-responsive element binding (CREB) binding protein, and the related protein p300 (Gerritsen *et al.*, 1997; Parker *et al.*, 1997). The repressive function of the adenoviral early protein on the NF- $\kappa$ B pathway by inhibiting IKK-mediated I $\kappa$ B phosphorylation has been shown for HAdV-C5 (Shao *et al.*, 1999). However, this inhibition could be mediated indirectly, as immunoprecipitation analysis indicated that there is no direct binding between E1A and IKK $\alpha$ /IKK $\beta$ , respectively (Shao *et al.*, 1999). Although the molecular mechanism of E1A after transfection has been investigated in detail, its regulatory role in concert with further viral proteins during HAdV-C5 infection on the NF- $\kappa$ B pathway had not been investigated yet.

Here we present results showing that the viral late non-structural L4-100K and the core proteins pV and pVII, which enter the cell with the viral capsid and are *de novo* expressed at late time point of infection, were also able to stimulate the NF- $\kappa$ B pathway, although at a lower rate (Figure 16).

In contrast, overexpression of E1B-55K and pIX proteins failed to activate the NF- $\kappa$ B promoter in our reporter gene assay (Figure 16). Nothing is reported regarding the role of pIX on the NF- $\kappa$ B pathway regulation. However, E1B-19K can inhibit NF- $\kappa$ B activation in epithelial cell lines (Schmitz *et al.*, 1996; Bergman & Shavit, 1988). Based

on our findings, it is likely that first activation of the NF- $\kappa$ B promoter is necessary in order to measure E1B-dependent inhibition of the NF- $\kappa$ B pathway.

Taken together, the results show that a regulatory interplay exists between HAdV-C5 proteins and the NF- $\kappa$ B pathway, suggesting a timely dependent regulation of the NF- $\kappa$ B pathway by different HAdV-C5 proteins, as both early as well as late expressed proteins are capable of activating the NF- $\kappa$ B promoter.

### 5.1.2 HAdV-C5 infection counteracts TNF $\alpha$ -induced NF- $\kappa$ B activation

The results of our studies in H1299 cells showed that the NF- $\kappa$ B pathway is not activated at early and late time point upon infection (Figure 17BC). This is in line with results from a publication investigating adenovirus respiratory tract infections (ARTI) of airway epithelial cells, which do not express inflammatory mediators (Zsengeller *et al.*, 2000). However, during ARTI alveolar macrophages rapidly phagocytose internalized adenovirus-infected cells, and therefore induce expression of inflammatory mediators (Zsengeller *et al.*, 2000). Furthermore, immediate early events in *in vivo* studies of HAdV-C5-mediated inflammation induce or release cytokines including TNF $\alpha$ , IL-6, IL-8, Mip-1 $\alpha$ , IL-1 and Mip-2 (Cartmell *et al.*, 1999; Muruve *et al.*, 1999; Otake *et al.*, 1998). This is also true after *in vivo* response to replication-deficient adenoviral vector transduction or infection with inactivated particles/capsids, suggesting that immune responses occur prior to detectable viral gene expression, potentially dependent only on binding and/or internalization of viral capsid components (Higginbotham *et al.*, 2002).

HAdV-C5 infection triggers the release of chemokines and cytokines by the immune cells, which are responsible in some cases for the physiopathology associated with severe HAdV infections (Guidotti & Chisari, 2001; Muruve *et al.*, 1999; Schnell *et al.*, 2001). Moreover, it has been shown that specific serotypes induce different cytokine/chemokine response depending on the cell type (Diaz *et al.*, 1999; Moro *et al.*, 2009; Teigler *et al.*, 2012; Zsengeller *et al.*, 2000). In order to mimic the effects of cytokine release by the immune cells upon the NF- $\kappa$ B pathway activation in epithelial cells infected by HAdV-C5, H1299 cells were treated with TNF $\alpha$  and infected them with HAdV-C5 (Figure 17DE). We excluded the immunomodulatory functions of the E3 proteins, which have been widely implicated in controlling the

immune response upon HAdV-C5 infection, by using a HAdV-C5 virus that lacks part of the E3 region (Kinds Müller *et al.*, 2007).

Our results (displayed in Figure 17DE) showed that HAdV-C5 infection inhibited TNF $\alpha$ -mediated NF- $\kappa$ B activation in epithelial cells 24 hours post infection (Zsengeller *et al.*, 2000). Similar results have been previously obtained during human cytomegalovirus (HCMV) infection, where TNF $\alpha$  as well as IL-1 $\beta$  signaling were blocked at later times post infection (Montag *et al.*, 2006). TNF $\alpha$  is a pro-inflammatory molecule, which is important in host defense against viruses and bacteria, in lymphoid organ architecture, and in immune cell activation and trafficking (Bradham *et al.*, 1998; Gantzer *et al.*, 2002; Lieber *et al.*, 1997; Sedgwick *et al.*, 2000). Therefore, circumventing the TNF $\alpha$ -induced immune response is beneficial for a successful virus infiltration in the host-targeted tissue. Moreover, understanding how HAdV-C5 regulates TNF $\alpha$ -mediated immune response could be useful to improve the design of adenovirus-based vector for the safe use in gene therapy approaches (Friedman & Horwitz, 2002).

### 5.1.3 IKK complex proteins are targeted upon adenoviral infection

Based on transcriptome data from Miller *et al.*, E1B-55K seems to be necessary for gene repression of genes that mediate antiviral and immune defenses (Miller *et al.*, 2009). Therefore, we decided to investigate the role of E1B-55K on interfering with NF- $\kappa$ B pathway protein complexes. We detected interaction between the viral protein E1B-55K and IKK $\alpha$ , IKK $\beta$  and NEMO after cotransfection (Figure 20). Besides, we could observe a significant reduction in the IKK complex formation upon HAdV-C5 infection, which indicates that HAdV-C5 targets the NF- $\kappa$ B pathway by physically affecting the IKK complex formation (Figure 20). The IKK complex is a common target for several viruses such as Merkel Cell Polyomavirus Small T Antigen (ST), which interacts with NEMO and thereby inhibits I $\kappa$ B phosphorylation by IKK $\alpha$ /IKK $\beta$  preventing NF- $\kappa$ B activation (Griffiths *et al.*, 2013). The reduction of the IKK complex formation upon HAdV-C5 infection could explain the inhibition of TNF $\alpha$  mediated NF- $\kappa$ B activation, which was detected in Figure 17DE. However, the decrease of IKK complex formation can only partially be responsible for the entire disruption of TNF $\alpha$  mediated NF- $\kappa$ B inhibition at 24 hpi as a significant amount of IKK complex formation was still detectable. In line with this, the remaining amount of IKK complexes could be responsible for reduced protein levels of I $\kappa$ B $\alpha$  upon HAdV-C5 infection (Figure 18, Figure 31, Figure 32). I $\kappa$ B $\alpha$  is the inhibitor of the NF-

$\kappa$ B pathway that is proteasomally degraded when this pathway is activated. By this, the transcription factor NF- $\kappa$ B consisting of p50/p65 (canonical pathway) can enter the nucleus and activate the expression of genes involved in the immune response. Although the I $\kappa$ B $\alpha$  levels upon HAdV-C5 infection is reduced (Figure 18, Figure 31, Figure 32), a nuclear relocalization of p65 after infection is not detectable (Figure 19). These results suggest that HAdV-C5 might not affect I $\kappa$ B $\alpha$  proteasomal degradation; in contrast, it might abrogate NF- $\kappa$ B pathway activation through the inhibition of p65 nuclear localization. This inhibition has already been shown for poxviruses. For example, chordopoxviruses like CPV (Cowpox virus), which express the CP77 protein that targets both p65 and the E3 ubiquitin ligase complex. Both functions are essential for inhibition of NF- $\kappa$ B relocalization into the nucleus (Chang *et al.*, 2009). Furthermore, other poxviral proteins directly interact with p65 or inhibit its phosphorylation to prevent its activation and/or nuclear relocalization (Camus-Bouclainville *et al.*, 2004; Mohamed *et al.*, 2009a). Further investigations are needed to describe the adenoviral factors that might inhibit NF- $\kappa$ B pathway activation by preventing p65 nuclear relocalization.

IL-1 and TNF $\alpha$  signaling converge in the IKK complex, which is phosphorylated, promoting the ubiquitinylation and subsequent degradation of the NF- $\kappa$ B inhibitory molecule I $\kappa$ B $\alpha$  (Basak & Hoffmann, 2008; Karin, 1999). Therefore, it seems logical that the virus targets the IKK complex because of its central role in controlling NF- $\kappa$ B pathway. This way, HAdV-C5 could benefit from NF- $\kappa$ B pathway-independent functions of the IKK complex proteins. In this regard, it is known that the activity of the IKK complex components is not only restricted to the NF- $\kappa$ B-dependent pathway, but it is also involved in cross-talk with further signalling cascades, such as mTOR and MAPK (Dan *et al.*, 2014). Besides, IKK $\alpha$  is a key component of the non-canonical NF- $\kappa$ B pathway that is activated by the NF- $\kappa$ B-inducing kinase (NIK). Up to date, the IKK $\alpha$  components form the central complex of the non-canonical NF- $\kappa$ B pathway, as all inducers of the pathway identified so far sense the signals through NIK (Claudio *et al.*, 2002; Coope *et al.*, 2002a; Dejardin *et al.*, 2002; Kayagaki *et al.*, 2002). IKK $\alpha$  and NIK process the p100 protein into a smaller isoform, named p52, which forms the RelB/p52 heterodimer that is translocated into the nucleus. Targeting IKK $\alpha$  during HAdV-C5 infection could be a mechanism to modulate the non-canonical NF- $\kappa$ B pathway. This has already been shown for EBV LMP1 protein, which activates the pathway via a NIK- and IKK $\alpha$  dependent mechanism (Soni *et al.*, 2007). Furthermore, KSHV and EBV activate the non-canonical NF- $\kappa$ B pathway via vFLIP, which occurs through a NIK-independent but NEMO- and IKK $\alpha$ -dependent

mechanism (Sun & Cesarman, 2011). It remains to be investigated whether HAdV-C5 targets NEMO and IKK $\alpha$  in order to modulate the non-canonical NF- $\kappa$ B pathway.

Taken together, these results provide first insights into the NF- $\kappa$ B pathway regulation in human epithelial cell lines by counteracting the formation of the IKK complex upon HAdV-C5 infection.

## 5.2 IKK $\alpha$ exerts pro-viral functions upon HAdV-C5 infection

The real time PCR data from this thesis indicated that IKK $\alpha$  activates the E1A promoter after HAdV-C5 infection, which was verified by IKK $\alpha$  knock-down experiments (Figure 32A). In line with these results, the amounts of E1A and E1B mRNA transcripts at 12 hpi were increased (Figure 32AB). Interestingly, at 24 hpi the mRNA levels of both E1A and E1B were downregulated, indicating a regulatory switch from slight activation to repression by IKK $\alpha$  upon HAdV-C5 infection (Figure 32AB). This switch was confirmed by an increase in the E1A levels upon IKK $\alpha$  knocked-down, although this increase was rather mild (Figure 32A). The repression of the viral gene expression correlates with the time point of IKK $\alpha$  nuclear localization, as detected by immunofluorescence analysis in Figure 27. However, although mRNA transcript levels of E1B are increased in the absence of IKK $\alpha$  (Figure 32B), the virus yield analysis indicates that this cellular protein is important for proper HAdV-C5 progeny production. Depletion of IKK $\alpha$  resulted in highly reduced virus yields in different cell lines (Figure 30), although at different degrees. While a six-fold reduction in virus yield in H1299 with IKK $\alpha$  knocked-down cells (Figure 30D) could be detected, a ten-fold decrease was observed in A549 IKK $\alpha$  knocked-down cells (Figure 30E). These results indicate that IKK $\alpha$  has important distinct pro-viral functions for HAdV-C5 early upon infection. In line with this, it has been shown that other pro-viral cellular proteins relocalize juxtaposed to viral replication centers into track like structures, such as Sp100A. There, these factors promote viral DNA replication that takes place at the periphery of the replication centers (Berscheminski *et al.*, 2014). Furthermore, the relocalization of IKK $\alpha$  is independent on E1B-55K (Figure 28) and that it does not affect the IKK complex formation (Figure 29). Therefore, we assume that the interaction between both proteins is important to regulate a NF- $\kappa$ B pathway-independent function of IKK $\alpha$  during lytic infection. It is known that various functions of E1B-55K are regulated by different posttranslational modifications such as phosphorylation and SUMOylation. Hence, we investigated the interaction between IKK $\alpha$  and mutants of E1B-55K in posttranslational modified

sites to reveal the nature of their interaction. Immunoprecipitation analysis showed that posttranslational modifications of E1B-55K are not necessary for these protein interactions (Figure 24). To further characterize the interaction between E1B-55K and IKK $\alpha$ , different single-amino acid substitution mutants throughout E1B-55K that have been well characterized were tested (Kindsmüller *et al.*, 2007; Schwartz *et al.*, 2008; Shen *et al.*, 2001). We could show that IKK $\alpha$  has reduced binding affinity to the E1B-55K-RF6 mutant, which could abolish the transformation potential of E1B-55K, although transactivation of p53 is repressed (Härtl *et al.*, 2008). This observation was unexpected, as repression of the transactivation activity of p53 was believed to be a prerequisite for efficient cellular transformation (Zeller, 2003). Furthermore, the E1B-55K-RF6 mutant disturbs the integrity of the perinuclear bodies as it localizes in many distinct dot-like structures within the cytoplasm, close to the nucleus. It is assumed that the contribution of one or several additional p53-independent factors together with E1B-55K could stimulate the E1A-induced transformation efficiency (Zeller, 2003). Therefore, it is reasonable to assume that IKK $\alpha$  could be such a factor, enhancing the transformation capability of E1B-55K by a so far unknown mechanism (Perkins, 2012). In general, previous studies showed that prolonged activation of NF- $\kappa$ B pathway can promote cell survival and malignant phenotypic changes, which is important in development and progression of squamous cell carcinomas (SCC) and other cancers (Van Waes *et al.*, 2007). Intriguingly, IKK $\alpha$ -mediated phosphorylation has been shown to positively regulate cell proliferation and consequently tumorigenesis via NF- $\kappa$ B-independent pathways (Chariot, 2009). Thereby, IKK $\alpha$  interacts with steroid receptor coactivator (SRC) that, in turn, regulates genes such as cyclin D1 and c-Myc, leading to oestrogen-dependent cell proliferation induction (Park *et al.*, 2005; Wu *et al.*, 2002). Additionally, prometastatic function was also linked to nuclear IKK $\alpha$ , which is correlated with phosphorylated nuclear IKK $\alpha$  and reduced expression of maspin, a gene suppressor that belongs to the serpin family (Luo *et al.*, 2007). Therefore, nuclear IKK $\alpha$  is recruited to the maspin promoter presumably through the recruitment of a so far unidentified DNA methyltransferase by IKK $\alpha$  (Luo *et al.*, 2007). However, there are several publications, which showed the role of IKK $\alpha$  as a tumor suppressor in SCC. In a murine model, expression of IKK $\alpha$  promoted terminal differentiation and reduced proliferation, angiogenesis and metastasis (Liu *et al.*, 2006; Maeda *et al.*, 2007). Therefore, it remains to be elusive, whether IKK $\alpha$  contributes to transformation with the adenoviral oncogenes E1A and E1B-55K.

HAdV-C5 targets IKK $\alpha$  and redirects it into the nucleus, juxtaposed to the viral replication centers (Figure 27; Figure 28). It has been shown that IKK $\alpha$  also exerts NF- $\kappa$ B pathway-independent regulatory functions within the cytoplasm and the nucleus (Chariot, 2009). Additional kinase substrates, which mainly localizes within the nucleus, have been identified. Therefore, the variety of its biological functions beside immune response regulation is obvious, which is increased by its cytoplasmic/nuclear shuttling capability (Jiang *et al.*, 2003; Lamberti *et al.*, 2001).

The first identified stimulant for IKK $\alpha$  nuclear translocation is TNF $\alpha$  (Anest *et al.*, 2003; Yamamoto *et al.*, 2003b), which was followed by lymphotoxin  $\beta$  and CD40 (Huang *et al.*, 2007). Later on, nuclear IKK $\alpha$  has been identified to regulate NF- $\kappa$ B-dependent and -independent gene transcription as reviewed by Huang and Hung (Huang & Hung, 2013). Therefore, IKK $\alpha$  translocates into the nucleus in response to a variety of stimuli, and enhances chromatin accessibility at NF- $\kappa$ B-responsive promoters, which is mediated by phosphorylation of Histone H3 at Ser10 (Yamamoto *et al.*, 2003b). Additionally, IKK $\alpha$  kinase activity regulates corepressor and coactivator complexes on chromatin, thereby enhancing acetylation of p65 by p300 and it enables full transcriptional activity (Hoberg *et al.*, 2006). Due to the described NF- $\kappa$ B-independent functions of IKK $\alpha$ , we could assume that a so far unidentified nuclear function of IKK $\alpha$  is beneficial for adenoviral lytic infection. Whether this function needs nuclear relocalization of IKK $\alpha$ , which has been observed at late time points upon HAdV-C5 infection, remains to be proved by mutation of the nuclear localization signal (NLS) of IKK $\alpha$ .

### 5.3 NEMO regulates stability of important HAdV-C5 regulatory proteins

This work demonstrates that E1B-55K protein levels were reduced upon cotransfection with NEMO independent of the proteasomal degradation pathway (Figure 35, 37). This reduction was also observed for E4orf6 (Figure 38), a viral protein that is known to exert important functions for the virus life cycle in cooperation with E1B-55K. These two proteins together are able to induce the proteasomal degradation of several antiviral factors such as p53, Mre11, the DNA ligase IV, the bloom helicase, ATRX, Tip60, SPOC1, and the integrin  $\alpha$ 3 (Blanchette *et al.*, 2004a; Blanchette *et al.*, 2004b; Boyer *et al.*, 1999; Dallaire *et al.*, 2009b; Forrester *et al.*, 2011; Gupta *et al.*, 2012; Harada *et al.*, 2002; Liu *et al.*, 2005b; Orazio *et al.*, 2011; Schreiner *et al.*, 2013a; Schreiner *et al.*, 2013b; Schreiner *et al.*, 2012b; Stracker *et al.*,

2002a; Stracker *et al.*, 2002b; Woo & Berk, 2007). Moreover, NEMO and E1B-55K overexpression were accompanied by relocalization of cytoplasmic E1B-55K into the perinuclear bodies (Figure 36b), whereas NEMO lost its diffuse cellular localization within the cytoplasm (Figure 36e) and relocalized into the nucleus as well as into perinuclear bodies (Figure 36i), where it colocalizes with E1B-55K (Figure 36l). Proteins are mainly degraded through proteasomal or lysosomal degradation. This is usually following a prior covalent linkage of proteins with ubiquitin, which targets them for degradation processes. Proteasomal degradation is mostly ubiquitin-dependent, whereas ubiquitylation is a rare event prior to lysosomal degradation (Glick *et al.*, 2010; Jariel-Encontre *et al.*, 2008; Kirkin *et al.*, 2009; Knecht *et al.*, 2009). Staining of E1B-55K does not indicate lysosomal degradation, as it is associated with cytoplasmic dot like structures in immunofluorescence staining. Therefore, it is remaining to be investigated how NEMO influences E1B-55K protein levels within the infected cell.

#### **5.4 The nuclear localization of NEMO might play a role upon adenovirus infection**

Besides reduced protein levels of E1B-55K and E4orf6 (Figure 21), cotransfection of E1B-55K and NEMO induces complete relocalization of diffusely cytoplasmic distributed E1B-55K into perinuclear bodies (Figure 36). Conversely, HAdV-C5 infection induces the nuclear relocalization of NEMO, which colocalizes with thereplication centers where viral DNA replication takes place (Figure 40). It has already been observed that cellular proteins, which have regulatory roles in lytic infection, are relocalized into replication centers. Some examples are ATRX, Daxx, SPOC1, STAT1 and Sp100 B, C and HMG, which exert antiviral functions (Berscheminski *et al.*, 2014; Schreiner *et al.*, 2013a; Schreiner *et al.*, 2013b). However, proviral cellular proteins such as Sp100A and TIF1 $\alpha$  have been observed to relocalize juxtaposed to the viral replication centers (Berscheminski *et al.*, 2014; Vink *et al.*, 2012). This is also true for IKK $\alpha$  as shown in Figure 33. NEMO dependent reduction of E1B-55K after cotransfection of NEMO and E1B-55K (Figure 35) and nuclear relocalization of NEMO into viral replication centers after infection (Figure 42) suggest its role as a negative regulator of adenovirus lytic infection. However, depletion of NEMO reduces adenovirus progeny production (Figure 45). More detailed investigations showed that although E1B-55K is regulated by NEMO, cells infected with a HAdV-C5 E1B-55K null mutant, still show relocalization of NEMO

into the viral replication centers (Figure 40). Interestingly, the relocalization of NEMO in replication/transcription active nuclear bodies has been shown in the presence of the viral protein Tax, from HTLV-1. Tax-containing nuclear bodies are constituted preferentially in close spatial proximity to a variety of proteinaceous nuclear structures, including PML bodies, Cajal bodies, and the nucleoli (Freiman & Tjian, 2003). Their loss prevents transcriptional activation due to the ineffective accumulation of components that are important for transcription, formation of splicing complexes, of the two subunits of NF- $\kappa$ B, and of the transcriptional co-activator CBP/p300 (Bex *et al.*, 1997; Bex *et al.*, 1998). SUMOylated Tax is important to drive NEMO nuclear localization, specifically within the nuclear bodies (Lamsoul *et al.*, 2005; McCool & Miyamoto, 2012). Both proteins have in common that they interact with the N-terminal domain of the transcriptional co-activator CBP. The interaction of NEMO with CBP counteracts the positive action of CBP/RelA/IKK $\alpha$  complexes on the transcription initiated at NF- $\kappa$ B-responsive promoters (Verma, 2003), whereas Tax-CBP interaction is critical for Tax transcriptional activities (Kwok *et al.*, 1996). Analogous to HTLV, HAdV-C5 encodes for two proteins (E1A and E2A), which target host cell regulation. Therefore, E1A and E2A disrupt the same cellular protein complex by targeting CBP and SrCap, respectively (Xu *et al.*, 2003). In this thesis we could show that NEMO interacts with the main viral replication center protein E2A (Figure 43), which could be in line with Tax being responsible for regulating the subcellular localization of NEMO upon infection, which could be needed to support HAdV-C5 progeny production (Figure 45). Moreover, NEMO interacts with the viral late non-structural protein L4-100K with multiple essential functions for efficient completion of lytic virus infection during the late phase of infection. These comprises the modulation of the cellular translation machinery in favor of translating large amounts of virus products and functioning as a chaperone for hexon trimerization and preventing apoptosis by inhibition of granzyme-B. Several different HAdV-C5 proteins with various functions interact with NEMO suggesting that it could have a broad range of functions in regulating adenovirus infection.

Besides the activation of the NF- $\kappa$ B pathway, NEMO is also functionally associated with an additional role to communicate between the nuclear DNA damage activated kinase ATM (Ataxia telangiectasia mutated) and the cytoplasmic IKK complex to induce NF- $\kappa$ B signaling in response to genotoxic agents (Miyamoto, 2010). Adenoviruses as DNA viruses are perceived by the cell as damaged DNA, which are protected from the DNA damage response (DDR) by the adenoviral core protein VII

upon cell entry (Karen & Hearing, 2011). However, after viral DNA entry into the nucleus, DDR is activated leading to concatenation of viral genomes, which has been shown to be counteracted by HAdV-C5 encoded early proteins in order to ensure proper virus propagation (Forrester *et al.*, 2011; Weitzman & Ornelles, 2005). Interestingly, NEMO targets the adenoviral proteins E1B-55K and E4orf6 which are known to inhibit the DNA damage response (DDR) by ubiquitin-mediated degradation of DDR proteins such as components of the MRN complex (Carson *et al.*, 2003; Forrester *et al.*, 2011; Stracker *et al.*, 2002a), the DNA ligase IV (Baker *et al.*, 2007; Forrester *et al.*, 2011), p53 (Forrester *et al.*, 2011; Harada *et al.*, 2002; Querido, 2001) and TOPBP1 (Blackford *et al.*, 2008; Forrester *et al.*, 2011) or by relocalizing MRN from viral replication centers (Carson *et al.*, 2009; Evans & Hearing, 2003; Stracker *et al.*, 2002a). For nuclear sensing of DNA damage response activation to induce NF- $\kappa$ B pathway, SUMO modification of NEMO is required (Huang *et al.*, 2003). One putative reason for relocalization of NEMO into viral replication centers could be the inhibition of NF- $\kappa$ B activation induced by DNA damage response sensing. Therefore, SUMOylated NEMO would be trapped within viral replication centers and cannot bridge the DDR to NF- $\kappa$ B pathway activation anymore. However, we could not detect changes in NEMO SUMOylation upon infection (Figure 44). Furthermore, expression of E1B-55K after adenoviral infection is not necessary to mediate nuclear relocalization of NEMO (Figure 41). Besides the already mentioned E1B-55K and E4orf6 proteins, there are further proteins known, which are involved in counteracting the DDR such as E4orf3 and E4orf4 (Brestovitsky *et al.*, 2016; Shah & O'Shea, 2015). Therefore, E4orf3 assembles a multivalent polymer network within the nucleus that sequesters MRN (Ou *et al.*, 2012; Stracker *et al.*, 2002a), whereas E4orf4 reduces phosphorylation of ATM and ATR (Ataxia telangiectasia and Rad3 related) and thereby inhibiting DNA damage repair (Brestovitsky *et al.*, 2016). More investigations are needed to examine whether relocalization of NEMO upon adenovirus infection into the viral replication centers has influence on the DDR.

It has been published that overexpression of NEMO can result in inhibition of NF- $\kappa$ B signaling, suggesting that the expression levels of NEMO regulate its own function. Therefore, it is important to take into account the different amounts of NEMO expressed in different cell systems, which could explain contradictory results upon comparison of infection or overexpression of E1B-55K protein levels with endogenous or overexpressed NEMO. We could detect reduced protein levels of E1B-55K and E4orf6 after cotransfection with NEMO (Figure 35). However, also depletion of NEMO resulted in reduced protein levels of E1B-55K and E4orf6 after

adenovirus infection (Figure 46). Furthermore, interaction of E1B-55K with NEMO is only detectable upon HAdV-C5 infection and overexpression of NEMO.

Beside functional switch dependent on the expression levels of NEMO, other viral proteins alone or together with E1B-55K could be responsible for the contradictory results.

All together, our data support already published studies, which indicate that adenoviruses efficiently infect susceptible cells that are then activated and secrete pro-inflammatory cytokines such as TNF $\alpha$ . On one hand, these cytokines activate different signaling pathway (i.e. apoptosis) in the surrounding epithelial cells, sensing the presence of an adenovirus infection that needs to be controlled. On the other hand, adenoviruses inhibit NF- $\kappa$ B activation in highly susceptible and permissive epithelial cell lines at late time points of infection in order to escape the immune response and to prolong cell survival, reaching a most efficient viral progeny production. In order to answer the question how adenoviruses inhibit TNF $\alpha$  mediated NF- $\kappa$ B activation, we investigated the IKK complex in which different upstream signaling pathways converge. In our experiments, we could show for the first time, that the IKK complex components IKK $\alpha$  and NEMO have an important role in adenoviral infection as their depletion affects viral progeny production. However, more experiments are needed to understand whether the NF- $\kappa$ B activation is inhibited through targeting the IKK complex. We hypothesize that these proteins might exert their proviral functions in a NF- $\kappa$ B pathway-independent manner, being the aim of current investigations.

- Abe, T., Kaname, Y., Hamamoto, I., Tsuda, Y., Wen, X., Taguwa, S., Moriishi, K., Takeuchi, O., Kawai, T., Kanto, T., Hayashi, N., Akira, S. & Matsuura, Y. (2007). Hepatitis C virus nonstructural protein 5A modulates the toll-like receptor-MyD88-dependent signaling pathway in macrophage cell lines. *Journal of Virology* **81**, 8953-8966.
- Adli, M., Merkhofer, E., Cogswell, P. & Baldwin, A. S. (2010). IKK  $\alpha$  and IKK  $\beta$  Each Function to Regulate NF- $\kappa$ B Activation in the TNF-Induced/Canonical Pathway. *PLoS ONE* **5**, e9428-9427.
- Agou, F., Traincard, F., Vinolo, E., Courtois, G., Yamaoka, S., Israel, A. & Veron, M. (2004). The trimerization domain of NEMO is composed of the interacting C-terminal CC2 and LZ coiled-coil subdomains. *J Biol Chem* **279**, 27861-27869.
- Agou, F., Ye, F., Goffinont, S., Courtois, G., Yamaoka, S., Israel, A. & Veron, M. (2002). NEMO trimerizes through its coiled-coil C-terminal domain. *J Biol Chem* **277**, 17464-17475.
- Akusjarvi, G. & Persson, H. (1981). Controls of RNA splicing and termination in the major late adenovirus transcription unit. *Nature* **292**, 420-426.
- Alharbi, S., Van Caesele, P., Consunji-Araneta, R., Zoubeidi, T., Fanella, S., Souid, A.-K. & Alsuwaidi, A. R. (2012). Epidemiology of severe pediatric adenovirus lower respiratory tract infections in Manitoba, Canada, 1991-2005. *BMC Infect Dis* **12**, 55.
- Ali, H., LeRoy, G., Bridge, G. & Flint, S. J. (2007). The adenovirus L4 33-kilodalton protein binds to intragenic sequences of the major late promoter required for late phase-specific stimulation of transcription. *Journal of Virology* **81**, 1327-1338.
- Amaya, M., Keck, F., Bailey, C. & Narayanan, A. (2014). The role of the IKK complex in viral infections. *Pathogens Disease* **72**, 32-44.
- Amir, R. E., Haecker, H., Karin, M. & Ciechanover, A. (2004). Mechanism of processing of the NF-kappa B2 p100 precursor: identification of the specific polyubiquitin chain-anchoring lysine residue and analysis of the role of NEDD8-modification on the SCF(beta-TrCP) ubiquitin ligase. *Oncogene* **23**, 2540-2547.
- Ampuero, J. S., Ocaña, V., Gómez, J., Gamero, M. E., Garcia, J., Halsey, E. S. & Laguna-Torres, V. A. (2012). Adenovirus respiratory tract infections in Peru. *PLoS ONE* **7**, e46898.
- Anderson, C. W., Young, M. E. & Flint, S. J. (1989). Characterization of the adenovirus 2 virion protein, mu. *Virology* **172**, 506-512.
- Anderson, K. P. & Fennie, E. H. (1987). Adenovirus early region 1A modulation of interferon antiviral activity. *Journal of Virology* **61**, 787-795.
- Andersson, M., Pääbo, S., Nilsson, T. & Peterson, P. A. (1985). Impaired intracellular transport of class I MHC antigens as a possible means for adenoviruses to evade immune surveillance. *Cell* **43**, 215-222.
- Anest, V., Hanson, J. L., Cogswell, P. C., Steinbrecher, K. A., Strahl, B. D. & Baldwin, A. S. (2003). A nucleosomal function for IkappaB kinase-alpha in NF-kappaB-dependent gene expression. *Nature* **423**, 659-663.
- Arany, Z., Newsome, D., Oldread, E., Livingston, D. M. & Eckner, R. (1995). A family of transcriptional adaptor proteins targeted by the E1A oncoprotein. *Nature* **374**, 81-84.
- Araujo, F. D., Stracker, T. H., Carson, C. T., Lee, D. V. & Weitzman, M. D. (2005). Adenovirus Type 5 E4orf3 Protein Targets the Mre11 Complex to Cytoplasmic Aggregates. *Journal of Virology* **79**, 11382-11391.
- Ashida, H., Kim, M., Schmidt-Supprian, M., Ma, A., Ogawa, M. & Sasakawa, C. (2010). A bacterial E3 ubiquitin ligase IpaH9.8 targets NEMO/IKKgamma to dampen the host NF-kappaB-mediated inflammatory response. *Nat Cell Biol* **12**, 66-73; sup pp 61-69.
- Avantaggiati, M. L., Carbone, M., Graessmann, A., Nakatani, Y., Howard, B. & Levine, A. S. (1996). The SV40 large T antigen and adenovirus E1a oncoproteins interact with distinct isoforms of the transcriptional co-activator, p300. *EMBO J* **15**, 2236-2248.
- Avvakumov, N., Sahbegovic, M., Zhang, Z., Shuen, M. & Mymryk, J. S. (2002a). Analysis of DNA binding by the adenovirus type 5 E1A oncoprotein. *J Gen Virol* **83**, 517-524.
- Avvakumov, N., Wheeler, R., D'Halluin, J.-C. & Mymryk, J. S. (2002b). Comparative sequence analysis of the largest E1A proteins of human and simian adenoviruses. *Journal of Virology* **76**, 7968-7975.

- Bachelier, F., Alcamí, J., Arenzana-Seisdedos, F. & Virelizier, J. L. (1991). HIV enhancer activity perpetuated by NF-kappa B induction on infection of monocytes. *Nature* **350**, 709-712.
- Bailey, A. & Mautner, V. (1994). Phylogenetic relationships among adenovirus serotypes. *Virology* **205**, 438-452.
- Baker, A., Rohleder, K. J., Hanakahi, L. A. & Ketner, G. (2007). Adenovirus E4 34k and E1b 55k Oncoproteins Target Host DNA Ligase IV for Proteasomal Degradation. *Journal of Virology* **81**, 7034-7040.
- Baldwin, A. S. (1996). The NF-kappa B and I kappa B proteins: new discoveries and insights. *Annu Rev Immunol* **14**, 649-683.
- Barbeau, D., Marcellus, R. C., Bacchetti, S., Bayley, S. T. & Branton, P. E. (1992). Quantitative analysis of regions of adenovirus E1A products involved in interactions with cellular proteins. *Biochem Cell Biol* **70**, 1123-1134.
- Barrero, P. R., Valinotto, L. E., Tittarelli, E. & Mistchenko, A. S. (2012). Molecular typing of adenoviruses in pediatric respiratory infections in Buenos Aires, Argentina (1999-2010). *J Clin Virol* **53**, 145-150.
- Basak, S. & Hoffmann, A. (2008). Crosstalk via the NF- $\kappa$ B signaling system. *Cytokine & Growth Factor Reviews* **19**, 187-197.
- Basak, S., Kim, H., Kearns, J. D., Tergaonkar, V., O'Dea, E., Werner, S. L., Benedict, C. A., Ware, C. F., Ghosh, G., Verma, I. M. & Hoffmann, A. (2007). A fourth IkappaB protein within the NF-kappaB signaling module. *Cell* **128**, 369-381.
- Benko, M., Elo, P., Ursu, K., Ahne, W., LaPatra, S. E., Thomson, D. & Harrach, B. (2002). First molecular evidence for the existence of distinct fish and snake adenoviruses. *Journal of Virology* **76**, 10056-10059.
- Benkő, M. & Harrach, B. (1998). A proposal for a new (third) genus within the family Adenoviridae. *Arch Virol* **143**, 829-837.
- Bennett, E. M., Bennink, J. R., Yewdell, J. W. & Brodsky, F. M. (1999). Cutting edge: adenovirus E19 has two mechanisms for affecting class I MHC expression. *J Immunol* **162**, 5049-5052.
- Berciaud, S., Rayne, F., Kassab, S., Jubert, C., Faure-Della Corte, M., Salin, F., Wodrich, H., Lafon, M. E. & Typadeno Study, M. (2012). Adenovirus infections in Bordeaux University Hospital 2008-2010: clinical and virological features. *J Clin Virol* **54**, 302-307.
- Bergman, Y. & Shavit, D. (1988). Regulation of the Ig kappa-chain enhancer by the adenovirus E1A gene products. Repression in lymphoid cells, activation in fibroblasts. *The Journal of Immunology* **140**, 2073-2080.
- Berk, A. J. (2007). *Adenoviridae: The Viruses and Their Replication*: Lippincott Williams & Wilkins.
- Berk, A. J., Lee, F., Harrison, T., Williams, J. & Sharp, P. A. (1979). Pre-early adenovirus 5 gene product regulates synthesis of early viral messenger RNAs. *Cell* **17**, 935-944.
- Berk, A. J. & Sharp, P. A. (1977). Ultraviolet mapping of the adenovirus 2 early promoters. *Cell* **12**, 45-55.
- Berscheminski, J., Wimmer, P., Brun, J., Ip, W. H., Groitl, P., Horlacher, T., Jaffray, E., Hay, R. T., Dobner, T. & Schreiner, S. (2014). Sp100 Isoform-Specific Regulation of Human Adenovirus 5 Gene Expression. *Journal of Virology* **88**, 6076-6092.
- Betts, J. C. & Nabel, G. J. (1996). Differential regulation of NF-kappaB2(p100) processing and control by amino-terminal sequences. *Molecular and Cellular Biology* **16**, 6363-6371.
- Bex, F., McDowall, A., Burny, A. & Gaynor, R. (1997). The human T-cell leukemia virus type 1 transactivator protein Tax colocalizes in unique nuclear structures with NF-kappaB proteins. *J Virol* **71**, 3484-3497.
- Bex, F., Yin, M. J., Burny, A. & Gaynor, R. B. (1998). Differential transcriptional activation by human T-cell leukemia virus type 1 Tax mutants is mediated by distinct interactions with CREB binding protein and p300. *Mol Cell Biol* **18**, 2392-2405.
- Beyer, W. R., Westphal, M., Ostertag, W. & von Laer, D. (2002). Oncoretrovirus and lentivirus vectors pseudotyped with lymphocytic choriomeningitis virus glycoprotein: generation, concentration, and broad host range. *J Virol* **76**, 1488-1495.

- Bhattacharya, S., Eckner, R., Grossman, S., Oldread, E., Arany, Z., D'Andrea, A. & Livingston, D. M. (1996). Cooperation of Stat2 and p300/CBP in signalling induced by interferon-alpha. *Nature* **383**, 344-347.
- Birbach, A., Gold, P., Binder, B. R., Hofer, E., de Martin, R. & Schmid, J. A. (2002). Signaling molecules of the NF-kappa B pathway shuttle constitutively between cytoplasm and nucleus. *J Biol Chem* **277**, 10842-10851.
- Blackford, A. N., Bruton, R. K., Dirlik, O., Stewart, G. S., Taylor, A. M. R., Dobner, T., Grand, R. J. A. & Turnell, A. S. (2008). A Role for E1B-AP5 in ATR Signaling Pathways during Adenovirus Infection. *Journal of Virology* **82**, 7640-7652.
- Blanchette, P., Cheng, C. Y., Yan, Q., Ketner, G., Ornelles, D. A., Dobner, T., Conaway, R. C., Conaway, J. W. & Branton, P. E. (2004a). Both BC-box motifs of adenovirus protein E4orf6 are required to efficiently assemble an E3 ligase complex that degrades p53. *Molecular and Cellular Biology* **24**, 9619-9629.
- Blanchette, P., Cheng, C. Y., Yan, Q., Ketner, G., Ornelles, D. A., Dobner, T., Conaway, R. C., Conaway, J. W. & Branton, P. E. (2004b). Both BC-box motifs of adenovirus protein E4orf6 are required to efficiently assemble an E3 ligase complex that degrades p53. *Molecular and Cellular Biology* **24**, 9619-9629.
- Blanchette, P., Kindsmuller, K., Groitl, P., Dallaire, F., Speiseder, T., Branton, P. E. & Dobner, T. (2008). Control of mRNA Export by Adenovirus E4orf6 and E1B55K Proteins during Productive Infection Requires E4orf6 Ubiquitin Ligase Activity. *Journal of Virology* **82**, 2642-2651.
- Bode, J. G., Ludwig, S., Ehrhardt, C., Albrecht, U., Erhardt, A., Schaper, F., Heinrich, P. C. & Haussinger, D. (2003). IFN-alpha antagonistic activity of HCV core protein involves induction of suppressor of cytokine signaling-3. *FASEB J* **17**, 488-490.
- Bonizzi, G. & Karin, M. (2004). The two NF-kappaB activation pathways and their role in innate and adaptive immunity. *Trends in Immunology* **25**, 280-288.
- Borgland, S. L., Bowen, G. P., Wong, N. C. W., Libermann, T. A. & Muruve, D. A. (2000). Adenovirus Vector-Induced Expression of the C-X-C Chemokine IP-10 Is Mediated through Capsid-Dependent Activation of NF-kappa B. *Journal of Virology* **74**, 3941-3947.
- Bosschaerts, T., Guilliams, M., Stijlemans, B., Morias, Y., Engel, D., Tacke, F., Herin, M., De Baetselier, P. & Beschin, A. (2010). Tip-DC development during parasitic infection is regulated by IL-10 and requires CCL2/CCR2, IFN-gamma and MyD88 signaling. *PLoS Pathog* **6**, e1001045.
- Bouchard, M. J., Wang, L. & Schneider, R. J. (2006). Activation of focal adhesion kinase by hepatitis B virus HBx protein: multiple functions in viral replication. *J Virol* **80**, 4406-4414.
- Bour, S., Perrin, C., Akari, H. & Strebel, K. (2001). The human immunodeficiency virus type 1 Vpu protein inhibits NF-kappa B activation by interfering with beta TrCP-mediated degradation of I kappa B. *J Biol Chem* **276**, 15920-15928.
- Bowie, A. G. & Unterholzner, L. (2008). Viral evasion and subversion of pattern-recognition receptor signalling. *Nat Rev Immunol* **8**, 911-922.
- Boyer, J., Rohleder, K. & Ketner, G. (1999). Adenovirus E4 34k and E4 11k inhibit double strand break repair and are physically associated with the cellular DNA-dependent protein kinase. *Virology* **263**, 307-312.
- Bradford, L. W. (1976). Problems of ethics and behavior in the forensic sciences. *Journal of forensic sciences* **21**, 763-768.
- Bradham, C. A., Plumpe, J., Manns, M. P., Brenner, D. A. & Trautwein, C. (1998). Mechanisms of hepatic toxicity. I. TNF-induced liver injury. *Am J Physiol* **275**, G387-392.
- Brady, G. & Bowie, A. G. (2014). Innate immune activation of NF  $\kappa$  B and its antagonism by poxviruses. *Cytokine & Growth Factor Reviews* **25**, 611-620.
- Braithwaite, A. W., Cheetham, B. F., Li, P., Parish, C. R., Waldron-Stevens, L. K. & Bellett, A. J. (1983). Adenovirus-induced alterations of the cell growth cycle: a requirement for expression of E1A but not of E1B. *Journal of Virology* **45**, 192-199.
- Bremner, K. H., Scherer, J., Yi, J., Vershinin, M., Gross, S. P. & Vallee, R. B. (2009). Adenovirus Transport via Direct Interaction of Cytoplasmic Dynein with the Viral Capsid Hexon Subunit. *Cell Host and Microbe* **6**, 523-535.

- Brestovitsky, A., Nebenzahl-Sharon, K., Kechker, P., Sharf, R. & Kleinberger, T. (2016). The Adenovirus E4orf4 Protein Provides a Novel Mechanism for Inhibition of the DNA Damage Response. *PLoS Pathog* **12**, e1005420.
- Bridge, E. & Ketner, G. (1989). Redundant control of adenovirus late gene expression by early region 4. *Journal of Virology* **63**, 631-638.
- Bridge, E. & Ketner, G. (1990). Interaction of adenoviral E4 and E1b products in late gene expression. *Virology* **174**, 345-353.
- Bridge, E., Mattsson, K., Aspegren, A. & Sengupta, A. (2003). Adenovirus early region 4 promotes the localization of splicing factors and viral RNA in late-phase interchromatin granule clusters. *Virology* **311**, 40-50.
- Brinkmann, M. M., Glenn, M., Rainbow, L., Kieser, A., Henke-Gendo, C. & Schulz, T. F. (2003). Activation of mitogen-activated protein kinase and NF-kappaB pathways by a Kaposi's sarcoma-associated herpesvirus K15 membrane protein. *J Virol* **77**, 9346-9358.
- Brinkmann, M. M. & Schulz, T. F. (2006). Regulation of intracellular signalling by the terminal membrane proteins of members of the Gammaherpesvirinae. *J Gen Virol* **87**, 1047-1074.
- Brown, A. M., Linhoff, M. W., Stein, B., Wright, K. L., Baldwin, A. S., Basta, P. V. & Ting, J. P. (1994). Function of NF-kappa B/Rel binding sites in the major histocompatibility complex class II invariant chain promoter is dependent on cell-specific binding of different NF-kappa B/Rel subunits. *Molecular and Cellular Biology* **14**, 2926-2935.
- Browne, E. P. & Shenk, T. (2003). Human cytomegalovirus UL83-coded pp65 virion protein inhibits antiviral gene expression in infected cells. *PNAS* **100**, 11439-11444.
- Brunetti, C. R., Amano, H., Ueda, Y., Qin, J., Miyamura, T., Suzuki, T., Li, X., Barrett, J. W. & McFadden, G. (2003). Complete genomic sequence and comparative analysis of the tumorigenic poxvirus Yaba monkey tumor virus. *J Virol* **77**, 13335-13347.
- Buchkovich, K., Dyson, N., Whyte, P. & Harlow, E. (1990). Cellular proteins that are targets for transformation by DNA tumour viruses. *Ciba Found Symp* **150**, 262-271- discussion 271-268.
- Buckwalter, S. P., Teo, R., Espy, M. J., Sloan, L. M., Smith, T. F. & Pritt, B. S. (2012). Real-time qualitative PCR for 57 human adenovirus types from multiple specimen sources. *J Clin Microbiol* **50**, 766-771.
- Burgert, H. G. & Blusch, J. H. (2000). Immunomodulatory functions encoded by the E3 transcription unit of adenoviruses. *Virus Genes* **21**, 13-25.
- Burgert, H. G. & Kvist, S. (1985). An adenovirus type 2 glycoprotein blocks cell surface expression of human histocompatibility class I antigens. *Cell* **41**, 987-997.
- Burgert, H. G., Ruzsics, Z., Obermeier, S., Hilgendorf, A., Windheim, M. & Elsing, A. (2002). Subversion of host defense mechanisms by adenoviruses. *Curr Top Microbiol Immunol* **269**, 273-318.
- Camus-Bouclainville, C., Fiette, L., Bouchiha, S., Pignolet, B., Counor, D., Filipe, C., Gelfi, J. & Messud-Petit, F. (2004). A virulence factor of myxoma virus colocalizes with NF-kappaB in the nucleus and interferes with inflammation. *J Virol* **78**, 2510-2516.
- Cardoso, F. M., Kato, S. E., Huang, W., Flint, S. J. & Gonzalez, R. A. (2008). An early function of the adenoviral E1B 55 kDa protein is required for the nuclear relocalization of the cellular p53 protein in adenovirus-infected normal human cells. *Virology* **378**, 339-346.
- Carr, M. J., Kajon, A. E., Lu, X., Dunford, L., O'Reilly, P., Holder, P., De Gascun, C. F., Coughlan, S., Connell, J., Erdman, D. D. & Hall, W. W. (2011). Deaths associated with human adenovirus-14p1 infections, Europe, 2009-2010. *Emerg Infect Dis* **17**, 1402-1408.
- Carson, C. T., Orazio, N. I., Lee, D. V., Suh, J., Bekker-Jensen, S., Araujo, F. D., Lakdawala, S. S., Lilley, C. E., Bartek, J., Lukas, J. & Weitzman, M. D. (2009). Mislocalization of the MRN complex prevents ATR signaling during adenovirus infection. *The EMBO Journal* **28**, 652-662.
- Carson, C. T., Schwartz, R. A., Stracker, T. H., Lilley, C. E., Lee, D. V. & Weitzman, M. D. (2003). The Mre11 complex is required for ATM activation and the G2/M checkpoint. *EMBO J* **22**, 6610-6620.

- Cartmell, T., Southgate, T., Rees, G. S., Castro, M. G., Lowenstein, P. R. & Luheshi, G. N. (1999). Interleukin-1 mediates a rapid inflammatory response after injection of adenoviral vectors into the brain. *J Neurosci* **19**, 1517-1523.
- Carvalho, T., Seeler, J. S., Ohman, K., Jordan, P., Pettersson, U., Akusjarvi, G., Carmo-Fonseca, M. & Dejean, A. (1995). Targeting of adenovirus E1A and E4-ORF3 proteins to nuclear matrix-associated PML bodies. *The Journal of Cell Biology* **131**, 45-56.
- Celik, C., Gozel, M. G., Turkay, H., Bakici, M. Z., Güven, A. S. & Elaldi, N. (2015). Rotavirus and adenovirus gastroenteritis: time series analysis. *Pediatr Int* **57**, 590-596.
- Centers for Disease, C. & Prevention (2013). Adenovirus-associated epidemic keratoconjunctivitis outbreaks--four states, 2008-2010. *MMWR Morb Mortal Wkly Rep* **62**, 637-641.
- Chan, J. Y., Li, L., Fan, Y. H., Mu, Z. M., Zhang, W. W. & Chang, K. S. (1997). Cell-cycle regulation of DNA damage-induced expression of the suppressor gene PML. *Biochemical and Biophysical Research Communications* **240**, 640-646.
- Chang, S. J., Hsiao, J. C., Sonnberg, S., Chiang, C. T., Yang, M. H., Tzou, D. L., Mercer, A. A. & Chang, W. (2009). Poxvirus host range protein CP77 contains an F-box-like domain that is necessary to suppress NF-kappaB activation by tumor necrosis factor alpha but is independent of its host range function. *J Virol* **83**, 4140-4152.
- Chariot, A. (2009). The NF- $\kappa$ B-independent functions of IKK subunits in immunity and cancer. *Trends in Cell Biology* **19**, 404-413.
- Che, X. Y., Qiu, L. W., Pan, Y. X., Xu, H., Hao, W., Liao, Z. Y., Mei, Y. B., Zhang, L. Y., Wan, Z. Y., Yuan, G. Y. & Huang, Z. (2003). Rapid and efficient preparation of monoclonal antibodies against SARS-associated coronavirus nucleocapsid protein by immunizing mice. *Di Yi Jun Yi Da Xue Xue Bao* **23**, 640-642.
- Chen, I. S., Mak, T. W., O'Rear, J. J. & Temin, H. M. (1981). Characterization of reticuloendotheliosis virus strain T DNA and isolation of a novel variant of reticuloendotheliosis virus strain T by molecular cloning. *Journal of Virology* **40**, 800-811.
- Chen, L.-F. & Greene, W. C. (2004). Shaping the nuclear action of NF-kappaB. *Nature Reviews Molecular Cell Biology* **5**, 392-401.
- Chen, M. J., Holskin, B., Strickler, J., Gorniak, J., Clark, M. A., Johnson, P. J., Mitcho, M. & Shalloway, D. (1987). Induction by E1A oncogene expression of cellular susceptibility to lysis by TNF. *Nature* **330**, 581-583.
- Chen, R. A., Ryzhakov, G., Cooray, S., Randow, F. & Smith, G. L. (2008). Inhibition of IkappaB kinase by vaccinia virus virulence factor B14. *PLoS Pathog* **4**, e22.
- Chen, S.-P., Huang, Y.-C., Chiu, C.-H., Wong, K.-S., Huang, Y.-L., Huang, C.-G., Tsao, K.-C. & Lin, T.-Y. (2013). Clinical features of radiologically confirmed pneumonia due to adenovirus in children. *J Clin Virol* **56**, 7-12.
- Chen, W. & Cooper, N. R. (1996). Epstein-Barr virus nuclear antigen 2 and latent membrane protein independently transactivate p53 through induction of NF-kappaB activity. *J Virol* **70**, 4849-4853.
- Chhabra, P., Payne, D. C., Szilagyi, P. G., Edwards, K. M., Staat, M. A., Shirley, S. H., Wikswo, M., Nix, W. A., Lu, X., Parashar, U. D. & Vinjé, J. (2013). Etiology of viral gastroenteritis in children <5 years of age in the United States, 2008-2009. *J INFECT DIS* **208**, 790-800.
- Chiocca, S., Kurzbauer, R., Schaffner, G., Baker, A., Mautner, V. & Cotten, M. (1996). The complete DNA sequence and genomic organization of the avian adenovirus CELO. *Journal of Virology* **70**, 2939-2949.
- Chirmule, N., Wang, X. P., Hu, R., Oyaizu, N., Roifman, C., Pahwa, R., Kalyanaraman, V. S. & Pahwa, S. (1994). Envelope glycoproteins of HIV-1 interfere with T-cell-dependent B cell differentiation: role of CD4-MHC class II interaction in the effector phase of T cell help. *Cell Immunol* **155**, 169-182.
- Choi, H. S., Kim, W.-T., Kim, H., Kim, J.-J., Ko, J.-Y., Lee, S.-W., Jang, Y. J., Kim, S. J., Lee, M.-J., Jung, H.-S., Kzhyshkowska, J., Um, S.-J., Lee, M.-Y., Lee, S.-H., Kim, C.-H. & Ryu, C. J. (2011). Identification and characterization of adenovirus early region 1B-associated protein 5 as a surface marker on undifferentiated human embryonic stem cells. *Stem Cells Dev* **20**, 609-620.

- Choi, S.-H., Park, K.-J., Ahn, B.-Y., Jung, G., Lai, M. M. C. & Hwang, S. B. (2006). Hepatitis C virus nonstructural 5B protein regulates tumor necrosis factor alpha signaling through effects on cellular IkappaB kinase. *Molecular and Cellular Biology* **26**, 3048-3059.
- Chow, L. C., Gelinas, R. E., Broker, T. R. & Roberts, R. J. (2000). *An amazing sequence arrangement at the 5' ends of adenovirus 2 messenger RNA*. 1977.
- Chu, Z.-L., Shin, Y.-A., Yang, J.-M., DiDonato, J. A. & Ballard, D. W. (1999). IKK  $\gamma$  Mediates the Interaction of Cellular I  $\kappa$  B Kinases with the Tax Transforming Protein of Human T Cell Leukemia Virus Type 1. *J Biol Chem* **274**, 15297-15300.
- Classon, M. & Dyson, N. (2001). p107 and p130: versatile proteins with interesting pockets. *Experimental Cell Research* **264**, 135-147.
- Claudio, E., Brown, K., Park, S., Wang, H. & Siebenlist, U. (2002). BAFF-induced NEMO-independent processing of NF-kappa B2 in maturing B cells. *Nat Immunol* **3**, 958-965.
- Compton, T., Kurt-Jones, E. A., Boehme, K. W., Belko, J., Latz, E., Golenbock, D. T. & Finberg, R. W. (2003). Human Cytomegalovirus Activates Inflammatory Cytokine Responses via CD14 and Toll-Like Receptor 2. *Journal of Virology* **77**, 4588-4596.
- Coope, H. J., Atkinson, P. G., Huhse, B., Belich, M., Janzen, J., Holman, M. J., Klaus, G. G., Johnston, L. H. & Ley, S. C. (2002a). CD40 regulates the processing of NF-kappaB2 p100 to p52. *EMBO J* **21**, 5375-5385.
- Cuconati, A. (2003). DNA damage response and MCL-1 destruction initiate apoptosis in adenovirus-infected cells. *Genes & Development* **17**, 2922-2932.
- Cuconati, A. & White, E. (2002). Viral homologs of BCL-2: role of apoptosis in the regulation of virus infection. *Genes & Development* **16**, 2465-2478.
- Cundy, K. C. (1999). Clinical pharmacokinetics of the antiviral nucleotide analogues cidofovir and adefovir. *Clin Pharmacokinet* **36**, 127-143.
- D'Amours, D. & Jackson, S. P. (2002). The Mre11 complex: at the crossroads of dna repair and checkpoint signalling. *Nature Reviews Molecular Cell Biology* **3**, 317-327.
- Dallaire, F., Blanchette, P. & Branton, P. E. (2009a). A Proteomic Approach To Identify Candidate Substrates of Human Adenovirus E4orf6-E1B55K and Other Viral Cullin-Based E3 Ubiquitin Ligases. *Journal of Virology* **83**, 12172-12184.
- Dallaire, F., Blanchette, P., Groitl, P., Dobner, T. & Branton, P. E. (2009b). Identification of Integrin 3 as a New Substrate of the Adenovirus E4orf6/E1B 55-Kilodalton E3 Ubiquitin Ligase Complex. *Journal of Virology* **83**, 5329-5338.
- Dan, H. C., Ebbs, A., Pasparakis, M., Van Dyke, T., Basseres, D. S. & Baldwin, A. S. (2014). Akt-dependent activation of mTORC1 complex involves phosphorylation of mTOR (mammalian target of rapamycin) by IkappaB kinase alpha (IKKalpha). *J Biol Chem* **289**, 25227-25240.
- Davison, A. J. (2003). Genetic content and evolution of adenoviruses. *Journal of general Virology* **84**, 2895-2908.
- de Jong, R. N., van der Vliet, P. C. & Brenkman, A. B. (2003). Adenovirus DNA replication: protein priming, jumping back and the role of the DNA binding protein DBP. *Curr Top Microbiol Immunol* **272**, 187-211.
- de Ory, F., Avellón, A., Echevarría, J. E., Sánchez-Seco, M. P., Trallero, G., Cabrerizo, M., Casas, I., Pozo, F., Fedele, G., Vicente, D., Pena, M. J., Moreno, A., Niubo, J., Rabella, N., Rubio, G., Pérez-Ruiz, M., Rodríguez-Iglesias, M., Gimeno, C., Eiros, J. M., Melón, S., Blasco, M., López-Miragaya, I., Varela, E., Martínez-Sapiña, A., Rodríguez, G., Marcos, M. Á., Gegúndez, M. I., Cilla, G., Gabilondo, I., Navarro, J. M., Torres, J., Aznar, C., Castellanos, A., Guisasola, M. E., Negredo, A. I., Tenorio, A. & Vázquez-Morón, S. (2013). Viral infections of the central nervous system in Spain: a prospective study. *J Med Virol* **85**, 554-562.
- Debbas, M. & White, E. (1993). Wild-type p53 mediates apoptosis by E1A, which is inhibited by E1B. *Genes & Development* **7**, 546-554.
- Dejardin, E., Droin, N. M., Delhase, M., Haas, E., Cao, Y., Makris, C., Li, Z.-W., Karin, M., Ware, C. F. & Green, D. R. (2002). The lymphotoxin-beta receptor induces different patterns of gene expression via two NF-kappaB pathways. *Immunity* **17**, 525-535.
- Delhalle, S., Blasius, R., Dicato, M. & Diederich, M. (2004). A Beginner's Guide to NF- $\kappa$ B Signaling Pathways. *Ann N Y Acad Sci* **1030**, 1-13.

- DeLuca, C., Petropoulos, L., Zmeureanu, D. & Hiscott, J. (1999). Nuclear I $\kappa$ B maintains persistent NF- $\kappa$ B activation in HIV-1-infected myeloid cells. *J Biol Chem* **274**, 13010-13016.
- Detrait, M., De Prophetis, S., Delville, J.-P. & Komuta, M. (2015). Fulminant isolated adenovirus hepatitis 5 months after haplo-identical HSCT for AML. *Clin Case Rep* **3**, 802-805.
- Diamant, G. & Dikstein, R. (2013). Transcriptional control by NF- $\kappa$ B: elongation in focus. *Biochim Biophys Acta* **1829**, 937-945.
- Diaz, P. V., Calhoun, W. J., Hinton, K. L., Avendano, L. F., Gaggero, A., Simon, V., Arredondo, S. M., Pinto, R. & Diaz, A. (1999). Differential effects of respiratory syncytial virus and adenovirus on mononuclear cell cytokine responses. *Am J Respir Crit Care Med* **160**, 1157-1164.
- DiDonato, J. A., Hayakawa, M., Rothwarf, D. M., Zandi, E. & Karin, M. (1997). A cytokine-responsive I $\kappa$ B kinase that activates the transcription factor NF- $\kappa$ B. *Nature* **388**, 548-554.
- Dingle, J. H. & Langmuir, A. D. (1968). Epidemiology of acute, respiratory disease in military recruits. *The American review of respiratory disease* **97**, Suppl:1-65.
- DiPerna, G., Stack, J., Bowie, A. G., Boyd, A., Kotwal, G., Zhang, Z., Arvikar, S., Latz, E., Fitzgerald, K. A. & Marshall, W. L. (2004). Poxvirus protein N1L targets the I $\kappa$ B kinase complex, inhibits signaling to NF- $\kappa$ B by the tumor necrosis factor superfamily of receptors, and inhibits NF- $\kappa$ B and IRF3 signaling by toll-like receptors. *J Biol Chem* **279**, 36570-36578.
- Dix, I. & Leppard, K. N. (1993). Regulated splicing of adenovirus type 5 E4 transcripts and regulated cytoplasmic accumulation of E4 mRNA. *Journal of Virology* **67**, 3226-3231.
- Dix, I. & Leppard, K. N. (1995). Expression of adenovirus type 5 E4 Orf2 protein during lytic infection. *J Gen Virol* **76** ( Pt 4), 1051-1055.
- Dobbelstein, M., Roth, J., Kimberly, W. T., Levine, A. J. & Shenk, T. (1997). Nuclear export of the E1B 55-kDa and E4 34-kDa adenoviral oncoproteins mediated by a rev-like signal sequence. *EMBO J* **16**, 4276-4284.
- Dobner, T., Horikoshi, N., Rubenwolf, S. & Shenk, T. (1996). Blockage by Adenovirus E4orf6 of Transcriptional Activation by the p53 Tumor Suppressor. *Science* **272**, 1470-1473.
- Dobrzanski, P., Ryseck, R. P. & Bravo, R. (1995). Specific inhibition of RelB/p52 transcriptional activity by the C-terminal domain of p100. *Oncogene* **10**, 1003-1007.
- Dosch, T., Horn, F., Schneider, G., Kratzer, F., Dobner, T., Hauber, J. & Stauber, R. H. (2001). The adenovirus type 5 E1B-55K oncoprotein actively shuttles in virus-infected cells, whereas transport of E4orf6 is mediated by a CRM1-independent mechanism. *J Virol* **75**, 5677-5683.
- Doucas, V. & Evans, R. M. (1996). The PML nuclear compartment and cancer. *Biochim Biophys Acta* **1288**, M25-29.
- Doucas, V., Ishov, A. M., Romo, A., Juguilon, H., Weitzman, M. D., Evans, R. M. & Maul, G. G. (1996). Adenovirus replication is coupled with the dynamic properties of the PML nuclear structure. *Genes & Development* **10**, 196-207.
- Doyle, S. L. & O'Neill, L. A. J. (2006). Toll-like receptors: from the discovery of NF $\kappa$ B to new insights into transcriptional regulations in innate immunity. *Biochemical Pharmacology* **72**, 1102-1113.
- DuBridg, R. B., Tang, P., Hsia, H. C., Leong, P. M., Miller, J. H. & Calos, M. P. (1987). Analysis of mutation in human cells by using an Epstein-Barr virus shuttle system. *Mol Cell Biol* **7**, 379-387.
- Duerksen-Hughes, P., Wold, W. S. & Gooding, L. R. (1989). Adenovirus E1A renders infected cells sensitive to cytolysis by tumor necrosis factor. *The Journal of Immunology* **143**, 4193-4200.
- Dull, T., Zufferey, R., Kelly, M., Mandel, R. J., Nguyen, M., Trono, D. & Naldini, L. (1998). A third-generation lentivirus vector with a conditional packaging system. *J Virol* **72**, 8463-8471.
- Dyson, N., Buchkovich, K., Whyte, P. & Harlow, E. (1989). Cellular proteins that are targetted by DNA tumor viruses for transformation. *Int Symp Princess Takamatsu Cancer Res Fund* **20**, 191-198.

- Dyson, N., Guida, P., Münger, K. & Harlow, E. (1992). Homologous sequences in adenovirus E1A and human papillomavirus E7 proteins mediate interaction with the same set of cellular proteins. *Journal of Virology* **66**, 6893-6902.
- Eckner, R., Ewen, M. E., Newsome, D., Gerdes, M., DeCaprio, J. A., Lawrence, J. B. & Livingston, D. M. (1994). Molecular cloning and functional analysis of the adenovirus E1A-associated 300-kD protein (p300) reveals a protein with properties of a transcriptional adaptor. *Genes & Development* **8**, 869-884.
- Enders, J. F., Bell, J. A., Dingle, J. H., Francis, T., Hilleman, M. R., Huebner, R. J. & Payne, A. M. (1956). Adenoviruses: group name proposed for new respiratory-tract viruses. *Science* **124**, 119-120.
- Endter, C. & Dobner, T. (2004). Cell transformation by human adenoviruses. *Curr Top Microbiol Immunol* **273**, 163-214.
- Endter, C., Kzhyshkowska, J., Stauber, R. & Dobner, T. (2001). SUMO-1 modification is required for transformation by adenovirus type 5 early region 1B 55-kDa oncoprotein. *Proc Natl Acad Sci USA* **98**, 11312-11317.
- Esposito, S., Daleno, C., Prunotto, G., Scala, A., Tagliabue, C., Borzani, I., Fossali, E., Pelucchi, C. & Principi, N. (2013). Impact of viral infections in children with community-acquired pneumonia: results of a study of 17 respiratory viruses. *Influenza Other Respi Viruses* **7**, 18-26.
- Esposito, S., Preti, V., Consolo, S., Nazzari, E. & Principi, N. (2012). Adenovirus 36 infection and obesity. *J Clin Virol* **55**, 95-100.
- Evans, J. D. & Hearing, P. (2003). Distinct roles of the Adenovirus E4 ORF3 protein in viral DNA replication and inhibition of genome concatenation. *Journal of Virology* **77**, 5295-5304.
- Evans, J. D. & Hearing, P. (2005). Relocalization of the Mre11-Rad50-Nbs1 Complex by the Adenovirus E4 ORF3 Protein Is Required for Viral Replication. *Journal of Virology* **79**, 6207-6215.
- Everett, R. D. (2001). DNA viruses and viral proteins that interact with PML nuclear bodies. *Oncogene* **20**, 7266-7273.
- Everett, R. D. & Chelbi-Alix, M. K. (2007). PML and PML nuclear bodies: implications in antiviral defence. *Biochimie* **89**, 819-830.
- Everitt, E., Lutter, L. & Philipson, L. (1975). Structural proteins of adenoviruses. XII. Location and neighbor relationship among proteins of adenovirion type 2 as revealed by enzymatic iodination, immunoprecipitation and chemical cross-linking. *Virology* **67**, 197-208.
- Fan, C. M. & Maniatis, T. (1991). Generation of p50 subunit of NF-kappa B by processing of p105 through an ATP-dependent pathway. *Nature* **354**, 395-398.
- Farley, D. C., Brown, J. L. & Leppard, K. N. (2004). Activation of the early-late switch in adenovirus type 5 major late transcription unit expression by L4 gene products. *Journal of Virology* **78**, 1782-1791.
- Fejer, G., Drechsel, L., Liese, J., Schleicher, U., Ruzsics, Z., Imelli, N., Greber, U. F., Keck, S., Hildenbrand, B., Krug, A., Bogdan, C. & Freudenberg, M. A. (2008). Key role of splenic myeloid DCs in the IFN-alpha response to adenoviruses in vivo. *PLoS Pathogens* **4**, e1000208.
- Feng, P., Scott, C. W., Cho, N. H., Nakamura, H., Chung, Y. H., Monteiro, M. J. & Jung, J. U. (2004). Kaposi's sarcoma-associated herpesvirus K7 protein targets a ubiquitin-like/ubiquitin-associated domain-containing protein to promote protein degradation. *Mol Cell Biol* **24**, 3938-3948.
- Ferrari, F. K., Samulski, T., Shenk, T. & Samulski, R. J. (1996). Second-strand synthesis is a rate-limiting step for efficient transduction by recombinant adeno-associated virus vectors. *J Virol* **70**, 3227-3234.
- Ferrari, R., Berk, A. J. & Kurdistani, S. K. (2009). Viral manipulation of the host epigenome for oncogenic transformation. *Nat Rev Genet* **10**, 290-294.
- Ferrari, R., Pellegrini, M., Horwitz, G. A., Xie, W., Berk, A. J. & Kurdistani, S. K. (2008). Epigenetic reprogramming by adenovirus e1a. *Science* **321**, 1086-1088.
- Field, N., Low, W., Daniels, M., Howell, S., Daviet, L., Boshoff, C. & Collins, M. (2003). KSHV vFLIP binds to IKK-gamma to activate IKK. *J Cell Sci* **116**, 3721-3728.

- Fisher, K. J. K., W. Mark John, Burda, F. and Wilson, James M. (1996). A novel adenovirus- adeno-associated virus hybrid vector that displays efficient rescue and delivery of the AAV genome. *Hum Gene Ther*, 2079-2087.
- Fiume, G., Vecchio, E., De Laurentiis, A., Trimboli, F., Palmieri, C., Pisano, A., Falcone, C., Pontoriero, M., Rossi, A., Scialdone, A., Fasanella Masci, F., Scala, G. & Quinto, I. (2012). Human immunodeficiency virus-1 Tat activates NF- $\kappa$ B via physical interaction with I $\kappa$ B- $\alpha$  and p65. *Nucleic Acids Research* 40, 3548-3562.
- Fliss, P. M. & Brune, W. (2012). Prevention of Cellular Suicide by Cytomegaloviruses. *Viruses* 4, 1928-1949.
- Fliss, P. M., Jowers, T. P., Brinkmann, M. M., Holstermann, B., Mack, C., Dickinson, P., Hohenberg, H., Ghazal, P. & Brune, W. (2012). Viral Mediated Redirection of NEMO/IKK  $\gamma$  to Autophagosomes Curtails the Inflammatory Cascade. *PLoS Pathogens* 8, e1002517.
- Fontan, E., Traincard, F., Levy, S. G., Yamaoka, S., Veron, M. & Agou, F. (2007). NEMO oligomerization in the dynamic assembly of the IkappaB kinase core complex. *FEBS J* 274, 2540-2551.
- Forrester, N. A., Sedgwick, G. G., Thomas, A., Blackford, A. N., Speiseder, T., Dobner, T., Byrd, P. J., Stewart, G. S., Turnell, A. S. & Grand, R. J. (2011). Serotype-specific inactivation of the cellular DNA damage response during adenovirus infection. *J Virol* 85, 2201-2211.
- Freiman, R. N. & Tjian, R. (2003). Regulating the regulators: lysine modifications make their mark. *Cell* 112, 11-17.
- Friedman, J. M. & Horwitz, M. S. (2002). Inhibition of tumor necrosis factor alpha-induced NF-kappa B activation by the adenovirus E3-10.4/14.5K complex. *J Virol* 76, 5515-5521.
- Frisch, S. M. & Mymryk, J. S. (2002). Adenovirus-5 e1a: paradox and paradigm. *Nature Reviews Molecular Cell Biology* 3, 441-452.
- Furcinitti, P. S., van Oostrum, J. & Burnett, R. M. (1989). Adenovirus polypeptide IX revealed as capsid cement by difference images from electron microscopy and crystallography. *EMBO J* 8, 3563-3570.
- Furuya, K., Ozaki, T., Hanamoto, T., Hosoda, M., Hayashi, S., Barker, P. A., Takano, K., Matsumoto, M. & Nakagawara, A. (2007). Stabilization of p73 by nuclear IkappaB kinase-alpha mediates cisplatin-induced apoptosis. *J Biol Chem* 282, 18365-18378.
- Ganapathi, L., Arnold, A., Jones, S., Patterson, A., Graham, D., Harper, M. & Levy, O. (2016). Use of cidofovir in pediatric patients with adenovirus infection. *F1000Res* 5, 758.
- Gantzer, M., Spitz, E., Accard, N. & Rooke, R. (2002). Constitutive expression of the adenovirus E3-14.7K protein does not prolong adenovirus vector DNA persistence but protects mice against lipopolysaccharide-induced acute hepatitis. *Hum Gene Ther* 13, 921-933.
- Gao, S., Song, L., Li, J., Zhang, Z., Peng, H., Jiang, W., Wang, Q., Kang, T., Chen, S. & Huang, W. (2012). Influenza A virus-encoded NS1 virulence factor protein inhibits innate immune response by targeting IKK. *Cellular Microbiology* 14, 1849-1866.
- Garcia-Mata, R., Gao, Y.-S. & Sztul, E. (2002). Hassles with taking out the garbage: aggravating aggresomes. *Traffic* 3, 388-396.
- Garnett, C. T., Erdman, D., Xu, W. & Gooding, L. R. (2002). Prevalence and quantitation of species C adenovirus DNA in human mucosal lymphocytes. *Journal of Virology* 76, 10608-10616.
- Garnett, C. T., Talekar, G., Mahr, J. A., Huang, W., Zhang, Y., Ornelles, D. A. & Gooding, L. R. (2009). Latent species C adenoviruses in human tonsil tissues. *Journal of Virology* 83, 2417-2428.
- Gavin P. J., K. B. Z. (2002). Intravenous Ribavirin Treatment for Severe Adenovirus Disease in Immunocompromised Children. *Pediatr Int* 110.
- Gerritsen, M. E., Williams, A. J., Neish, A. S., Moore, S., Shi, Y. & Collins, T. (1997). CREB-binding protein/p300 are transcriptional coactivators of p65. *Proc Natl Acad Sci U S A* 94, 2927-2932.

- Ghosh, S., May, M. J. & Kopp, E. B. (1998). NF-kappa B and Rel proteins: evolutionarily conserved mediators of immune responses. *Annu Rev Immunol* **16**, 225-260.
- Giard, R. J., Aaronson, S. A., Todaro, G. J., Arnstein, P., Kersey, J. H., Dosik, H. & Parks, W. P. (1973). *In vitro* cultivation of human tumors: establishment of cell lines derived from a series of solid tumors. *J Natl Cancer Inst* **51**, 1417-1423.
- Gilmore, T. D. (2006). Introduction to NF- $\kappa$ B: players, pathways, perspectives. *Oncogene* **25**, 6680-6684.
- Gimble, J. M., Duh, E., Ostrove, J. M., Gendelman, H. E., Max, E. E. & Rabson, A. B. (1988). Activation of the human immunodeficiency virus long terminal repeat by herpes simplex virus type 1 is associated with induction of a nuclear factor that binds to the NF-kappa B/core enhancer sequence. *Journal of Virology* **62**, 4104-4112.
- Ginsberg, H. S., Badger, G. F., Dingle, J. H., Jordan, W. S. & Katz, S. (1955). Etiologic relationship of the RI-67 agent to acute respiratory disease (ARD). *J Clin Invest* **34**, 820-831.
- Ginsberg, H. S., Moldawer, L. L., Sehgal, P. B., Redington, M., Kilian, P. L., Chanock, R. M. & Prince, G. A. (1991). A mouse model for investigating the molecular pathogenesis of adenovirus pneumonia. *PNAS* **88**, 1651-1655.
- Giordano, A., McCall, C., Whyte, P. & Franza, B. R. (1991). Human cyclin A and the retinoblastoma protein interact with similar but distinguishable sequences in the adenovirus E1A gene product. *Oncogene* **6**, 481-485.
- Gitlin, L., Barchet, W., Gilfillan, S., Cella, M., Beutler, B., Flavell, R. A., Diamond, M. S. & Colonna, M. (2006). Essential role of mda-5 in type I IFN responses to polyriboinosinic:polyribocytidylic acid and encephalomyocarditis picornavirus. *Proc Natl Acad Sci U S A* **103**, 8459-8464.
- Glick, D., Barth, S. & Macleod, K. F. (2010). Autophagy: cellular and molecular mechanisms. *J Pathol* **221**, 3-12.
- Gloria P Bowen, S. L. B. M. L. T. A. L. N. C. W. W. & Daniel, A. M. (2004). Adenovirus Vector-Induced Inflammation: Capsid-Dependent Induction of the C-C Chemokine RANTES Requires NF- $\kappa$ B. 1-13.
- Gong, G., Waris, G., Tanveer, R. & Siddiqui, A. (2001). Human hepatitis C virus NS5A protein alters intracellular calcium levels, induces oxidative stress, and activates STAT-3 and NF-kappa B. *Proc Natl Acad Sci U S A* **98**, 9599-9604.
- Gonzalez, R. A. & Flint, S. J. (2002). Effects of mutations in the adenoviral E1B 55-kilodalton protein coding sequence on viral late mRNA metabolism. *Journal of Virology* **76**, 4507-4519.
- Gooding, L. R., Elmore, L. W., Tollefson, A. E., Brady, H. A. & Wold, W. S. (1988). A 14,700 MW protein from the E3 region of adenovirus inhibits cytolysis by tumor necrosis factor. *Cell* **53**, 341-346.
- Gräble, M. & Hearing, P. (1992). cis and trans requirements for the selective packaging of adenovirus type 5 DNA. *Journal of Virology* **66**, 723-731.
- Graef, I. A., Gastier, J. M., Francke, U. & Crabtree, G. R. (2001). Evolutionary relationships among Rel domains indicate functional diversification by recombination. *PNAS* **98**, 5740-5745.
- Graff, J. W., Ettayebi, K. & Hardy, M. E. (2009). Rotavirus NSP1 inhibits NFkappaB activation by inducing proteasome-dependent degradation of beta-TrCP: a novel mechanism of IFN antagonism. *PLoS Pathog* **5**, e1000280.
- Graham, F. L., Smiley, J., Russel, W. C. & Nairn, R. (1977). Characteristics of a human cell line transformed by DNA from human adenovirus type 5. *J Gen Virol* **36**, 59-72.
- Granja, A. G., Sabina, P., Salas, M. L., Fresno, M. & Revilla, Y. (2006). Regulation of inducible nitric oxide synthase expression by viral A238L-mediated inhibition of p65/RelA acetylation and p300 transactivation. *J Virol* **80**, 10487-10496.
- Gribaudo, G., Ravaglia, S., Guandalini, L., Cavallo, R., Gariglio, M. & Landolfo, S. (1996). The murine cytomegalovirus immediate-early 1 protein stimulates NF-kappa B activity by transactivating the NF-kappa B p105/p50 promoter. *Virus Research* **45**, 15-27.
- Griffiths, D. A., Abdul-Sada, H., Knight, L. M., Jackson, B. R., Richards, K., Prescott, E. L., Peach, A. H., Blair, G. E., Macdonald, A. & Whitehouse, A. (2013). Merkel cell

- polyomavirus small T antigen targets the NEMO adaptor protein to disrupt inflammatory signaling. *J Virol* **87**, 13853-13867.
- Guidotti, L. G. & Chisari, F. V. (2001).** Noncytolytic control of viral infections by the innate and adaptive immune response. *Annu Rev Immunol* **19**, 65-91.
- Guilfoyle, R. A., Osheroff, W. P. & Rossini, M. (1985).** Two functions encoded by adenovirus early region 1A are responsible for the activation and repression of the DNA-binding protein gene. *EMBO J* **4**, 707-713.
- Guilliams, M., Movahedi, K., Bosschaerts, T., VandenDriessche, T., Chuah, M. K., Herin, M., Acosta-Sanchez, A., Ma, L., Moser, M., Van Ginderachter, J. A., Brys, L., De Baetselier, P. & Beschin, A. (2009).** IL-10 dampens TNF/inducible nitric oxide synthase-producing dendritic cell-mediated pathogenicity during parasitic infection. *J Immunol* **182**, 1107-1118.
- Guo, L., Gonzalez, R., Zhou, H., Wu, C., Vernet, G., Wang, Z. & Wang, J. (2012).** Detection of three human adenovirus species in adults with acute respiratory infection in China. *Eur J Clin Microbiol Infect Dis* **31**, 1051-1058.
- Gupta, A., Jha, S., Engel, D. A., Ornelles, D. A. & Dutta, A. (2012).** Tip60 degradation by adenovirus relieves transcriptional repression of viral transcriptional activator E1A. *Oncogene*.
- Häcker, H. & Karin, M. (2006).** Regulation and function of IKK and IKK-related kinases. *Sci STKE* **2006**, re13.
- Haddad, J. J., Saade, N. E. & Safieh-Garabedian, B. (2003).** Interleukin-10 and the regulation of mitogen-activated protein kinases: are these signalling modules targets for the anti-inflammatory action of this cytokine? *Cell Signal* **15**, 255-267.
- Hanahan, D. & Meselson, M. (1983).** Plasmid screening at high colony density. *Methods Enzymol* **100**, 333-342.
- Hansen, S. K., Baeuerle, P. A. & Blasi, F. (1994a).** Purification, reconstitution, and I kappa B association of the c-Rel-p65 (RelA) complex, a strong activator of transcription. *Molecular and Cellular Biology* **14**, 2593-2603.
- Hansen, S. K., Guerrini, L. & Blasi, F. (1994b).** Differential DNA sequence specificity and regulation of HIV-1 enhancer activity by cRel-RelA transcription factor. *J Biol Chem* **269**, 22230-22237.
- Harada, J. N., Shevchenko, A., Pallas, D. C. & Berk, A. J. (2002).** Analysis of the adenovirus E1B-55K-anchored proteome reveals its link to ubiquitination machinery. *J Virol* **76**, 9194-9206.
- Harlow, E., Franza, B. R., Jr. & Schley, C. (1985).** Monoclonal antibodies specific for adenovirus early region 1A proteins: extensive heterogeneity in early region 1A products. *J Virol* **55**, 533-546.
- Harte, M. T., Haga, I. R., Maloney, G., Gray, P., Reading, P. C., Bartlett, N. W., Smith, G. L., Bowie, A. & O'Neill, L. A. (2003).** The poxvirus protein A52R targets Toll-like receptor signaling complexes to suppress host defense. *J Exp Med* **197**, 343-351.
- Härtl, B., Zeller, T., Blanchette, P., Kremmer, E. & Dobner, T. (2008).** Adenovirus type 5 early region 1B 55-kDa oncoprotein can promote cell transformation by a mechanism independent from blocking p53-activated transcription. *Oncogene* **27**, 3673-3684.
- Hatzivassiliou, E., Miller, W. E., Raab-Traub, N., Kieff, E. & Mosialos, G. (1998).** A fusion of the EBV latent membrane protein-1 (LMP1) transmembrane domains to the CD40 cytoplasmic domain is similar to LMP1 in constitutive activation of epidermal growth factor receptor expression, nuclear factor-kappa B, and stress-activated protein kinase. *J Immunol* **160**, 1116-1121.
- Hayden, M. S. & Ghosh, S. (2004).** Signaling to NF-kappaB. *Genes & Development* **18**, 2195-2224.
- Hayden, M. S. & Ghosh, S. (2011).** NF- $\kappa$ B in immunobiology. *Nature Publishing Group* **21**, 223-244.
- Hearing, P., Samulski, R. J., Wishart, W. L. & Shenk, T. (1987).** Identification of a repeated sequence element required for efficient encapsidation of the adenovirus type 5 chromosome. *Journal of Virology* **61**, 2555-2558.
- Hendrickx, R., Stichling, N., Koelen, J., Kuryk, L., Lipiec, A. & Greber, U. F. (2014).** Innate Immunity to Adenovirus. *Hum Gene Ther.*

- Herscovitch M., C. W., Ennis T., Coleman K., Yong S., Armstead B., Kalaitzidis D., Chandani S., Gilmore T. (2008). Intermolecular disulfide bond formation in the NEMO dimer requires Cys54 and Cys347. *Biochem Biophys Res Commun* **367**, 103-108.
- Higginbotham, J. N., Seth, P., Blaese, R. M. & Ramsey, W. J. (2002). The release of inflammatory cytokines from human peripheral blood mononuclear cells in vitro following exposure to adenovirus variants and capsid. *Hum Gene Ther* **13**, 129-141.
- Hiscott, J., Kwon, H. & Génin, P. (2001). Hostile takeovers: viral appropriation of the NF- $\kappa$ B pathway. *J Clin Invest* **107**, 143-151.
- Hiscott, J., Nguyen, T. L. A., Arguello, M., Nakhaei, P. & Paz, S. (2006). Manipulation of the nuclear factor- $\kappa$ B pathway and the innate immune response by viruses. *Oncogene* **25**, 6844-6867.
- Hoberg, J. E., Popko, A. E., Ramsey, C. S. & Mayo, M. W. (2006). IkappaB kinase alpha-mediated derepression of SMRT potentiates acetylation of RelA/p65 by p300. *Mol Cell Biol* **26**, 457-471.
- Hodge, L. D., Mancini, P., Davis, F. M. & Heywood, P. (1977). Nuclear matrix of HeLa S3 cells. Polypeptide composition during adenovirus infection and in phases of the cell cycle. *J Cell Biol* **72**, 194-208.
- Hodgson, A. & Wan, F. (2015). Interference with nuclear factor kappaB signaling pathway by pathogen-encoded proteases: global and selective inhibition. *Mol Microbiol*.
- Hoesel, B. & Schmid, J. A. (2013). The complexity of NF- $\kappa$ B signaling in inflammation and cancer. *Molecular Cancer* **12**, 1-1.
- Hoffmann, A., Natoli, G. & Ghosh, G. (2006). Transcriptional regulation via the NF-kappaB signaling module. *Oncogene* **25**, 6706-6716.
- Hofland, C. A., Eron, L. J. & Washecka, R. M. (2004). Hemorrhagic adenovirus cystitis after renal transplantation. *Transplant Proc* **36**, 3025-3027.
- Holloway, G. & Coulson, B. S. (2006). Rotavirus activates JNK and p38 signaling pathways in intestinal cells, leading to AP-1-driven transcriptional responses and enhanced virus replication. *J Virol* **80**, 10624-10633.
- Honda, K., Takaoka, A. & Taniguchi, T. (2006). Type I Interferon Gene Induction by the Interferon Regulatory Factor Family of Transcription Factors. *Immunity* **25**, 349-360.
- Hoppe, A., Beech, S. J., Dimmock, J. & Leppard, K. N. (2006). Interaction of the Adenovirus Type 5 E4 Orf3 Protein with Promyelocytic Leukemia Protein Isoform II Is Required for ND10 Disruption. *Journal of Virology* **80**, 3042-3049.
- Howe, J. A., Mymryk, J. S., Egan, C., Branton, P. E. & Bayley, S. T. (1990). Retinoblastoma growth suppressor and a 300-kDa protein appear to regulate cellular DNA synthesis. *PNAS* **87**, 5883-5887.
- Hu, F. Q., Smith, C. A. & Pickup, D. J. (1994). Cowpox virus contains two copies of an early gene encoding a soluble secreted form of the type II TNF receptor. *Virology* **204**, 343-356.
- Huang, M. M. & Hearing, P. (1989). Adenovirus early region 4 encodes two gene products with redundant effects in lytic infection. *Journal of Virology* **63**, 2605-2615.
- Huang, T. T., Wuerzberger-Davis, S. M., Wu, Z. H. & Miyamoto, S. (2003). Sequential modification of NEMO/IKKgamma by SUMO-1 and ubiquitin mediates NF-kappaB activation by genotoxic stress. *Cell* **115**, 565-576.
- Huang, W.-C. & Hung, M.-C. (2013). Beyond NF- $\kappa$ B activation: nuclear functions of I $\kappa$ B kinase a. *J Biomed Sci* **20**, 1-1.
- Huang, W. C., Ju, T. K., Hung, M. C. & Chen, C. C. (2007). Phosphorylation of CBP by IKKalpha promotes cell growth by switching the binding preference of CBP from p53 to NF-kappaB. *Mol Cell* **26**, 75-87.
- Iha, H., Kibler, K. V., Yedavalli, V. R., Peloponese, J. M., Haller, K., Miyazato, A., Kasai, T. & Jeang, K. T. (2003). Segregation of NF-kappaB activation through NEMO/IKKgamma by Tax and TNFalpha: implications for stimulus-specific interruption of oncogenic signaling. *Oncogene* **22**, 8912-8923.
- Imperiale, M. J., Akusjarvi, G. & Leppard, K. N. (1995). Post-transcriptional control of adenovirus gene expression. *Curr Top Microbiol Immunol* **199** ( Pt 2), 139-171.
- Ishiko, H., Shimada, Y., Konno, T., Hayashi, A., Ohguchi, T., Tagawa, Y., Aoki, K., Ohno, S. & Yamazaki, S. (2008). Novel human adenovirus causing nosocomial epidemic keratoconjunctivitis. *Journal of Clinical Microbiology* **46**, 2002-2008.

- Ison, M. G. (2006). Adenovirus infections in transplant recipients. *Clinical Infectious Diseases* **43**, 331-339.
- Janaswami, P. M., Kalvakolanu, D. V., Zhang, Y. & Sen, G. C. (1992). Transcriptional repression of interleukin-6 gene by adenoviral E1A proteins. *J Biol Chem* **267**, 24886-24891.
- Janeway Jr, C. A. & Medzhitov, R. (2002). Innate Immune Recognition. *Annu Rev Immunol* **20**, 197-216.
- Jariel-Encontre, I., Bossis, G. & Piechaczyk, M. (2008). Ubiquitin-independent degradation of proteins by the proteasome. *Biochim Biophys Acta* **1786**, 153-177.
- Javier, R. T. (1994). Adenovirus type 9 E4 open reading frame 1 encodes a transforming protein required for the production of mammary tumors in rats. *Journal of Virology* **68**, 3917-3924.
- Jawetz, E., Kimura, S., Nicholas, A. N., Thygeson, P. & Hanna, L. (1955). new type of APC virus from epidemic keratoconjunctivitis. *Science* **122**, 1190-1191.
- Jenner, R. G. & Young, R. A. (2005). Insights into host responses against pathogens from transcriptional profiling. *Nat Rev Microbiol* **3**, 281-294.
- Jiang, X., Takahashi, N., Ando, K., Otsuka, T., Tetsuka, T. & Okamoto, T. (2003). NF-kappa B p65 transactivation domain is involved in the NF-kappa B-inducing kinase pathway. *Biochem Biophys Res Commun* **301**, 583-590.
- Jones, M. S., Harrach, B., Ganac, R. D., Gozum, M. M. A., Dela Cruz, W. P., Riedel, B., Pan, C., Delwart, E. L. & Schnurr, D. P. (2007). New adenovirus species found in a patient presenting with gastroenteritis. *Journal of Virology* **81**, 5978-5984.
- Jones, N. & Shenk, T. (1979). Isolation of adenovirus type 5 host range deletion mutants defective for transformation of rat embryo cells. *Cell* **17**, 683-689.
- Joo, M., Hahn, Y. S., Kwon, M., Sadikot, R. T., Blackwell, T. S. & Christman, J. W. (2005). Hepatitis C virus core protein suppresses NF-kappaB activation and cyclooxygenase-2 expression by direct interaction with IkappaB kinase beta. *Journal of Virology* **79**, 7648-7657.
- Jost, P. J. & Ruland, J. (2007). Aberrant NF-kappaB signaling in lymphoma: mechanisms, consequences, and therapeutic implications. *Blood* **109**, 2700-2707.
- Juang, Y. T., Lowther, W., Kellum, M., Au, W. C., Lin, R., Hiscott, J. & Pitha, P. M. (1998). Primary activation of interferon A and interferon B gene transcription by interferon regulatory factor 3. *PNAS* **95**, 9837-9842.
- Kallunki, T., Deng, T., Hibi, M. & Karin, M. (1996). c-Jun can recruit JNK to phosphorylate dimerization partners via specific docking interactions. *Cell* **87**, 929-939.
- Kang, S. M., Tran, A. C., Grilli, M. & Lenardo, M. J. (1992). NF-kappa B subunit regulation in nontransformed CD4+ T lymphocytes. *Science* **256**, 1452-1456.
- Kanno, T., Franzoso, G. & Siebenlist, U. (1994). Human T-cell leukemia virus type I Tax-protein-mediated activation of NF-kappa B from p100 (NF-kappa B2)-inhibited cytoplasmic reservoirs. *PNAS* **91**, 12634-12638.
- Karen, K. A. & Hearing, P. (2011). Adenovirus Core Protein VII Protects the Viral Genome from a DNA Damage Response at Early Times after Infection. *Journal of Virology* **85**, 4135-4142.
- Karin, M. (1999). How NF-kB is activated: the role of the Ikb kinase (IKK) complex. *Oncogene* **13**, 6867-6874.
- Karin, M. (2011). *NF-kB in Health and Disease*. Berlin, Heidelberg: Springer Science & Business Media.
- Kawai, T. & Akira, S. (2006). TLR signaling. *Cell Death and Differentiation* **13**, 816-825.
- Kawai, T. & Akira, S. (2010). The role of pattern-recognition receptors in innate immunity: update on Toll-like receptors. *Nat Immunol* **11**, 373-384.
- Kayagaki, N., Yan, M., Seshasayee, D., Wang, H., Lee, W., French, D. M., Grewal, I. S., Cochran, A. G., Gordon, N. C., Yin, J., Starovasnik, M. A. & Dixit, V. M. (2002). BAFF/BLYS receptor 3 binds the B cell survival factor BAFF ligand through a discrete surface loop and promotes processing of NF-kappaB2. *Immunity* **17**, 515-524.
- Keicho, N., Higashimoto, Y., Bondy, G. P., Elliott, W. M., Hogg, J. C. & Hayashi, S. (1999). Endotoxin-specific NF-kappaB activation in pulmonary epithelial cells harboring adenovirus E1A. *Am J Physiol* **277**, L523-532.

- Keller, S. A., Hernandez-Hopkins, D., Vider, J., Ponomarev, V., Hyjek, E., Schattner, E. J. & Cesarman, E. (2006). NF-kappaB is essential for the progression of KSHV- and EBV-infected lymphomas in vivo. *Blood* **107**, 3295-3302.
- Kim, J. C., Lee, S. Y., Kim, S. Y., Kim, J. K., Kim, H. J., Lee, H. M., Choi, M. S., Min, J. S., Kim, M. J., Choi, H. S. & Ahn, J. K. (2008). HSV-1 ICP27 suppresses NF-kappaB activity by stabilizing IkappaBalpha. *FEBS Lett* **582**, 2371-2376.
- Kimelman, D., Miller, J. S., Porter, D. & Roberts, B. E. (1985). E1a regions of the human adenoviruses and of the highly oncogenic simian adenovirus 7 are closely related. *J Virol* **53**, 399-409.
- Kindsmüller, K., Groitl, P., Härtl, B., Blanchette, P., Hauber, J. & Dobner, T. (2007). Intranuclear targeting and nuclear export of the adenovirus E1B-55K protein are regulated by SUMO1 conjugation. *Proc Natl Acad Sci USA* **104**, 6684-6689.
- Kirkin, V., McEwan, D. G., Novak, I. & Dikic, I. (2009). A role for ubiquitin in selective autophagy. *Mol Cell* **34**, 259-269.
- Kitajewski, J., Schneider, R. J., Safer, B., Munemitsu, S. M., Samuel, C. E., Thimmappaya, B. & Shenk, T. (1986). Adenovirus VAI RNA antagonizes the antiviral action of interferon by preventing activation of the interferon-induced eIF-2 alpha kinase. *Cell* **45**, 195-200.
- Knecht, E., Aguado, C., Carcel, J., Esteban, I., Esteve, J. M., Ghislat, G., Moruno, J. F., Vidal, J. M. & Saez, R. (2009). Intracellular protein degradation in mammalian cells: recent developments. *Cell Mol Life Sci* **66**, 2427-2443.
- Kong, K., Kumar, M., Taruishi, M. & Javier, R. T. (2014). The human adenovirus E4-ORF1 protein subverts discs large 1 to mediate membrane recruitment and dysregulation of phosphatidylinositol 3-kinase. *PLoS Pathogens* **10**, e1004102.
- Kong, K., Kumar, M., Taruishi, M. & Javier, R. T. (2015). Adenovirus E4-ORF1 Dysregulates Epidermal Growth Factor and Insulin/Insulin-Like Growth Factor Receptors To Mediate Constitutive Myc Expression. *Journal of Virology* **89**, 10774-10785.
- König, C., Roth, J. & Dobbelstein, M. (1999). Adenovirus type 5 E4orf3 protein relieves p53 inhibition by E1B-55-kilodalton protein. *Journal of Virology* **73**, 2253-2262.
- König, C., Roth, J. & Dobbelstein, M. (1999). Adenovirus type 5 E4orf3 protein relieves p53 inhibition by E1B-55-kilodalton protein. *Journal of Virology* **73**, 2253-2262.
- Kopito, R. R. (2000). Aggresomes, inclusion bodies and protein aggregation. *Trends in Cell Biology* **10**, 524-530.
- Krätzer, F., Rosorius, O., Heger, P., Hirschmann, N., Dobner, T., Hauber, J. & Stauber, R. H. (2000). The adenovirus type 5 E1B-55K oncoprotein is a highly active shuttle protein and shuttling is independent of E4orf6, p53 and Mdm2. *Oncogene* **19**, 850-857.
- Kumar, H., Kawai, T. & Akira, S. (2011). Pathogen recognition by the innate immune system. *Int Rev Immunol* **30**, 16-34.
- Kwok, R. P., Lurance, M. E., Lundblad, J. R., Goldman, P. S., Shih, H., Connor, L. M., Marriott, S. J. & Goodman, R. H. (1996). Control of cAMP-regulated enhancers by the viral transactivator Tax through CREB and the co-activator CBP. *Nature* **380**, 642-646.
- Lam, E. & Falck-Pedersen, E. (2014). Unabated Adenovirus replication following activation of the cGAS/STING dependent antiviral response in human cells. *Journal of Virology*.
- Lamberti, C., Lin, K. M., Yamamoto, Y., Verma, U., Verma, I. M., Byers, S. & Gaynor, R. B. (2001). Regulation of beta-catenin function by the IkappaB kinases. *J Biol Chem* **276**, 42276-42286.
- Lamsoul, I., Lodewick, J., Lebrun, S., Bresseur, R., Burny, A., Gaynor, R. B. & Bex, F. (2005). Exclusive Ubiquitination and Sumoylation on Overlapping Lysine Residues Mediate NF- B Activation by the Human T-Cell Leukemia Virus Tax Oncoprotein. *Molecular and Cellular Biology* **25**, 10391-10406.
- Le Negrate, G. (2011). Viral interference with innate immunity by preventing NF-κ B activity. *Cellular Microbiology* **14**, 168-181.
- Le, V. T. K., Trilling, M., Zimmermann, A. & Hengel, H. (2008). Mouse cytomegalovirus inhibits beta interferon (IFN-beta) gene expression and controls activation pathways of the IFN-beta enhanceosome. *J Gen Virol* **89**, 1131-1141.
- Lee, M. S. & Kim, Y.-J. (2007). Signaling pathways downstream of pattern-recognition receptors and their cross talk. *Annu Rev Biochem* **76**, 447-480.

- Leen, A. M. & Rooney, C. M. (2005). Adenovirus as an emerging pathogen in immunocompromised patients. *Br J Haematol* **128**, 135-144.
- Leonard, G. T. & Sen, G. C. (1996). Effects of adenovirus E1A protein on interferon-signaling. *Virology* **224**, 25-33.
- Leonard, G. T. & Sen, G. C. (1997). Restoration of interferon responses of adenovirus E1A-expressing HT1080 cell lines by overexpression of p48 protein. *Journal of Virology* **71**, 5095-5101.
- Leopold, P. L., Kreitzer, G., Miyazawa, N., Rempel, S., Pfister, K. K., Rodriguez-Boulan, E. & Crystal, R. G. (2000). Dynein- and microtubule-mediated translocation of adenovirus serotype 5 occurs after endosomal lysis. *Hum Gene Ther* **11**, 151-165.
- Leppard, K. N. & Everett, R. D. (1999). The adenovirus type 5 E1b 55K and E4 Orf3 proteins associate in infected cells and affect ND10 components. *J Gen Virol* **80** ( Pt 4), 997-1008.
- Leppard, K. N. & Shenk, T. (1989). The adenovirus E1B 55 kd protein influences mRNA transport via an intranuclear effect on RNA metabolism. *EMBO J* **8**, 2329-2336.
- Lethbridge, K. J. (2003). Nuclear matrix localization and SUMO-1 modification of adenovirus type 5 E1b 55K protein are controlled by E4 Orf6 protein. *Journal of general Virology* **84**, 259-268.
- Lewis, P. F., Schmidt, M. A., Lu, X., Erdman, D. D., Campbell, M., Thomas, A., Cieslak, P. R., Grenz, L. D., Tsaknardis, L., Gleaves, C., Kendall, B. & Gilbert, D. (2009). A community-based outbreak of severe respiratory illness caused by human adenovirus serotype 14. *J INFECT DIS* **199**, 1427-1434.
- Li, E., Stupack, D., Klemke, R., Cheresch, D. A. & Nemerow, G. R. (1998). Adenovirus endocytosis via alpha(v) integrins requires phosphoinositide-3-OH kinase. *Journal of Virology* **72**, 2055-2061.
- Li, K., Foy, E., Ferreon, J. C., Nakamura, M., Ferreon, A. C., Ikeda, M., Ray, S. C., Gale, M., Jr. & Lemon, S. M. (2005). Immune evasion by hepatitis C virus NS3/4A protease-mediated cleavage of the Toll-like receptor 3 adaptor protein TRIF. *Proc Natl Acad Sci U S A* **102**, 2992-2997.
- Li, X., Massa, P. E., Hanidu, A., Peet, G. W., Aro, P., Savitt, A., Mische, S., Li, J. & Marcu, K. B. (2002). IKKalpha, IKKbeta, and NEMO/IKKgamm are each required for the NF-kappa B-mediated inflammatory response program. *J Biol Chem* **277**, 45129-45140.
- Li, Y., Kang, J., Friedman, J., Tarassishin, L., Ye, J., Kovalenko, A., Wallach, D. & Horwitz, M. S. (1999). Identification of a cell protein (FIP-3) as a modulator of NF-kappaB activity and as a target of an adenovirus inhibitor of tumor necrosis factor alpha-induced apoptosis. *PNAS* **96**, 1042-1047.
- Lieber, A., He, C. Y., Meuse, L., Schowalter, D., Kirillova, I., Winther, B. & Kay, M. A. (1997). The role of Kupffer cell activation and viral gene expression in early liver toxicity after infusion of recombinant adenovirus vectors. *Journal of Virology* **71**, 8798-8807.
- Liebermann, H., Mentel, R., Döhner, L., Modrow, S. & Seidel, W. (1996). Inhibition of cell adhesion to the virus by synthetic peptides of fiber knob of human adenovirus serotypes 2 and 3 and virus neutralisation by anti-peptide antibodies. *Virus Research* **45**, 111-122.
- Lim, K. H., Choi, H. S., Park, Y. K., Park, E. S., Shin, G. C., Kim, D. H., Ahn, S. H. & Kim, K. H. (2013). HBx-induced NF-kappaB signaling in liver cells is potentially mediated by the ternary complex of HBx with p22-FLIP and NEMO. *PLoS ONE* **8**, e57331.
- Lin, K.-H., Lin, Y.-C., Chen, H.-L., Ke, G.-M., Chiang, C.-J., Hwang, K.-P., Chu, P.-Y., Lin, J.-H., Liu, D.-P. & Chen, H.-Y. (2004). A two decade survey of respiratory adenovirus in Taiwan: the reemergence of adenovirus types 7 and 4. *J Med Virol* **73**, 274-279.
- Lindemans, C. A., Leen, A. M. & Boelens, J. J. (2010). How I treat adenovirus in hematopoietic stem cell transplant recipients. *Blood* **116**, 5476-5485.
- Link, E., Kerr, L. D., Schreck, R., Zabel, U., Verma, I. & Baeuerle, P. A. (1992). Purified I kappa B-beta is inactivated upon dephosphorylation. *J Biol Chem* **267**, 239-246.
- Lion, T. (2014). Adenovirus Infections in Immunocompetent and Immunocompromised Patients. *Clinical Microbiology Reviews* **27**, 441-462.
- Lion, T., Baumgartinger, R., Watzinger, F., Matthes-Martin, S., Suda, M., Preuner, S., Futterknecht, B., Lawitschka, A., Peters, C., Potschger, U. & Gadner, H. (2003).

- Molecular monitoring of adenovirus in peripheral blood after allogeneic bone marrow transplantation permits early diagnosis of disseminated disease. *Blood* **102**, 1114-1120.
- Lion, T., Kosulin, K., Landlinger, C., Rauch, M., Preuner, S., Jugovic, D., Pötschger, U., Lawitschka, A., Peters, C., Fritsch, G. & Matthes-Martin, S. (2010). Monitoring of adenovirus load in stool by real-time PCR permits early detection of impending invasive infection in patients after allogeneic stem cell transplantation. *Leukemia* **24**, 706-714.
- Liu, B., Park, E., Zhu, F., Bustos, T., Liu, J., Shen, J., Fischer, S. M. & Hu, Y. (2006). A critical role for I kappaB kinase alpha in the development of human and mouse squamous cell carcinomas. *Proc Natl Acad Sci U S A* **103**, 17202-17207.
- Liu, B., Sun, L., Liu, Q., Gong, C., Yao, Y., Lv, X., Lin, L., Yao, H., Su, F., Li, D., Zeng, M. & Song, E. (2015). A cytoplasmic NF- $\kappa$ B interacting long noncoding RNA blocks I $\kappa$ B phosphorylation and suppresses breast cancer metastasis. *Cancer Cell* **27**, 370-381.
- Liu, F. & Green, M. R. (1994). Promoter targeting by adenovirus E1a through interaction with different cellular DNA-binding domains. *Nature* **368**, 520-525.
- Liu, H., Jin, L., Koh, S. B. S., Atanasov, I., Schein, S., Wu, L. & Zhou, Z. H. (2010). Atomic structure of human adenovirus by cryo-EM reveals interactions among protein networks. *Science* **329**, 1038-1043.
- Liu, X., Chen, W., Wang, Q., Li, L. & Wang, C. (2013). Negative Regulation of TLR Inflammatory Signaling by the SUMO-deconjugating Enzyme SENP6. *PLoS Pathogens* **9**, e1003480.
- Liu, Y., Colosimo, A. L., Yang, X.-J. & Liao, D. (2000). Adenovirus E1B 55-Kilodalton Oncoprotein Inhibits p53 Acetylation by PCAF. *Molecular and Cellular Biology* **20**, 5540-5553.
- Liu, Y., Shevchenko, A., Shevchenko, A. & Berk, A. J. (2005a). Adenovirus exploits the cellular aggresome response to accelerate inactivation of the MRN complex. *J Virol* **79**, 14004-14016.
- Liu, Y., Shevchenko, A., Shevchenko, A. & Berk, A. J. (2005b). Adenovirus exploits the cellular aggresome response to accelerate inactivation of the MRN complex. *Journal of Virology* **79**, 14004-14016.
- Ljungman, P., Ribaud, P., Eyrich, M., Matthes-Martin, S., Einsele, H., Bleakley, M., Machaczka, M., Bierings, M., Bosi, A., Gratecos, N., Cordonnier, C., Infectious Diseases Working Party of the European Group for, B. & Marrow, T. (2003). Cidofovir for adenovirus infections after allogeneic hematopoietic stem cell transplantation: a survey by the Infectious Diseases Working Party of the European Group for Blood and Marrow Transplantation. *Bone Marrow Transplant* **31**, 481-486.
- Long, B. H., Huang, C. Y. & Pogo, A. O. (1979). Isolation and characterization of the nuclear matrix in Friend erythroleukemia cells: chromatin and hnRNA interactions with the nuclear matrix. *Cell* **18**, 1079-1090.
- Look, D. C., Roswit, W. T., Frick, A. G., Gris-Alevy, Y., Dickhaus, D. M., Walter, M. J. & Holtzman, M. J. (1998). Direct suppression of Stat1 function during adenoviral infection. *Immunity* **9**, 871-880.
- Loparev, V. N., Parsons, J. M., Knight, J. C., Panus, J. F., Ray, C. A., Buller, R. M., Pickup, D. J. & Esposito, J. J. (1998). A third distinct tumor necrosis factor receptor of orthopoxviruses. *Proc Natl Acad Sci U S A* **95**, 3786-3791.
- Lowe, S. W. & Ruley, H. E. (1993). Stabilization of the p53 tumor suppressor is induced by adenovirus 5 E1A and accompanies apoptosis. *Genes & Development* **7**, 535-545.
- Lukashev, A. N., Ivanova, O. E., Eremeeva, T. P. & Iggo, R. D. (2008). Evidence of frequent recombination among human adenoviruses. *J Gen Virol* **89**, 380-388.
- Lundblad, J. R., Kwok, R. P., Laurance, M. E., Harter, M. L. & Goodman, R. H. (1995). Adenoviral E1A-associated protein p300 as a functional homologue of the transcriptional co-activator CBP. *Nature* **374**, 85-88.
- Luo, J.-L., Tan, W., Ricono, J. M., Korchynskyi, O., Zhang, M., Gonias, S. L., Cheresch, D. A. & Karin, M. (2007). Nuclear cytokine-activated IKK $\alpha$  controls prostate cancer metastasis by repressing Maspin. *Nature* **446**, 690-694.

- Lutz, P. & Kedinger, C. (1996). Properties of the adenovirus IVa2 gene product, an effector of late-phase-dependent activation of the major late promoter. *Journal of Virology* **70**, 1396-1405.
- Lysakova-Devine, T., Keogh, B., Harrington, B., Nagpal, K., Halle, A., Golenbock, D. T., Monie, T. & Bowie, A. G. (2010). Viral inhibitory peptide of TLR4, a peptide derived from vaccinia protein A46, specifically inhibits TLR4 by directly targeting MyD88 adaptor-like and TRIF-related adaptor molecule. *J Immunol* **185**, 4261-4271.
- Ma, Y. & Mathews, M. B. (1996). Structure, function, and evolution of adenovirus-associated RNA: a phylogenetic approach. *Journal of Virology* **70**, 5083-5099.
- Machitani, M., Sakurai, F., Wakabayashi, K., Nakatani, K., Shimizu, K., Tachibana, M. & Mizuguchi, H. (2016). NF-kappaB promotes leaky expression of adenovirus genes in a replication-incompetent adenovirus vector. *Sci Rep* **6**, 19922.
- Mack, C., Sickmann, A., Lembo, D. & Brune, W. (2008). Inhibition of proinflammatory and innate immune signaling pathways by a cytomegalovirus RIP1-interacting protein. *Proc Natl Acad Sci* **105**, 3094-3099.
- Madisch, I., Wölfel, R., Harste, G., Pommer, H. & Heim, A. (2006). Molecular identification of adenovirus sequences: a rapid scheme for early typing of human adenoviruses in diagnostic samples of immunocompetent and immunodeficient patients. *J Med Virol* **78**, 1210-1217.
- Maeda, G., Chiba, T., Kawashiri, S., Satoh, T. & Imai, K. (2007). Epigenetic inactivation of IkappaB Kinase-alpha in oral carcinomas and tumor progression. *Clin Cancer Res* **13**, 5041-5047.
- Mahr, J. A. & Gooding, L. R. (1999). Immune evasion by adenoviruses. *Immunological Reviews* **168**, 121-130.
- Makris, C., Roberts, J. L. & Karin, M. (2002). The carboxyl-terminal region of IkappaB kinase gamma (IKKgamma) is required for full IKK activation. *Molecular and Cellular Biology* **22**, 6573-6581.
- Marienfeld, R. B., Palkowitsch, L. & Ghosh, S. (2006). Dimerization of the I kappa B kinase-binding domain of NEMO is required for tumor necrosis factor alpha-induced NF-kappa B activity. *Mol Cell Biol* **26**, 9209-9219.
- Martin, M. E. & Berk, A. J. (1999). Corepressor required for adenovirus E1B 55,000-molecular-weight protein repression of basal transcription. *Molecular and Cellular Biology* **19**, 3403-3414.
- Marton, M. J., Baim, S. B., Ornelles, D. A. & Shenk, T. (1990). The adenovirus E4 17-kilodalton protein complexes with the cellular transcription factor E2F, altering its DNA-binding properties and stimulating E1A-independent accumulation of E2 mRNA. *J Virol* **64**, 2345-2359.
- Matsushima, Y., Shimizu, H., Kano, A., Nakajima, E., Ishimaru, Y., Dey, S. K., Watanabe, Y., Adachi, F., Mitani, K., Fujimoto, T., Phan, T. G. & Ushijima, H. (2013). Genome sequence of a novel virus of the species human adenovirus d associated with acute gastroenteritis. *Genome Announc* **1**, e00068-00012-e00068-00012.
- Matthews, D. A. & Russell, W. C. (1998). Adenovirus core protein V is delivered by the invading virus to the nucleus of the infected cell and later in infection is associated with nucleoli. *Journal of general Virology*, 1671-1675.
- May, M. J., D'Acquisto, F., Madge, L. A., Glöckner, J., Pober, J. S., Ghosh, S. (2000). Selective Inhibition of NF-kB Activation by a Peptide That Blocks the Interaction of NEMO with the IkB Kinase Complex. *Science* **289**, 1550-1554.
- May, M. J., Marienfeld, R. B. & Ghosh, S. (2002). Characterization of the Ikappa B-kinase NEMO binding domain. *J Biol Chem* **277**, 45992-46000.
- McCaffrey, A. P., Fawcett, P., Nakai, H., McCaffrey, R. L., Ehrhardt, A., Pham, T.-T. T., Pandey, K., Xu, H., Feuss, S., Storm, T. A. & Kay, M. A. (2008). The Host Response to Adenovirus, Helper-dependent Adenovirus, and Adeno-associated Virus in Mouse Liver. *Mol Ther* **16**, 931-941.
- McCool, K. W. & Miyamoto, S. (2012). DNA damage-dependent NF- $\kappa$ B activation: NEMO turns nuclear signaling inside out. *Immunological Reviews* **246**, 311-326.
- Medzhitov, R. (2001). Toll-like receptors and innate immunity. *Nat Rev Immunol* **1**, 135-145.
- Medzhitov, R. (2007). Recognition of microorganisms and activation of the immune response. *Nature* **449**, 819-826.

- Mercurio, F., Murray, B. W., Shevchenko, A., Bennett, B. L., Young, D. B., Li, J. W., Pascual, G., Motiwala, A., Zhu, H., Mann, M. & Manning, A. M. (1999). IkappaB kinase (IKK)-associated protein 1, a common component of the heterogeneous IKK complex. *Molecular and Cellular Biology* **19**, 1526-1538.
- Mercurio, F., Zhu, H., Murray, B. W., Shevchenko, A., Bennett, B. L., Li, J., Young, D. B., Barbosa, M., Mann, M., Manning, A. & Rao, A. (1997). IKK-1 and IKK-2: cytokine-activated IkappaB kinases essential for NF-kappaB activation. *Science* **278**, 860-866.
- Merlo, J. J. & Tsygankov, A. Y. (2001). Herpesvirus saimiri oncoproteins Tip and StpC synergistically stimulate NF-kappaB activity and interleukin-2 gene expression. *Virology* **279**, 325-338.
- Miller, D. L., Rickards, B., Mashiba, M., Huang, W. & Flint, S. J. (2009). The Adenoviral E1B 55-Kilodalton Protein Controls Expression of Immune Response Genes but Not p53-Dependent Transcription. *Journal of Virology* **83**, 3591-3603.
- Miller, W. E., Zagorski, W. A., Breneman, J. D., Avery, D., Miller, J. L. & O'Connor, C. M. (2012). US28 is a potent activator of phospholipase C during HCMV infection of clinically relevant target cells. *PLoS ONE* **7**, e50524.
- Mirza, M. A. & Weber, J. (1982). Structure of adenovirus chromatin. *Biochim Biophys Acta* **696**, 76-86.
- Mirza, M. A. & Weber, J. M. (1981). Structure of adenovirus chromatin as probed with restriction endonucleases. *Virology* **108**, 351-360.
- Mitchell, L. S., Taylor, B., Reimels, W., Barrett, F. F. & Devincenzo, J. P. (2000). Adenovirus 7a: a community-acquired outbreak in a children's hospital. *Pediatr Infect Dis J* **19**, 996-1000.
- Mitsudomi, T., Steinberg, S. M., Nau, M. M., Carbone, D., D'Amico, D., Bodner, H. K., Oie, H. K., Linnoila, R. I., Mulshine, J. L., Minna, J. D. & Gazdar, A. F. (1992). p53 gene mutations in non-small-lung cell cancer cell lines and their correlation with the presence of ras mutations and clinical features. *Oncogene* **7**, 171-180.
- Miyamoto, S. (2010). Nuclear initiated NF- $\kappa$ B signaling: NEMO and ATM take center stage. *Nature Publishing Group* **21**, 116-130.
- Mock, B. A., Connelly, M. A., McBride, O. W., Kozak, C. A. & Marcu, K. B. (1995). CHUK, a conserved helix-loop-helix ubiquitous kinase, maps to human chromosome 10 and mouse chromosome 19. *Genomics* **27**, 348-351.
- Mohamed, M. R., Rahman, M. M., Lanchbury, J. S., Shattuck, D., Neff, C., Dufford, M., van Buuren, N., Fagan, K., Barry, M., Smith, S., Damon, I. & McFadden, G. (2009a). Proteomic screening of variola virus reveals a unique NF-kappaB inhibitor that is highly conserved among pathogenic orthopoxviruses. *Proc Natl Acad Sci U S A* **106**, 9045-9050.
- Mohamed, M. R., Rahman, M. M., Rice, A., Moyer, R. W., Werden, S. J. & McFadden, G. (2009b). Cowpox virus expresses a novel ankyrin repeat NF-kappaB inhibitor that controls inflammatory cell influx into virus-infected tissues and is critical for virus pathogenesis. *J Virol* **83**, 9223-9236.
- Monaghan, A., Webster, A. & Hay, R. T. (1994). Adenovirus DNA binding protein: helix destabilising properties. *Nucleic Acids Research* **22**, 742-748.
- Montag, C., Wagner, J., Gruska, I. & Hagemeyer, C. (2006). Human cytomegalovirus blocks tumor necrosis factor alpha- and interleukin-1beta-mediated NF-kappaB signaling. *Journal of Virology* **80**, 11686-11698.
- Moran, E., Grodzicker, T., Roberts, R. J., Mathews, M. B. & Zerler, B. (1986). Lytic and transforming functions of individual products of the adenovirus E1A gene. *Journal of Virology* **57**, 765-775.
- Moro, M. R., Bonville, C. A., Suryadevara, M., Cummings, E., Faddoul, D., Kobayaa, H., Branigan, P. J. & Domachowske, J. B. (2009). Clinical features, adenovirus types, and local production of inflammatory mediators in adenovirus infections. *Pediatr Infect Dis J* **28**, 376-380.
- Morris, S. J. & Leppard, K. N. (2009). Adenovirus serotype 5 L4-22K and L4-33K proteins have distinct functions in regulating late gene expression. *Journal of Virology* **83**, 3049-3058.
- Morris, S. J., Scott, G. E. & Leppard, K. N. (2010). Adenovirus Late-Phase Infection Is Controlled by a Novel L4 Promoter. *Journal of Virology* **84**, 7096-7104.

- Mortola, E., Noad, R. & Roy, P. (2004). Bluetongue virus outer capsid proteins are sufficient to trigger apoptosis in mammalian cells. *J Virol* **78**, 2875-2883.
- Mosmann, T. R., Kobie, J. J., Lee, F. E. & Quataert, S. A. (2009). T helper cytokine patterns: defined subsets, random expression, and external modulation. *Immunol Res* **45**, 173-184.
- Müller, J. R. & Siebenlist, U. (2003). Lymphotoxin beta receptor induces sequential activation of distinct NF-kappa B factors via separate signaling pathways. *J Biol Chem* **278**, 12006-12012.
- Murray, K. D., Etheridge, C. J., Shah, S. I., Matthews, D. A., Russell, W., Gurling, H. M. & Miller, A. D. (2001). Enhanced cationic liposome-mediated transfection using the DNA-binding peptide mu (mu) from the adenovirus core. *Gene Ther* **8**, 453-460.
- Muruve, D. A., Barnes, M. J., Stillman, I. E. & Libermann, T. A. (1999). Adenoviral gene therapy leads to rapid induction of multiple chemokines and acute neutrophil-dependent hepatic injury in vivo. *Hum Gene Ther* **10**, 965-976.
- Nevins, J. R. & Wilson, M. C. (1981). Regulation of adenovirus-2 gene expression at the level of transcriptional termination and RNA processing. *Nature* **290**, 113-118.
- Nichols, D. B. & Shisler, J. L. (2009). Poxvirus MC160 protein utilizes multiple mechanisms to inhibit NF-kappaB activation mediated via components of the tumor necrosis factor receptor 1 signal transduction pathway. *J Virol* **83**, 3162-3174.
- Nolan, G. P., Fujita, T., Bhatia, K., Huppi, C., Liou, H. C., Scott, M. L. & Baltimore, D. (1993). The bcl-3 proto-oncogene encodes a nuclear I kappa B-like molecule that preferentially interacts with NF-kappa B p50 and p52 in a phosphorylation-dependent manner. *Molecular and Cellular Biology* **13**, 3557-3566.
- Nordqvist, K. & Akusjarvi, G. (1990). Adenovirus early region 4 stimulates mRNA accumulation via 5' introns. *PNAS* **87**, 9543-9547.
- Nordqvist, K., Ohman, K. & Akusjarvi, G. (1994). Human adenovirus encodes two proteins which have opposite effects on accumulation of alternatively spliced mRNAs. *Molecular and Cellular Biology* **14**, 437-445.
- Orazio, N. I., Naeger, C. M., Karlseder, J. & Weitzman, M. D. (2011). The adenovirus E1b55K/E4orf6 complex induces degradation of the Bloom helicase during infection. *Journal of Virology* **85**, 1887-1892.
- Orlando, J. S. & Ornelles, D. A. (1999). An arginine-faced amphipathic alpha helix is required for adenovirus type 5 e4orf6 protein function. *Journal of Virology* **73**, 4600-4610.
- Ornelles, D. A. & Shenk, T. (1991). Localization of the adenovirus early region 1B 55-kilodalton protein during lytic infection: association with nuclear viral inclusions requires the early region 4 34-kilodalton protein. *J Virol* **65**, 424-429.
- Ostapchuk, P., Anderson, M. E., Chandrasekhar, S. & Hearing, P. (2006). The L4 22-kilodalton protein plays a role in packaging of the adenovirus genome. *Journal of Virology* **80**, 6973-6981.
- Otake, K., Ennist, D. L., Harrod, K. & Trapnell, B. C. (1998). Nonspecific inflammation inhibits adenovirus-mediated pulmonary gene transfer and expression independent of specific acquired immune responses. *Hum Gene Ther* **9**, 2207-2222.
- Ou, H. D., Kwiatkowski, W., Deerinck, T. J., Noske, A., Blain, K. Y., Land, H. S., Soria, C., Powers, C. J., May, A. P., Shu, X., Tsien, R. Y., Fitzpatrick, J. A., Long, J. A., Ellisman, M. H., Choe, S. & O'Shea, C. C. (2012). A structural basis for the assembly and functions of a viral polymer that inactivates multiple tumor suppressors. *Cell* **151**, 304-319.
- Pahl, H. L. (1999). Activators and target genes of Rel/NF-kappaB transcription factors. *Oncogene* **18**, 6853-6866.
- Pahl, H. L., Sester, M., Burgert, H. G. & Baeuerle, P. A. (1996). Activation of transcription factor NF-kappaB by the adenovirus E3/19K protein requires its ER retention. *The Journal of Cell Biology* **132**, 511-522.
- Palombella, V. J., Rando, O. J., Goldberg, A. L. & Maniatis, T. (1994). The ubiquitin-proteasome pathway is required for processing the NF-kappa B1 precursor protein and the activation of NF-kappa B. *Cell* **78**, 773-785.

- Pang, I. K., Pillai, P. S. & Iwasaki, A. (2013). Efficient influenza A virus replication in the respiratory tract requires signals from TLR7 and RIG-I. *Proc Natl Acad Sci U S A* **110**, 13910-13915.
- Panus, J. F., Smith, C. A., Ray, C. A., Smith, T. D., Patel, D. D. & Pickup, D. J. (2002). Cowpox virus encodes a fifth member of the tumor necrosis factor receptor family: a soluble, secreted CD30 homologue. *Proc Natl Acad Sci U S A* **99**, 8348-8353.
- Park, K. J., Krishnan, V., O'Malley, B. W., Yamamoto, Y. & Gaynor, R. B. (2005). Formation of an IKK $\alpha$ -dependent transcription complex is required for estrogen receptor-mediated gene activation. *Mol Cell* **18**, 71-82.
- Parker, S. F., Felzien, L. K., Perkins, N. D., Imperiale, M. J. & Nabel, G. J. (1997). Distinct domains of adenovirus E1A interact with specific cellular factors to differentially modulate human immunodeficiency virus transcription. *J Virol* **71**, 2004-2012.
- Pauli, E.-K., Schmolke, M., Wolff, T., Viemann, D., Roth, J., Bode, J. G. & Ludwig, S. (2008). Influenza A Virus Inhibits Type I IFN Signaling via NF- $\kappa$ B-Dependent Induction of SOCS-3 Expression. *PLoS Pathogens* **4**, e1000196.
- Pelka, P., Ablack, J. N., Fonseca, G. J., Yousef, A. F. & Mymryk, J. S. (2008). Intrinsic structural disorder in adenovirus E1A: a viral molecular hub linking multiple diverse processes. *J Virol* **82**, 7252-7263.
- Pennella, M. A., Liu, Y., Woo, J. L., Kim, C. A. & Berk, A. J. (2010). Adenovirus E1B 55-Kilodalton Protein Is a p53-SUMO1 E3 Ligase That Represses p53 and Stimulates Its Nuclear Export through Interactions with Promyelocytic Leukemia Nuclear Bodies. *Journal of Virology* **84**, 12210-12225.
- Pérez-Berná, A. J., Marabini, R., Scheres, S. H. W., Menéndez-Conejero, R., Dmitriev, I. P., Curiel, D. T., Mangel, W. F., Flint, S. J. & San Martín, C. (2009). Structure and uncoating of immature adenovirus. *Journal of Molecular Biology* **392**, 547-557.
- Perkins, N. D. (2012). The diverse and complex roles of NF- $\kappa$ B subunits in cancer. *Nat Rev Cancer*, 1-12.
- Petrini, J. H. J. & Stracker, T. H. (2003). The cellular response to DNA double-strand breaks: defining the sensors and mediators. *Trends in Cell Biology* **13**, 458-462.
- Pham, A. M. & Tenover, B. R. (2010). The IKK Kinases: Operators of Antiviral Signaling. *Viruses* **2**, 55-72.
- Philipson, L. (1983). Structure and Assembly of Adenoviruses. In *NF- $\kappa$ B in Health and Disease*, pp. 1-52. Berlin, Heidelberg: Springer Science & Business Media Springer Berlin Heidelberg.
- Pichler, A. & Melchior, F. (2002). Ubiquitin-related modifier SUMO1 and nucleocytoplasmic transport. *Traffic* **3**, 381-387.
- Pieper, G. M., Olds, C. L., Bub, J. D. & Lindholm, P. F. (2002). Transfection of human endothelial cells with HIV-1 tat gene activates NF-kappa B and enhances monocyte adhesion. *Am J Physiol Heart Circ Physiol* **283**, H2315-2321.
- Pombo, A., Ferreira, J., Bridge, E. & Carmo-Fonseca, M. (1994). Adenovirus replication and transcription sites are spatially separated in the nucleus of infected cells. *EMBO J* **13**, 5075-5085.
- Popkin, D. L. & Virgin, H. W. (2003). Murine cytomegalovirus infection inhibits tumor necrosis factor alpha responses in primary macrophages. *Journal of Virology* **77**, 10125-10130.
- Pronk, R., Stuiver, M. H. & van der Vliet, P. C. (1992). Adenovirus DNA replication: the function of the covalently bound terminal protein. *Chromosoma* **102**, S39-45.
- Punga, T. & Akusjarvi, G. (2000). The adenovirus-2 E1B-55K protein interacts with a mSin3A/histone deacetylase 1 complex. *FEBS Letters* **476**, 248-252.
- Puvion-Dutilleul, F., Chelbi-Alix, M. K., Koken, M., Quignon, F., Puvion, E. & de The, H. (1995). Adenovirus infection induces rearrangements in the intranuclear distribution of the nuclear body-associated PML protein. *Experimental Cell Research* **218**, 9-16.
- Qing, G., Yan, P. & Xiao, G. (2006). Hsp90 inhibition results in autophagy-mediated proteasome-independent degradation of IkappaB kinase (IKK). *Cell Res* **16**, 895-901.
- Quackenbush, S. L., Linton, A., Brewster, C. D. & Rovnak, J. (2009). Walleye dermal sarcoma virus rv-cyclin inhibits NF-kappaB-dependent transcription. *Virology* **386**, 55-60.

- Querido, E. (2001). Degradation of p53 by adenovirus E4orf6 and E1B55K proteins occurs via a novel mechanism involving a Cullin-containing complex. *Genes & Development* **15**, 3104-3117.
- Querido, E., Blanchette, P., Yan, Q., Kamura, T., Morrison, M., Boivin, D., Kaelin, W. G., Conaway, R. C., Conaway, J. W. & Branton, P. E. (2001). Degradation of p53 by adenovirus E4orf6 and E1B55K proteins occurs via a novel mechanism involving a Cullin-containing complex. *Genes & Development* **15**, 3104-3117.
- Querido, E., Chu-Pham-Dang, H. & Branton, P. E. (2000). Identification and elimination of an aberrant splice product from cDNAs encoding the human adenovirus type 5 E4orf6 protein. *Virology* **275**, 263-266.
- Querido, E., Marcellus, R. C., Lai, A., Charbonneau, R., Teodoro, J. G., Ketner, G. & Branton, P. E. (1997). Regulation of p53 levels by the E1B 55-kilodalton protein and E4orf6 in adenovirus-infected cells. *Journal of Virology* **71**, 3788-3798.
- Qurei, L., Seto, D., Salah, Z. & Azzeh, M. (2012). A Molecular Epidemiology Survey of Respiratory Adenoviruses Circulating in Children Residing in Southern Palestine. *PLoS ONE* **7**, e42732.
- Rahman, M. M., Barrett, J. W., Brouckaert, P. & McFadden, G. (2006). Variation in ligand binding specificities of a novel class of poxvirus-encoded tumor necrosis factor-binding protein. *J Biol Chem* **281**, 22517-22526.
- Rahman, M. M. & McFadden, G. (2011). Modulation of NF- $\kappa$ B signalling by microbial pathogens. *Nat Rev Micro* **9**, 291-306.
- Rahman, M. M., Mohamed, M. R., Kim, M., Smallwood, S. & McFadden, G. (2009). Co-regulation of NF-kappaB and inflammasome-mediated inflammatory responses by myxoma virus pyrin domain-containing protein M013. *PLoS Pathog* **5**, e1000635.
- Rajaiya, J., Xiao, J., Rajala, R. V. S. & Chodosh, J. (2008). Human adenovirus type 19 infection of corneal cells induces p38 MAPK-dependent interleukin-8 expression. *Virology Journal* **5**, 17.
- Ranganathan, P. N. & Khalili, K. (1993). The transcriptional enhancer element, kappa B, regulates promoter activity of the human neurotropic virus, JCV, in cells derived from the CNS. *Nucleic Acids Research* **21**, 1959-1964.
- Rao, L., Debbas, M., Sabbatini, P., Hockenbery, D., Korsmeyer, S. & White, E. (1992). The adenovirus E1A proteins induce apoptosis, which is inhibited by the E1B 19-kDa and Bcl-2 proteins. *PNAS* **89**, 7742-7746.
- Reich, N., Pine, R., Levy, D. & Darnell, J. E. (1988). Transcription of interferon-stimulated genes is induced by adenovirus particles but is suppressed by E1A gene products. *Journal of Virology* **62**, 114-119.
- Reich, N. C., Sarnow, P., Duprey, E. & Levine, A. J. (1983). Monoclonal antibodies which recognize native and denatured forms of the adenovirus DNA-binding protein. *Virology* **128**, 480-484.
- Reimers, K., Buchholz, K. & Werchau, H. (2005). Respiratory syncytial virus M2-1 protein induces the activation of nuclear factor kappa B. *Virology* **331**, 260-268.
- Richardson, P. M. & Gilmore, T. D. (1991). vRel is an inactive member of the Rel family of transcriptional activating proteins. *J Virol* **65**, 3122-3130.
- Robin, M., Marque-Juillet, S., Scieux, C., Peffault de Latour, R., Ferry, C., Rocha, V., Molina, J.-M., Bergeron, A., Devergie, A., Gluckman, E., Ribaud, P. & Socié, G. (2007). Disseminated adenovirus infections after allogeneic hematopoietic stem cell transplantation: incidence, risk factors and outcome. *Haematologica* **92**, 1254-1257.
- Robinson, C. M., Rajaiya, J., Walsh, M. P., Seto, D., Dyer, D. W., Jones, M. S. & Chodosh, J. (2009). Computational analysis of human adenovirus type 22 provides evidence for recombination among species D human adenoviruses in the penton base gene. *Journal of Virology* **83**, 8980-8985.
- Robinson, C. M., Singh, G., Henquell, C., Walsh, M. P., Peigue-Lafeuille, H., Seto, D., Jones, M. S., Dyer, D. W. & Chodosh, J. (2011). Computational analysis and identification of an emergent human adenovirus pathogen implicated in a respiratory fatality. *Virology* **409**, 141-147.
- Robinson, C. M., Singh, G., Lee, J. Y., Dehghan, S., Rajaiya, J., Liu, E. B., Yousuf, M. A., Betensky, R. A., Jones, M. S., Dyer, D. W., Seto, D. & Chodosh, J. (2013). Molecular evolution of human adenoviruses. *Sci Rep* **3**, 1812.

- Rodriguez, C. I., Nogal, M. L., Carrascosa, A. L., Salas, M. L., Fresno, M. & Revilla, Y. (2002). African Swine Fever Virus IAP-Like Protein Induces the Activation of Nuclear Factor Kappa B. *Journal of Virology* **76**, 3936-3942.
- Roelvink, P. W., Lizonova, A., Lee, J. G., Li, Y., Bergelson, J. M., Finberg, R. W., Brough, D. E., Kovesdi, I. & Wickham, T. J. (1998). The coxsackievirus-adenovirus receptor protein can function as a cellular attachment protein for adenovirus serotypes from subgroups A, C, D, E, and F. *Journal of Virology* **72**, 7909-7915.
- Romagnani, S. (2006). Regulation of the T cell response. *Clin Exp Allergy* **36**, 1357-1366.
- Rong, B. L., Libermann, T. A., Kogawa, K., Ghosh, S., Cao, L. X., Pavan-Langston, D. & Dunkel, E. C. (1992). HSV-1-inducible proteins bind to NF-kappa B-like sites in the HSV-1 genome. *Virology* **189**, 750-756.
- Rothwarf, D. M., Zandi, E., Natoli, G. & Karin, M. (1998). IKK-gamma is an essential regulatory subunit of the I-kappaB kinase complex. *Nature* **395**, 297-300.
- Roy, S., Calcedo, R., Medina-Jaszek, A., Keough, M., Peng, H. & Wilson, J. M. (2011). Adenoviruses in lymphocytes of the human gastro-intestinal tract. *PLoS ONE* **6**, e24859.
- Rubenwolf, S., Schutt, H., Nevels, M., Wolf, H. & Dobner, T. (1997). Structural analysis of the adenovirus type 5 E1B 55-kilodalton-E4orf6 protein complex. *J Virol* **71**, 1115-1123.
- Rudolph, D., Yeh, W. C., Wakeham, A., Rudolph, B., Nallainathan, D., Potter, J., Elia, A. J. & Mak, T. W. (2000). Severe liver degeneration and lack of NF-kappaB activation in NEMO/IKKgamma-deficient mice. *Genes & Development* **14**, 854-862.
- Russell, W. C. (1969). Internal components of adenovirus. *J Gen Microbiol* **57**, ix.
- Russell, W. C. (2009). Adenoviruses: update on structure and function. *Journal of general Virology* **90**, 1-20.
- Rux, J. J. & Burnett, R. M. (2004). Adenovirus structure. *Hum Gene Ther* **15**, 1167-1176.
- Sadowski, I. & Ptashne, M. (1989). A vector for expressing GAL4(1-147) fusions in mammalian cells. *Nucleic acids research* **17**, 7539.
- Safrin, S., Cherrington, J. & Jaffe, H. S. (1997). Clinical uses of cidofovir. *Rev Med Virol* **7**, 145-156.
- Sambrook, J., E. F. Fritsch, und T. Maniatis. (1989). *Molecular cloning: A laboratory manual*. Cold Spring Harbor: Cold Spring Harbor Laboratory Press.
- Sambucetti, L. C., Cherrington, J. M., Wilkinson, G. W. & Mocarski, E. S. (1989). NF-kappa B activation of the cytomegalovirus enhancer is mediated by a viral transactivator and by T cell stimulation. *EMBO J* **8**, 4251-4258.
- Samulski, R. J. & Shenk, T. (1988). Adenovirus E1B 55-Mr polypeptide facilitates timely cytoplasmic accumulation of adeno-associated virus mRNAs. *J Virol* **62**, 206-210.
- San Martin, C. & Burnett, R. M. (2003). Structural studies on adenoviruses. *Curr Top Microbiol Immunol* **272**, 57-94.
- Sandford, G., Choi, Y. B. & Nicholas, J. (2009). Role of ORF74-encoded viral G protein-coupled receptor in human herpesvirus 8 lytic replication. *J Virol* **83**, 13009-13014.
- Saraiva, M. & Alcami, A. (2001). CrmE, a novel soluble tumor necrosis factor receptor encoded by poxviruses. *J Virol* **75**, 226-233.
- Sarnow, P., Hearing, P., Anderson, C. W., Halbert, D. N., Shenk, T. & Levine, A. J. (1984). Adenovirus early region 1B 58,000-dalton tumor antigen is physically associated with an early region 4 25,000-dalton protein in productively infected cells. *Journal of Virology* **49**, 692-700.
- Sarnow, P., Sullivan, C. A. & Levine, A. J. (1982). A monoclonal antibody detecting the adenovirus type 5-E1b-58Kd tumor antigen: characterization of the E1b-58Kd tumor antigen in adenovirus-infected and -transformed cells. *Virology* **120**, 510-517.
- Savelyeva, I. & Dobbstein, M. (2011). Infection with E1B-mutant adenovirus stabilizes p53 but blocks p53 acetylation and activity through E1A. *Oncogene* **30**, 865-875.
- Savón, C., Acosta, B., Valdés, O., Goyenechea, A., Gonzalez, G., Piñón, A., Más, P., Rosario, D., Capó, V., Kourí, V., Martínez, P. A., Marchena, J. J., González, G., Rodríguez, H. & Guzmán, M. G. (2008). A myocarditis outbreak with fatal cases associated with adenovirus subgenera C among children from Havana City in 2005. *J Clin Virol* **43**, 152-157.
- Schaack, J. (2005). Induction and inhibition of innate inflammatory responses by adenovirus early region proteins. *Viral Immunol* **18**, 79-88.

- Schaeper, U., Subramanian, T., Lim, L., Boyd, J. M. & Chinnadurai, G. (1998). Interaction between a cellular protein that binds to the C-terminal region of adenovirus E1A (CtBP) and a novel cellular protein is disrupted by E1A through a conserved PLDLS motif. *J Biol Chem* **273**, 8549-8552.
- Schmitz, H., Wigand, R. & Heinrich, W. (1983). Worldwide epidemiology of human adenovirus infections. *American journal of epidemiology* **117**, 455-466.
- Schmitz, M. L., Indorf, A., Limbourg, F. P., Städtler, H., Traenckner, E. B. & Baeuerle, P. A. (1996). The dual effect of adenovirus type 5 E1A 13S protein on NF-kappaB activation is antagonized by E1B 19K. *Molecular and Cellular Biology* **16**, 4052-4063.
- Schneider-Brachert, W., Tchikov, V., Merkel, O., Jakob, M., Hallas, C., Kruse, M.-L., Groitl, P., Lehn, A., Hildt, E., Held-Feindt, J., Dobner, T., Kabelitz, D., Krönke, M. & Schütze, S. (2006). Inhibition of TNF receptor 1 internalization by adenovirus 14.7K as a novel immune escape mechanism. *J Clin Invest* **116**, 2901-2913.
- Schnell, M. A., Zhang, Y., Tazelaar, J., Gao, G. P., Yu, Q. C., Qian, R., Chen, S. J., Varnavski, A. N., LeClair, C., Raper, S. E. & Wilson, J. M. (2001). Activation of innate immunity in nonhuman primates following intraportal administration of adenoviral vectors. *Mol Ther* **3**, 708-722.
- Schreiner, S., Bürck, C., Glass, M., Groitl, P., Wimmer, P., Kinkley, S., Mund, A., Everett, R. D. & Dobner, T. (2013a). Control of human adenovirus type 5 gene expression by cellular Daxx/ATRAX chromatin-associated complexes. *Nucleic Acids Research* **41**, 3532-3550.
- Schreiner, S., Kinkley, S., Bürck, C., Mund, A., Wimmer, P., Schubert, T., Groitl, P., Will, H. & Dobner, T. (2013b). SPOC1-mediated antiviral host cell response is antagonized early in human adenovirus type 5 infection. *PLoS Pathogens* **9**, e1003775.
- Schreiner, S., Martinez, R., Groitl, P., Rayne, F., Vaillant, R., Wimmer, P., Bossis, G., Sternsdorf, T., Marcinowski, L., Ruzsics, Z., Dobner, T. & Wodrich, H. (2012a). Transcriptional Activation of the Adenoviral Genome Is Mediated by Capsid Protein VI. *PLoS Pathogens* **8**, e1002549.
- Schreiner, S., Wimmer, P. & Dobner, T. (2012b). Adenovirus degradation of cellular proteins. *Future Microbiol* **7**(2), 211-225.
- Schreiner, S., Wimmer, P., Sirma, H., Everett, R. D., Blanchette, P., Groitl, P. & Dobner, T. (2010). Proteasome-Dependent Degradation of Daxx by the Viral E1B-55K Protein in Human Adenovirus-Infected Cells. *Journal of Virology* **84**, 7029-7038.
- Schutze, S., Wiegmann, K., Machleidt, T. & Kronke, M. (1995). TNF-induced activation of NF-kappa B. *Immunobiology* **193**, 193-203.
- Schwartz, R. A., Lakdawala, S. S., Eshleman, H. D., Russell, M. R., Carson, C. T. & Weitzman, M. D. (2008). Distinct Requirements of Adenovirus E1b55K Protein for Degradation of Cellular Substrates. *Journal of Virology* **82**, 9043-9055.
- Schwarz, M. & Murphy, P. M. (2001). Kaposi's Sarcoma-Associated Herpesvirus G Protein-Coupled Receptor Constitutively Activates NF- $\kappa$ B and Induces Proinflammatory Cytokine and Chemokine Production Via a C-Terminal Signaling Determinant. *The Journal of Immunology* **167**, 505-513.
- Sebban, H., Yamaoka, S. & Courtois, G. (2006). Posttranslational modifications of NEMO and its partners in NF- $\kappa$ B signaling. *Trends in Cell Biology* **16**, 569-577.
- Sedgwick, J. D., Riminton, D. S., Cyster, J. G. & Korner, H. (2000). Tumor necrosis factor: a master-regulator of leukocyte movement. *Immunol Today* **21**, 110-113.
- Senftleben, U., Cao, Y., Xiao, G., Greten, F. R., Krähn, G., Bonizzi, G., Chen, Y., Hu, Y., Fong, A., Sun, S. C. & Karin, M. (2001). Activation by IKKalpha of a second, evolutionary conserved, NF-kappa B signaling pathway. *Science* **293**, 1495-1499.
- Seo, T., Park, J., Lim, C. & Choe, J. (2004). Inhibition of nuclear factor kappaB activity by viral interferon regulatory factor 3 of Kaposi's sarcoma-associated herpesvirus. *Oncogene* **23**, 6146-6155.
- Shah, G. A. & O'Shea, C. C. (2015). Viral and Cellular Genomes Activate Distinct DNA Damage Responses. *Cell* **162**, 987-1002.
- Shao, R., Hu, M. C., Zhou, B. P., Lin, S. Y., Chiao, P. J., von Lindern, R. H., Spohn, B. & Hung, M. C. (1999). E1A sensitizes cells to tumor necrosis factor-induced apoptosis through inhibition of IkappaB kinases and nuclear factor kappaB activities. *J Biol Chem* **274**, 21495-21498.

- Sharp, P. A., Gallimore, P. H. & Flint, S. J. (1975). Mapping of adenovirus 2 RNA sequences in lytically infected cells and transformed cell lines. *Cold Spring Harb Symp Quant Biol* **39 Pt 1**, 457-474.
- Shauer, A., Gotsman, I., Keren, A., Zwas, D. R., Hellman, Y., Durst, R. & Admon, D. (2013). Acute viral myocarditis: current concepts in diagnosis and treatment. *Isr Med Assoc J* **15**, 180-185.
- Shaw, A. R. & Ziff, E. B. (1980). Transcripts from the adenovirus-2 major late promoter yield a single early family of 3' coterminal mRNAs and five late families. *Cell* **22**, 905-916.
- Shen, Y., Kitzes, G., Nye, J. A., Fattaey, A. & Hermiston, T. (2001). Analyses of single-amino-acid substitution mutants of adenovirus type 5 E1B-55K protein. *J Virol* **75**, 4297-4307.
- Shenk, T. (2001). Adenoviridae: the viruses and their replication. In *Virology*, Fourth edn, pp. 2265-2300. Edited by D. M. Knipe & P. M. Howley. New York: Lippincott-Raven.
- Shepard, R. N. & Ornelles, D. A. (2004). Diverse roles for E4orf3 at late times of infection revealed in an E1B 55-kilodalton protein mutant background. *Journal of Virology* **78**, 9924-9935.
- Shisler, J., Duerksen-Hughes, P., Hermiston, T. M., Wold, W. S. & Gooding, L. R. (1996). Induction of susceptibility to tumor necrosis factor by E1A is dependent on binding to either p300 or p105-Rb and induction of DNA synthesis. *Journal of Virology* **70**, 68-77.
- Shisler, J., Yang, C., Walter, B., Ware, C. F. & Gooding, L. R. (1997). The adenovirus E3-10.4K/14.5K complex mediates loss of cell surface Fas (CD95) and resistance to Fas-induced apoptosis. *J Virol* **71**, 8299-8306.
- Shisler, J. L. & Jin, X. L. (2004). The vaccinia virus K1L gene product inhibits host NF-kappaB activation by preventing IkappaBalpha degradation. *J Virol* **78**, 3553-3560.
- Shurman, L., Sen, R. & Bergman, Y. (1989). Adenovirus E1A products activate the Ig k-chain enhancer in fibroblasts. A possible involvement of the NF-kB binding site. *The Journal of Immunology* **143**, 3806-3812.
- Siebenlist, U., Franzoso, G. & Brown, K. (1994). Structure, regulation and function of NF-kappa B. *Annu Rev Cell Biol* **10**, 405-455.
- Siminovich, M. & Murtagh, P. (2011). Acute lower respiratory tract infections by adenovirus in children: histopathologic findings in 18 fatal cases. *Pediatr Dev Pathol* **14**, 214-217.
- Smith, S. A., Mullin, N. P., Parkinson, J., Shchelkunov, S. N., Totmenin, A. V., Loparev, V. N., Srisatjaluk, R., Reynolds, D. N., Keeling, K. L., Justus, D. E., Barlow, P. N. & Kotwal, G. J. (2000). Conserved surface-exposed K/R-X-K/R motifs and net positive charge on poxvirus complement control proteins serve as putative heparin binding sites and contribute to inhibition of molecular interactions with human endothelial cells: a novel mechanism for evasion of host defense. *J Virol* **74**, 5659-5666.
- Söderlund, H., Pettersson, U., Vennström, B., Philipson, L. & Mathews, M. B. (1976). A new species of virus-coded low molecular weight RNA from cells infected with adenovirus type 2. *Cell* **7**, 585-593.
- Sohn, S. Y. & Hearing, P. (2011). Adenovirus Sequesters Phosphorylated STAT1 at Viral Replication Centers and Inhibits STAT Dephosphorylation. *Journal of Virology* **85**, 7555-7562.
- Somasundaram, K. & El-Deiry, W. S. (1997). Inhibition of p53-mediated transactivation and cell cycle arrest by E1A through its p300/CBP-interacting region. *Oncogene* **14**, 1047-1057.
- Soni, V., Cahir-McFarland, E. & Kieff, E. (2007). LMP1 TRAFficking activates growth and survival pathways. *Adv Exp Med Biol* **597**, 173-187.
- Spindler, K. R., Rosser, D. S. & Berk, A. J. (1984). Analysis of adenovirus transforming proteins from early regions 1A and 1B with antisera to inducible fusion antigens produced in Escherichia coli. *Journal of Virology* **49**, 132-141.
- Spitkovsky, D., Hehner, S. P., Hofmann, T. G., Moller, A. & Schmitz, M. L. (2002). The human papillomavirus oncoprotein E7 attenuates NF-kappa B activation by targeting the Ikappa B kinase complex. *J Biol Chem* **277**, 25576-25582.
- Sprengel, J., Schmitz, B., Heuss-Neitzel, D., Zock, C. & Doerfler, W. (1994). Nucleotide sequence of human adenovirus type 12 DNA: comparative functional analysis. *Journal of Virology* **68**, 379-389.

- Stack, J., Haga, I. R., Schroder, M., Bartlett, N. W., Maloney, G., Reading, P. C., Fitzgerald, K. A., Smith, G. L. & Bowie, A. G. (2005). Vaccinia virus protein A46R targets multiple Toll-like-interleukin-1 receptor adaptors and contributes to virulence. *J Exp Med* **201**, 1007-1018.
- Stein, G. H., Beeson, M. & Gordon, L. (1990). Failure to phosphorylate the retinoblastoma gene product in senescent human fibroblasts. *Science* **249**, 666-669.
- Stephens, C. & Harlow, E. (1987). Differential splicing yields novel adenovirus 5 E1A mRNAs that encode 30 kd and 35 kd proteins. *EMBO J* **6**, 2027-2035.
- Stevens, J. L. (2002). Transcription Control by E1A and MAP Kinase Pathway via Sur2 Mediator Subunit. *Science* **296**, 755-758.
- Stewart, P. L., Burnett, R. M., Cyrklaff, M. & Fuller, S. D. (1991). Image reconstruction reveals the complex molecular organization of adenovirus. *Cell* **67**, 145-154.
- Stewart, P. L., Fuller, S. D. & Burnett, R. M. (1993). Difference imaging of adenovirus: bridging the resolution gap between X-ray crystallography and electron microscopy. *EMBO J* **12**, 2589-2599.
- Stracker, T. H., Carson, C. T. & Weitzman, M. D. (2002). Adenovirus oncoproteins inactivate the Mre11 Rad50 NBS1 DNA repair complex. *Nature* **418**, 348-352.
- Strunze, S., Trotman, L. C., Boucke, K. & Greber, U. F. (2005). Nuclear targeting of adenovirus type 2 requires CRM1-mediated nuclear export. *Molecular Biology of the Cell* **16**, 2999-3009.
- Sun, S.-C. & Cesarman, E. (2011). NF- $\kappa$ B as a target for oncogenic viruses. *Curr Top Microbiol Immunol* **349**, 197-244.
- Sun, S. C., Ganchi, P. A., Ballard, D. W. & Greene, W. C. (1993). NF-kappa B controls expression of inhibitor I kappa B alpha: evidence for an inducible autoregulatory pathway. *Science* **259**, 1912-1915.
- Swaminathan, S. & Thimmapaya, B. (1996). Transactivation of adenovirus E2-early promoter by E1A and E4 6/7 in the context of viral chromosome. *Journal of Molecular Biology* **258**, 736-746.
- Symeonidis, N., Jakubowski, A., Pierre-Louis, S., Jaffe, D., Pamer, E., Sepkowitz, K., O'Reilly, R. J. & Papanicolaou, G. A. (2007). Invasive adenoviral infections in T-cell-depleted allogeneic hematopoietic stem cell transplantation: high mortality in the era of cidofovir. *Transpl Infect Dis* **9**, 108-113.
- Takeuchi, O. & Akira, S. (2010). Pattern Recognition Receptors and Inflammation. *Cell* **140**, 805-820.
- Tamanini, A., Nicolis, E., Bonizzato, A., Bezzerri, V., Melotti, P., Assael, B. M. & Cabrini, G. (2006). Interaction of Adenovirus Type 5 Fiber with the Coxsackievirus and Adenovirus Receptor Activates Inflammatory Response in Human Respiratory Cells. *Journal of Virology* **80**, 11241-11254.
- Tamanoi, F. & Stillman, B. W. (1982). Function of adenovirus terminal protein in the initiation of DNA replication. *PNAS* **79**, 2221-2225.
- Taylor, R. T. & Bresnahan, W. A. (2006). Human cytomegalovirus IE86 attenuates virus- and tumor necrosis factor alpha-induced NFkappaB-dependent gene expression. *Journal of Virology* **80**, 10763-10771.
- Taylor, S. L., Frias-Staheli, N., Garcia-Sastre, A. & Schmaljohn, C. S. (2009a). Hantaan virus nucleocapsid protein binds to importin alpha proteins and inhibits tumor necrosis factor alpha-induced activation of nuclear factor kappa B. *J Virol* **83**, 1271-1279.
- Taylor, S. L., Krempel, R. L. & Schmaljohn, C. S. (2009b). Inhibition of TNF-alpha-induced activation of NF-kappaB by hantavirus nucleocapsid proteins. *Ann N Y Acad Sci* **1171 Suppl 1**, E86-93.
- Teigler, J. E., Iampietro, M. J. & Barouch, D. H. (2012). Vaccination with Adenovirus Serotypes 35, 26, and 48 Elicits Higher Levels of Innate Cytokine Responses than Adenovirus Serotype 5 in Rhesus Monkeys. *Journal of Virology* **86**, 9590-9598.
- tenOever, B. R., Sharma, S., Zou, W., Sun, Q., Grandvaux, N., Julkunen, I., Hemmi, H., Yamamoto, M., Akira, S., Yeh, W. C., Lin, R. & Hiscott, J. (2004). Activation of TBK1 and IKKvarepsilon kinases by vesicular stomatitis virus infection and the role of viral ribonucleoprotein in the development of interferon antiviral immunity. *J Virol* **78**, 10636-10649.

- Teodoro, J. G. & Branton, P. E. (1997). Regulation of p53-dependent apoptosis, transcriptional repression, and cell transformation by phosphorylation of the 55-kilodalton E1B protein of human adenovirus type 5. *Journal of Virology* **71**, 3620-3627.
- Teodoro, J. G., Halliday, T., Whalen, S. G., Takayesu, D., Graham, F. L. & Branton, P. E. (1994). Phosphorylation at the carboxy terminus of the 55-kilodalton adenovirus type 5 E1B protein regulates transforming activity. *Journal of Virology* **68**, 776-786.
- Thaci, B., Ulasov, I. V., Wainwright, D. A. & Lesniak, M. S. (2011). The challenge for gene therapy: innate immune response to adenoviruses. *Oncotarget* **2**, 113-121.
- Thompson, M. R., Kaminski, J. J., Kurt-Jones, E. A. & Fitzgerald, K. A. (2011). Pattern recognition receptors and the innate immune response to viral infection. *Viruses* **3**, 920-940.
- Tollefson, A. E., Scaria, A., Hermiston, T. W., Ryerse, J. S., Wold, L. J. & Wold, W. S. (1996). The adenovirus death protein (E3-11.6K) is required at very late stages of infection for efficient cell lysis and release of adenovirus from infected cells. *Journal of Virology* **70**, 2296-2306.
- Törmänen, H., Backström, E., Carlsson, A. & Akusjärvi, G. (2006). L4-33K, an adenovirus-encoded alternative RNA splicing factor. *J Biol Chem* **281**, 36510-36517.
- Totzke, G., Essmann, F., Pohlmann, S., Lindenblatt, C., Jänicke, R. U. & Schulze-Osthoff, K. (2006). A novel member of the IkappaB family, human IkappaB-zeta, inhibits transactivation of p65 and its DNA binding. *J Biol Chem* **281**, 12645-12654.
- Traenckner, E. B., Wilk, S. & Baeuerle, P. A. (1994). A proteasome inhibitor prevents activation of NF-kappa B and stabilizes a newly phosphorylated form of I kappa B-alpha that is still bound to NF-kappa B. *EMBO J* **13**, 5433-5441.
- Trentin, J. J., Yabe, Y. & Taylor, G. (1962). The quest for human cancer viruses. *Science* **137**, 835-841.
- Tribouley, C., Lutz, P., Staub, A. & Kedinger, C. (1994). The product of the adenovirus intermediate gene IVa2 is a transcriptional activator of the major late promoter. *Journal of Virology* **68**, 4450-4457.
- Tufariello, J. M., Cho, S. & Horwitz, M. S. (1994). Adenovirus E3 14.7-kilodalton protein, an antagonist of tumor necrosis factor cytotoxicity, increases the virulence of vaccinia virus in severe combined immunodeficient mice. *Proc Natl Acad Sci U S A* **91**, 10987-10991.
- Ugolini, S., Moulard, M., Mondor, I., Barois, N., Demandolx, D., Hoxie, J., Brelot, A., Alizon, M., Davoust, J. & Sattentau, Q. J. (1997). HIV-1 gp120 induces an association between CD4 and the chemokine receptor CXCR4. *J Immunol* **159**, 3000-3008.
- Ulfendahl, P. J., Linder, S., Kreivi, J. P., Nordqvist, K., Sevansson, C., Hultberg, H. & Akusjärvi, G. (1987). A novel adenovirus-2 E1A mRNA encoding a protein with transcription activation properties. *The EMBO Journal* **6**, 2037-2044.
- Vallabhapurapu, S., Matsuzawa, A., Zhang, W., Tseng, P.-H., Keats, J. J., Wang, H., Vignali, D. A. A., Bergsagel, P. L. & Karin, M. (2008). Nonredundant and complementary functions of TRAF2 and TRAF3 in a ubiquitination cascade that activates NIK-dependent alternative NF-kappaB signaling. *Nat Immunol* **9**, 1364-1370.
- van Breukelen, B., Kanellopoulos, P. N., Tucker, P. A. & van der Vliet, P. C. (2000). The formation of a flexible DNA-binding protein chain is required for efficient DNA unwinding and adenovirus DNA chain elongation. *J Biol Chem* **275**, 40897-40903.
- Van Damme, E., Laukens, K., Dang, T. H. & Van Ostade, X. (2010). A manually curated network of the PML nuclear body interactome reveals an important role for PML-NBs in SUMOylation dynamics. *Int J Biol Sci* **6**, 51-67.
- van den Bosch, M., Bree, R. T. & Lowndes, N. F. (2003). The MRN complex: coordinating and mediating the response to broken chromosomes. *EMBO Rep* **4**, 844-849.
- van Eekelen, C. A. & van Venrooij, W. J. (1981). hnRNA and its attachment to a nuclear protein matrix. *J Cell Biol* **88**, 554-563.
- van Lint, A. L., Murawski, M. R., Goodbody, R. E., Severa, M., Fitzgerald, K. A., Finberg, R. W., Knipe, D. M. & Kurt-Jones, E. A. (2010). Herpes simplex virus immediate-early ICP0 protein inhibits Toll-like receptor 2-dependent inflammatory responses and NF-kappaB signaling. *J Virol* **84**, 10802-10811.
- van Ormondt, H., Maat, J. & Dijkema, R. (1980). Comparison of nucleotide sequences of the early E1a regions for subgroups A, B and C of human adenoviruses. *Gene* **12**, 63-76.

- Van Waes, C., Yu, M., Nottingham, L. & Karin, M. (2007). Inhibitor-kappaB kinase in tumor promotion and suppression during progression of squamous cell carcinoma. *Clin Cancer Res* **13**, 4956-4959.
- Varin, A., Manna, S. K., Quivy, V., Decrion, A. Z., Van Lint, C., Herbein, G. & Aggarwal, B. B. (2003). Exogenous Nef protein activates NF-kappa B, AP-1, and c-Jun N-terminal kinase and stimulates HIV transcription in promonocytic cells. Role in AIDS pathogenesis. *J Biol Chem* **278**, 2219-2227.
- Veckman, V., Osterlund, P., Fagerlund, R., Melen, K., Matikainen, S. & Julkunen, I. (2006). TNF-alpha and IFN-alpha enhance influenza-A-virus-induced chemokine gene expression in human A549 lung epithelial cells. *Virology* **345**, 96-104.
- Verma, U. N. (2003). Nuclear Role of I B Kinase- /NF- B Essential Modulator (IKK /NEMO) in NF- B-dependent Gene Expression. *Journal of Biological Chemistry* **279**, 3509-3515.
- Vink, E. I., Yondola, M. A., Wu, K. & Hearing, P. (2012). Adenovirus E4-ORF3-dependent relocalization of TIF1  $\alpha$  and TIF1  $\gamma$  relies on access to the Coiled-Coil motif. *Virology* **422**, 317-325.
- Vinolo, E., Sebban, H., Chaffotte, A., Israel, A., Courtois, G., Veron, M. & Agou, F. (2006). A point mutation in NEMO associated with anhidrotic ectodermal dysplasia with immunodeficiency pathology results in destabilization of the oligomer and reduces lipopolysaccharide- and tumor necrosis factor-mediated NF-kappa B activation. *J Biol Chem* **281**, 6334-6348.
- Virtanen, A., Gilardi, P., Näslund, A., LeMoulllec, J. M., Pettersson, U. & Perricaudet, M. (1984). mRNAs from human adenovirus 2 early region 4. *Journal of Virology* **51**, 822-831.
- Viruses, I. C. o. T. o. (2012). International Committee on Taxonomy of Viruses, Feb. 21, 2012 edn.
- Wadell, G. (1984). Molecular epidemiology of human adenoviruses. *Curr Top Microbiol Immunol* **110**, 191-220.
- Waldhoer, M., Kledal, T. N., Farrell, H. & Schwartz, T. W. (2002). Murine cytomegalovirus (CMV) M33 and human CMV US28 receptors exhibit similar constitutive signaling activities. *J Virol* **76**, 8161-8168.
- Walsh, M. P., Chintakuntlawar, A., Robinson, C. M., Madisch, I., Harrach, B., Hudson, N. R., Schnurr, D., Heim, A., Chodosh, J., Seto, D. & Jones, M. S. (2009). Evidence of molecular evolution driven by recombination events influencing tropism in a novel human adenovirus that causes epidemic keratoconjunctivitis. *PLoS ONE* **4**, e5635.
- Wang, X. & Sonenshein, G. E. (2005). Induction of the RelB NF-kappaB subunit by the cytomegalovirus IE1 protein is mediated via Jun kinase and c-Jun/Fra-2 AP-1 complexes. *J Virol* **79**, 95-105.
- Wang, Y., Zhou, J., Ruan, C. & Du, Y. (2012). Inhibition of type I interferon production via suppressing IKK-gamma expression: a new strategy for counteracting host antiviral defense by influenza A viruses? *J Proteome Res* **11**, 217-223.
- Webster, L. C. & Ricciardi, R. P. (1991). trans-dominant mutants of E1A provide genetic evidence that the zinc finger of the trans-activating domain binds a transcription factor. *Molecular and Cellular Biology* **11**, 4287-4296.
- Weiden, M. D. & Ginsberg, H. S. (1994). Deletion of the E4 region of the genome produces adenovirus DNA concatemers. *PNAS* **91**, 153-157.
- Weigel, S. & Dobbelstein, M. (2000). The nuclear export signal within the E4orf6 protein of adenovirus type 5 supports virus replication and cytoplasmic accumulation of viral mRNA. *Journal of Virology* **74**, 764-772.
- Weitzman, M. D., Fisher, K. J. & Wilson, J. M. (1996). Recruitment of wild-type and recombinant adeno-associated virus into adenovirus replication centers. *J Virol* **70**, 1845-1854.
- Weitzman, M. D. & Ornelles, D. A. (2005). Inactivating intracellular antiviral responses during adenovirus infection. *Oncogene* **24**, 7686-7696.
- White, E., Cipriani, R., Sabbatini, P. & Denton, A. (1991). Adenovirus E1B 19-kilodalton protein overcomes the cytotoxicity of E1A proteins. *Journal of Virology* **65**, 2968-2978.
- White, L., Blair, G. E. (2012). Adenoviruses and Gene Therapy: The Role of the Immune System. In *Small DNA Tumour Viruses*. Bristol, UK: Caister Academic Press.

- Whiteside, S. T., Epinat, J. C., Rice, N. R. & Israel, A. (1997). I kappa B epsilon, a novel member of the I kappa B family, controls RelA and cRel NF-kappa B activity. *EMBO J* **16**, 1413-1426.
- Whiteside, S. T. & Israel, A. (1997). I kappa B proteins: structure, function and regulation. *Semin Cancer Biol* **8**, 75-82.
- Wickham, T. J., Mathias, P., Cheresch, D. A. & Nemerow, G. R. (1993). Integrins alpha v beta 3 and alpha v beta 5 promote adenovirus internalization but not virus attachment. *Cell* **73**, 309-319.
- Williams, B. R. (1999). PKR; a sentinel kinase for cellular stress. *Oncogene* **18**, 6112-6120.
- Williams, J. L. J., Garcia, J. J., Harrich, D. D., Pearson, L. L., Wu, F. F. & Gaynor, R. R. (1990). Lymphoid specific gene expression of the adenovirus early region 3 promoter is mediated by NF-kappa B binding motifs. *EMBO J* **9**, 4435-4442.
- Wilson, J. R., de Sessions, P. F., Leon, M. A. & Scholle, F. (2008). West Nile virus nonstructural protein 1 inhibits TLR3 signal transduction. *J Virol* **82**, 8262-8271.
- Wilson, M. C., Fraser, N. W. & Darnell, J. E. (1979). Mapping of RNA initiation sites by high doses of uv irradiation: evidence for three independent promoters within the left 11% of the Ad-2 genome. *Virology* **94**, 175-184.
- Wimmer, P., Blanchette, P., Schreiner, S., Ching, W., Groitl, P., Berscheminski, J., Branton, P. E., Will, H. & Dobner, T. (2012). Cross-talk between phosphorylation and SUMOylation regulates transforming activities of an adenoviral oncoprotein. *Oncogene*, 1-12.
- Windheim, M. & Burgert, H. G. (2002). Characterization of E3/49K, a novel, highly glycosylated E3 protein of the epidemic keratoconjunctivitis-causing adenovirus type 19a. *J Virol* **76**, 755-766.
- windheim, M., Stafford, M., Peggie, M. & Cohen, P. (2008). Interleukin-1 (IL-1) induces the Lys63-linked polyubiquitination of IL-1 receptor-associated kinase 1 to facilitate NEMO binding and the activation of IkappaBalpha kinase. *Molecular and Cellular Biology* **28**, 1783-1791.
- Wold, W. S. (1993). Adenovirus genes that modulate the sensitivity of virus-infected cells to lysis by TNF. *J Cell Biochem* **53**, 329-335.
- Wold, W. S. & Gooding, L. R. (1991). Region E3 of adenovirus: a cassette of genes involved in host immunosurveillance and virus-cell interactions. *Virology* **184**, 1-8.
- Wold, W. S., Tollefson, A. E. & Hermiston, T. W. (1995). E3 transcription unit of adenovirus. *Curr Top Microbiol Immunol* **199** ( Pt 1), 237-274.
- Woo, J. L. & Berk, A. J. (2007). Adenovirus ubiquitin-protein ligase stimulates viral late mRNA nuclear export. *J Virol* **81**, 575-587.
- Wu, C.-J., Conze, D. B., Li, T., Srinivasula, S. M. & Ashwell, J. D. (2006). NEMO is a sensor of Lys 63-linked polyubiquitination and functions in NF- $\kappa$ B activation. *Nat Cell Biol* **8**, 398-406.
- Wu, R. C., Qin, J., Hashimoto, Y., Wong, J., Xu, J., Tsai, S. Y., Tsai, M. J. & O'Malley, B. W. (2002). Regulation of SRC-3 (pCIP/ACTR/AIB-1/RAC-3/TRAM-1) Coactivator activity by I kappa B kinase. *Mol Cell Biol* **22**, 3549-3561.
- Xiao, G., Fong, A. & Sun, S. C. (2004). Induction of p100 Processing by NF- $\kappa$ B-inducing Kinase Involves Docking IB Kinase (IKK $\alpha$ ) to p100 and IKK $\alpha$ -mediated Phosphorylation. *J Biol Chem* **279**, 30099-30105.
- Xiao, G., Harhaj, E. W. & Sun, S. C. (2001). NF-kappaB-inducing kinase regulates the processing of NF-kappaB2 p100. *Molecular Cell* **7**, 401-409.
- Xu, X., Tarakanova, V., Chrivia, J. & Yaciuk, P. (2003). Adenovirus DNA binding protein inhibits SrCap-activated CBP and CREB-mediated transcription. *Virology* **313**, 615-621.
- Yageta, M., Tsunoda, H., Yamanaka, T., Nakajima, T., Tomooka, Y., Tsuchida, N. & Oda, K. (1999). The adenovirus E1A domains required for induction of DNA rereplication in G2/M arrested cells coincide with those required for apoptosis. *Oncogene* **18**, 4767-4776.
- Yamamoto, M., Sato, S., Hemmi, H., Hoshino, K., Kaisho, T., Sanjo, H., Takeuchi, O., Sugiyama, M., Okabe, M., Takeda, K. & Akira, S. (2003a). Role of Adaptor TRIF in the MyD88-Independent Toll-Like Receptor Signaling Pathway. *Science* **301**, 640-643.

- Yamamoto, Y., Verma, U. N., Prajapati, S., Kwak, Y. T. & Gaynor, R. B. (2003b).** Histone H3 phosphorylation by IKK-alpha is critical for cytokine-induced gene expression. *Nature* **423**, 655-659.
- Yamaoka, S., Courtois, G., Bessia, C., Whiteside, S. T., Weil, R., Agou, F., Kirk, H. E., Kay, R. J. & Israel, A. (1998).** Complementation cloning of NEMO, a component of the IkappaB kinase complex essential for NF-kappaB activation. *Cell* **93**, 1231-1240.
- Yang, X. J., Ogryzko, V. V., Nishikawa, J., Howard, B. H. & Nakatani, Y. (1996).** A p300/CBP-associated factor that competes with the adenoviral oncoprotein E1A. *Nature* **382**, 319-324.
- Yew, P. R. & Berk, A. J. (1992).** Inhibition of p53 transactivation required for transformation by adenovirus early 1B protein. *Nature* **357**, 82-85.
- Yew, P. R., Kao, C. C. & Berk, A. J. (1990).** Dissection of functional domains in the adenovirus 2 early 1B 55K polypeptide by suppressor-linker insertional mutagenesis. *Virology* **179**, 795-805.
- Yew, P. R., Liu, X. & Berk, A. J. (1994).** Adenovirus E1B oncoprotein tethers a transcriptional repression domain to p53. *Genes & Development* **8**, 190-202.
- Ylihärsilä, M., Harju, E., Arppe, R., Hattara, L., Hölsä, J., Saviranta, P., Soukka, T. & Waris, M. (2013).** Genotyping of clinically relevant human adenoviruses by array-in-well hybridization assay. *Clin Microbiol Infect* **19**, 551-557.
- Yolken, R. H., Lawrence, F., Leister, F., Takiff, H. E. & Strauss, S. E. (1982).** Gastroenteritis associated with enteric type adenovirus in hospitalized infants. *J Pediatr* **101**, 21-26.
- Yondola, M. A. & Hearing, P. (2007).** The Adenovirus E4 ORF3 Protein Binds and Reorganizes the TRIM Family Member Transcriptional Intermediary Factor 1 Alpha. *Journal of Virology* **81**, 4264-4271.
- Yoon, D. W., Lee, H., Seol, W., DeMaria, M., Rosenzweig, M. & Jung, J. U. (1997).** Tap: a novel cellular protein that interacts with tip of herpesvirus saimiri and induces lymphocyte aggregation. *Immunity* **6**, 571-582.
- Yoshida, K., Ozaki, T., Furuya, K., Nakanishi, M., Kikuchi, H., Yamamoto, H., Ono, S., Koda, T., Omura, K. & Nakagawara, A. (2008).** ATM-dependent nuclear accumulation of IKK-alpha plays an important role in the regulation of p73-mediated apoptosis in response to cisplatin. *Oncogene* **27**, 1183-1188.
- Yurochko, A. D., Hwang, E. S., Rasmussen, L., Keay, S., Pereira, L. & Huang, E. S. (1997).** The human cytomegalovirus UL55 (gB) and UL75 (gH) glycoprotein ligands initiate the rapid activation of Sp1 and NF-kappaB during infection. *Journal of Virology* **71**, 5051-5059.
- Yurochko, A. D., Kowalik, T. F., Huong, S. M. & Huang, E. S. (1995).** Human cytomegalovirus upregulates NF-kappa B activity by transactivating the NF-kappa B p105/p50 and p65 promoters. *Journal of Virology* **69**, 5391-5400.
- Zabel, U. & Baeuerle, P. A. (1990).** Purified human I kappa B can rapidly dissociate the complex of the NF-kappa B transcription factor with its cognate DNA. *Cell* **61**, 255-265.
- Zandi, E., Rothwarf, D. M., Delhase, M., Hayakawa, M. & Karin, M. (1997).** The IkappaB kinase complex (IKK) contains two kinase subunits, IKKalpha and IKKbeta, necessary for IkappaB phosphorylation and NF-kappaB activation. *Cell* **91**, 243-252.
- Zantema, A., Schrier, P. I., Davis-Olivier, A., van Laar, T., Vaessen, R. T. & van der Eb, A. J. (1985).** Adenovirus serotype determines association and localization of the large E1B tumor antigen with cellular tumor antigen p53 in transformed cells. *Molecular and Cellular Biology* **5**, 3084-3091.
- Zaragoza, C., Saura, M., Padalko, E. Y., Lopez-Rivera, E., Lizarbe, T. R., Lamas, S. & Lowenstein, C. J. (2006).** Viral protease cleavage of inhibitor of kappaBalpha triggers host cell apoptosis. *PNAS* **103**, 19051-19056.
- Zarnegar, B. J., Wang, Y., Mahoney, D. J., Dempsey, P. W., Cheung, H. H., He, J., Shiba, T., Yang, X., Yeh, W. C., Mak, T. W., Korneluk, R. G. & Cheng, G. (2008).** Noncanonical NF-kappaB activation requires coordinated assembly of a regulatory complex of the adaptors cIAP1, cIAP2, TRAF2 and TRAF3 and the kinase NIK. *Nat Immunol* **9**, 1371-1378.
- Zeller, T. (2003).** In-vitro- und In-vivo-Untersuchungen funktioneller Bereiche des Adenovirus Typ 5 E1B-55kDa-Proteins, p. 166. Regensburg: Universität Regensburg.

- Zerler, B., Roberts, R. J., Mathews, M. B. & Moran, E. (1987).** Different functional domains of the adenovirus E1A gene are involved in regulation of host cell cycle products. *Molecular and Cellular Biology* **7**, 821-829.
- Zhang, J. J., Vinkemeier, U., Gu, W., Chakravarti, D., Horvath, C. M. & Darnell, J. E. (1996).** Two contact regions between Stat1 and CBP/p300 in interferon gamma signaling. *PNAS* **93**, 15092-15096.
- Zhang, S. Q., Kovalenko, A., Cantarella, G. & Wallach, D. (2000).** Recruitment of the IKK signalosome to the p55 TNF receptor: RIP and A20 bind to NEMO (IKKgamma) upon receptor stimulation. *Immunity* **12**, 301-311.
- Zhang, X., Hussain, R., Turnell, A. S., Mymryk, J. S., Gallimore, P. H. & Grand, R. J. A. (2005).** Accumulation of p53 in response to adenovirus early region 1A sensitizes human cells to tumor necrosis factor alpha-induced apoptosis. *Virology* **340**, 285-295.
- Zhao, J., He, S., Minassian, A., Li, J. & Feng, P. (2015).** Recent advances on viral manipulation of NF- $\kappa$ B signaling pathway. *Current Opinion in Virology* **15**, 103-111.
- Zsengeller, Z., Otake, K., Hossain, S. A., Berclaz, P. Y. & Trapnell, B. C. (2000).** Internalization of adenovirus by alveolar macrophages initiates early proinflammatory signaling during acute respiratory tract infection. *J Virol* **74**, 9655-9667.

**I Publications in Scientific Journals**

Berscheminski J., Wimmer P., Brun J., **Ip W. H.**, Groitl P., Horlacher T., Jaffray E., Hay R. T., Dobner T., Schreiner S. (2014). Sp100 Isoform-Specific Regulation of Human Adenovirus 5 Gene Expression. *J. Virol.* 2014, 88(11): 6076-92.

Berscheminski J., Brun J., Speiseder T., Wimmer P., **Ip W. H.**, Terzic M., Dobner T., Schreiner S. (2015) SP100 is a tumor suppressor that activates p53-dependent transcription and counteracts E1A/E1B-55K-mediated transformation. *Oncogene.* 2015

Lüdtke A., Oestereich L., Ruibal P., Wurr S., Pallasch E., Bockholt S., **Ip W. H.**, Rieger T., Gómez-Medina S., Stocking C., Rodríguez E., Günther S., Muñoz-Fontela C., (2015). Ebola virus disease in mice with translated human hematopoietic stem cells. *J. Virol.*, 89(8): 4700-4.

Rodríguez E., **Ip W. H.**, Kolbe V., Hartmann K., Pilnitz-Stolze G., Tekin N., Gómez-Medina S., Muñoz-Fontela C., Krasemann S., Dobner T., (2016). Humanized Mice Reproduce Acute and Persistent Infection of Human Adenovirus. *J. Infect. Dis.* (under review)

**Ip W. H.**, Dobner T., Schreiner S., (2016). HAdV-C5 mediated modulation of IKK $\alpha$  promotes efficient productive infection. (manuscript in preparation)

**Ip W. H.**, Dobner T., Schreiner S., (2016). NEMO is a novel restriction factor during HAdV-C5 productive infection. (manuscript in preparation)

**II Oral presentations at scientific meeting**

HPI Retreat, Hamburg, Germany (2014)

**III. Participation in scientific meetings/Workshops**

22<sup>nd</sup> Annual Meeting of the GfV (Society for Virology) and DVV, Essen, Germany (2012)

Soft skill course: Scientific Writing Workshop (2013)

Soft skill course: Data Analysis (2014)

Felasa B course (2014)

The Ubiquitin Family, Cold Spring Harbor (2015)

## 8 Acknowledgements

---

First, I would like to thank my supervisor Prof. Dr. Thomas Dobner for giving me the opportunity to work on this project, and the nice atmosphere in the lab. He has given me enough freedom to develop my own ideas and to establish my own scientific thinking, which will help me in my future career.

Second, I would like to thank the members of the advisory committee, including Prof. Dr. Nicole Fischer, for evaluating my thesis, and Prof. Dr. Julia Kehr for chairing the oral thesis defense.

A special thank goes to Sabrina Schreiner for encouraging me to start this project and to focus the goals. Thanks to my lab mates: Carolin Bürck, Nora Freudenberger, Jana Kondrajew, Tina Meyer, Sarah Müncheberg and Maggie Valdes Aleman.

I wish to thank the former lab members, Julia Berscheminski, Elena Lam; and current lab members Willi Ching, Marie Fiedler, Helga Hofmann-Sieber, Shankar Kapnoor, Viktoria Kolbe, Lisa Kieweg, Michael Melling, Steewen Speck, Thomas Speiseder and Nilgün Tekin-Bubenheim.

I am grateful to Estefania Rodriguez-Burgos for introducing me into the mouse work and thoroughly reading and correcting my thesis manuscript.

Further, I am particularly grateful for the assistance given by Gabi Dobner and Britta Wilkens and the administrative assistance of Edda Renz that support me during all these years.

